NASA/TM-2001-211054
ARL-TR-2564

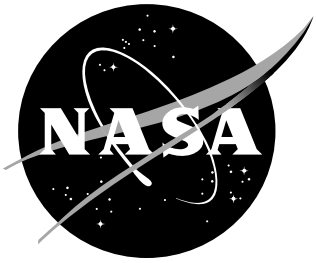

A Historical Overview of Aeroelasticity Branch and Transonic Dynamics Tunnel Contributions to Rotorcraft Technology and Development

William T. Yeager, Jr.
U.S. Army Research Laboratory
Vehicle Technology Directorate
Langley Research Center, Hampton, Virginia

Raymond G. Kvaternik
Langley Research Center, Hampton, Virginia

August 2001

The NASA STI Program Office ... in Profile

Since its founding, NASA has been dedicated to the advancement of aeronautics and space science. The NASA Scientific and Technical Information (STI) Program Office plays a key part in helping NASA maintain this important role.

The NASA STI Program Office is operated by Langley Research Center, the lead center for NASA's scientific and technical information. The NASA STI Program Office provides access to the NASA STI Database, the largest collection of aeronautical and space science STI in the world. The Program Office is also NASA's institutional mechanism for disseminating the results of its research and development activities. These results are published by NASA in the NASA STI Report Series, which includes the following report types:

- TECHNICAL PUBLICATION. Reports of completed research or a major significant phase of research that present the results of NASA programs and include extensive data or theoretical analysis. Includes compilations of significant scientific and technical data and information deemed to be of continuing reference value. NASA counterpart of peer-reviewed formal professional papers, but having less stringent limitations on manuscript length and extent of graphic presentations.

- TECHNICAL MEMORANDUM. Scientific and technical findings that are preliminary or of specialized interest, e.g., quick release reports, working papers, and bibliographies that contain minimal annotation. Does not contain extensive analysis.

- CONTRACTOR REPORT. Scientific and technical findings by NASA-sponsored contractors and grantees.

- CONFERENCE PUBLICATION. Collected papers from scientific and technical conferences, symposia, seminars, or other meetings sponsored or co-sponsored by NASA.

- SPECIAL PUBLICATION. Scientific, technical, or historical information from NASA programs, projects, and missions, often concerned with subjects having substantial public interest.

- TECHNICAL TRANSLATION. English-language translations of foreign scientific and technical material pertinent to NASA's mission.

Specialized services that complement the STI Program Office's diverse offerings include creating custom thesauri, building customized databases, organizing and publishing research results ... even providing videos.

For more information about the NASA STI Program Office, see the following:

- Access the NASA STI Program Home Page at ***http://www.sti.nasa.gov***

- E-mail your question via the Internet to help@sti.nasa.gov

- Fax your question to the NASA STI Help Desk at (301) 621-0134

- Phone the NASA STI Help Desk at (301) 621-0390

- Write to:
  NASA STI Help Desk
  NASA Center for AeroSpace Information
  7121 Standard Drive
  Hanover, MD 21076-1320

NASA/TM-2001-211054
ARL-TR-2564

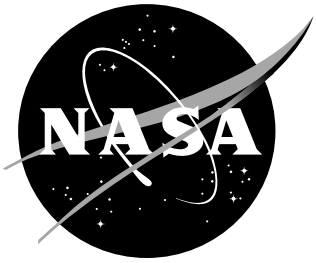

A Historical Overview of Aeroelasticity Branch and Transonic Dynamics Tunnel Contributions to Rotorcraft Technology and Development

William T. Yeager, Jr.
U.S. Army Research Laboratory
Vehicle Technology Directorate
Langley Research Center, Hampton, Virginia

Raymond G. Kvaternik
Langley Research Center, Hampton, Virginia

National Aeronautics and
Space Administration

Langley Research Center
Hampton, Virginia 23681-2199

August 2001

Acknowledgments

The authors wish to acknowledge the work of the research staff of the Aeroelasticity Branch at NASA Langley Research Center and our partners from government, industry, and academia whose research has been reviewed in this report.

Available from:

NASA Center for AeroSpace Information (CASI)
7121 Standard Drive
Hanover, MD 21076-1320
(301) 621-0390

National Technical Information Service (NTIS)
5285 Port Royal Road
Springfield, VA 22161-2171
(703) 605-6000

This report is also available in electronic form at URL http://techreports.larc.nasa.gov/ltrs/

Table of Contents

Abstract

A historical account of the contributions of the Aeroelasticity Branch (AB) and the Langley Transonic Dynamics Tunnel (TDT) to rotorcraft technology and development since the tunnel's inception in 1960 is presented. The paper begins with a summary of the major characteristics of the TDT and a description of the unique capability offered by the TDT for testing aeroelastic models by virtue of its heavy gas test medium. This is followed by some remarks on the role played by scale models in the design and development of rotorcraft vehicles and a review of the basic scaling relationships important for designing and building dynamic aeroelastic models of rotorcraft vehicles for testing in the TDT. Chronological accounts of helicopter and tiltrotor research conducted in AB/TDT are then described in separate sections. Both experimental and analytical studies are reported and include a description of the various physical and mathematical models employed, the objectives of the investigations, and illustrative experimental and analytical results.

Introduction

The Langley Transonic Dynamics Tunnel (TDT) (fig. 1) and the Aeroelasticity Branch (AB) with which it is associated have a long and substantive history of aeroelastic research that has made creditable contributions to rotorcraft technology and development. That research, extending from shortly after the tunnel's inception in 1960 to the present, has included a wide range of experimental investigations using a variety of scale models and testbeds, and the development and application of essential analyses. The results of that research have contributed substantially to the technology base needed by the industry for designing and building advanced rotorcraft systems. In particular, the work has contributed to supporting rotorcraft research and development programs, to the fundamental understanding of phenomena involved, and to resolving anomalies. For convenience of discussion, the rotorcraft investigations may be divided into two categories: helicopters and tiltrotors.

Helicopter model testing has been conducted in the TDT since 1963, and has generally taken the form of research testing rather than testing in direct support of any specific helicopter development program. Several testbeds have been used for helicopter testing in the TDT (fig. 2). The first (fig. 2a) was built by Lockheed Aircraft Company and was used for testing of hingeless rotor configurations in support of the XH-51 research helicopter development program. A testbed developed by Bell Helicopter Company was used for two-bladed teetering rotor studies (fig. 2b). The Lockheed testbed was later refurbished in-house at Langley and became known as the Generalized Rotor Aeroelastic Model, or GRAM (fig. 2c). This testbed was used for helicopter rotor testing at the TDT until the late 1970s. The current testbed, known as the Aeroelastic Rotor Experimental System, or ARES (fig. 2d), has been used for all helicopter rotor testing in the TDT since 1977. The ARES testbed has been used for investigations involving rotor performance, loads, stability, and acoustics for a number of rotor models. For example, the ARES has been used for the study of conformable rotors to define their potential for altering blade spanwise and azimuthal airload distributions to improve rotor performance and reduce loads. An active control concept known as Higher Harmonic Control (HHC) was tested on the ARES to confirm predictions as to the level of reduction in fixed-system vibration and blade-vortex interaction noise. The ARES testbed has also been used to obtain aeromechanical stability and loads data for hingeless and bearingless rotor models and to validate existing analytical models. The ARES testbed has also been used for studies to evaluate rotors incorporating advanced technologies that will be needed to meet military requirements for increased mission effectiveness

and improved safety and survivability in future helicopters.

Tiltrotor aeroelastic research in the TDT (fig. 3) has been about equally divided between supporting research and development programs. This work has its roots in propeller whirl flutter studies conducted in the TDT in the early 1960s, and some later fundamental studies into the whirl flutter behavior of propellers having flapping blades. Tiltrotor aeroelastic studies began in 1968 in an exploratory parametric investigation of stability, dynamics, and loads using a model of a proposed Bell Helicopter Company tiltrotor design designated the Model 266. In the early 1970s, aerodynamic and flutter clearance tests were conducted in support of the development program that led to the NASA/Army XV-15 tiltrotor research aircraft. During this same period, a parametric investigation of proprotor whirl flutter was conducted using an off-design research configuration of a proposed Grumman tiltrotor design. There was a hiatus in tiltrotor research activity at AB from 1974 until 1984, after which tests were conducted on a Bell tiltrotor model in support of the V-22 development program. A second hiatus in tiltrotor research occurred from 1985 to 1994, after which there was a resurgence of tiltrotor activity within AB/TDT, primarily in anticipation of NASA's Short Haul Civil Tiltrotor program. This led to a new tiltrotor research program using a refurbished version of the V-22 model that was tested earlier in the TDT in support of the V-22 program. The refurbished model has been incorporated into a tiltrotor research testbed called the Wing and Rotor Aeroelastic Testing System (WRATS). In collaboration with Bell Helicopter Textron, studies under the current research program are focused on a range of aeroelastic technical areas that have been identified as having the potential for enhancing the commercial and military viability of tiltrotor aircraft. In particular, emphasis is being placed on the development of active and passive techniques for vibration control, stability augmentation, and increased aerodynamic performance of tiltrotor aircraft.

Several overviews of AB/TDT aeroelastic research activities have been published over the years (see, for example, refs. 1-9). However, these reviews have either been generic discussions of work conducted in the TDT without any particular emphasis on rotorcraft, or specific to rotorcraft but incomplete with respect to the scope of the work reviewed. The purpose of this paper is to present a complete and unified historical account of the AB/TDT aeroelastic research accomplishments that have contributed to rotorcraft technology and development since the inception of the TDT in 1960. Relevant ancillary studies contributing to this technology base are also included. The paper begins with a summary of the major characteristics of the TDT and a description of the unique capability offered by the TDT for testing aeroelastic models by virtue of its heavy gas test medium. This is followed by some remarks on the use of scale models in the design and development of rotorcraft vehicles, and a review of the basic scaling relationships important for designing and building dynamic aeroelastic rotorcraft models for testing in the TDT. Helicopter and tiltrotor research conducted in AB/TDT is then described in separate sections. In each of these sections, a chronological account of the pertinent experimental and analytical work and contributions is given. These discussions include a description of the various physical and mathematical models employed, the specific objectives of the investigations, and illustrative experimental and analytical results. Where and when appropriate, an explanation of the pertinent fundamental mechanisms and interactions involved in the phenomena under investigation is included in the discussion. Each section concludes with a résumé of current and planned research activities.

Tunnel Characteristics

The Langley Transonic Dynamics Tunnel (TDT) is a single-return, closed-loop, continuous-flow, variable-pressure, slotted-throat wind tunnel having a test section 16-feet square (with cropped corners). An aerial view of the wind tunnel and its adjoining engineering and equipment building is shown in figure 1. A schematic depicting the general arrangement of the tunnel is shown in figure 4. The tunnel uses either air or a heavy gas as the test medium and can operate at total (stagnation) pressures from near vacuum to atmospheric. It has a Mach number range from near zero to

about 1.2, with attendant maximum Reynolds numbers of about three million per foot in air to about ten million per foot in heavy gas. Both Mach number and pressure are independently controllable.

The TDT is specially configured for aeroelastic testing. Large windows are provided for close, unobstructed viewing of the model from the control room. A set of four by-pass valves is present in the wind-tunnel circuit to allow quick reduction in the dynamic pressure in the test section in case of model instability. The tunnel fan blades are protected from debris of damaged models by a wire-mesh safety screen. A variety of model mount systems are available. For helicopter testing, stand-mounted testbeds have been used. For tiltrotor testing, stand-mounted, sidewall-mounted, sting-mounted, and rod-mounted models have been used. The TDT also offers an airstream oscillator system for gust studies. The system consists of an arrangement of biplane vanes located on either side of the tunnel entrance section (fig. 5). Vane frequency and amplitude are adjustable and the two pairs of vanes may be operated either in phase or out of phase to provide vertical or rolling gust fields.

The tunnel was originally constructed as a 19-foot diameter subsonic pressure tunnel in 1938 (ref. 10). In the late 1950s, the facility was converted to a transonic dynamics tunnel to fill the need for a wind tunnel dedicated to the testing of large aeroelastic models of aerospace flight vehicles from low subsonic through transonic speeds. This new aeroelastic testing capability was made possible by using the high-molecular-weight gas R-12 as the test medium (ref. 11). A number of subsequent comparative tests (see, for example, refs. 12-15) confirmed pre-conversion studies as to the soundness of testing aeroelastic models in R-12 instead of air. Environmental concerns raised in the late-1980s regarding the continued widespread use of R-12 led to a NASA decision to replace the R-12 used in the TDT with the environmentally acceptable and essentially equivalent refrigerant R-134a. Conversion of the TDT heavy gas test medium from R-12 to R-134a was completed in 1997 and is described in references 16-17. Subsequent wind tunnel characterization and calibration tests were completed in 1998, after which normal tunnel operations resumed. Because R-12 and R-134a have comparable properties, the primary flow characteristics of the TDT for R-134a operations are not much different from those for R-12, as was expected. For this reason, the advantages of testing in heavy gas will continue with R-134a. However, because the speed of sound in R-134a is slightly higher than in R-12 rotorcraft models tested in R-134a must be operated at higher rotor rotational speeds to maintain Mach scaling.

Since its inception, the TDT has been a unique national facility for testing aeroelastic models of a variety of aircraft, spacecraft, and launch vehicles (see, for example, refs. 1-2). The heavy gas feature of the tunnel (in combination with its large size) offers several advantages over air with respect to designing, building, and testing aeroelastic models. For example, improved model-to-full scale similitude, eased fabrication requirements, lower model vibration frequencies, reduced test section flow velocities, larger test Reynolds numbers, and reduced tunnel power requirements. The size of the test section easily accommodates model rotors up to 10 feet in diameter. More detailed descriptions of the TDT and its capabilities may be found in references 16-17.

Some Remarks on the Use of Scale Models

Aeroelastically-scaled wind-tunnel models have played an important role in the design, development, and verification process in diverse fields of engineering, including aerospace engineering (see, for example, refs. 18-23). Their use is particularly prolific in the field of aeronautics wherein dynamic aeroelastic (i.e., flutter) models are extensively employed both to substantiate that an aircraft design is free of aeroelastic instabilities within its flight envelope, and to validate analyses. Analytical capabilities for addressing aeroelastic design issues of aircraft have improved significantly over the years. However, because aircraft have continued to increase in structural and aerodynamic complexity, the need to rely on wind-tunnel tests of sub-scale models to verify predicted behavior and performance before entering the flight test stage of a development program

remains. Such models are also widely used in research investigations dealing with such issues as active control of aeroelastic stability and response, buffet load alleviation, and for the validation of analytical and computational methods used in design.

The importance of sub-scale models for helicopter research has been recognized as early as 1953 (refs. 24-25). Sub-scale models have also played a valuable, although perhaps less prominent, role in the design and development of helicopters, tiltrotors, and V/STOL aircraft (for example, see refs. 22-23, 26-27). Both government and industry have acknowledged the significance and role of sub-scale models in rotorcraft research and development on many occasions. For example, references 28-29 emphasized the importance of a properly conducted wind-tunnel test program that includes both model-scale and full-scale testing to reduce the technical risk of a rotorcraft development program, and to lessen the chance for surprises in the flight test stage.

Model Scaling Considerations

Dynamic aeroelastic models may be classified into two general groups: (1) research models, and (2) prediction models. Research models do not represent any particular aircraft and are at most only broadly representative of full-scale designs. They are used primarily to gain insight into aeroelastic problems (e.g., identify the types of flutter which may be associated with a new or unusual configuration), to provide experimental data for comparison with analysis, and to provide general design information on flutter trends that occur with variations in system parameters. Prediction models are based on actual full-scale designs and are intended to predict the full-scale behavior of specific aircraft. These models are related to the full-scale designs that they represent by certain scaling relationships. It should be noted that prediction models can also be used effectively as research models.

A model will exhibit similitude or similarity to a full-scale structure provided certain dimensionless ratios have the same values for both. These dimensionless ratios may be determined by dimensional analysis of all the quantities involved in the problem or (if the structure is simple enough) from the differential equations which define the system. The objective of the theory of similitude (refs. 18, 19, 30-32) is to establish those relationships that must be maintained to permit reliable predictions to be made from measured model behavior. Usually, not all dimensionless ratios can be maintained at full-scale values with reasonable choices of materials and scale factors in available test facilities. In such cases, complete similarity cannot be maintained and compromises must be made, based on experience and knowledge of the problem, by which the less important dimensionless ratios are allowed to deviate from full-scale values. Fortunately, a model is usually designed to study only a particular phenomenon (or class of phenomena), in which case only those dimensionless ratios important for the phenomena of interest need be maintained at their full-scale values.

The requirements for achieving dynamic and aeroelastic similitude of model and full-scale aircraft and helicopters are replete in the literature (see, for example, refs. 31-36) and will be reviewed here only briefly as they apply to rotorcraft. As mentioned above, the similarity requirements can be obtained either by applying dimensional analysis to the problem or by examining the appropriate governing equations written in nondimensional form. Application of such procedures results in the identification of the basic independent nondimensional parameters that must have a one-to-one correspondence between model and full scale to ensure adequate representation. For the study of dynamic aeroelasticity and unsteady aerodynamics phenomena, five basic similarity parameters are indicated: Mach number, advance ratio (reduced frequency), Lock number (mass ratio), Reynolds number, and Froude number. The other dependent ratios relating model quantities to full-scale quantities can be derived from these basic similarity parameters. The models must also be geometrically similar to their full-scale equivalents in external shape as well as in their distribution of mass and stiffness. In addition, any important body degrees-of-freedom must be included in the models.

The simultaneous satisfaction of the five similarity parameters noted above is not possible because of conflicting requirements that result for the design of a model. In conventional wind tunnels using atmospheric pressure air as the test medium, only three of the five parameters can be maintained at their full-scale values. For the simulation of flight conditions where compressibility effects are important, it is well established that the full-scale values of Mach number, advance ratio, and Lock number must be maintained in the model. This is true whether the model is to be tested in air or heavy gas. However, if the model is designed for testing in heavy gas, Froude number may be maintained simultaneously with Mach number, advance ratio, and Lock number by selecting an appropriate length scale factor (about .20 to .29 depending on the simulated full-scale altitude). For simulation of flight conditions where compressibility effects are not important models are usually designed to maintain full-scale values of advance ratio, Froude number, and Lock number when tested in air. However, for suitable length scale factors, these models can simultaneously obtain near full-scale values of Mach number when tested in heavy gas. It is generally not possible to simulate full-scale Reynolds number in either the air or heavy gas test mediums of the TDT. However, the use of heavy gas permits a nearly three-fold increase in Reynolds number over comparable conditions in air.

Some of the more important aeroelastic scale factors applicable to rotorcraft models in the TDT are summarized in table 1. Scale factors are tabulated for testing in air, R-12, and R-134a for the cases in which either Mach number or Froude number is maintained at its full-scale value in addition to Lock number and advance ratio.

Helicopter Research Contributions

Tests Using Lockheed Aircraft Testbed

1963 - 1964

The initial model helicopter tests in the TDT were conducted in 1963 and 1964 as part of a cooperative effort between the U. S. Army, Lockheed Aircraft, and NASA to conduct hingeless rotor research investigations (refs. 37-40). The tests were conducted using a 1/3-size hingeless rotor model that was 10 feet in diameter (fig. 2a). The model blades were ballasted to allow testing in R-12 at a density of 0.008 slugs/ft^3. A number of configurations were tested resulting in research information that included structural loads and aerodynamic data for all the configurations tested. The 1963 and 1964 tests included rotor configurations with three, four, and six blades as well as variations in the blade flapwise and chordwise stiffnesses and stiffness distributions. Each configuration was tested through a forward speed and load factor range simulating conventional helicopter and compound helicopter operation (refs. 37-38).

The 1963 test involved only a three-bladed hingeless rotor configuration with matched root stiffness. Testing was conducted at simulated forward speeds from 60 to 240 mph over a range of rotor load factors at advancing tip Mach numbers up to 0.91. Data were obtained for helicopter, unloaded rotor, and compound helicopter modes of operation and indicated a beneficial influence of blade twist on chordwise cyclic loads in forward flight. This rotor was designed to enable wide variations in dynamic characteristics and therefore was not representative of an optimized design. The test in 1964 was conducted using a blade and rotor hub design that was optimized for low drag. The blade flapwise and chordwise stiffnesses were also approximately matched along the blade span. This test involved three-, four-, and six- bladed rotors with the four-bladed configuration considered as the baseline. As in the 1963 test, all configurations were tested over a range of forward speeds and rotor load factors to obtain structural loads and performance data. Results indicated that the optimized rotor design with low chordwise stiffness blades showed considerable promise from the standpoint of structural loads, vibration, and performance. The results of these two hingeless rotor tests were encouraging with regard to the use of hingeless rotor configurations and were of use in the development of the Lockheed XH-51 helicopter.

Tests Using Bell Helicopter Company Testbed

In the late 1960s and into the 1970s, the emphasis in helicopter testing at the TDT was on two-bladed teetering rotor configurations. The tests conducted in this timeframe used 1/4- and 1/5- size teetering rotor models mounted on the testbed developed by Bell Helicopter Company (fig. 2b).

1969

In 1969, a teetering rotor test (ref. 13) was conducted to obtain data to assess three areas of interest: 1) the aerodynamic characteristics of rotors operating at combinations of high advance ratio and high advancing tip Mach number; 2) the feasibility of obtaining rotor structural and aerodynamic loads from a dynamically similar scaled model; and 3) the validity of data obtained in an R-12 atmosphere. This test used a 1/4-size, geometrically and dynamically scaled rotor system representative of those used on Bell Helicopter Company UH-1C and AH-1G aircraft. An additional 1/4-size model rotor was used that had different twist and airfoil characteristics than the scaled rotor system. Assessment of the wind-tunnel results was made by comparing to existing full-scale wind-tunnel data and full-scale flight data. Comparisons of theoretical calculations with the wind-tunnel data were also made. Results documented in reference 13 show that model and full-scale experimental rotor performance as a function of advance ratio showed no significant trend differences. Comparisons of model and full-scale rotor performance showed good agreement with variations in advancing tip Mach number. Calculated rotor performance trends with advance ratio and with advancing tip Mach number were not found to be in as good agreement with full-scale data as was the wind-tunnel results. Correlation of model and full-scale blade oscillatory loads did not yield the accuracy desired. It was concluded that non-scaled rotor hub impedance and discrepancies in the full-scale blade stiffness values used to produce the model blades probably caused this lack of agreement. Finally, it was concluded that trend correlations showed that full-scale loads could be determined in an R-12 atmosphere using a properly scaled rotor model.

1973

References 15 and 41 document results of a teetering rotor test conducted in 1973 using the same testbed as the 1969 test. This test continued the evaluation of R-12 as a suitable test medium for model helicopter rotors (ref. 15), and investigated the effects of hub inplane support parameters ("hub impedance") on the chordwise oscillatory loads of a two-bladed teetering rotor (ref. 41). To evaluate the suitability of R-12 as a test medium, the studies involved testing a 1/5-size aeroelastically scaled helicopter rotor in R-12 at the same advance ratios, tip Mach numbers, shaft angles of attack, and collective pitch values as a full-size helicopter rotor tested in air. Reynolds number variations were achieved through controlled R-12 density changes and the use of a wide chord model rotor that was not aeroelastically scaled. Integrated rotor performance from the aeroelastically scaled model rotor provided data trends and magnitudes that agreed well with full-scale rotor data (figs. 6-7) even at the lower values of model Reynolds numbers. An exact match of full-scale rotor Reynolds number was accomplished by utilizing the wide chord model rotor, but with accompanying mismatches in rotor solidity and aeroelastic scaling. Performance results obtained for the full-scale and model-scale rotors are summarized in figure 8. Region B of figure 8 illustrates the expected performance trend with decreasing Reynolds number for the wide chord blade, i.e., more torque required at a given rotor lifting task. An unexpected result of these tests is illustrated by Region A of figure 8 which shows that better model performance correlation with full-scale values was achieved with a dynamically scaled rotor of the correct solidity than with a rotor that matched Reynolds number but was not dynamically scaled. It was concluded that Reynolds number effects might be minor in rotor aerodynamic performance testing in comparison to the combined effects of rotor solidity and blade elastic properties.

The determination of the effect of hub inplane support parameters on two-bladed teetering rotor chordwise oscillatory loads consisted of : 1) a shake test to define the impedance of several testbed configurations as a function of frequency, and 2) testing of the configurations in the TDT. Wind-

tunnel test results showed that the one-per-rev inplane bending moments could be changed by a factor of two, depending on the testbed configuration, at the same aerodynamic operating condition. The higher harmonic blade loads and pitch link loads were not affected by changes in inplane hub impedance. Additionally, the test results generally substantiated the predicted trends, although differences in the magnitude of the blade bending moments were observed when compared to predicted results. Some of these differences were attributed to the influence of the testbed strain-gage balance or tunnel floor on hub impedance. A definitive reason for the difference between the measured and calculated blade bending moments was not arrived at since neither of these effects were accounted for in the analysis.

Tests Using the GRAM Testbed

In 1974 and 1975 teetering rotor tests were conducted utilizing the GRAM testbed (fig. 2c). These teetering rotor tests (ref. 6) involved a 1/4-size aeroelastically scaled model of a Bell Helicopter Company AH-1G "Cobra" rotor (fig. 9), and two 1/5-size aeroelastically scaled wide-chord rotor configurations, with (fig. 10) and without a mid-span flap hinge (fig. 11).

1974

The purpose of the AH-1G rotor test (ref. 6) was to determine whether two-bladed teetering rotors can experience stall flutter, which is a factor that limits the forward flight speed of articulated rotor configurations. Stall flutter is a phenomenon that is characterized by high oscillatory blade loads at the first torsional frequency of the blade occurring on the retreating side of the rotor disk. Blade loads and rotor performance data were obtained for the AH-1G model rotor up to advance ratios of 0.40. In order to compare the model test conditions with the full-scale aircraft flight envelope, model thrust values for selected test points were converted to full-scale load factors. These results were plotted on the aircraft flight envelope as shown in figure 12. Based on the comparison with the full-scale load factors in figure 12 it was determined that model data were obtained that corresponded to full-scale thrust values both within and without the aircraft sustained operating envelope. Model thrust data were also obtained outside the sustained operating value of the aircraft, but within the maneuver, or transient, envelope. It should be noted that the model tests did not simulate maneuvers, but rather the model thrust simulated the full-scale thrust required in maneuvering flight. For three of the test points presented in figure 12, the model blade torsional moment waveforms at 45% blade radius are shown for two rotor revolutions. Note that at an advance ratio of 0.2, the torsional waveform at a low thrust condition does not indicate any oscillations on the retreating side of the disk (180 deg. to 360 deg. azimuth) that could be attributable to stall flutter. However, for the higher thrust condition at an advance ratio of 0.2 there are significant torsional oscillations of the model blade on the retreating side of the disk and these oscillations are at the first torsional frequency of the model blade. At an advance ratio of 0.4, the torsional waveform shown corresponds to a maneuver thrust condition for the aircraft, and large torsional oscillations are evident on the retreating side of the rotor disk. The results presented in figure 12 indicate that two-bladed teetering rotors could experience the stall flutter phenomenon experienced by articulated rotor systems. With regard to control system loads, the implications of stall flutter for a teetering rotor may not be as severe as for an articulated rotor since, even for non-stalled conditions, the control system of a teetering rotor must be designed to withstand the typically higher control loads.

1975

The test of the wide-chord teetering rotor (ref. 42) had two purposes. The primary purpose of the test was to evaluate the use of a wide chord blade to increase the aerodynamic performance capabilities of a two-bladed teetering rotor, and to obtain loads data on the wide chord configuration. The secondary purpose of the test was to determine the effectiveness of a mid-span flapping hinge in reducing the flapwise blade loads of the wide-chord blade configuration. Figure 13 shows a comparison of the oscillatory flapwise blade loads as a function of blade radius for the rotor configurations with and without the hinge. As the results in figure 13 show, the mid-span hinge was effective in reducing the oscillatory flapwise bending mo-

ments. The hinged rotor was also found to exhibit no tendency to become dynamically unstable, nor were any excessive outboard blade motions about the hinge observed. From an operational point of view, the blades with the mid-span hinge behaved much like the blades without the hinge.

In addition to testing two-bladed teetering rotor configurations, the GRAM testbed was used in 1975 for testing of a four-bladed flex-hinge rotor configuration (refs. 6 and 43). Figure 14 shows the flex-hinge rotor mounted on the GRAM testbed in the TDT. The flex-hinge rotor was hingeless in the flapping direction, using low bending stiffness flexures to allow blade flapping motions. The blades were hinged in the lead-lag direction with an elastomeric damper used to provide inplane damping and stiffness. This inplane configuration allowed the rotor to behave dynamically as a soft-inplane hingeless rotor. The flex-hinge model had a diameter of 10 feet and was Froude-scaled for operation in air, as opposed to R-12, because the test required a large number of configuration changes. Typically, tests in R-12 required as much as 3 hours of gas handling for each model configuration change. The objectives of the tests were to provide performance, loads, and stability data for the flex-hinge configuration. These data were intended to aid the development and eventual flight test of full-scale hardware by Bell Helicopter Company as part of its internal research and development efforts. Figure 15 shows samples of the flex-hinge rotor performance data obtained at an advance ratio of 0.35. The results in figure 15 are plots of the rotor torque coefficient versus rotor thrust coefficient and rotor lift coefficient versus rotor drag coefficient for three values of rotor shaft angle of attack. Similar performance results were obtained over the intended operational envelope to determine how the flex-hinge rotor could be expected to perform.

A concern for testing of the flex-hinge rotor was whether the configuration would experience the air resonance phenomenon that can occur for soft-inplane hingeless rotors. Air resonance involves coupling between the first blade inplane mode and fuselage pitch and roll modes. In order to examine the stability characteristics of the flex-hinge rotor, an on-line subcritical testing technique (refs. 44-45) was used to determine the frequency and damping in the mode of interest at each test condition. By monitoring the damping as a function of the test parameters the stability boundary may be defined. Although no instabilities were experienced during testing of the flex-hinge rotor, damping trends were obtained to determine an optimum level of damping from both a stability and blade response point of view. Figure 16 shows the trend of damping for the blade lead-lag mode as a function of advance ratio for the nominal damper configuration.

Tests Using the ARES Testbed

In 1977, the ARES testbed (fig. 2d) was put into service at the TDT and has been used since then for all studies of aeroelastically scaled main-rotor systems. A description of the ARES and associated instrumentation can be found in references 7 and 8. Initial use of the ARES testbed was accompanied by a change in emphasis from the testing of two-bladed teetering rotor configurations to the testing of four-bladed articulated rotor configurations. The initial series of articulated rotor tests was conducted in the late 1970's and early 1980's to investigate conformable rotor configurations. A conformable rotor (refs. 46-50) is intended to use passive means of inducing dynamic twist along a rotor blade to alter unfavorable blade spanwise and azimuthal load distributions to improve rotor performance and reduce vibratory loads. The tests in the TDT investigated the use of tip geometry as a means of inducing rotor blade dynamic twist.

1977

Reference 51 documents the initial TDT test that investigated the use of blade tip geometry to improve rotor performance and reduce loads. This test used model rotor blades that were aeroelastically designed but did not represent any full-scale rotor in production. The blades were originally designed to be Mach-scaled for operation in air, but were converted for operation in R-12 by adding ballast weights that produced the proper Lock number. The tests were conducted at combinations of rotor shaft angle of attack, rotor lift, and rotor advance ratio to evaluate the effects of tip geometries incorporating sweep, taper, and anhedral. Tip geometry changes were made through the use of interchangeable blade tips. Results from this test indicated that the use of tip sweep

reduced blade flapwise and chordwise bending moments and torsional moments as well as control system loads, while improving rotor forward flight performance above an advance ratio of 0.30. The use of blade tip anhedral was found to increase blade bending moments while reducing torsional moments. Anhedral was found to improve rotor performance in hover as well as in forward flight up to an advance ratio of 0.30.

1978

In 1978 a test was conducted in the TDT as a follow-up to the 1977 test. The follow-up test used the same model rotor blades as the 1977 test, and was conducted to evaluate the impact of additional tip geometries on the interaction between blade torsional loads and rotor performance. This test is documented in reference 52. The data acquired were evaluated to determine if the tip geometries tested produced the torsional moments required for a successful conformable rotor, i.e., reducing nose-down twist on the advancing side of the rotor disk while avoiding stall on the retreating side of the disk. Results from the test indicated that there does not appear to be a strong correlation between blade torsional loads and the prediction of rotor performance. It was also determined that reducing the nose-down twist on the advancing blade appeared to be more important to rotor forward flight performance than increasing the nose-down twist on the retreating blade. Reference 52 also includes analytical results that addressed the effect of using uniform and nonuniform inflow models on the correlation between measured rotor torsional loads and performance. It was shown in reference 52 that the nonuniform inflow model more accurately predicted the angle-of-attack environment that would result in the blade torsional moments needed for a successful conformable rotor.

1979

Based on the results of the 1977 and 1978 tests, tests were conducted at the TDT to investigate additional conformable rotor configurations. The 1979 test was conducted to investigate the effects of blade torsional stiffness, tip sweep, and camber on blade dynamic twist as suggested by the analysis described in reference 49. This test (refs. 53-54) used two sets of aeroelastically scaled model rotor blades. The baseline blade set was generally based on the full-scale UH-60A blade design. Blade weight, torsional inertia and flapwise, chordwise and torsional stiffnesses were scaled from UH-60A blade properties although no attempt was made to match the detailed distributions of the full-scale blades. The second blade set was geometrically identical to the baseline blade but incorporated a nominal 4-to-1 reduction in torsional stiffness outboard of the fifty-percent radius station. The blade set with reduced torsional stiffness is referred to as the aeroelastically conformable rotor, or ACR. Each blade set incorporated adjustable trailing edge tabs to allow changes in local pitching moment, as well as the capability to vary the tip geometry outboard of the 89% radial station by using interchangeable blade tips. Data were obtained in R-12 at a nominal density of 0.006 slugs/ft^3 at advance ratios from 0.2 to 0.45 and at hover tip Mach numbers of 0.62, 0.65, and 0.68. The results of this test indicated that blade dynamic twist is controllable through blade design. It was shown (fig. 17) that the use of the blade trailing edge tabs produced more elastic twist than either tip sweep or tip anhedral. Blade flapwise, chordwise and torsion loads were found to be reduced, and rotor performance improved for configurations that reduced advancing blade twist. This result is in agreement with results obtained during the 1978 test documented in reference 52. One concern of using blades with reduced torsional stiffness is the possible effect on aircraft stability and control characteristics. The variation of blade torsional response with the application of controls or with airspeed, for example, can affect the rotor contribution to aircraft stability and control derivatives. However, test results showed that the control inputs required to achieve trim (fig. 18) and the control derivatives of the reduced torsional stiffness configuration were not significantly different from those of the baseline rotor.

1980 to 1983

A second test of an ACR configuration was conducted in the TDT in 1980 (ref. 55). This test used a new set of baseline and ACR model blades. The characteristics of both sets of blades were based on the rotor system of the U.S. Army YAH-64 helicopter; however, the ACR blade torsional

stiffness was reduced by a factor of 6, compared to the baseline blade, from 23% radial station to the tip. The model blades had a chord of 4.24 inches with −8 deg of linear twist over the full blade span and used a NACA 23012 airfoil section. The blade mass and elastic properties had mean values such that Mach, Froude, and Lock scaling from the full-scale blade were correct when tested in an R-12 environment. The test was conducted in R-12 at a density of 0.007134 slugs/ft^3, three times standard air density. Both the baseline and ACR blades used a rectangular planform, however, the ACR blade had an interchangeable tip that could be used to introduce 20 deg of sweep over the outboard 8% of the blade span.

The test was conducted to evaluate potential benefits of the ACR concept over a range of advance ratios and rotor thrust conditions. The test was conducted by "flying" the model to an analytically pre-determined trim condition that represented loadings a rotor system must develop in flight to trim a helicopter for steady-state operation. This procedure was followed for both the baseline and ACR blade sets. Sample results from this test are shown in figures 19-20. The results show the performance improvements offered by the ACR configuration with a swept tip at high blade loading values (fig. 19). Figure 20 also indicates reduced flapwise oscillatory bending loads for the ACR configuration compared to the baseline configuration. However, data not presented here indicates that this trend of reduced oscillatory bending loads for the ACR configuration is not always the case at higher advance ratios.

During the conformable rotor tests conducted in the TDT, the aeroelastic mechanism linking rotor configuration performance and loads to blade deflection wasn't always easy to determine. Therefore, tests were conducted in 1981 and 1982 in an effort to understand the coupling between configuration response and the resulting rotor aeroelastic environment. Because earlier conformable rotor studies had indicated the importance of the rotor blade tip geometry in producing the necessary dynamic twist, emphasis was given to parameter changes in this area. Seven blade tip shapes were tested (ref. 56) on a four-bladed articulated hub using the baseline and ACR blade sets used in the 1979 test (refs. 53-54). The different tip shapes coupled with the different blade torsional stiffnesses of the two blade sets produced significant differences in both performance and loads. Configurations that exhibited low oscillatory loads also had the best performance, while the configurations with poor performance generated the highest loads. Another interesting result of these tests was the strong correlation between azimuthal variation of elastic twist and rotor behavior. As noted in reference 52, the configurations that exhibited small azimuthal activity in elastic twist were the best performers.

The utilization of a conformable rotor concept should be evaluated not only for how successfully it achieves improved performance and reduced loads, but also how well it can be "fielded". That is, how much change, if any, in current installation, maintenance, and rotor tuning is necessary for the rotor concept to be employed. One aspect of this "fielding" process is rotor tracking sensitivity and its implications to rotor and fuselage loads. As part of the conformable rotor studies in the TDT, a rotor track sensitivity investigation was conducted, again using the same blade set as in the 1979 test (refs. 53-54). The blades were subjected to a test matrix that included a perturbation in the track on one blade. This perturbation was accomplished by a deflection of the blade trailing edge tabs. The elastic response of the baseline and ACR torsionally soft blades to tab deflection was correlated with fixed-system loads (ref. 57). The torsionally soft blades were found to respond very differently than the baseline blades to the same tab deflection. As shown in figure 21, the torsional moments for both stiff and soft blades, due to tab deflection, resulted in different blade flapping magnitudes, flapwise loads, and fixed-system vibration. These results indicate a potential coupling of blade torsional deflection, blade oscillatory loads, and fixed-system vibration which results from a high sensitivity of the conformable rotor to practical tracking procedures.

The interest in reducing helicopter fixed-system vibration led to the investigation of the use of active as well as passive means of controlling rotor vibratory loads. These active control tests were conducted in conjunction with the conformable rotor studies and involved the higher har-

monic control (HHC) concept of references 58-63. The approach combined HHC experimental studies with the development of control algorithms suitable for real-time implementation of the required control inputs, and presented the first opportunity to evaluate an adaptive control system using optimal control theory for model helicopter vibration reduction. The HHC concept involves superimposing fixed-system swashplate motions at the blade passage frequency on the basic collective and cyclic requirements. The phase and amplitude of the HHC inputs are chosen to minimize the blade passage responses transmitted to the fixed-system. Details of the choice of electronic control designs and software can be found in references 60 and 61.

Experimental verification of the HHC concept was conducted during two tests in 1980 using a four-bladed articulated model rotor tested over a range of advance ratios simulating 1g flight with the rotor first harmonic flapping trimmed to the shaft. Data were recorded to quantify the vibratory load levels without the HHC operating. The HHC closed-loop system was then activated and allowed to stabilize. With the controller still operating at its stabilized condition, data were recorded to establish the vibratory responses with higher harmonic control. The success of the HHC in reducing fixed-system vibratory responses is shown in figure 22. Variations in the fixed-system signals with and without the HHC operating indicated substantial control of the fixed-system vibration levels. It should be noted that although the required control inputs are small (less than one degree) the blade and control system loads usually increase with the HHC system operating as shown in figure 23. These experimental studies helped to accelerate the successful application of the HHC concept in a full-scale helicopter flight test described in references 62 and 63.

It has already been noted that the initial helicopter tests in the TDT were conducted to investigate hingeless rotor configurations. Soft in-plane hingeless rotors were of primary interest when two tests, combined with analytical studies, were conducted in 1982 and 1983 to investigate the ground resonance characteristics of these configurations (refs. 64-65). These efforts were intended to aid in the identification of an analysis that can be used in both the design and testing phases of hingeless and bearingless rotor development.

The rotor model used for these tests was a soft in-plane hingeless rotor that was not a dynamically scaled representation of a specific aircraft hub, but rather was representative of a typical full-scale design based on Mach number, Lock number, and frequency simulation. The model blades used were fabricated specifically for testing in R-12. The rotor hub (fig. 24) consisted of metal flap and lead-lag flexures each strain-gaged and calibrated to measure motion in those directions. The hub also utilized a mechanical feathering hinge to allow blade pitch motion.

The first generation Comprehensive Analytical Model of Rotorcraft Aerodynamics and Dynamics (CAMRAD) (refs. 66-67) computer program was used as the analytical tool for these tests. The structural dynamic model of the rotor included elastic degrees of freedom in flap bending, lead-lag bending, torsion, and a rigid pitch degree of freedom. The blade was represented by a spanwise distribution of mass, flapwise and chordwise bending stiffness and torsion stiffness, and moment of inertia. An estimated structural damping was also included in the rotor data and body characteristics were also included in the CAMRAD model. The rotor blade aerodynamic forces were calculated using lifting line theory and steady two-dimensional airfoil characteristics with corrections for unsteady and three-dimensional flow effects. The degrees of freedom used in the stability analysis were the blade flap and lag motions, the body pitch and roll motions, and rotor dynamic inflow.

Testing was conducted in both hover and forward flight. A sample of the predicted and measured hover results is shown in figure 25 for a blade collective pitch of eight degrees. The predicted and experimental lead-lag frequencies are seen to be in good agreement. The regressing lag mode damping in the fixed-system is also well predicted. An unstable region is indicated near the regressing lag-roll coalescence rotor speed. Due to rotor stress level limitations, the test could not be carried out for rotor speeds above 650 rpm.

Figures 26 and 27 present analytical and experimental lead-lag damping results that show the effect of blade droop and pre-cone angles on the damping levels in forward flight. These wind-tunnel tests of a hingeless rotor configuration aided the further development of a satisfactory technique for aeromechanical stability testing at the TDT, as well as identifying an analysis that produced good correlation with experimental results.

1985

In the mid-1980s the emphasis of helicopter testing in the TDT changed once again to an area referred to as "advanced rotor design studies." Testing in this area has been continued up to the present time. These tests, like others previously discussed, have focused on improving rotor performance and reducing vibratory loads. The first of these tests was conducted in 1985 in support of a U.S. Army program that was intended to upgrade the UH-60 Blackhawk helicopter. This planned upgrade involved the design and qualification of new main-rotor blades to improve aircraft performance. In support of this effort, the aerodynamic characteristics (airfoil section, planform, twist, and solidity) of an advanced rotor blade were analytically designed at the U.S. Army Aerostructures Directorate, located at Langley Research Center, using the approach described in reference 68. The advanced blade planform geometry is shown in figure 28. The baseline blades for this investigation were models of the UH-60A rotor (fig. 29) that were used in the conformable rotor studies conducted in 1979. Both the baseline and advanced blade sets were nominally 1/6-size and aeroelastically scaled. The tests were conducted to reduce the risk of full-scale development by providing comparative data between a candidate advanced rotor design and the baseline rotor.

The purpose of this test (ref. 69-70) was to compare the performance and loads characteristics of the baseline and advanced rotor systems. Therefore, each rotor was evaluated at the same nominal test conditions defined by advance ratio, hover tip Mach number, and rotor lift and drag coefficients. The range of advance ratio covered in these tests was from 0.0 to 0.40. Some illustrative rotor performance and fixed-system vibratory loads results are shown in figures 30 and 31, respectively. These results are for a nominal design condition used by the Army, namely, 4000 feet geometric altitude and 95 deg F ambient temperature. The data in figure 30 show the improvement in performance provided by the advanced rotor throughout the speed range for two simulated gross weight conditions. Similar results were obtained for the other simulated gross weight conditions tested. Although the data are not presented here, the advanced rotor also showed performance improvements in hover. Figure 31 shows the 4-per-rev fixed-system vertical loads produced by the baseline and advanced rotor. The data show that the 4-per-rev fixed system loads produced by the advanced rotor are higher than those produced by the baseline rotor throughout the speed range. This trend was consistent for all gross weight conditions tested.

1987

The first helicopter rotor test using a bearingless rotor hub configuration was conducted in the TDT in 1987. The objective of the test described in reference 71 was to investigate the use of a Bell Helicopter Textron rotor structural tailoring concept known as rotor nodalization (refs. 72 - 73) in conjunction with advanced blade aerodynamics and to evaluate rotor blade aerodynamic design methodologies. A nodalized rotor design is intended to cancel the inertial and aerodynamic loads at the rotor hub at a frequency equal to the blade passage frequency (ref. 72). This test was a part of ongoing programs of the U.S. Army and NASA to improve the aerodynamic performance of helicopters and to reduce helicopter vibrations. The model rotor hub used in this investigation was a 1/5-size, four-bladed bearingless hub (fig. 32). Rotor flap, lag, and pitch motions are accommodated by flexural arms that are constructed of fiberglass, extend outward from the center of rotation, and are pre-coned 2.75 deg upward at their inboard end. Five sets of 1/5-size model blades designed to represent those of an intermediate-weight civil helicopter were used during these tests. Two of the five blade sets were Froude scaled for testing in air at standard density. The remaining three blade sets were Mach scaled for testing in R-12 at a density of 0.006 slugs/ft^3, and included a rectangular planform blade and two ta-

pered planform blades. The Froude scale blades tested in air were used to evaluate structural tailoring, while the blades tested in R-12 were used to evaluate the use of structural tailoring in conjunction with advanced blade aerodynamics. The planforms of the Froude scaled blade sets are shown in figure 33 and the planforms of the Mach scaled blades are shown in figure 34.

Each blade set was evaluated at the same nominal test conditions defined by advance ratio, rotor rpm, and rotor lift and drag. The rotor rpm used for all of the test points was 780 rpm. The values of rotor lift and drag used for all five blade sets were chosen to represent an aircraft of 7850 lbs gross weight with an equivalent parasite area of 20.65 ft^2 operating at 4000 ft geometric altitude and an ambient temperature of 95 deg F. The range of advance ratio covered in this test was from 0.06 to 0.35, which includes the region from transition to high-speed forward flight. Reference 71 documents this test and presents a tabulation of the data pertaining to the evaluation of the structural tailoring concept. These data consist of fixed-system and rotating system vibratory loads measured during the test. No results are presented in reference 71 pertaining to an evaluation of the aerodynamic design methodologies used to create the model rotor blades used in the test.

1988

At the conclusion of the 1987 test, it was determined that insufficient rotor performance data were acquired for the evaluation of the aerodynamic design methodologies. To obtain the required data a test was conducted in 1988 using the Mach scaled model rotor blade sets (fig. 34) tested in 1987. Because structural tailoring was not an issue during this test, the rotor performance data were obtained using an articulated rotor hub instead of the bearingless rotor hub used during the 1987 test. The test was conducted in R-12 and data were acquired in hover and forward flight at advance ratios from 0.10 to 0.45.

Sample hover and forward flight performance results from this test are shown in figures 35 and 36. The hover data presented in figure 35, for a condition of 4000 ft geometric altitude and an ambient temperature of 95 deg F, show that the tapered planform blade required less rotor torque coefficient over the entire range of rotor lift coefficient than did the rectangular planform blade. Similar results not shown here, for the tapered and rectangular planform blades were also obtained at a condition representative of sea level standard conditions. Figure 36 shows the rotor torque coefficient required versus advance ratio for both the tapered and rectangular planform blades. These data were obtained at rotor lift and drag coefficients representative of a 7850 lb gross weight aircraft with an equivalent parasite area of 20.65 ft^2 operating at sea level standard conditions. The data in figure 36 show little difference in rotor torque required between the two blade configurations except at advance ratios of 0.15 and 0.35. Although not shown here, it was also determined that as advance ratio was increased to 0.40 and 0.425 the rectangular planform blades attained higher lift and propulsive force coefficients than the tapered blades before encountering high blade loads. However, the tapered planform blades were designed for a maximum advance ratio of 0.36. It should be noted that at this time none of these results have been documented in a formal report.

In 1988, another test of the advanced rotor design developed and tested in 1985 was conducted to investigate a passive method of reducing the 4-per-rev fixed-system vibratory loads. The passive method makes use of concentrated non-structural masses to "tune" the blade, similar to the approach used in reference 74, so that vibratory shear loads transmitted to the fixed-system are reduced. The model blades were aerodynamically identical to the previously tested advanced blades, and were comprised of two major components: an airfoil glove, which had an internal channel centered about its quarter chord; and a steel spar that could be inserted in the channel (fig. 37). The steel spar had 13 cutouts located every 5% of span beginning at the 30% radial station. A tungsten or steel mass could be mounted in any of the cutouts on the steel spar that was then mated with the airfoil glove to form the complete blade assembly. Testing was conducted at advance ratios up to 0.35 at several rotor thrust levels while maintaining constant rotor rotational speed. A sample of the results obtained during these tests is shown in figure 38. Each data point represents the effect of adding a mass equivalent to approximately 10%

of the total blade mass at the radial location specified by the abscissa. The results show the 4-per-rev vertical fixed-system loads for a simulated 1g thrust condition (Thrust = 285 lbs model scale) at an advance ratio of 0.35. The results may be compared directly with the baseline condition, in which no insertable masses were installed in the blades, represented by the horizontal line in figure 38. A more thorough description of this research as well as additional results may be found in references 75 and 76.

1989

A test conducted in 1989, while not dealing strictly with "advanced rotor designs", evaluated an "advanced" method of addressing rotor blade vortex interaction (BVI) noise. Impulsive BVI noise, due to blade interaction with shed vortices of preceding blades, has been a major focus of rotorcraft acoustics research for a number of years. One noise reduction concept (ref. 77) purported that decreases in blade lift and/or vortex strength at the blade-vortex encounters should reduce the intensity of the interactions and thus the noise produced by the interaction. This idea involves the application of higher harmonic pitch (HHP) to the rotor blades to modify the strengths of the shed vortices and alter the location of the blade vortex interactions (fig. 39). The amplitude and phase of such HHP inputs are important since the strongest BVI occurrences tend to be located within a limited rotor azimuth angle range roughly between 45 deg and 75 deg (ref. 78).

The test was conducted using an articulated, 4-bladed rotor with rectangular blades having NACA 0012 airfoil sections. Because this was the first acoustics test to be conducted in an R-12 test medium, detail flow-noise calibrations were performed in the TDT for both air and R-12. The results reinforced the conclusions that acoustic pressures are readily scaled between test media. Microphone sensitivity questions for R-12 were also addressed by conducting calibrations prior to conducting the wind-tunnel test. The results of these calibrations showed that the microphone response at specific harmonics of blade passage frequency is the same whether the tests were to be conducted in air or R-12. A total of 12 microphones were used for this test, and because of the reverberant character of the TDT test section it was decided not to attempt directivity measurements but to determine only sound power spectra.

Open-loop HHP inputs were superimposed on top of the rotor trim values of collective and cyclic pitch for a broad range of rotor operating conditions while maintaining a constant rotor thrust coefficient. The HHP inputs included 4-per-rev collective pitch inputs, as well as inputs developed to simulate individual blade control. It was found that the application of the HHP inputs could increase or decrease the intensity of the BVI noise depending on the amplitude and phase of the inputs. A sample of the results obtained during these tests is presented in figure 40, showing the potential of using HHP inputs for reducing BVI noise levels. A complete documentation of this effort is presented in reference 79.

1992

Between 1990 and 1992 there were no rotorcraft tests conducted in the TDT because of a moratorium on the use of R-12 due to environmental concerns. When the moratorium was lifted in 1992, a test was conducted to evaluate two advanced rotor blade design concepts that were under development prior to the moratorium. The first concept involved the use of paddle-type tip technology (refs. 80-83) that could be used in future U.S. advanced rotor designs. During this test, data were obtained, using a 4-bladed articulated hub, for both a baseline main-rotor blade and a main-rotor blade with a paddle-type tip. The main-rotor blade with the paddle-type tip has the same planform as that developed under the British Experimental Rotor Program (BERP) but uses different airfoils, and so is referred to as a "BERP-type" blade. The intent of using these two blade sets was to evaluate the effect of the BERP planform geometry on performance and loads, not to conduct an exhaustive study of the BERP concept. The baseline and BERP-type blades (fig. 41) were compared with regard to rotor performance, oscillatory pitch-link loads, and 4-per-rev vertical fixed-system loads. Data were obtained in hover and forward flight over a nominal range of advance ratios from 0.15 to 0.425. Sample performance and loads results are presented in figures 42-45. Results from this test indicate that the BERP-type blade offers no performance improvements in

either hover or forward flight, when compared to the baseline rotor. Pitch link oscillatory loads for the BERP-type blade were found to be higher than for the baseline blade, whereas 4-per-rev vertical fixed-system loads are generally lower. A complete documentation of this test is presented in reference 84.

The second concept evaluated during the 1992 test was a configuration that used slotted airfoils in the rotor blade tip region (85% - 100% radius). This configuration, known as the HIMARCS - I (first generation HIgh Maneuverability and Agility Rotor and Control System) was of interest because of the U.S. Army's need for increased helicopter mission effectiveness and improved safety and survivability. The test was conducted using a 4-bladed articulated hub. Four rotor configurations were tested in forward flight at advance ratios from 0.15 to 0.45 and in hover in ground effect. The rotor hover tip Mach number was 0.627, which is representative of a design point of 4000 ft. geometric altitude and an ambient temperature of 95 deg F. The baseline rotor configuration had a conventional single-element airfoil in the tip region. A second rotor configuration had a forward-slotted airfoil with a -6 deg slat, a third configuration had a forward-slotted airfoil with a -10 deg slat, and a fourth configuration had an aft-slotted airfoil with a 3 deg flap (trailing edge down). These rotor blade configurations are shown in figure 46. Sample performance and normalized loads results from this test are presented in figures 47-50 and indicate that the -6 deg slat configuration offers some performance and loads benefits over the other three configurations at higher rotor lift coefficients. A complete documentation of this test is presented in reference 85.

1995

During the moratorium on the use of R-12 that was imposed between 1990 and 1992 no new research efforts for model hardware development were initiated. Further, declining budgets permitted little latitude for the development of new model hardware. For this reason, in 1995 an in-house model rotor development program was started. The purpose of this program was to determine if elementary, basic research rotor blades could be designed by personnel at the TDT and built in the model shops at Langley. These blades were designed to acquire loads data for correlation with analyses. The design utilized for these blades involved uniform mass and stiffness distributions with values representative of aeroelastically scaled model blades typically tested in heavy gas at the TDT. The blades were rectangular in planform, used NACA 0012 airfoils, and were untwisted. Blade construction used an aluminum spar as the primary load carrying member, foam for the airfoil shape, and a fiberglass outer skin. The aluminum spar was particularly attractive for the attachment of strain-gages for the measurement of blade bending moments and torsion moments. These blades were tested in October 1995 on a 4-bladed articulated hub in both air and R-134a using the ARES testbed. Data were acquired at advance ratios up to 0.35 at moderate rotor lift coefficients before encountering stall problems attributable to the untwisted design. Additional measurements were made in air at higher advance ratios and rotor lift coefficients specifically for the purpose of acquiring rotor stall data for correlation with analyses. While none of these research results have been published, the entire effort was considered useful due to the experience gained in the design and fabrication of aeroelastically scaled model blades. This effort also helped to bridge the gap between the end of testing with R-12 and the initiation of testing in R-134a.

1999

Recent analytical and experimental investigations have indicated that piezoelectric active fiber composites (AFC) imbedded in composite rotor blade structures may be capable of meeting the performance requirements necessary for a useful individual blade control (IBC) system (refs. 86-92). The use of rotor IBC is of interest because active control concepts can be used to address multiple helicopter problem areas such as vibrations, acoustics, and performance. In 1999, a hover test of a prototype active twist rotor (ATR) blade was conducted in the TDT. The ATR blade design employs embedded piezoelectric AFC plies to generate dynamic blade twisting. Mathematical models indicate that from one to two degrees of twisting amplitude over a relatively wide frequency bandwidth is possible using the high strain actuation capabilities of AFC plies. Such

levels of twist actuation authority are also possible with only modest increases in blade weight and low levels of power consumption. For these reasons, AFC twist actuated helicopter rotor systems have become an important area of research at the TDT.

Investigation of the potential of AFC rotors was initiated with two ATR mathematical modeling efforts. The first of these modeling efforts was performed in collaboration with researchers at the University of Colorado and focused on the development of a simple mathematical model for helicopter rotor blades incorporating active fiber composite plies. The resulting computer implementation of this mathematical model is the Piezoelectric Twist Rotor Analysis (PETRA) (ref. 88), which is ideally suited for conceptual active twist rotor design and optimization studies. The second mathematical modeling effort used the second generation of the Comprehensive Analytical Model of Rotorcraft Aerodynamics and Dynamics (CAMRAD-II) (ref. 93) code. The use of the CAMRAD-II code allowed detailed active twist rotor numerical studies to be conducted using a state-of-the-art rotorcraft aerodynamics and dynamics computer analysis.

The model prototype ATR blade was dynamically scaled and was designed and constructed in a cooperative effort with the Massachusetts Institute of Technology Active Materials and Structures Laboratory (refs. 91-92). The prototype ATR blade utilizes low weight active fiber composites embedded along the blade, which under appropriate electric fields produce controllable twisting in the blade. The prototype ATR blade was tested using a four-bladed articulated hub with three passive structure blades, identical in twist and planform to the prototype ATR blade, mounted on the hub for balance. This rotor configuration was tested at 688 rpm, at collective pitch settings of 0 and 8 degrees in both air and R-134a. Blade actuation was accomplished by sine-dwell signals at a fixed 1kV amplitude. Peak torsional magnitudes were extracted from FFTs of blade strain gage signal time histories. The torsional load amplitude induced by the piezoelectric actuators was found to be essentially the same for both collective pitch values. This indicates that blade actuation frequency response remains relatively unaffected by rotor thrust conditions; a trend predicted in pretest analytical studies.

Preliminary results of the prototype ATR blade hover test indicate that peak twist magnitudes of about one degree were attainable at full design rotor speed, test medium density, and collective pitch. This level of twist actuation performance is sufficient to produce 70% reductions in fixed-system vibration amplitudes based on CAMRAD-II active twist simulation studies (ref. 92). Endurance of the active fiber composite actuator plies was also found to be acceptable, with only one actuator electrical failure, out of 19 original actuators, encountered over the course of the testing. A set of four model ATR blades, based on the prototype blade design, has been fabricated for forward flight testing.

An additional test, also conducted in 1999, was intended to acquire data for correlation with analysis. Throughout the descriptions of the helicopter tests conducted in the TDT there has been the recurring theme of reducing fixed-system vibrations. The primary contributor to helicopter vibration is the main rotor. Accurate prediction of main-rotor vibratory loads enables researchers to develop an understanding of the roles played by various design parameters with regard to helicopter vibration (refs. 94 - 95). The prediction of rotor vibratory loads has produced less than satisfactory results over the years. References 96-98 indicate that throughout the 1970s and 1980s the state-of-the-art of rotor loads analyses made successful prediction of rotor loads difficult, particularly for the higher frequency loads that are of primary interest when addressing helicopter vibrations. Reference 99 indicates that the prediction capability of current analyses has not improved greatly from that of 1970's and 1980's technology. The search for analyses that can accurately predict rotor vibratory loads will continue until an analysis is identified that can give a designer confidence that the goal of lower vibration can be met before committing to a costly fabrication process. To aid in the identification of such an analysis, a test was conducted in the TDT to acquire data for comparison with the CAMRAD-II computer code to evaluate the capability of this code to predict rotor performance and vibratory loads.

The model blades used in this test were 0.16-size, aeroelastically scaled representations of advanced main-rotor blades intended as an upgrade for Sikorsky S-61 helicopters used in commercial applications. The blades incorporate a swept, tapered tip and RC-series airfoils designed at NASA Langley Research Center (refs. 100 - 101). Figure 51 shows a planform view of the model blades. Unlike the helicopter tests conducted in previous years at the TDT, this test was conducted in the new R-134a test medium using a 5-bladed rotor system. Rotor performance and loads data were acquired in hover and forward flight up to an advance ratio of 0.375. The data were obtained by trimming the model to rotor lift and drag coefficients representative of a 20,000 lb S-61 helicopter operating at sea level standard conditions. The model was operated at a constant rotor speed that produced the nominal required tip Mach number. Experimental data were compared to CAMRAD-II results obtained at the same conditions. Samples of the comparison between experimental and analytical results are shown in figures 52-53. Figure 52 presents the rotor forward flight performance comparison in terms of rotor torque coefficient required versus advance ratio. It should be noted that experimental and analytical results were obtained at advance ratios beyond the capabilities of the full-scale S-61. This was done in order to obtain information on the advanced S-61 blade design over as wide a range of test conditions as possible. Figure 52 shows that the CAMRAD-II results indicate less rotor torque required than the experimental results at advance ratios above 0.125. The reduced rotor torque coefficient indicated by the analysis can be attributed to the use of airfoil data obtained at full-scale values of Reynolds number, while the experimental results were obtained at less than full-scale Reynolds numbers even though a heavy gas test medium was utilized. The analytical results in figure 52 below an advance ratio of 0.125 are attributed to the free-wake model in the analysis not being fully representative of the experimental environment. Figure 53 shows a comparison of the mean flapwise and chordwise blade bending moments and the mean blade torsional moments versus blade radial station at an advance ratio of 0.25. The results in figure 53 indicate the analysis captures the mean bending moment trends along the blade span at this advance ratio, but is not as successful at predicting the mean blade torsional moments. Results not presented here indicate the analysis, using the free wake model, does a good job of predicting the 5-per-rev fixed-system vibratory loads up to an advance ratio of 0.15, but above that advance ratio the correlation between experimental and analytical results is poor. Reduction and analysis of the experimental results from this test will continue along with continued correlation of the experimental and analytical results.

2000

The most recent TDT test involved the active twist rotor (ATR) concept (ref. 102). This test was a cooperative effort among the NASA Langley Research Center, the Army Research Laboratory, and the MIT Active Materials and Structures Laboratory. The ATR was a four-bladed, aeroelastically-scaled model rotor designed and fabricated for testing in the TDT heavy gas test medium. The test was conducted to assess the impact of active blade twist on fixed- and rotating-system vibratory loads in forward flight. The active twist control was found to have a pronounced effect on all system loads and was shown to generally offer reductions in fixed-system loads of 60% to 95%, depending upon flight condition, with 1.1ºto 1.4ºof dynamic blade twist observed. Additional tests of the ATR concept are planned.

Helicopter Analysis Development

Helicopter analytical research at AB/TDT was initiated in 1973 and since that time has addressed a variety of problems and issues, either in support of experimental work being conducted in the TDT or in support of other closely related work being conducted in the AB. These activities have included theoretical investigations, analytical studies, and development of computational algorithms. A summary of this work is given below.

Ground Resonance

The first helicopter-related analytical effort to be conducted at AB/TDT involved the application of Floquet theory (ref. 103) to an analysis of helicopter mechanical instability, or ground resonance (refs. 104-105). This effort was undertaken to ad-

dress the Army requirement that a helicopter be free of ground resonance even with one blade lag damper inoperative. The problem of ground resonance had been recognized and understood for many years, with the analysis by Coleman and Feingold (ref. 106) being recognized as the standard reference on this phenomenon. The analysis of reference 106, and others, defines the ground resonance problem as being due primarily to a coupling of the rotor blade inplane motion with the rigid body degrees of freedom of a helicopter on its landing gear. All of the ground resonance analyses in use in the early 1970s assumed that all blades had identical properties. This is a reasonable assumption under ordinary circumstances, but the Army requirement for stability with one lag damper inoperative had a serious impact on classical methods of ground resonance analysis. At the time the subject effort was undertaken there was no published method available for treating a case where each of the blades was permitted to have different properties, and so the dilemma was in trying to satisfy a requirement with an analysis in which one of the basic assumptions was violated.

Two methods were available to address the problem of an inoperative blade lag damper. The first method involved a smearing technique that redistributed lag damping over all blades after one damper is considered to be inoperative. With this approach, the system being analyzed is quite different than the actual situation of having one lag damper inoperative. The second method used involves reformatting the equations of motion to allow differing blade characteristics and obtaining the stability characteristics from a time history integration of the resulting equations. The drawback to this method is that the interpretation of system stability characteristics from time history calculations is often difficult and open to question (refs. 104-105). The use of Floquet theory was introduced as an alternate procedure for directly determining the stability characteristics of rotor systems with one blade lag damper inoperative.

References 104-105 present results from the use of the smearing technique, time history integration, and Floquet theory to determine the ground resonance characteristics of a sample helicopter configuration with and without an inoperative blade lag damper. It was determined that the smearing technique produced unconservative results and the use of time history integration could lead to erroneous conclusions relative to the determination of system stability. The use of Floquet theory indicated that using additional blade lag damping would have no effect on the region of instability when one blade lag damper is inoperative (fig. 54). An effective and viable means of addressing the case of an inoperative blade lag damper was found to involve variations in the rotor hub lateral and longitudinal stiffness and damping as represented by the results in figures 55 and 56. The Floquet theory method was found to be an effective analytical tool for directly determining stability boundaries and thus eliminating uncertainties associated with other solution methods.

Blade Modes Program

An existing analysis and computer program (ref. 107) used for calculating the rotating natural frequencies and mode shapes of the model helicopter rotor blades tested at the TDT was refined to improve its accuracy and versatility. The program is based on the Holzer-Myklestad approach adapted for rotating beams and represents a rotor blade as a series of lumped masses connected by stiffness elements. Elastic and inertia coupling between vertical, horizontal, and torsional deflections are included in the analysis. Spanwise variations in structural stiffness, mass, blade twist, rotary inertia, and center of gravity and shear center offsets from the blade pitch axis may be input. A unique feature of this program is the ability to include the effects of support system impedance on the blade natural frequencies and mode shapes. This is a capability that is not generally found in computer programs for computing the modes of rotating blades.

Because of the uniqueness of the program, considerable use was made of it at the TDT. This experience identified several errors and limitations in the program, and in anticipation of future needs and possible expansion of its capabilities the analysis was improved and all known errors corrected. Changes to the program included a different iteration scheme for the determination of natural frequencies, an improved technique for

computing mode shapes, and a new technique for identifying the predominant motion (flap, lag, or torsion) of the computed coupled modes. Changes were also made to the program to reduce the size of the source program and core requirements needed for execution, increase run-time efficiency, and expand the program capabilities by increasing the number of blade mass stations and rotor rotational speeds allowed. Changes were also made to the recursion equations that relate the state vectors at adjacent stations, and these changes were substantiated by the work reported in reference 108.

The analysis resulting from these changes was considerably different from the original version (ref. 107). The accuracy of the new program was demonstrated by correlating predicted results with both exact solutions for classical problems and with experimental data. The results of these correlations and a documentation of the revised computer program are presented in reference 109.

Rotor Blade Aeroelasticity and Dynamics

Throughout the 1970s, a rather substantial effort in the rotorcraft research community was directed at deriving nonlinear equations of motion for calculating the aeroelastic stability of rotor blades in forward flight and at conducting analytical studies to identify and assess the importance of parameters governing blade stability. Both articulated rotor blades that were treated as rigid, centrally or offset-hinged, spring-restrained beams, and hingeless rotor blades that were treated as flexible, twisted cantilevered beams were the subjects of these studies. AB researchers were also active in this area, particularly during 1975-78. A summary of their work is given below.

Stability of Rigid Articulated Blades: The flap-lag stability of rigid articulated rotor blades in forward flight was studied by AB researchers during 1975-76 (refs. 110-112). Reference 110 addressed the problem of flap-lag stability of both helicopters and wind turbines using a unified aerodynamic formulation that included the velocity gradient experienced by a wind turbine operating in the earth's boundary layer. The paper derived the governing nonlinear equations of motion for an individual blade in a coordinate system rotating with the blade. These equations were then reduced to linear equations by the usual practice of perturbing them about a steady-state equilibrium position and discarding all perturbation terms of second degree or higher. The resulting linear equations, which contain periodic coefficients, were then transformed into a nonrotating (space-fixed) coordinate system using the method of multiblade coordinates (ref. 113). Stability of systems described by such equations is typically assessed by examining the eigenvalues of the Floquet transition matrix (FTM) that is obtained by numerically integrating the state equations over one period using the identity matrix as the initial state (ref. 103). However, often useful predictions of stability can be made by employing the simpler equations obtained by dropping the periodic terms in the multiblade equations (ref. 114). The motivation for this "constant coefficient approximation" is the fact that the multiblade coordinate transformation leads to a set of fixed-system equations in which the periodic terms in the blade equations written in the rotating coordinate system are transformed into constant and higher harmonic terms. Thus, dropping the periodic terms that remain after this transformation leads to a set of differential equations with constant coefficients that retain some of the periodic effects of the original equations. System stability can then be determined by examining the eigenvalues of the (constant) state matrix obtained by writing these equations of motion in first order form in the usual manner. Both methods of stability analysis were employed in the studies reported in reference 110 and the results compared to establish the range of applicability of the approximate equations. Calculation of the FTMs for these studies was based on an algorithm (ref. 115) that was developed for use in conjunction with the work of reference 104 that allowed the matrices to be determined with a single integration pass through the N equations of motion rather than N passes as had been customary. A comparison of the stability boundaries obtained from a Floquet analysis of the multiblade equations containing all the periodic terms with the corresponding boundaries obtained from the approximate constant coefficient equations indicated that a constant coefficient approximation could be satisfactory for advance ratios up to about 0.4, depending on the particular system pa-

rameters. Some results from reference 110 for the special case of a flapping blade with and without kinematic pitch-flap coupling (δ_3) are shown in figure 57.

References 111-112 present a critical examination of the analytical basis for deriving the nonlinear equations of motion for flap-lag stability of a rigid articulated rotor blade in forward flight. This examination was motivated by differences that were observed in the linear perturbation equations obtained from the nonlinear equations derived by AB researchers and those found in the literature. The differences that were identified involved aerodynamic pitch-lag and pitch-flap coupling terms associated with blade steady-state flapping and lagging, respectively. A careful comparative examination of the derivation of the various sets of equations of motion revealed that the differences were a consequence of the physical arrangement (position) of the flapping and lagging hinges; that is, whether the lag hinge is outboard of the flap hinge and thus flaps with the blade (a flap-lag hinge sequence) or whether the flap hinge is outboard of the lag hinge and thus lags with the blade (a lag-flap hinge sequence). Both kinematic conditions are also possible for the case of coincident hinges. For a rigid hinged blade or a hingeless blade treated by virtual hinges, the appearance of these coupling terms depends on the particular order in which the flap and lag rotational transformations are imposed while deriving the nonlinear equations of motion. Equations then in the literature dealing with the problem of flap-lag stability of rigid articulated blades dealt with one or the other of the hinge sequences, and then usually only implicitly. The differences in the equations of motion that are associated with the hinge sequence and the role of that hinge sequence on flap-lag stability were not clearly recognized or addressed in the literature. The purpose of the subject investigation was to explain the differences by deriving in detail the flap-lag equations of motion of a rigid blade in forward flight assuming both flap-lag and lag-flap hinge sequences, and to examine the implications of the differences on blade flap-lag stability in both hover and forward flight.

The implications of the differences on stability for a range of values of flap and lag frequencies were examined in references 111-112 for the two hinge sequences depicted in figure 58. Based on these studies, it was shown that the subject coupling terms have varying degrees of influence on flap-lag stability in both hover and forward flight, depending on the system parameters. In particular, the pitch-lag coupling terms associated with a blade having a flap-lag hinge sequence were found to have a marked influence on stability. Some illustrative results for hover and forward flight are given in figures 59 and 60, respectively, where the calculated stability boundaries are plotted as a function of the blade rotating per-rev lag and flap frequencies. Combinations of blade flapping and lagging frequencies leading to instability are given by the areas inside the boundaries. It is clear that the stability of the system is different depending on which hinge sequence is employed and that the magnitude of the difference depends on the particular combination of flap and lag frequencies that are selected. These results indicated that the equations of motion used to analyze an articulated rotor must be based on a derivation in which the blade rotational transformations imposed in deriving the underlying nonlinear equations of motion are consistent with the physical arrangement of the hinges.

Nonlinear Equations for Flexible Hingeless Blades: The effect of hinge sequence on the equations of motion and stability of a rigid articulated rotor blade noted in reference 111 led those authors to speculate that there might be differences in the aeroelastic equations of flexible rotor blades depending on the order in which the rotational transformations associated with blade bending and torsion are imposed when deriving the equations. A preliminary investigation of this possibility was made in reference 111 where attention was limited to an inspection of the blade bending and torsional curvatures and the aerodynamic velocity components for two rotational transformation sequences. Based on the differences noted there, it was concluded that differences would also occur in the resulting governing aeroelastic equations of motion for a flexible blade. The preliminary findings of reference 111 with respect to the implications of the rotational transformation sequence on the resulting form of the blade equations of motion prompted those authors to conduct (1976-78) a careful examination (refs. 116-118) of the theo-

retical and analytical foundations on which nonlinear aeroelastic equations for flexible rotor blades were being derived at that time. A few comments on the role of rotational transformations in deriving blade equations of motion are given below before summarizing the contributions of references 116-118.

The need for considering the rotational transformation sequence arises from the need to specify the position vector of an arbitrary point on the blade in a deformed configuration when deriving the equations of motion. This position vector is obtained by performing a sequence of rotations and translations from inertial axes fixed in space to axes fixed at an arbitrary point on the deformed blade. In this case, rotation of coordinate axes corresponds to matrix multiplication and translation of coordinate axes corresponds to matrix addition. The sequence in which the rotations of a blade section due to flapwise bending, edgewise bending, and torsional deformations are imposed is of importance here because of the nonlinear nature of the governing equations of motion. The angles of rotation associated with the deformations must be treated as finite and the transformation matrices associated with the individual rotations are not commutative. In the case of a rigid articulated blade, the physical arrangement of the hinges dictates the order in which the component rotations must be imposed while specifying the position vector. However, for a flexible hingeless blade, the order in which the individual rotations are imposed is a prerogative of the analyst. Out of the six possible rotational transformation sequences that can be imposed, the lag-flap-pitch sequence was the basis for most of the hingeless rotor blade equations appearing in the literature at the time of the subject investigation, although no rationale for such preferential treatment was given.

Reference 116 summarizes the results of several preliminary studies that were made in conjunction with the preparatory derivation of the nonlinear equations of motion for the simpler case of transverse bending and extension of a rotating beam. These special-case equations (no torsion and no aerodynamics) were independent of the rotational transformation sequence. The studies made with these equations were intended to clarify the role of the geometric nonlinear theory of elasticity (ref. 119) in the derivation of the equations of motion for rotating beams, and to evaluate the analytical implications of explicitly considering radial foreshortening of the elastic axis due to bending by including its effect in the assumed axial displacement field when deriving the equations of motion (ref. 120). To this end, reference 116 compared and discussed the popular approaches found in the literature for developing the linear and nonlinear equations of motion for a rotating beam. This study demonstrated that all the proper approaches used the geometric nonlinear theory of elasticity, either explicitly or implicitly. Indeed, recourse had to be made to geometric nonlinearity even in formulating the linear equations of a rotating beam. These findings had not been generally recognized in the literature at that time. Reference 116 also derived the title equations by a variational (energy) approach in which the component of beam radial displacement associated with foreshortening of the elastic axis due to bending (a second-degree nonlinear effect) is included as a term separate from the component due to elastic axial deformation in the assumed axial displacement field in the expression for the position vector to a generic point on the deformed blade. The explicit use of foreshortening in this way was introduced in reference 120 as an alternative to the artifice of the effective applied load concept for deriving linear bending equations for radial beams on spin-stabilized satellites. The implications of explicitly accounting for foreshortening in this manner when deriving the linear and nonlinear flap-lag-axial equations of motion of a rotating beam were discussed in reference 116. For example, the explicit use of foreshortening was found to enable a derivation in which the retention of second-degree nonlinear terms in the kinetic and potential energy expressions leads to linear equations, retention of third-degree nonlinear terms leads to second-degree nonlinear equations, and so forth. It was also found that the assumption of inextensibility (an expedient usually employed to eliminate the axial equation of motion) could be made at any stage of the development of those equations. Conversely, special considerations are required in all phases of the derivation if foreshortening is not included in the assumed axial displacement field. Special considerations are also needed even if the analyst

chooses to employ a Newtonian approach to derive the equations by applying Newton's second law to the beam in a deformed configuration.

Reference 117 addressed the problem of deriving the second-degree nonlinear rotational transformation matrix between the blade-fixed coordinates of the deformed and undeformed blade and the corresponding expressions for the bending and torsional curvatures of a twisted helicopter rotor blade undergoing combined flapwise bending, chordwise bending, torsion, and extension. Two of the six possible rotational transformation sequences were examined: flap-lag-pitch and lag-flap-pitch. The general nonlinear expressions were systematically reduced to four levels of approximation by imposing various simplifying assumptions in the spirit of reference 119, and the implications of these assumptions with respect to the nonlinear theory of elasticity as applied to beams was pointed out. The nonlinear curvature expressions and transformation matrices of reference 117 were compared with corresponding results in the literature and a number of discrepancies identified. The reasons for these discrepancies are discussed. A by-product of the study of reference 117 was the resolution of a controversy that existed in the literature regarding whether, under the assumption of small strains, the uncoupled extensional frequency of a rotating beam increases or decreases with increasing rotational speed –it decreases.

The culmination of the subject examination was the derivation of the second-degree nonlinear aeroelastic equations of motion for the combined flapwise bending, chordwise bending, torsion, and extension of a twisted nonuniform rotor blade in forward flight using Hamilton's variational principle (ref. 118). A unique feature of the subject derivation was the explicit inclusion of a foreshortening term in the assumed axial displacement field for the blade. Because of the inherent geometric nonlinearity of the problem, the derivation was made with strict adherence to the fundamental principles of the geometric nonlinear theory of elasticity as discussed in reference 119. In particular, based on the results of reference 117, the derivation was based on the small deformation approximation in which the elongations and shears (and hence strains) are negligible compared to unity, with no restrictions on the rotations of the cross sections of the blade. The implications of applying a slender beam approximation in the derivation of the second-degree nonlinear equations of motion of a rotor blade are discussed and a mathematical ordering scheme that is consistent with the assumption of a slender beam is introduced. The blade aerodynamic loading is obtained from strip theory based on a quasi-steady approximation of two-dimensional, incompressible unsteady airfoil theory. The influence of the assumed rotational transformation sequence on the form of the resultant equations of motion was examined for two of the six possible rotational transformation sequences: flap-lag-pitch and lag-flap-pitch. The resulting sets of equations were found to differ in the nonlinear terms in both the aerodynamic and elastic terms, in contrast to the rigid articulated blade where there are differences only in the aerodynamic terms. The implications of these differences are discussed. A comparison of the subject equations with those found in the literature was also made. Several discrepancies in some nonlinear equations appearing in the literature at that time were identified and shown to be a consequence of a partial linearization of the resultant rotational transformation matrix between the coordinates of the deformed and undeformed blade or the use of an incorrect expression for the torsional curvature.

The methodology developed in connection with the rotor blade studies described in references 116-118 was later employed in the derivation of the aeroelastic equations of motion for the blades of both vertical-axis and horizontal-axis wind turbines (refs. 121-122). The insight gained from the rotor blade studies was also used to identify the proper procedure for applying unsteady airfoil theory to rotor blades (ref. 123). In particular, the correct relationship between the variables used in unsteady airfoil theory and the variables required to describe the more complex motion of a rotor blade was clarified.

Dynamics of Rotating Beams and Shafts

The dynamic behavior of rotating beams and shafts was addressed by AB researchers via both in-house and sponsored research during 1977-88 (refs. 124-131). This work is characterized by the

use and exploitation of integrating matrices as the basis for the numerical solution of the governing partial differential equations of motion. Integrating matrices were introduced in reference 132 as a numerically accurate method for solving the ordinary differential equations appearing in structural mechanics. An integrating matrix provides a means for numerically integrating a function that is expressed in terms of the values of the function at increments of the independent variable by a single matrix multiplication. The elements of the integrating matrix depend on the numerical procedure chosen to evaluate the integral (ref. 132 assumed a third-degree interpolating polynomial to approximate the function to be integrated). The method is applicable to the differential equations describing either the static or dynamic behavior of nonuniform beam-type structures. With regard to dynamic analyses, by expressing the equations of motion in matrix notation, utilizing the integrating matrix as an operator, and applying the boundary conditions, the spatial dependence is removed from the partial differential equations and the resulting ordinary differential equations can be cast into standard eigenvalue form for solution using standard eigensolution techniques. The method was more fully discussed in references 133-134 where the mechanics of its application to a rotating propeller blade were described. Integrating matrices based upon polynomials of degree one to seven were given in reference 133, which treated the linear equations for coupled inplane and out-of-plane bending. Reference 134 used the seventh-degree integrating matrix of reference 133 to solve the coupled bending-torsion equations but accounted for the nonlinear effects of blade steady-state twist induced by rotation on the torsion natural frequencies. Summaries of the contributions of references 124-131 are given below.

Reference 124 was intended to unify and extend the analytical basis of several aspects of the dynamic behavior of flexible rotating beams. To this end, the second-degree nonlinear equations of motion for the coupled flapwise bending, lagwise bending, and axial extension of an untwisted, torsionally rigid, nonuniform, rotating cantilever beam having an arbitrary angle of built-in coning or "precone" with the plane perpendicular to the axis of rotation were derived using Hamilton's variational principle. The derivation is characterized by the use of an axial displacement field that includes the second-degree nonlinear terms associated with radial foreshortening of the elastic axis due to bending, and the inclusion of both internal and external viscous damping. For zero and small values of the precone angle, the equations are applicable to beams that are oriented perpendicular to or nearly perpendicular to the axis of rotation, while for a precone angle of ninety degrees the equations are applicable to a rotating shaft. The nonlinear equations of motion were linearized by perturbing them about a steady-state equilibrium position in the usual manner. The resulting linear perturbation equations of motion and the nonlinear steady-state equilibrium equations were solved using the integrating matrix-based computer program used in reference 134, after the program was modified by its author for application to the present equations. The modified program was designated NLFLA (NonLinear Flap-Lag-Axial). The applicability of the subject equations of motion and method of solution for assessing the stability characteristics of rotating beams and shafts was demonstrated in reference 124 through a variety of numerical examples. Some illustrative results are given in figures 61 and 62. Figure 61 shows the effects of the steady-state deformation induced by rotation for non-zero values of the precone angle on the first flapwise and lagwise bending natural frequencies of a symmetric uniform beam. The effect of external viscous damping on the stability of a uniform asymmetric shaft for the particular case in which the internal damping is zero is given in figure 62, where the viscous damping coefficients have been non-dimensionalized by the product of the mass distribution and the first non-rotating flapping natural frequency.

The stability of a beam subjected to compressive centrifugal forces arising from steady rotation about an axis that does not pass through the clamped end of the beam (fig. 63) was analyzed in reference 125 to determine the critical rotational speeds for buckling in the inplane and out-of-plane directions. The linear differential equations of motion were solved numerically using program NLFLA, the only modification being the introduction of a "tension" expression appropriate to the subject configuration. The results (fig. 64) resolved several differences that appeared in the literature relating to the proper behavior of the criti-

cal rotational speed for buckling as the radius of rotation of the clamped end of the beam is reduced.

Historically, integrating matrices were derived for equal increments of the independent variable while expressing the function to be integrated as a polynomial in the form of Newton's forward-difference interpolation formula. However, many practical beam configurations have lengthwise variations in the sectional properties that require the use of an integrating matrix that can treat unequal increments. Reference 126 developed an analysis for computing integrating matrices for arbitrarily spaced grid points using either the customary interpolating polynomials or least-squares fit orthogonal polynomials. A subroutine for computing the new integrating matrices was written and incorporated into program NLFLA. The resulting program was designated NLFLAV (NonLinear Flap-Lag-Axial with Variable grid spacing). A companion differentiating matrix was developed later (ref. 127) to accommodate those cases in which the boundary conditions are such that both integrating and differentiating matrices are needed.

The integrating matrix as originally developed also required that the mass and stiffness distributions of the beam be at least piecewise continuous along its length. The important case in which one or more concentrated masses are located along the beam was thus excluded. Reference 128 describes the generalization of the integrating matrix method required to treat rotating beams with concentrated masses at arbitrary positions along their lengths. Reference 128 extended the integrating matrix method to treat the linear differential equations governing the flap, lag, or axial vibrations of rotating beams with concentrated masses at arbitrary positions along their lengths. It was found that the inclusion of concentrated masses leads to a standard eigenvalue problem of the same form as before, but with slightly modified matrices. A subroutine for computing the additional matrices was written and incorporated into a linear version of NLFLAV, which was designated LFLAVC (Linear Flap-Lag-Axial with Variable grid spacing and Concentrated masses). The analysis was applied to the problem of rotation induced buckling of a beam with discrete masses (ref. 129) (fig. 65). This study identified an error in the treatment of this problem in the literature concerning the behavior of the critical rotational speed for in-plane buckling as the radius of rotation of the clamped end of the beam is reduced.

The derivation of a two-dimensional integrating matrix for integrating a function of two variables whose values are known on a two-dimensional rectangular grid with arbitrary grid spacing allowed in one direction was given in reference 130. Reference 131 extended the work of references 126, 127 and 130 and developed a combined integrating/differentiating-matrix formulation for partial differential equations involving two space variables on a rectangular grid with nonuniform spacing in both directions. These are believed to be the first published attempts at deriving an integrating matrix for application to two-dimensional plate-like structures.

Finite Element Modeling of Rotor Blades

Several studies dealing with the development and validation of finite-element modeling techniques for application to metal and composite rotor blades were conducted by AB researchers during 1985-91 (refs. 135-145). The primary focus of these studies was on developing a beam theory applicable to composite rotor blades that are elastically tailored through an appropriate choice of ply fiber orientation and ply stacking sequence to exhibit extension-twist elastic coupling. Attention was directed to extension-twist coupling because of its potential for improving the aerodynamic performance of tiltrotor aircraft that are designed to operate at different rotor rotational speeds in the helicopter and airplane modes of flight (such as the XV-15 and the V-22). A conventional (untailored) blade designed for such aircraft has a twist distribution that produces acceptable performance in hover at the expense of a reduced propulsive efficiency in the airplane mode of flight. The hope was that elastic tailoring could be exploited to design an extension-twist-coupled blade that can utilize the change in centrifugal force associated with the change in rotor speed and produce a twist distribution that is more nearly optimum in the airplane mode of flight.

The derivation and validation of a tapered, p-version beam finite element suitable for dynamic applications were described in reference 135. A p-version element allows the user to select the order of the shape functions that relate the discrete nodal displacements of an element to the continuous displacements within the element, in contrast to h-version finite elements that use fixed-order shape functions to describe the displacement behavior of the element. In general, the higher the order of the shape functions, the more accurate the results. Increasing the order of the shape functions in a p-version model is analogous to increasing the number of elements for a comparable h-version model. However, for large finite-element models increasing the order of the shape functions in a p-version model is much easier than increasing the number of elements in an h-version model. The subject p-version beam element is implemented through a set of polynomial shape functions, where the lower-order shape functions are identical to the classical cubic and linear shape functions usually associated with a beam element and the higher-order shape functions are a hierarchical set of polynomials that are integrals of orthogonal polynomials. The taper in the element is represented by allowing the area moments of inertia to vary as quartic polynomials along the length of the beam and the cross-sectional area to vary as a quadratic polynomial. Reference 135 presents explicit expressions for the mass and stiffness matrices for the element for an arbitrary value of p. The element, which has been verified to be numerically stable with shape functions through 22^{nd} order, is capable of emulating four different types of beam elements: uniform h-version, uniform p-version, tapered h-version, and tapered p-version. Figure 66 presents results from reference 135 indicating the type of improvement in convergence that is realized by using tapered p- and h-version elements instead of uniform h-version elements to model a tapered cantilever beam. The figure shows the percent error in the calculated lowest (fundamental) bending, torsion, and axial frequencies versus the total number of degrees of freedom represented by the elements used to model the beam.

Reference 136 summarizes the results of an analytical study conducted in a preliminary assessment of a (then) new coupled-beam theory (ref. 146) for the structural analysis of thin-walled, single-cell composite rotor blades, including the effects of extension-twist elastic coupling achieved through unbalanced ply orientation. The analytical study employed the graphite-epoxy D-spar of a scale model rotor blade that was designed to demonstrate the coupling. The effectiveness of the new composite beam analysis was demonstrated in reference 136 through comparison of results obtained using the coupled-beam analysis with results obtained from an MSC/NASTRAN analysis using a detailed finite element model based on anisotropic plate elements. Computed deformations were compared for three scaled static load cases typical of those experienced by a rotor blade in flight. Some illustrative results for the case of a centrifugal force loading are shown in figure 67, where the twist computed using the coupled-beam analysis is compared with that obtained from a detailed finite element analysis. The comparative studies of reference 136 indicated that the coupled-beam analysis gives results with acceptable engineering accuracy. A byproduct of the study was the identification of a new and convenient approach for obtaining the extensional (EA), torsional (GJ), and bending (EI) engineering beam stiffnesses.

The investigation described in reference 137 was conducted to determine if the twist deformation required for the design of full-scale extension-twist-coupled tiltrotor blades could be achieved within material design limit loads, and to experimentally validate the coupled-beam analysis of reference 146 in predicting twist deformations for axially loaded extension-twist-coupled structures. The blade twists that would be required for optimum aerodynamic performance of the XV-15 and V-22 tiltrotor aircraft in both the hover and airplane modes of flight were estimated and used as a basis for comparison to the results of static torsion and axial tension tests conducted on extension-twist-coupled composite circular tubes assumed to be representative of the rotor blade spars of those aircraft. The tubes consisted of two different composite laminates ($[(+20/-70)_2]_S$ and $[(+40/+50)_2]_S$) and two different graphite/epoxy material systems (IM6/R6376 and T300/5208), for a total of four differently designed tube specimens. The tubes were 24 inches long, had an outside diameter of 1.64 inches, and a wall thickness

of .040 inches. The purpose of the tests was to correlate the measured twist deformation under combined axial and torsion loads with results from the coupled-beam analysis. Measured twist rates as a function of torque for the tubes having the $[(+20/-70)_2]_S$ lay-up are shown in figure 68 along with the corresponding analytical predictions. Figure 69 shows the analytical predictions and experimental results for the twist rate of the $[(+20/-70)_2]_S$ tubes as a function of axial load. The deviation between test and analysis at the higher loads in figure 69 is due to the effects of material nonlinearity that occur as the loading approaches the design limit loads. The coupled-beam analysis does not account for material nonlinearities. The experimental results showed that the twist deformations associated with axial loading of the $[(+20/-70)_2]_S$ ply specimens were sufficient to satisfy the blade twist rate requirements that were identified for optimum rotor aerodynamic performance of tiltrotor aircraft in both hover and airplane modes of flight.

Reference 138 describes the results of a design study aimed at identifying the improvements to tiltrotor aerodynamic performance in both hover and forward flight that might be possible through passive control of blade twist by the use of extension-twist structural coupling. The conventional metal blade design of the XV-15 tiltrotor research aircraft was chosen as the basis for the design study. To this end, the subject paper first determined the aerodynamically optimum linear twist distributions for the XV-15 in hover and forward flight and identified the performance gains that can be realized using these twists rather than those of the conventional blades. Based on these optimum twist distributions, three extension-twist-coupled blade designs were developed using the coupled-beam analysis of reference 146 (but extended to treat the case of a two-cell structure such as that used in the present investigation) and a laminate analysis (to determine the material strength margins of safety) integrated with an optimization algorithm (ref. 147). The blade structural model used in this design study is depicted in figure 70. The spar and airfoil skin were composed entirely of IM6/R6376 graphite/epoxy laminates. Design variables (see fig. 70) included the thicknesses of the D-spar laminates in the three sections of the blade, the thickness of the airfoil skin, the angle of the plies in the spar and in the skin, the length of the twisting section, the tip weight, and the nonstructural weight per unit length added to increase centrifugal loading. The designs were optimized for maximum twist deformation subject to material strength limits. Side constraints were imposed to ensure that realistic values of the design variables were maintained during the optimization process. The gains in aerodynamic performance associated with the final designs showed that the passive control of blade twist by the use of extension-twist structural coupling is a viable approach for the constraints considered, and has the potential for enhancing the performance of tiltrotor aircraft. The change in twist distribution with rotor rotational speed for one of the blade designs is presented in figure 71.

The study of reference 139 was aimed at developing an anisotropic beam finite element analysis, which can predict the static behavior of general thin-walled anisotropic beams with accuracy sufficient for use in the preliminary structural design of composite rotor blades. An anisotropic beam finite element was formulated based on an existing single-cell anisotropic beam theory (ref. 146) that included the effects of shear deformation but did not account for the full effects of cross-sectional warping. It is well known that the cross sections of thin-walled beams tend to warp out of plane when subjected to loads. This warping influences both the bending and torsion response of beams and its effects can be important in elastically-coupled composite blades. The manner of extending the subject analysis to treat multi-cell beams and to (approximately) account for the effects of warping are described. The accuracy of a finite element beam (FEB) analysis developed to implement the resulting beam element was assessed through comparison to results obtained from standard engineering beam theory and MSC/NASTRAN analysis of detailed plate models in which shear deformation and warping are inherently included, and through comparison to results obtained from a companion experimental study. The analytical assessments were based on analysis of 24-inch long cantilevered tubes of circular and square cross section having walls constructed of four plies of graphite/epoxy fabric in lay-ups with and without extension-twist coupling. Comparisons of computed global responses

and local axial and shear strains were made under axial, torsional, and bending loading conditions. Considerable insight was gained from these comparisons as to the importance of shear deformation and warping on global and local responses. Based on this insight, a simple method for modifying the FEB analysis to include the influences of torsion-related warping restraint was developed. The importance of bending-related warping effects on the bending solution of extension-twist-coupled beams was identified, and a formula was derived for the calculation of a shear stiffness reduction factor (dependent on ply orientation, stacking sequence, laminate thickness, and cross section geometry) that leads to considerably improved predictions of the bending behavior. On the experimental side, a set of static axial tests was performed for several different configurations of single-cell, thin-walled, extension-twist-coupled tubular beams to determine if strains and twist deformations could be accurately predicted by the FEB analysis. All specimens were constructed of graphite/epoxy woven cloth fabric, and used a symmetric material lay-up composed of a set of plies rotated off-axis to produce extension-twist coupling. Sixteen tubular test specimens were fabricated, all of which were 24 inches long with a four-ply lay-up of the material as assumed in the analytical studies mentioned earlier. Four different cross section shapes exhibiting warping were used: a square, a rectangle, a flattened ellipse, and a D-shape. Twist rate, principal fiber strain, and principal shear strain were measured for all the specimens. Prediction errors were generally less than one percent over most of the design load range of the specimens. The results for the D-shaped tube are compared with the results of the FEB analysis in figures 72-74. Analytical studies showed that the FEB analysis with warping included predicts global response to within 5% of values obtained from an MSC/NASTRAN analysis using a detailed plate model of the tubular beam structure.

Building on the results of references 135 and 139, reference 140 formulated a one-dimensional (beam) analysis to predict the rotating natural frequencies of highly-pretwisted elastically-coupled composite rotor blades. The formulation of reference 140 includes the nonclassical effects of transverse shear deformation and cross section warping and separates the geometrically nonlinear three-dimensional elasticity problem into two simpler problems: a nonlinear one-dimensional set of equations describing the global behavior of the beam and a linear two-dimensional set of equations describing the behavior of a cross section. The nonclassical effects are treated in a detailed cross section (local) analysis that is uncoupled from the beam (global) analysis and which yields the effective beam stiffnesses needed in the one-dimensional beam analysis. Thus, warping is accounted for in a local cross section analysis without explicit inclusion of these effects in the beam analysis. Degrees of freedom associated with shear deformation are statically condensed from the formulation, leading to a rotating beam analysis that uses only those degrees of freedom associated with classical beam theory. The resulting analysis was implemented as a p-version beam finite element into a program called CORBA (COmposite Rotating Beam Analysis). Numerical studies conducted with the program showed that the approach was able to capture the most significant effect of shear deformation, namely the reduction in effective bending stiffness that occurs when a substantial amount of bending-shear coupling is present in the beam. The results of the study also showed that a one-dimensional global dynamic analysis based on classical beam kinematics could accurately predict the bending and torsion frequencies of modes important to an aeroelastic analysis. However, the section properties used in the global analysis must account for the important nonclassical effects associated with shear deformation, warping, and elastic couplings. Nonclassical effects were shown to have significant influence on the frequencies of the fundamental modes of highly coupled composite beam structures. Errors on the order of 15-percent were reduced to less than five-percent by accounting for the nonclassical effects. The effects of shear deformation and warping on predicted dynamic behavior were only slightly influenced by large pretwist angles. In addition, the computational efficiency associated with using higher order elements when analyzing an untwisted beam was not realized for the case of beams with large pretwist.

The emphasis of the analytical work in references 135-140 was on developing and validating a beam-based analysis for computing the static and

dynamic behavior of extension-twist-coupled composite rotor blades that could be used in preliminary design. However, it was recognized that detailed finite-element models representing the three-dimensional built-up structure characteristic of real blades would be required for final analytical verification of such designs. Therefore, a companion experimental and analytical investigation was conducted with the objective of evaluating the use of MSC/NASTRAN for detailed finite-element modeling and analysis of extension-twist-coupled blades (refs. 141-144). Results from a preliminary investigation using an extension-twist-coupled circular tube that was fabricated for a static test are reported in reference 141. The specimen was 24 inches long, had an outer diameter of 1.640 inches, and a wall thickness of .046 inches. The tube was fabricated from unidirectional T300/5203 graphite fiber/epoxy resin, with a $[(+20°\text{-}70°)_2]_S$ lay-up. Because the tube was prepared for a static test, it had an aluminum plug and potting compound at each end to facilitate static testing. These components could not be removed for the dynamic tests. The body of the tube was modeled with 684 quadrilateral plate elements for the baseline model. Concentrated mass elements were used for modeling the aluminum end plugs and potting compound. In addition, the end plugs were assumed rigid. For vibration testing, the tube was suspended horizontally by two bungee cords attached near each end of the tube. Three natural frequencies (first and second bending and first torsion) were identified in the vibration test and were in reasonable agreement with those computed using the detailed finite element model (maximum error of 13.4%).

A more extensive analytical and experimental investigation of the vibration characteristics of extension-twist-coupled composite tubular beams representative of the primary load-carrying spars within a rotor blade is described in reference 142. A set of extension-twist coupled tubular beams was manufactured with four plies of T-650/42 graphite fiber with ERLX 1925-2 epoxy resin in a plain weave cloth pre-preg. The 0º90º cloth weave was rotated off-axis to achieve a $[+20°]_4$ laminate. Three different cross-sectional geometries were manufactured: D-shape, square, and flattened ellipse (fig. 75). The spars had a nominal wall thickness of .030 inches. A discussion of the fabrication process, vibration test setup, data acquisition system, data reduction, and test-analysis correlation techniques used are fully described in the report. Results from free-free vibration tests of the tubes were compared with results from a normal modes analysis of companion shell-finite-element models developed in MSC/NASTRAN. Agreement was reasonable, with errors ranging from about 5 to 13% depending on the cross section (elliptic best, D-shape worst). The spars were modeled using two-dimensional, quadrilateral flat plate (CQUAD4) elements having anisotropic properties. All finite element models were formed with 25 plate elements in the lengthwise direction, with the number of circumferential elements varying with cross-section type (12, 8, and 14, respectively). The FEM of the D-shaped spar is depicted in figure 76. Structural mass was accounted for using the consistent mass matrix option in the analyses. Results from normal mode and frequency analyses of the finite-element models were compared with those obtained from free-free dynamic tests of the fabricated spars. Five global or nonshell-type mode shapes were identified for each of the tubes in the frequency range from 0 to 2000 Hz. The measured and calculated global mode shapes for the D-shaped spar are shown in figure 77 for illustration. The results of reference 142 demonstrated that the structural dynamic characteristics of thin-walled composite structures employing extension-twist coupling can be determined with acceptable engineering accuracy using three-dimensional finite element models formed from shell-type elements that are available in commercial finite element analysis codes such as MSC/NASTRAN.

References 143-144 summarize the results of an experimental demonstration of passive blade twist control using extension-twist coupling on a model rotor. A set of low-twist model-scale helicopter rotor blades was manufactured from existing blade molds for hover testing on the ARES testbed. A four-bladed articulated rotor hub with coincident flap and lag hinges was used in the investigation. The blades were rectangular in planform with a NACA 0012 airfoil shape and a built-in linear twist of -8.25º. The blades were 55.0 inches in radius and had a chord of 4.24 inches. The D-spar was fabricated using four plies of graphite/epoxy in a plain weave cloth "pre-preg".

The 0º/90º cloth weave was rotated off-axis to achieve a ($[+20º]_4$) extension-twist-coupled laminate. The trailing edge of the blade was composed of honeycomb filler wrapped by a single layer of fiberglass skin. Two hollow fiberglass weight tubes running the length of the blade and located immediately forward and aft of the D-spar were incorporated into the blade design to provide a means of changing the nonstructural mass distribution. A cross section of the blade is shown in figure 78. Hover testing was conducted in AB's Rotorcraft Hover Test Facility located in the high-bay area of a building adjacent to the TDT. The change in blade twist was measured as a function of rpm and collective pitch. The blades were spun from 0 to 800 rpm in 100 rpm increments. Collective pitch was swept at each rpm. Data were obtained for both an unballasted (both weight tubes empty) and a ballasted (both weight tubes full) blade configuration at sea-level atmospheric air conditions, where maximum twist changes of 2.54º and 5.24º were observed, respectively. These results were in reasonable agreement with those obtained from a detailed MSC/NASTRAN finite-element analysis model of the rotor blade (fig. 79), which yielded maximum twist angles of 3.01ºand 5.61ºfor the unballasted and ballasted blade configurations, respectively. Figure 80 presents the blade elastic twist plotted as a function of rotor speed for test and analysis using both mass distributions. A ballasted blade configuration was also tested in a near-vacuum condition in the TDT as a means of determining the effect of aerodynamic loading on the total twist obtained. Aerodynamic-induced effects on the blade elastic twist were minimal, with the blade twist remaining nearly unchanged between atmospheric and near-vacuum conditions. The effect of collective pitch on blade elastic twist was also demonstrated to be minimal, as no appreciable degradation in twist was observed at increased collective pitch angles.

The blade design studies noted above showed that passive twist control of composite rotor blades via elastic extension-twist coupling has the potential for improving the aerodynamic performance of tiltrotor aircraft. However, none of the aforementioned studies addressed the effect of such blade designs on aeroelastic stability. Such a study was conducted as part of a broader investigation of tiltrotor aeroelasticity in reference 145. It was found that an extension-twist coupled blade design has a significant detrimental impact on aeroelastic stability of the rotor/pylon/wing system in the airplane mode of flight. This adverse effect is associated with the need to add considerable additional weight to the tips of the blades (over that for an uncoupled design) to achieve the level of centrifugal force needed to produce the blade twist changes necessary for increased aerodynamic performance. The additional weight reduces the wing torsion frequency and brings it closer to the wing beam frequency, which is destabilizing, while the increased centrifugal forces acting on each blade have an adverse effect on blade pitch-lag coupling due to precone. For the XV-15, the subject of this study, an increase in wing torsional stiffness on the order of 20-percent or a reduction in rotor precone to near zero would be required to achieve an acceptable level of stability.

Rotorcraft Vibrations

The problem of rotorcraft vibrations was addressed by Aeroelasticity Branch researchers in a variety of in-house and funded research activities during the period 1978-91. The major technical areas investigated included airframe finite-element modeling, analysis of coupled rotor-airframe vibrations, and airframe structural optimization. Several other ancillary studies of a specialized nature related to these major areas of research were also conducted.

Blade Pendulum Absorbers: Analytical studies that were conducted with the objective of expanding the analytical database for designing effective blade-mounted pendulum absorbers to reduce helicopter vibration are described in references 148-150. The oscillatory airloads acting on a rotor in forward flight are the primary source of vibration in helicopters. The character and magnitude of these loads have led to the design and implementation of a variety of vibration control devices for placement in the rotor and the fuselage by the helicopter manufacturers in their efforts to reduce vibrations (ref. 151). In particular, pendulum absorbers mounted near the root of each blade have proven to be quite successful in absorbing a large portion of the hub shears and moments that

would otherwise be transmitted to the fuselage (refs. 152-155). A properly tuned pendulum can attenuate vibratory loads by shifting the original natural frequencies of the blade away from an aerodynamic excitation frequency, and by generating appropriate forces at its point of attachment that causes a spanwise redistribution of the structural loads such that the hub reactions are reduced.

References 148-149 present the results of what are thought to be the first published analytical investigation of the effects of a spherical pendulum absorber on the natural frequencies and modes of a rotor blade. A spherical pendulum absorber was investigated because of its potential for simultaneously controlling the inplane, out-of-plane, and torsional blade vibratory loads, in contrast to conventional simple pendulums that affect only inplane or out-of-plane loads depending on their orientation. The nonlinear equations of motion of a spherical pendulum assumed to be attached to a rotor blade undergoing coupled flapwise bending, chordwise bending, and torsion were derived and then linearized for small oscillations about the steady state position of the pendulum. These equations were then combined with the linear blade equations of reference 156 using a transfer matrix approach (ref. 157) to obtain the transfer matrix of the coupled system. The natural frequencies and associated mode shapes are computed using the reduced transfer matrix that results from imposing the blade boundary conditions on the system transfer matrix. The spherical pendulum introduces two new modes between the displaced original blade modes, while the simple flapping and lead-lag pendulums each introduce only one mode. Illustrative results showing the variation with rotor speed of the natural frequencies of a hingeless blade with a spherical pendulum are shown in figure 81. The radial location of the pendulum was found to play the most important role in displacing the initial natural frequencies of a blade. Blade torsional frequencies were also affected by the offset of the pendulum hinge above the blade elastic axis. The spherical pendulum was found to significantly attenuate all blade root forces and moments while the simple pendulum was found to only attenuate forces and moments in the direction for which it was designed, i.e., either flapwise or chordwise.

A comprehensive analytical investigation of the dynamic and aeroelastic response of hingeless rotor blades with simple pendulum absorbers is reported in reference 150. The objective of the study was to establish analytical design procedures and criteria for the installation of flapping and lead-lag pendulums on the blades of a rotor to attenuate the forces and moments acting at the hub of a helicopter in forward flight. The study involved conducting frequency response analyses of both uniform and nonuniform blades excited by a harmonic variation of spanwise airload distributions as well as a concentrated tip load. The linearized aeroelastic equations of motion describing the coupled flapwise bending, chordwise bending, and torsion of a twisted, preconed blade in forward flight were expressed in state vector form and combined with the corresponding linearized equations for the pendulums using transfer matrix techniques. The resulting transfer matrix was then used for the frequency response analyses. Pendulum frequency, mass, spanwise location, and damping were systematically varied to identify the optimum tuning conditions for each of the blade/pendulum combinations studied. An example of one set of curves that were generated and used to identify an optimum spanwise location and tuning frequency is given in figure 82. The effects of variations in blade collective pitch, built-in twist, precone angle, and pendulum hinge offset on the optimum pendulum configurations of the nonuniform blade were also established. This investigation determined that a pendulum can be tuned and its optimum mass determined by excitation with a concentrated simple harmonic load at the blade tip. However, it was found that distributed airloads were required to accurately determine the attenuation of blade root reactions.

Rotor-Airframe Coupling: The problem of defining a practical computational procedure for calculating the flight vibrations of coupled rotor-airframe systems that is usable during helicopter design was addressed by AB researchers during 1978-81. The objective of this study was to establish foundations for adequate representation and treatment of airframe structures in design analysis of helicopter vibrations. The results of that study are documented in reference 158. The report presents a body of formulations for rotor-airframe coupling intended for flight vibration analysis in

airframe structural design work. The formulation assumes that the airframe structure is represented by a general, three-dimensional finite-element model, and that the rotor is represented by a set of linear, second-order, matrix differential equations with periodic coefficient matrices that are expanded in harmonic series form. The rotor equations are the linear perturbation equations that result from perturbing the nonlinear aeroelastic equations of the rotor with a free hub about a steady-state (trimmed) flight condition. The linear impedance characteristics of the airframe are computed using its finite-element model. The calculation involves imposing unit oscillatory displacements on the interface degrees of freedom (DOF) at each of the rotor harmonic frequencies of interest and computing the interface forces required to maintain the imposed motion. The interface forces so computed are used to form the desired impedance matrices. Coupling of the rotor to the airframe is specified through general linear equations of constraint relating rotor interface DOF to airframe interface DOF. The resulting equations of the combined rotor-airframe system are solved by the method of harmonic balance for the system's steady-state vibrations. A method is also presented for quick recalculation of vibrations when only relatively few members of the airframe finite-element model are identified as candidates for variation, as often happens in design studies of helicopter vibrations. Explicit relations required to generate the rotor-airframe equations and solve for the system vibratory responses are presented in a form suitable for direct computer implementation. Block diagrams illustrating computing sequences are included and discussed.

Four computer programs (MHB, RATTLE, ROTOR, and SHAKE) were written in 1979 to help verify concepts and procedures that were being developed as part of the coupled rotor-airframe formulations described in reference 158. The programs were initially written in FORTRAN 66 for execution on CDC 6000-series mainframe computers. PC-based FORTRAN 77 versions of the programs were developed in 1996. A summary of these programs follows:

(1) MHB employs the method of harmonic balance to compute the periodic solution of a system of linear, second-order, non-homogeneous matrix differential equations with periodic coefficients and periodic external forcing. Data required for the program include user-supplied harmonic series expansions for the mass, damping, stiffness, and external force matrices, and user specification of the sine and cosine harmonics of the desired solution vector.

(2) RATTLE couples a user-supplied linearized aeroelastic math model of a rotor to a user-supplied impedance math model of an airframe and calculates the vibratory response of the coupled system and the associated interface forces by the method of harmonic balance. The rotor is assumed to be represented by a set of linear, second-order, matrix differential equations with periodic coefficients whose mass, damping, stiffness, and external force matrices are expanded in harmonic series. The airframe is assumed to be represented by impedances that have been calculated externally using a finite-element model of the airframe. The RATTLE program is a special-case implementation of the primary method for rotor-airframe coupling and harmonic balance solution described in reference 158.

(3) ROTOR employs user-supplied linearized differential equations for a rotor aeroelastic math model with a free hub to calculate both the vibratory loads acting at the hub assuming no hub motion (the so-called "fixed-hub forces") and the hub load increments resulting from imposed harmonic displacements of the hub degrees of freedom (the so-called "hub impedances") by the method of harmonic balance. Fixed-hub forces have often been used to approximate the effect of a rotor on an airframe in analysis of "coupled" rotor-airframe vibrations by treating the forces as external loads acting on the hub degrees of freedom in a finite-element model of the airframe. Both the fixed-hub forces and the rotor hub impedances are employed in analyses based on so-called "impedance matching" techniques that take into account the dynamic interaction between the rotor and the airframe. The ROTOR program is a special-case implementation of the alternative representation of a rotor system by impedances described in Appendix H of reference 158.

(4) SHAKE employs a rotor impedance/airframe mobility matching technique for rotor-airframe coupling and vibratory response analysis. The program uses user-supplied lin-

earized matrix differential equations for a rotor with a free hub to calculate both the fixed-hub forces and the hub impedances by the method of harmonic balance as in program ROTOR. The airframe hub mobilities, representing hub responses to unit harmonic forces imposed on the hub degrees of freedom, must be calculated externally and supplied to the program. The SHAKE program is a special-case implementation of the alternative technique for rotor-airframe coupling and vibratory response analysis described in Appendix H of reference 158.

The four programs were verified using the equations of motion for a two-bladed, horizontal-axis, wind turbine under gravity excitation that were available from an earlier and unrelated investigation. Results obtained from these programs were in exact agreement with each other as well as with results obtained from the special-purpose harmonic balance program used to solve the wind turbine equations in the earlier investigation.

Airframe Finite-Element Modeling: Vibrations are a critical consideration in the design of all new rotorcraft. Unfortunately, all too often new rotorcraft unexpectedly exhibit excessive vibrations in flight test, and vibration mitigation solutions at that stage of development are usually add-on fixes that adversely impact cost, schedule, and performance. The problems facing analysts charged with predicting helicopter vibrations are formidable (fig. 83). The rotor system generates complex periodic aerodynamic and dynamic loads that are transmitted to the airframe both mechanically through the mounting system and aerodynamically by the rotor wake. These forces occur at the so-called blade passage frequency, which is equal to the product of the number of blades and the rotor rotational speed. This frequency is typically in the 10-20 Hz range. The airframe structural dynamics problem is complicated by the fact that helicopter airframes are lightweight, shell-type structures having multiple large cutouts and supporting several rather heavy components.

Even with the advanced analysis capabilities of finite-element methods such as embodied in NASTRAN (and later MSC/NASTRAN) that were adopted for structural analysis by the major helicopter manufacturers in the early 1970s, airframe structural designers achieved only limited success in designing airframes that exhibited low levels of vibratory response in flight. A major deficiency was an incomplete understanding of the modeling requirements for adequate vibration analysis of complex helicopter structures. Because of this experience, during the late 1970s, industry advisory groups began urging NASA to work with them on improving the predictive capability of finite-element models. In 1978, NASA's Office of Aeronautics and Space Technology, in an unrelated move, formed a special rotorcraft task force to review rotorcraft technology needs and to prepare an appropriate industry-wide rotorcraft program aimed at advancing technology readiness over a broad front. The draft plan cited vibrations as one of the key areas NASA intended to work as part of a new 10-year rotorcraft research program. As lead center for structures research, NASA Langley was asked to define a research activity aimed at addressing the industry's needs with respect to improving the predictive capability of finite-element dynamics models. The proposed task, which appeared in the final report of the task force (ref. 159), called for an application of finite-element modeling (with emphasis on predicting structural vibrations) in a workshop environment to assess and document industry modeling techniques and ground vibration test procedures. All work was to be done on a production aircraft. As a result of a competitive procurement, a contract was awarded to Boeing Helicopters in 1980 to conduct the subject study on the CH-47D tandem-rotor helicopter (fig. 84).

An unusual requirement of the contract was that each major step of the program be presented to and critiqued by the other three major helicopter airframe manufacturers. The study was deliberately slow-paced to allow for the necessary extensive government/industry interactions and technical exchanges. Plans for the modeling and ground vibration testing as well as the results of the modeling phase of the study were presented on-site to the other companies for critique by a NASA/Boeing team. The results of the test and correlation tasks were presented to industry representatives at Langley in February 1983. The finite-element model of the CH-47D airframe that was developed by Boeing is shown in figure 85.

An extensive ground vibration test was also conducted on the airframe (fig. 86), in which the airframe was excited by forces vertically, longitudinally, and laterally and moments in pitch and roll at both the forward and aft hubs over a frequency range from 5 to 35 Hz. Acceleration measurements in three orthogonal directions were recorded at 35 locations distributed throughout the airframe. Illustrative results showing the type of comparisons that were obtained between measured and calculated forced responses for lateral excitation at the forward hub are given in figure 87. The studies conducted on the CH-47D have been extensively documented in a series of NASA Contractor Reports (refs. 160-164). A concise summary of the work is given in reference 165.

Taken as a whole, the CH-47D test/analysis comparisons obtained were considerably improved over similar earlier attempts, particularly at the lower frequencies, and went a long way toward removing the uncertainty about the limits of applicability of finite-element models for the prediction of in-flight vibrations. However, the agreement was deemed acceptable only up through about 15-20 Hz. The modeling work demonstrated that a finite-element model suitable for static internal loads and vibrations can be developed simultaneously and that there is no need to form separate static and dynamic models as had been customary previously. The cost of such a combined static and dynamic model was established to be about 5-percent of the work-hours of a typical airframe design effort. Of the 5-percent, 4-percent is already typically expended in most companies to form the static model; the vibrations model is another 1-percent. The modeling and correlation studies also identified several items that have the potential for improving the correlation. These included: use of nonuniform modal damping in the frequency response calculations, and the inclusion of so-called "secondary effects" such as stringer shear area, stringer shear continuity across splice joints, and suspension system dynamics.

DAMVIBS: During the course of the studies conducted on the CH-47D helicopter, it became clear that the key to improving modeling technology and engendering in the industry the needed confidence to use finite-element models for vibrations design work was an industry-wide program in which all the companies conduct modeling, testing and correlation activities along the lines of the CH-47D work. Also identified as being essential was a workshop environment that fostered the open discussion of airframe finite-element modeling issues, techniques, and experiences. An expanded program directed at the long-term needs of the industry with respect to predicting and controlling vibrations, with primary attention to issues related to finite-element modeling, was defined by AB researchers in 1983. The proposed program was approved by NASA and the industry and subsequently implemented in 1984 with the award of task contracts to the (then) four major helicopter airframe manufacturers - Bell Helicopter Textron, Boeing Helicopters, McDonnell Douglas Helicopter Company, and Sikorsky Aircraft. Because the objective of this new program was to establish the technology base needed by the industry for developing an advanced finite-element-based dynamics design analysis capability for vibrations, the new program came to be called DAMVIBS (Design Analysis Methods for VIBrationS).

The overall objective of the DAMVIBS Program was the establishment in the U. S. helicopter industry of an advanced capability to utilize airframe finite-element models in analysis of rotorcraft vibrations as part of the regular airframe structural design process. The intent was to achieve a capability to make useful analytical predictions of helicopter vibration levels during design, and to design with confidence based on those predictions. The DAMVIBS Program was positioned as the focus of a new and broader rotorcraft structural dynamics program that was just getting underway within AB at that time. Four technology areas were to be worked under the DAMVIBS Program: (1) Airframe Finite-Element Modeling; (2) Difficult Components Studies; (3) Coupled Rotor-Airframe Vibrations; and (4) Airframe Structural Optimization. Primary emphasis was to be on the first two elements of the program, which were intended to be mainly an industry effort focusing on industrial modeling techniques. Under the last two elements of the program, the finite-element models formed by the industry were to be used by government, industry and academia as the basis for the development,

application, and evaluation of advanced analytical and computational techniques related to coupled rotor-airframe vibrations and to airframe structural optimization under vibration constraints.

Under the first element of the DAMVIBS Program, industry teams formed finite-element models (fig. 88), conducted companion ground vibration tests (fig. 89), and made extensive test/analysis comparisons (fig. 90) of both metal and composite airframes in an industry-wide assessment and critique of basic modeling techniques. The results of these studies are described in references 166-175. Three other efforts related to this program element were also funded. The first was aimed at describing a previously developed company method for identifying modeling errors that may arise in developing a finite-element model (ref. 176). The procedure is implemented as a set of MSC/NASTRAN DMAP alters. The second activity involved ground vibration testing and finite-element modeling and analysis of the tail boom of a Sikorsky S-55 helicopter under a grant with Rensselaer Polytechnic Institute (ref. 177). The third activity was a preliminary investigation into methods for significantly reducing the size of large finite-element models for increased computational efficiency in aeroelastic and dynamic analyses while preserving the essential dynamic characteristics of the full model (ref. 178).

Under the second element of the DAMVIBS Program unique experimental/analytical studies were conducted to identify an airframe's "difficult components", that is, those components that require better representation in the finite-element model for improved correlation (agreement) with test results. Special ground vibration tests were conducted during which components were progressively removed from an airframe to provide data for critically examining the effects of modeling assumptions on predicted vibrations. Difficult component studies were conducted on the all-metal AH-1G (ref. 179) and the all-composite D292 (refs. 180-181) airframes. The difficult components studies shed new light on the importance of many airframe components on vibratory response at the higher frequencies of interest. The AH-1G in its full-up ground vibration test configuration for this investigation is shown in figure 91a. Components were then progressively removed from the airframe to arrive at the configuration shown in figure 91b. The canopy glass, various black boxes, and the stub wings were removed in the last step of the strip down. At each stage, a ground vibration test and an analysis based on an existing FEM (ref. 182) that was modified to reflect the specific configuration tested were performed and the results compared. Comparisons of the measured and predicted changes in response were then used to identify components which were causing prediction difficulties and which therefore required better modeling treatment. Based on the results of such comparisons, the FEM was updated to include some of the effects that were found to be important. The improved model was then used to reanalyze each of the configurations tested. The improvement in the predicted frequencies is indicated in figure 92. In that figure the predicted natural frequencies are plotted versus the measured frequencies for all of the major configurations tested using both the initial and updated FEMs. In each case, perfect agreement is along the solid line. It is seen that the natural frequencies calculated using the updated model are generally within 5 percent of test values, compared to 20 percent using the initial model. The difficult component studies conducted on the AH-1G and D292 airframes showed that considerably improved correlation is possible if secondary effects that were historically regarded as unimportant dynamically are taken into account when forming the FEM. This finding means that FEMs for vibration analyses need to be substantially more detailed than the usual static model, contrary to what was previously thought.

The third element of the DAMVIBS Program was aimed at evaluating and improving existing industry codes for comprehensive analysis of the coupled rotor-airframe vibrations of a helicopter in forward flight, and to develop new computational procedures that are better suited to the repetitive analyses which are required in airframe design work. With regard to the first objective, teams from each of the four companies separately and independently applied different analysis techniques, one method per company, to calculate the vibrations of the AH-1G helicopter (fig. 93) in steady level flight and compared the results with existing flight vibration data. As the manufacturer

of the subject aircraft, Bell was required to provide to the other companies a summary of the modeling, testing and correlation work conducted on the AH-1G (ref. 183). Bell was further required to assemble the flight vibration data to be used in the correlations and to describe the rotor system both mechanically and aerodynamically to the other participants (ref. 184). An existing NASTRAN finite-element model of the airframe (ref. 182), adjusted by Bell to correspond to the flight condition for which the comparisons were to be made, was furnished by Bell to the other participating manufacturers as part of the common data to be utilized for the subject activity. The results of this study (refs. 185-188) showed that (then) current codes were not yet good enough to be relied on fully in design and spurred the industry to reexamine their codes and make them more accurate. With regard to the second objective, no tasks related to developing new computational procedures were issued to the industry participants. However, some work relevant to the area that was begun in-house is described in a later section. In addition, under a grant with Rensselaer Polytechnic Institute, a report was published (ref. 189) which describes two new methods for modeling the dynamics of general, multi-body elastic systems undergoing large arbitrary motions.

Under the fourth element of the program, industry studies aimed at establishing (identifying) the potential role of structural optimization in airframe vibrations design work were planned. Although no airframe structural optimization tasks were issued to the industry participants, relevant studies were conducted in AB as part of the Branch's rotorcraft structural dynamics program. This work is described in the next section. There were two university activities funded under the DAMVIBS Program that are related to this program element. Both dealt with the use of system identification techniques to improve airframe finite-element models using frequency response test data while preserving the physical interpretability of the system mass, damping, and stiffness matrices. At Georgia Tech, a method based on using linear sensitivity matrices to relate changes in selected physical parameters to changes in the total system matrices was developed (ref. 190). The values for the physical parameters were determined using constrained optimization techniques in combination with singular value decomposition. Applications were made to the AH-1G airframe using the finite-element model and data generated as part of the difficult components study of that aircraft. At the University of Bridgeport, a method that relies on the design sensitivity analysis procedures in MSC/NASTRAN to determine the physical parameter changes needed for correlation was implemented using the DMAP language. Applications were made using data from ground vibration tests of a 7-ft long composite semi-monocoque cylinder with cutouts and concentrated masses.

Five government-industry workshops were held at NASA-Langley during the course of the DAMVIBS Program to review and discuss completed work and to critique plans for future work. These meetings provided an excellent forum for technical discussions related to airframe finite-element modeling issues, particularly as they related to airframe design (something rarely presented or discussed in more formal public forums). Indeed, the workshops provided the necessary atmosphere where difficult-to-obtain experiences (not usually recorded in journals or discussed at conferences) were freely discussed. With the phasing out of the DAMVIBS Program in 1991, a government/industry assessment of the program was made to identify those accomplishments and contributions that could be ascribed to the program (refs. 191-194). References 191-193 provide an assessment from the perspective of the government sponsoring organization. Reference 194 contains assessments from the perspective of the industry participants. The assessments indicated that the DAMVIBS Program provided the leadership role and focal point for the type of structural dynamics research that was needed by the rotorcraft industry. The program has resulted in notable technical achievements and changes in industrial design practice, all of which have advanced the industry's capability to use and rely on airframe finite-element models in analysis of vibrations during design. As a result, it is expected that the industry will emerge with a substantially improved finite-element-based dynamics design analysis capability to meet the dynamics design challenges of the next generation rotorcraft. The assessment also identified a number of key con-

tinuing and new structural dynamics technology needs that must be met if the industry is to achieve a "jet smooth" ride for helicopters.

Airframe Structural Optimization: Structural design involves the merging of an analysis procedure with a resizing/reanalysis procedure in which changes are made to the structure in an iterative process until a converged design that is best or optimum in some sense is obtained. The objective of structural optimization is to design a structure that minimizes a specified function while satisfying a set of restrictions imposed on the design. The function with respect to which the design is optimized is called the objective function. For aircraft structures, weight is often taken to be the objective function. However, the objective function can be any quantity of interest. The restrictions placed on the design that must be satisfied to produce an acceptable design are collectively called constraints. Optimization procedures start with an arbitrary (but usually feasible) initial design and proceed by varying structural parameters in stepwise fashion so that the value of the objective function is reduced without violating the constraints. The parameters that are varied during the iterative design process are called design variables. Examples of design variables include member sizes such as thicknesses of panels and cross-sectional areas of stringers, ply thickness and fiber orientation angles in composite material laminates, and material properties. The set of quantities consisting of the design variables, objective function, and constraints is called the design model.

With regard to the helicopter airframe structural design process, the design of an airframe that meets all static and dynamic design requirements, in particular the vibration requirements, is a difficult task. During the definition of the DAMVIBS Program, it was recognized that structural optimization techniques, if properly brought to bear by the airframe designer, could go a long way toward achieving the goal of a low-vibration helicopter. Consequently, "Airframe Structural Optimization" was identified as a lucrative element of both the DAMVIBS and in-house research programs. Unfortunately, no airframe design optimization tasks were issued to the industry participants before the phasing-out of the DAMVIBS Program. However, extensive exploratory studies were conducted in-house under the rotorcraft structural dynamics program during 1985-90 with the objective of establishing the potential role of nonlinear-programming (NLP)-based structural optimization techniques in airframe vibrations design work. Emphasis in these studies was on developing and implementing a computational procedure for vibrations optimization of airframe structures subject to dynamic response constraints along with the customary strength and frequency constraints. This work, which is fully described in references 195-200, is summarized below.

One of the essential elements needed in the development of a computational procedure for airframe optimization is a method for efficient calculation of derivatives of the constraints and the objective function with respect to the design variables. These derivatives are usually referred to as design sensitivity derivatives. A semi-analytical method for computing the necessary sensitivity derivatives for an airframe subject to constraints on vibratory forced response was formulated and implemented into MSC/NASTRAN (ref. 201) as a new solution sequence (ref. 195). An application of the method to a simple elastic-line finite-element model (fig. 94) of the AH-1G helicopter airframe for the case of vertical vibratory response due to 2/rev vertical excitation at the hub is presented and discussed in reference 195. The sensitivity derivatives computed indicated that the elements in the tail boom would be the most likely candidates for modification to effect a reduction in the response at the pilot and gunner locations.

Reference 196 addresses several important issues involved in the application of formal optimization techniques to helicopter airframe structures for vibration reduction. An optimization strategy is suggested for minimization of vibration in airframe structures during the design process. Considerations needed in the formulation and solution of optimization problems during the conceptual, preliminary, detailed, and ground and flight test phases of airframe design and development are discussed. The formulation of optimization problems for helicopter airframes is described and pertinent expressions for objective and constraint functions and their sensitivity derivatives are derived. The application of the optimization meth-

odology is demonstrated using the airframe structure of the Bell AH-1G helicopter. Numerical results are presented for both a preliminary and detailed design model of the airframe. A computer program system called DYNOPT (DYNamics OPTimization) was developed to carry out the airframe optimization computations as a nonlinear mathematical programming problem. The program featured a unique operational combination of the MSC/NASTRAN finite-element structural analysis code (ref. 201) extended to include calculation of the sensitivity derivatives of steady-state dynamic response constraints, with the CONMIN (ref. 147) optimizer. The latter uses the method of feasible directions for design change computations. The primary computational steps used in the DYNOPT program are illustrated in figure 95. Approximation techniques based on Taylor series approximation with respect to direct and reciprocal design variables were incorporated into the code. The structure of the AH-1G helicopter airframe with its skin panels removed is depicted in figure 96. The fuselage portion of the airframe is built around two main beams that provide the primary vertical bending stiffness in the fuselage structure. The tailboom is of semi-monocoque construction having aluminum skins, stringers, and longerons. Two different finite element models of the airframe were used in the optimization studies: the elastic-line (or "stick") finite-element model (ref. 202) shown in figure 94, and the built-up fuselage/elastic-line tail boom model (ref. 182) shown in figure 97. In the stick model of figure 94, the fuselage, tail boom, wings, and rotor shaft were modeled with beam elements. In the model of figure 97, the fuselage and wing structures were modeled primarily with rods, shear panels, and membrane elements, while the tail boom, vertical fin, and tail rotor shaft were modeled with beam elements in the same manner as they were in the stick model. Corresponding to the two different-fidelity finite-element models, two different design models were developed for the optimization studies, one appropriate for preliminary design (fig. 98) and one for detail design (fig. 99). The preliminary design model takes as its design variables the overall depth of the cross section of the primary structure at several stations along the airframe, for a total of 46 independent design variables. An empirical relationship between the design variables of the design model and the element section properties of the stick finite-element model was established to update the MSC/NASTRAN bulk data deck during optimization iterations. The detailed design model in figure 99 is compatible with the finite-element model of figure 97 and was developed to permit optimization of the sizes of the many individual structural members comprising the airframe structure. The design variables consisted of the thickness of the outer skin of each of the panels and the cross-sectional areas of the stiffeners, for a total of 108 independent design variables. The design variables were related to the element properties of the built-up finite-element model by empirical relationships in a manner similar to that employed for the stick model. The preliminary design model was used in an optimization problem formulated for tuning the natural frequencies of the airframe to avoid resonance with the rotor exciting forces. The objective function was the weight of the primary structure. Constraints were placed on the upper and lower values of the natural frequencies of the five predominant modes of the airframe. Figure 100 shows the distribution of sensitivity coefficients for the constraints on the first and second vertical bending mode frequencies. The results indicate that the design variables in the rear fuselage and most of the tail boom would be effective in changing the first vertical bending mode frequency, while the variables in both the fuselage and the tail boom would be effective for changing the second vertical bending mode. The iteration histories of the objective function and the constraints are given in figure 101. The detailed design model was used in an optimization problem formulated for reducing the 2/rev vertical vibratory response at the pilot seat location in the forward fuselage. The objective function was the forced response displacement at the pilot seat. Constraints were placed on the forced response displacements at five other locations throughout the airframe. Figure 102 shows the distribution of sensitivity derivatives for the forced response displacement at the pilot seat location with respect to the fuselage and tail boom design variables. The results indicate that the response is much more sensitive to changes in the design variables in the tail boom portion of the airframe than it is to changes in the fuselage portion. The optimization histories of the objective and constraint functions

in the various iterations of the DYNOPT program are shown in figure 103.

Reference 197 describes the extension of the DYNOPT program to include fatigue stress constraints in the optimization procedure and demonstrates the application of the extended code using the elastic-line model of the AH-1G helicopter airframe. References 198-199 are unified summaries of the results and experiences from the in-house study to investigate the use of formal, nonlinear programming-based optimization techniques for helicopter airframe vibrations design work. The papers discuss the formulation and solution of airframe optimization problems, describe the DYNOPT computer program system that was developed for optimization of airframes subject to strength, frequency, dynamic response, and fatigue constraints, and illustrate its application to the AH-1G helicopter.

Reference 200 was intended to be a primer on airframe dynamics for NASA-Langley researchers who were involved in rotor blade optimization. To this end, the reference provides an overview and discussion of those aspects of airframe structural dynamics that have a strong influence on rotor design. The role of airframe response in rotor design is described, and the types of constraints that need to be imposed on rotor design due to airframe dynamics are discussed.

Based on the in-house studies, it was concluded that formal, NLP-based structural optimization techniques have considerable potential for playing a major role in airframe vibrations design work, but only if the design models which are required in optimization algorithms adequately reflect the nuances of airframe design. The same studies identified an essential need of those who are engaged in optimization work, namely, at least a rudimentary understanding of the airframe structural design process. Such an understanding is necessary if the structural optimization engineer is to properly and adequately formulate the types of design models that are required for industrial design work.

The next phase of this study was to have been an application of DYNOPT to a complete built-up three-dimensional finite-element model of the AH-1G airframe. Unfortunately, the NASA-Langley rotorcraft structural dynamics program was terminated in October 1991 and all work in this area ceased.

Airframe Damping: Airframe structural damping plays an important role in airframe vibrations, particularly at resonant and near resonant conditions. However, because of the complex nature of most damping mechanisms, usual practice has been to use the same (usually assumed) value of modal damping for each airframe mode when computing airframe responses to rotor-induced vibratory forces. There has been little attention directed either at formulating mathematical models of real damping mechanisms suitable to incorporate with airframe finite-element models or at devising methods for quickly evaluating the effects of localized damping treatment in preliminary design analyses. The results of research supported by AB that was aimed at addressing the latter need are described in references 203-207.

Reference 207 develops engineering preliminary design methods for approximating and predicting the effects of viscous or equivalent viscous-type damping treatments on the free and forced vibration of lightly damped aircraft structures. Similar developments are presented for dynamic hysteresis-viscoelastic-type damping treatments. The basis of the methods is an energy quotient analogous to Rayleigh's quotient for predicting undamped natural frequencies of vibration. The energy quotient employs the undamped modes of vibration to compute the generalized damping, mass, and stiffness terms that appear in the quotient to evaluate the influence of damping treatment types, locations, and magnitudes on the various modal damping fractions. It was shown that the intermodal coupling of the undamped modes arising from the introduction of damping may be neglected in applying these preliminary design methods, except when the dissimilar modes have identical or nearly identical natural frequencies. In such cases, it was shown that a relatively simple, additional interaction calculation between pairs of modes exhibiting this "modal resonance" phenomenon suffices in the prediction of modal damping fractions in the interacting modes. The methods are applied to both beam and plate structures. The accuracy of the methods

is shown to be good to excellent, depending on the normal frequency separation of the system modes.

The structural damping studies identified an anomalous behavior for damped systems that have different modal patterns with close or identical frequencies (see, also, refs. 203-204). In this case, one damping-coupled mode loses its damping, while the companion mode gains the damping lost by the other mode. An example of this behavior is illustrated in figure 104 for the case of a binary-mode system representing the first symmetric and anti-symmetric modes of a simply-supported beam in which the specified uncoupled modal damping ratios are 0.020 and 0.010, respectively. As the frequency ratio increases to unity, the effective damping ratio of the second damping-coupled mode progressively decreases from its uncoupled value of 0.010 to zero. As the frequency ratio increases beyond unity, the effective damping ratio of the second mode recovers its initial uncoupled value. The first mode, in effect, steals damping from the second mode when their natural frequencies match or nearly match. This indicates that care must be exercised in designing damping treatments for vibration reduction because a resonating mode may not benefit from a damping treatment to reduce its vibratory response as expected. The analytical method described in references 205 and 207 includes a modal interaction analysis that computes the effectiveness of damping treatment when two different modes of vibration have matching or nearly matching natural frequencies. This permits the structural designer to better employ damping treatments in conjunction with structural mass and stiffness considerations that influence natural frequency placement.

Reference 206 examines the dynamic stability of binary systems with emphasis on the influence of natural frequency proximity and those instabilities that stem from skew symmetric stiffness matrices. The paper shows that the modal natural frequency ratio is of crucial importance in binary system dynamic stability. It also shows that severe (and perhaps unattainable) damping requirements result when two natural frequencies match or nearly match.

Rotor Math Model for Airframe Vibrations Design Work: The final analytical verification of a new helicopter design for acceptable flight vibrations generally requires the use of a comprehensive coupled rotor-airframe system analysis that is based on a sophisticated rotor aeroelastic mathematical model. However, based on insight gained while conducting studies that led to the rotor-airframe coupling formulation described in reference 158, those authors were led to speculate as to whether analytical predictions of airframe vibrations that would be useful during preliminary design could be made with much simpler rotor models. The investigation of this thesis was put on AB's list of planned rotorcraft research activities, but it was not until 1990 that the opportunity arose to initiate the study.

In 1990, a cooperative study was undertaken by AB and the U. S. Military Academy (USMA) with the overall objectives of: (1) developing an impedance matching method for coupling the rotor to the airframe that is tailored for use in preliminary design analyses of helicopter airframe vibrations; and (2) identifying the minimum levels of structural and aerodynamic sophistication that are required in rotor aeroelastic math models that are going to be employed to compute rotor impedances for use in airframe vibrations design work. The approach defined to meet the stated objectives included: modifying an existing nonlinear helicopter simulation program called DYSCO (Dynamic System Coupler) (ref. 208) to calculate rotor impedances; developing an impedance-based rotor-airframe coupling procedure along the lines described in Appendix H of reference 158; applying the new coupling procedure to the OH-6A helicopter; and then conducting extensive studies of the sensitivity of calculated airframe vibrations to rotor structural and aerodynamic modeling assumptions.

The initial effort in this study was undertaken by (then) LTC Kip P. Nygren of the USMA while he was in residence at AB during the summer of 1990 under a NASA/ASEE Summer Faculty Fellowship, and then for three weeks in the summer of 1991. LTC Nygren developed a procedure for calculating the needed rotor hub impedances within the DYSCO program, and then incorporated the procedure into the program as a new so-

lution module. Initial verification of the new procedure was made by comparing the time history solution obtained from DYSCO for the two-bladed, horizontal-axis, wind turbine under gravity excitation mentioned earlier with the harmonic balance solutions obtained from programs ROTOR, SHAKE and RATTLE.

The next step in the study was to have been the development and implementation of a computational procedure for rotor-airframe coupling by impedance matching. However, the elimination of rotorcraft structural dynamics base research at NASA-Langley in the fall of 1991 led to the demise of this activity as well as several other related in-house activities.

Impedance Model of ARES Testbed

In the early 1990s, design of an active-mount version of the ARES rotorcraft testbed was underway in AB with the aim of providing a testbed for studying the effects of rotor/body coupling on rotor aeromechanical behavior. The new testbed was to be capable of imposing motion in up to six-degrees-of-freedom simultaneously at the rotor hub by means of six actuators located beneath a Stewart platform to which the rotor pylon was mounted (fig. 105). Because this testbed was to be a second-generation version of the ARES testbed, it was designated ARES-II.

In anticipation of this planned upgrade to the capabilities of the ARES testbed, an impedance-based analytical method for coupling an aeroelastically-scaled model rotor system to the ARES-II testbed was developed (ref. 209). The rotor system chosen for the study was a four-bladed articulated basic research rotor (BRR) that was intended for generic experimental research in the TDT at that time. The BRR hub has coincident flap and lag hinges offset three inches from the center of rotation. The blades are untwisted, have a rectangular planform (56.224" by 3.625"), and NACA 0012 airfoils.

CAMRAD-II, the second-generation version of the Comprehensive Analytical Model of Rotorcraft Aerodynamics and Dynamics program (ref. 210), was chosen to develop the aerodynamic and dynamic model of the BRR. The Dynamic Analysis and Design System (DADS) multi-body dynamics analysis code (refs. 211-212) was used to develop the dynamic model of ARES-II. A multi-body dynamics code was chosen to model ARES-II because of the inherently multi-body character of the components comprising the testbed (fig. 105), and because such codes offer a superior capability for representing the motions of the actuators on which the Stewart platform is mounted.

The impedance matching method that was developed in reference 209 was extended beyond most treatments found in the literature in that it included the motions introduced by the platform, and representation of two mechanical load paths between the rotor and the testbed – the hub and the rotor control system. The DADS model of ARES-II and the CAMRAD-II model of the BRR are described, as is the development of the equations necessary to prescribe the motion of the Stewart platform. A complete description of the steps necessary to develop the impedance models of the components and the coupling equations are included. Numerical results are presented for the rotor and the testbed, both as separate and coupled systems. Some illustrative numerical results for the uncoupled BRR model are given in figure 106, which shows the variation of the fixed-hub 4-per-rev normal force and pitching moment with advance ratio. The sine and cosine components of the loads transmitted through both the hub and control system load paths as well as the total loads are shown. These as well as other results presented in reference 209 indicate that the loads transmitted to the airframe through the rotor control system may have to be included to provide an accurate assessment of the total loads.

The upgrade of the ARES testbed to the ARES-II configuration was not completed. Changing research priorities within the Branch, as well as problems related to providing the staffing and funding needed to complete the work, led to the termination of the effort.

Active Twist Rotors

During the mid-1990s, analytical efforts were initiated by AB researchers to investigate the potential of active twist rotors (ATR) employing

embedded piezoelectric active fiber composite (AFC) plies to generate dynamic blade twisting. The first of these analytical efforts focused on the development of a simple mathematical model for helicopter rotor blades incorporating AFCs. The resulting computer program is the Piezoelectric Twist Rotor Analysis (PETRA), and is designed for rapid and efficient control law and design optimization studies. A complete description of the development of the PETRA analysis is presented in reference 88. The primary components and features of the PETRA analysis are described below in a discussion adapted from reference 92.

The blade equations of motion used in the PETRA analysis are adapted from the second-degree nonlinear equations of reference 118. These equations are simplified to a linear out-of-plane bending-torsion model. A classical laminated plate theory approach is used to develop the composite laminate properties of the spar wall, and Rehfield theory (ref. 146) is then applied to obtain the beam properties of the spar structure. The piezoelectric beam actuation forces and moments are also obtained using linear piezoelectric constitutive relations and a procedure adapted from the Rehfield approach (refs. 88 and 213). The aerodynamic loads acting on the rotating blade are derived from an existing finite-state, unsteady aerodynamics formulation, which includes the ONERA dynamic stall model (refs. 214-216). For simplicity, a uniform inflow model is used.

Because the aerodynamic terms are highly nonlinear, a numerical time integration procedure is used to obtain a solution to the aeroelastic equations of motion. This is accomplished by first obtaining a system of ordinary differential equations using a modified Galerkin procedure and then integrating these equations in a MATLAB-based numerical analysis procedure (ref. 217). A numerical autopilot technique is also used during the time integration process to obtain trimmed, steady state flight conditions (ref. 216). This enables vibratory loads for active twist blades and conventional passive structure blades to be compared equally under identical flight conditions. For hovering flight cases an alternative solution approach is available that uses a linearized system of equations developed about a steady-state hovering flight solution. This approach is particularly useful for stability and control studies and is easily used with traditional eigenanalysis techniques.

As previously discussed in an earlier section of this report, the PETRA analysis has been used in conjunction with the CAMRAD-II code in numerical studies to investigate the theoretical actuation capabilities of active fiber composites (AFC) for controllable blade twist applications. In addition to quantifying the relative performance of AFC actuators, the ability to alleviate rotor vibrations has also been examined. Results of these analytical studies are presented in reference 92.

Current and Planned Helicopter Research

Helicopter research in the AB/TDT continues to involve testing of both passive and active rotor configurations, with comprehensive analyses being used in the design of models and planning of tests. Currently, the emphasis is on continued testing and development of the active twist rotor (ATR) concept with research on additional active controls concepts under consideration. For example, the use of smart materials in the development of a "swashplate-less" rotor system will be of interest in the next few years. Testing of additional high-lift rotor configurations using slotted airfoils is planned. Continued analysis using CAMRAD-II will be conducted to investigate the role played by various rotor parameters in the reduction of fixed-system vibration. It is hoped that additional testing will also be conducted in support of the efforts using CAMRAD-II.

Tiltrotor Research Contributions

The Bell/Boeing V-22 Osprey (fig. 107) that is being built for the U. S. Military is a tiltrotor aircraft combining the versatility of a helicopter with the range and speed of a turboprop airplane. The V-22 represents a tiltrotor lineage that goes back fifty years, during which time contributions to the technology base needed for its development were made by both government and industry. NASA Langley Research Center has made substantial contributions to tiltrotor technology and development in several areas, in particular in the area of aeroelasticity. The purpose of this section of the paper is to present a chronological summary of the

tiltrotor aeroelastic research conducted in AB/TDT that has contributed to that technology.

Tiltrotor aeroelastic research in the TDT formally began in 1968, but its roots actually extend back to 1960 when an extensive test program was initiated to study the phenomenon of propeller whirl flutter. A brief review of these early studies that are relevant to the subject area is presented first. This work includes the whirl flutter studies conducted initially for conventional propellers, then for propellers having blades with flapping hinges, and finally for high-bypass-ratio ducted fan-jet engines. The major portion of this section addresses the tiltrotor aeroelastic studies which were conducted later, first (1968-1974) in support of the program which led to the XV-15 tiltrotor research aircraft, then (1984-1985) in support of the V-22 tiltrotor aircraft development program, and finally (1994-present) as part of Langley's base research in tiltrotor aeroelasticity. The development of essential computer programs for aeroelastic stability and response analyses of tiltrotor aircraft was initiated in 1970 and has proceeded concurrently with the experimental studies (table 2). Illustrative results obtained from these wind-tunnel tests as well as from companion analyses are presented and discussed. The section concludes with a résuméof current and planned research activities in tiltrotor aeroelasticity.

Relevant Early Work

Propeller Whirl Flutter

Propeller whirl flutter is a self-excited whirling instability that can occur in a flexibly-mounted aircraft propeller-engine combination. The possibility that such an instability might occur was first mentioned as early as 1938. However, the very large margins of safety prevalent at that time and in later years resulted in the phenomenon being accorded only academic interest. In particular, the instability was studied extensively at Rensselaer Polytechnic Institute in the early 1950s by Professor Robert H. Scanlan and his group. The instability remained of academic interest until 1960 when it became of practical concern following the loss of two Lockheed Electra aircraft in fatal accidents. Extensive studies were conducted in the TDT on a 1/8-scale, full-span, dynamic aeroelastic model of the subject aircraft (fig. 108) as part of a national investigation into identifying the cause of the accidents. The TDT studies showed that propeller whirl flutter was possible if the engine support stiffnesses were sufficiently reduced, say due to damage (refs. 218-219). The initial propeller whirl flutter analyses were also developed at this time (refs. 220-221). Following wind-tunnel tests of the Electra model, a more general investigation of propeller whirl flutter was initiated with the aim of identifying and studying the pertinent parameters influencing the phenomenon and to obtain data for verifying analyses. The first study (ref. 222) involved a model of an isolated propeller/pylon/engine system mounted with flexibility in pitch and yaw on a rigid sting support structure (fig. 109). The second study (ref. 223) employed the propeller of reference 222 mounted on a cantilever semispan wing (fig. 110) to determine the effects of a flexible wing on whirl flutter. Reference 223 also extended the analyses of references 220-221 to include the fundamental bending and torsion degrees of freedom of the wing.

Tests of the Electra model, and the ensuing whirl flutter tests of propeller/pylon and propeller/pylon/wing components from the complete model, were the first significant series of flutter tests of a real aircraft to be conducted in the newly constructed TDT. The experimental studies on the Electra model clearly identified propeller whirl flutter as the most likely culprit in the accidents and pointed the way to the necessary structural changes that needed to be made in the aircraft to preclude whirl flutter. These studies also established the initial credibility of the TDT as a unique national facility for testing large flutter models. The experimental and analytical studies conducted on isolated components from the Electra model resulted in a wealth of new information on important design parameters influencing the whirl flutter phenomenon and established in the open literature a large database for validation of analyses.

Whirl Flutter of Flapping-Blade Propellers

Several V/STOL aircraft concepts based on the use of propellers having blades which had a hinge at their root to permit flapping motion out of the plane of rotation were proposed as research vehicles in the 1960s, some reaching flight test status.

These included the Grumman proposal in the Tri-Service VTOL Transport Competition, the Vertol VZ-2 built for the Army, and the Kaman K-16B amphibian built for the Navy. Because of the attention that was being directed to propeller whirl flutter, it became of interest to consider the manner in which whirl flutter might be altered by the use of hinged blades (ref. 224). Experimental studies using small models (all having propeller diameters of about one foot) were conducted by researchers in government, industry, and academia. These studies showed that either backward or forward whirl flutter could occur for propellers having blades with flapping hinges, in contrast to propellers with fixed blades that flutter only in the backward whirl mode. In parallel with these experimental studies, several researchers extended conventional propeller whirl flutter analyses to include the blade flapping degree of freedom. The whirl flutter equations for propellers with hinged blades developed by Richardson and Naylor (ref. 225) appeared in the open literature at about this time and were used by several researchers, including those in AB. However, none of the analyses that were developed was able to successfully predict the forward whirl instabilities that were obtained experimentally (ref. 226).

The low-speed model tested and studied by AB researchers is shown in figure 111. It consisted of a windmilling propeller mounted on a spring-restrained rod that could rotate in pitch and yaw about a set of gimbal axes behind the propeller. The (symmetric) stiffness could be controlled by varying the tension in a spring connected axially at the other end of the rod. Each blade was attached to the hub by means of two pins, such that when both pins were in position the blades were fixed (fig. 111a); and when one of the pins was removed the other pin became a flapping hinge (fig. 111b). The hub geometry was such that hinge offsets of 8% and 13% could be set. Testing was conducted in both a working model of the Langley Full-Scale Tunnel and the Langley 12-foot Low-Speed Wind Tunnel. Analysis predicted the backward whirl flutter that occurred for the fixed and 13% hinge offset cases but failed to predict the forward whirl flutter that occurred for the 8% hinge offset case. Similar difficulties were being experienced by other researchers in predicting forward whirl flutter on their models. The inability of analyses to predict the forward whirl flutter behavior observed in tests of these model propellers caused considerable dismay in the analysis community. This concern was formally expressed by Eugene Baird of Grumman Aircraft at a meeting of the Aerospace Flutter and Dynamics Council in November 1969. In prepared comments made to the Council summarizing the state of affairs, Baird questioned whether proprotor whirl flutter could be predicted with confidence and asked that NASA Langley look into the issue. The predictability question was settled in 1971 by tests conducted in the TDT using a research configuration of a Grumman tiltrotor model, the results of which are discussed in a later section.

Whirl Flutter of Turbofan Engines

In the mid-1960s, high-bypass-ratio turbofan jet engines were being developed for the Boeing 747 and Lockheed C-5A. These engines are characterized by a large-diameter ducted fan ahead of the engine nacelle. Because of the large gyroscopic and aerodynamic forces acting on the fan, it was thought that a flexibly mounted engine could be susceptible to a whirl-type instability analogous to propeller whirl flutter. Preliminary studies to explore the possibility of whirl flutter in such engines were conducted by AB researchers in 1966-68. The initial studies used the low-speed model shown in figure 112. The model employed a windmilling fan inside a duct that was mounted on a sting and elastically restrained with freedom to oscillate in pitch and yaw about a set of gimbal axes located behind the fan. A range of duct chord-to-diameter ratios, restraint stiffnesses, and gimbal axis locations were investigated experimentally (in the Langley 12-foot Low-Speed Wind Tunnel) and the results compared with analysis. Static and dynamic stability derivatives of importance to whirl flutter were also measured. An existing three-dimensional theory for computing the static derivatives of ducted propellers at angle of attack was extended under contract to include the calculation of the important dynamic derivatives. The resulting quasi-static analysis using measured derivatives was found to give good agreement with the measured instability boundaries. The results of this investigation are summarized in a Langley internal report (Rao, K. V. K.: *A Preliminary Investigation of Whirl-Flutter*

Characteristics of High By-Pass Ratio Ducted Fan-Jet Engines. LWP 523, 1967).

Some limited testing was conducted later by the second author in the Langley 8-foot Transonic Pressure Tunnel using the high-speed engine model shown in figure 113 to measure the static stability derivatives at full-scale Mach numbers. The engine was mounted on a six-component balance that was attached to the end of a cantilevered wing. A balsa wood aerodynamic fairing fixed to the wing tip surrounded the balance and its fittings. The extended theory mentioned above and the derivatives measured on the high-speed model were applied to a typical set of full-scale nacelle parameters but using a reduced value of nacelle-pylon support stiffness to approximate a partially failed structural condition. The calculated stability boundaries, taken from reference 227, are shown in figure 114. The velocities associated with the two instability boundaries, whirl flutter and static divergence, are shown in the figure as a function of cowl-length-to-diameter ratio. In spite of the lowered support stiffness assumed in the calculations, both stability boundaries are at relatively high velocities. These results suggested that whirl flutter of high-bypass-ratio fan-jet engines as (then) being planned for the 747 and C-5A should not be a serious problem. The results also indicated that relatively simple whirl flutter analyses using measured stability derivatives are probably adequate.

Tiltrotor Aeroelastic Research

Preparatory Remarks

A number of essential aeroelastic analyses have been developed and implemented into computer programs by AB researchers, either in support of the tiltrotor testing in the TDT or as part of broader studies being conducted by the AB. Because several of these programs will be mentioned by name and results obtained from them will be shown in this section of the paper, a brief summary of these aeroelastic analyses is appropriate before beginning discussion of the tests. In addition, due to the significant role played by proprotor-induced aerodynamic forces on all facets of tiltrotor aircraft stability, a brief comment on these forces here would aid in understanding the stability results to be presented.

Aeroelastic Analysis Development: The development of tiltrotor aeroelastic analyses at AB has proceeded along the lines indicated in table 2. Most of the analytical work encompassed the periods during which testing was being conducted in the TDT. The initial phase of the analytical development (1970-72) was intended to support the experimental work being done in the TDT at that time in support of what would become the XV-15, as well as to serve as part of a Ph.D. dissertation (ref. 228). The second phase (1973-74) involved some enhancements and extensions to the codes developed during the initial phase as a prelude to the phasing out of this research area by the Branch. Several major extensions and enhancements to the stability code were made in the period 1984-85 to provide analysis support both during and after the tests conducted on a V-22 flutter model in the TDT. The latest phase of aeroelastic analysis development began in 1991. The development during 1991-93 was primarily intended for a Ph.D. dissertation (ref. 145). However, this analytical work was continued, and several other analyses were initiated later, in support of the new tiltrotor research program initiated within the AB in 1994.

Programs PRSTAB1 - PRSTAB9 are a series of linear stability analysis codes of increasing dynamic and aerodynamic complexity in the rotor modeling, all of which are based on a lumped mass-spring-damper representation of the wing structure. The analysis on which PRSTAB6 is based is described in reference 228. HFORCE1 is a code for computing rotor oscillatory force and moment derivatives due to shaft pitching oscillations. GUST1 is a version of HFORCE1 that includes a vertical sinusoidal gust in the computation of the rotor hub oscillatory inplane shear forces. ROTDER1 - ROTDER4 are codes for computing rotor oscillatory flapping derivatives due to shaft pitching oscillations. The analytical bases of programs HFORCE1 and ROTDER4 are described in reference 228. The lumped parameter model of the wing in PRSTAB9 was replaced by a modal model in 1984 and the new program called PASTA1 (Proprotor Aeroelastic STability Analysis, version 1.0). PASTA2 and 3 were ex-

tensions of PASTA1 to include first a blade coning hinge (1984) and then an airplane rigid-body stability analysis capability (1985). A PC version of PASTA3 was developed in 1987. Several upgrades of the PC version of the code were made in 1995-96. Major enhancements made at that time include: engine gyroscopic effects, improved treatment of airframe support springs for representing spring-supported wind-tunnel models, addition of a five-degree-of-freedom drive system dynamic model, provision for reading in externally-computed (MSC/NASTRAN) quasi-steady generalized aerodynamic force matrices for the wing elastic modes, and the QZ algorithm for solving the generalized matrix eigenvalue problem. PASTA4.1 is the most recent version of the code that is available for public distribution. This is also the version that is typically used in AB. A MATLAB version of PASTA4.1 was developed in 1998.

PASTA4.1 is a code for the aeroelastic and rigid-body stability analysis of a tiltrotor aircraft in the airplane mode of flight. The analysis is based on a ten-degree-of-freedom linear mathematical model of the rotor and drive system. The rotor is assumed to be windmilling (i.e., nonthrusting) but perturbations in the rotor rotational speed can be mechanically coupled to the airframe through the torsional dynamics of the drive system. The blades are assumed to undergo rigid flapping motion due to both the gimbal action of the hub and an offset coning hinge. The blades are also assumed to execute rigid lead-lag motion about a virtual lag hinge. Quasi-steady strip-theory aerodynamics is employed for the blade airloading. Compressibility effects are introduced using a Ribner Mach number correction that is applied to the blade lift curve slope. A modal representation is employed for the airframe (up to ten modes). Either full-span or semi-span configurations can be treated. The aerodynamic forces acting on the airframe rigid-body modes are expressed in terms of stability derivatives. No airloads are assumed to be acting on the wing elastic modes. Stability is determined by examining the eigenvalues that are obtained by solving the system equations as a matrix eigenvalue problem.

UMARC/G is a general-purpose aeroelastic analysis applicable to tiltrotor aircraft operating in the helicopter, conversion and airplane modes of flight that was the subject of a Ph.D. dissertation (ref. 145). It is an extensive modification of a helicopter analysis called UMARC (University of Maryland Advanced Rotorcraft Code) developed at the University of Maryland. A finite-element methodology using anisotropic beam elements is employed for structurally modeling the rotor blades and the wings. Quasi-steady aerodynamics are assumed for the wing airloading. Either quasi-steady or Leishman unsteady aerodynamics can be employed for the blade airloads. The rotor wake can either be prescribed or treated as a free-wake using either the Scully or Baigai wake models. The resulting nonlinear equations are linearized about a trim solution that is calculated using a time-finite-element method. Stability is determined by solving for the eigenvalues of the matrix that results by applying either the constant coefficient approximation or Floquet theory to the linear perturbation equations with periodic coefficients. Blade loads can also be calculated as part of the trim solution. UMARC/G is currently being extended as part of a Ph.D. investigation to include aerodynamic interaction effects between the rotor and the wing, and a drive train dynamics model including the rotor speed perturbation (ref. 229). UMARC/S is the Sikorsky Aircraft version of UMARC/G that has been modified to analyze blades with multiple load paths such as those associated with the bearingless rotor design of the variable diameter tiltrotor (VDTR), a Sikorsky concept aimed at improving the tiltrotor's performance in the helicopter and airplane modes of flight (refs. 230-231).

MBDyn is a multi-body code that is under development at the *Dipartimento di Ingegneria Aerospaziale of the Politecnico di Milano*, Italy. MBDyn is intended to be a general-purpose tool for the multi-disciplinary analysis of complex aerospace systems. Extensions of the analysis and the code to tiltrotor configurations were begun by a Ph.D. candidate from the university while he was in residence at AB during the summer of 1998. Since that time, a number of applications of that code have been made to the Wing and Rotor Aeroelastic Testing System (WRATS) testbed (refs. 232-234).

Rotor-Induced Aerodynamic Forces: Disturbances occurring in flight can, depending on their frequency content, excite either the elastic or rigid-body modes of an aircraft in an oscillatory manner. For a tiltrotor aircraft, any motions of this type effectively represent oscillatory motions of the proprotor shaft in space. This leads to proprotor-generated forces and moments that are a function of these oscillatory motions (ref. 228). Figure 115 shows the perturbation rotor aerodynamic forces acting on an aircraft executing small pitching and yawing motions when operating in an airplane mode of flight. From the position of these forces on the aircraft, it is clear that the forces shown can influence aircraft longitudinal and lateral-directional stability. However, the shear forces H and Y can, quite independently of any rigid-body motions, also destabilize the proprotor-pylon-wing system aeroelastically. In fact, it is precisely these forces that are the drivers for proprotor-pylon whirl flutter. Propeller whirl flutter, on the other hand, is driven by aerodynamic cross-stiffness moments. A discussion of these and other important differences in the aeromechanical behavior of propellers and proprotors is given in reference 228.

Bell Model 266

In 1965, the U. S. Army started the Composite Aircraft Program with the objective of producing a rotary-wing research vehicle combining the characteristics of an airplane and a helicopter. Bell Helicopter Company proposed a tiltrotor design designated the Model 266 (fig. 116) and was awarded one of the two exploratory definition contracts that were let under the program. The design features a three-bladed proprotor with highly twisted blades that are rigidly attached to a hub assembly that is gimbal-mounted to the mast. Hub flapping restraint is employed to increase control power when operating in the helicopter mode. Three degrees of precone is built into the pitch axis of each blade to ensure blade pitch-lag stability. The proprotor is designed so that the blade lowest inplane natural frequency remains well above the rotor rpm over the entire operating range, thus precluding mechanical (ground resonance) instability. The blades have a built-in structural twist of −27.7°. A blade root cuff extending from the hub to 30% blade radius results in an overall aerodynamic twist of −43.5°. Blade kinematic (mechanical) pitch-flap coupling (δ_3) is employed to reduce flapping in maneuvers and gusts when operating in the airplane mode of flight. Positive pitch-flap coupling (negative δ_3) was selected for the Model 266 rather than the more conventional use of negative pitch-flap coupling (positive δ_3) to preclude blade flap-lag instability (ref. 235). The value of positive pitch-flap coupling used on the Model 266 ($\delta_3 = -22.5°$) lowers the blade rigid-body flapping frequency below one-per-rev (1P), and as the inflow angle increases with airspeed the frequency is further decreased. This ensures an adequate separation of this mode from the blade inplane mode whose frequency is also decreasing with airspeed, thus preventing the coupling necessary for a flap-lag instability. The Model 266 wing is designed to be soft in bending (the fundamental cantilevered vertical and fore-and-aft bending (beam and chord) mode frequencies are below 1P) but stiff in torsion (torsion mode frequency is above 1P).

A 1/7.5-scale semi-span model that is a dynamic and aeroelastic representation of the Model 266 proprotor, pylon and wing was built by Bell in support of their studies. When the program was terminated in 1967, the model was given to the Aeroelasticity Branch by the Army. Both NASA and Bell were interested in continuing the experimental work initiated by Bell with the model to further define the aeroelastic and dynamic characteristics of proprotor-type aircraft. This common interest led to a joint NASA/Bell investigation in the TDT of proprotor stability, dynamics, and loads using the model in September 1968. The model is shown in airplane and conversion modes in figures 117 and 118, respectively. The model was Froude-scaled for operation in air and could be run with the proprotor either powered or windmilling. The model proprotor has a diameter of 5.1 feet. For windmilling operation the rotor rpm was controlled remotely by adjusting blade collective pitch. The rotor was disconnected from the drive train when windmilling to reduce wear on the bearings. A close-up view of the pylon with its spinner and aerodynamic fairings removed is shown in figure 119. Scale factors pertinent to the model are given in table 3. Since the high-speed (airplane) mode of flight is critical in-

sofar as proprotor-pylon instability is concerned, most of the effort was devoted to investigating the airplane mode of flight with the pylon fully converted forward and the airflow passing axially through the rotor.

Some results pertaining to stability and gust response while operating in an airplane mode with a windmilling proprotor are shown in figures 120-124, where equivalent full-scale values are given. The effects of several system parameters on stability over the design rpm range of the Model 266 are shown in figure 120. The calculated stability boundaries shown were obtained using program PRSTAB6. Figure 120 shows that, with respect to the stability boundary of the reference configuration, altitude is stabilizing, increased pylon yaw flexibility is destabilizing, and both hub flapping restraint and wing aerodynamics are stabilizing. The wing beam mode (consisting primarily of wing vertical bending) was the system mode that went unstable in all of the cases shown. Figures 121 and 122 provide an indication of the relative degree to which stability of the wing beam mode is affected by rotor-induced aerodynamic forces and wing aerodynamics. The calculated results were computed using program PRSTAB8. Figure 121 illustrates the dominant role played by rotor aerodynamic forces in the balance of forces leading to flutter of the proprotor-pylon-wing system. Figures 121 and 122 show that wing aerodynamic forces have only a slight stabilizing effect. The calculated results in figure 122 also show the stabilizing effects of blade inplane flexibility. The sharp rise in the damping at about 170 kt in figure 122 is associated with the coupling of the blade inplane (lag) bending mode with the wing vertical bending (beam) mode. The dynamic response characteristics of the model due to excitation by a vertical sinusoidal gust that was generated by the TDT airstream oscillator (fig. 5) were also studied. The measured variation of gust-induced angle of attack versus vane oscillation frequency is shown in figure 123, where the quantities have been normalized as indicated to make them independent of vane amplitude and airspeed. These data were measured using a flow direction transmitter that was mounted at the upstream end of a boom extending from the nose of the model as seen in figure 118. Some results showing the variation of wing vertical bending moment with gust frequency for the rotor-on and rotor-off conditions are shown in figure 124. Calculated results were obtained with program GUST1 using the gust curve of figure 123. It is clear that proprotors operating at advance ratios typical of airplane mode flight are quite sensitive to vertical gusts.

The results of this wind tunnel investigation as well as companion analytical studies that were conducted are described in references 228, 236, and 237. Reference 228, in particular, contains the results of an extensive analytical parametric investigation into the effects of several important system design parameters on stability.

Bell Model 266 - Folding Proprotor Variant

A joint NASA/Bell/Air Force test was conducted in the TDT in January 1970 to investigate any potential problem areas associated with the folding proprotor variant of the tiltrotor concept. The model used in this study was the same model employed in the previous investigation, but modified to include a collective drive motor that permitted rapid feathering and unfeathering of the proprotor and a manually adjustable blade folding hinge (figs. 125 and 126). The main objectives of the test were to investigate stability in the airplane mode of flight at low (including zero) rotor rotational speeds, during rotor stopping and starting, and during blade folding. The rotor was unpowered for this test. The stability boundary obtained for one of the configurations tested is shown in figure 127, where equivalent full-scale values are shown. The variation of flutter airspeed with rotor rpm as rpm is reduced from its maximum design value to zero is shown. As indicated in the figure, the model experienced several different modes of instability as rpm was reduced. The instability experienced at low and zero rpm was unexpected as no pretest predictions were made at those rpm. Based on analytical studies conducted after the test to gain an understanding of the phenomenon, it was concluded that blade precone was the primary cause of the instability (refs. 228, 237). The subcritical response through flutter for the 172 rpm condition is shown in figure 128 where, in addition to the measured wing beam mode damping and frequency, the calculated

variation of both the wing beam and low-frequency rotor flapping modes is shown. These results indicate a changeover from a dominant (least stable) wing beam mode to a dominant (least stable) rotor flapping mode as airspeed is increased. The effect of the blade flapping degree of freedom on stability is illustrated in figure 129, which compares the wing beam mode damping versus airspeed at 300 rpm for flapping locked and unlocked. Stability calculations were made using program PRSTAB6.

The variation of steady-state one-per-rev blade flapping response with rotor rotational speed for a (nominally) constant shaft angle-of-attack is shown in figure 130. These data were taken to establish a steady-state flapping response baseline for evaluating the transient flapping response during the rotor feathering portion of the test (ref. 238). The calculated results shown were obtained using program ROTDER4. The peak in the flapping response occurs when the rotor rotational speed is in resonance with the blade flapping natural frequency in the rotating system.

Bell Model 300-A1A

In 1968, Bell Helicopter initiated an in-house development program for a tiltrotor aircraft designated the Model 300 that would ultimately evolve into the XV-15. This design, like the Model 266, features a three-bladed proprotor with highly twisted blades that are rigidly attached to a hub assembly that is gimbal-mounted to the mast. Hub flapping restraint is employed to increase control power when operating in the helicopter mode. Blade precone is 2.5º and $\delta_3 = -15º$. The blade first inplane natural frequency again is well above the rotor rpm, thus precluding ground resonance instability. The cantilevered wing beam and chord mode frequencies are well below 1P but the torsion mode frequency is only slightly below 1P. In support of this aircraft design activity, Bell designed and built a 1/5-scale, full-span dynamic aeroelastic model for testing on a vertical rod mount in the TDT. The model was Froude scaled for air because of testing that was to be conducted in the LTV Low-Speed Wind Tunnel before coming to the TDT for flutter clearance testing. However, the model was sized so that it would also be Mach scaled when tested in R-12 (recall discussion in Model Scaling Considerations section). The model proprotor had a diameter of five feet. Scale factors for the model are given in table 4.

The Bell Model 300-A1A was tested in the TDT in August 1970 (fig. 131). This test was intended to be the required flutter clearance demonstration for the aircraft over its simulated flight envelope. However, unexpectedly poor lateral-directional flying qualities exhibited by the model during the test precluded the conduct of a flutter clearance test. The test convinced Bell to change the design of the tail from a single-vertical-tail configuration to an H-tail configuration (ref. 239).

Grumman Helicat

A joint NASA/Grumman investigation of a 1/4.5-scale semi-span model (fig. 132) of a Grumman tiltrotor design called Helicat was conducted in two entries in the TDT during February/March 1971. The Helicat design featured a stiff (strut-supported) wing that resulted in the wing beam, chord and torsion mode frequencies all being well above 1P. The three-bladed proprotor had blades with 5% offset flapping hinges and 30º positive δ_3. The blades were also stiff-inplane so that their first inplane natural frequency was well above rotor rpm. The model was targeted for flutter clearance testing in the TDT and thus was Mach scaled for R-12. However, the model was sized so that it would also be Froude scaled if tested in R-12 (recall discussion in Model Scaling Considerations section). The model proprotor had a diameter of 4.9 feet. Scale factors for the model are listed in table 5.

A blade flap-lag instability that destroyed one blade and damaged another occurred unexpectedly during an early checkout run of the model in air. It was found that the model blades were considerably softer inplane than expected and this, in combination with the value of positive δ_3 used, led to a coalescence of the blade flap and lag natural frequencies with increasing airspeed and the resulting instability (ref. 235). The model was repaired, the design value of δ_3 reduced from +30º to +20º, and a flutter clearance test conducted in the second (March) entry without incident (ref. 240).

During the second entry, an off-design research configuration of the model (fig. 133) was employed in an extensive investigation of proprotor whirl flutter. This portion of the test was aimed at establishing the whirl flutter database needed to respond to Gene Baird's 1969 challenge of resolving the whirl flutter predictability issue. A range of pylon pitch and yaw stiffnesses, blade hinge offsets, and blade kinematic pitch-flap couplings were investigated over a wide range of windmilling advance ratios in air. To obtain flutter at low tunnel speeds, a reduced-stiffness pylon-to-wing-tip restraint mechanism (fig. 134) that permitted independent variations in pylon pitch and yaw stiffness was employed. The restraint was sufficiently soft so that the wing was effectively rigid. Fifty cases of forward whirl flutter and 26 cases of backward whirl flutter were clearly identified (ref. 241). Some whirl flutter results from reference 241 showing the effect of pitch-flap coupling (δ_3) on stability of a symmetric pylon configuration are given in figure 135, where the flutter advance ratio, $V_F/\Omega R$, is plotted versus pylon frequency nondimensionalized by the rotor speed. For the cases shown, all flutter occurred in the forward whirl mode, except for the two points denoted by the solid symbols, which were in the backward whirl mode. The calculated results were obtained using program PRSTAB5. The measured whirl flutter characteristics (flutter speed and frequency, direction of pylon whirl, and pylon yaw-to-pitch amplitude ratio and phase angle) were in excellent agreement with predictions from two different four-degree-of-freedom linear stability analyses (PRSTAB5 and ref. 225) for all of the configurations tested (ref. 241). This study clearly demonstrated that proprotor whirl flutter, both backward and forward, can be predicted with confidence using linear analyses based on relatively simple math models and quasi-steady strip-theory aerodynamics for the blade airloads.

Aerodynamic Test of Bell Model 300-A2A

A joint NASA/Bell investigation employing a 1/5-scale full-span sting-mounted aerodynamic (force) model of the Bell Model 300 with the new H-tail (designated the Model 300-A2A) was conducted in the TDT in August 1971 for the purpose of determining the longitudinal and lateral static stability and control characteristics and establishing the effect of the proprotors (windmilling only) on the basic airframe characteristics. The model is shown in figure 136. The rotors used on this model were the same ones used on the aeroelastic model. Use of R-12 permitted testing at full-scale Mach numbers and near full-scale Reynolds numbers (ref. 239). Blade flapping was measured in both air and R-12 for several values of tunnel airspeed over a range of sting pitch angles. The resulting flapping derivatives are shown in figure 137. Since the range of inflow (advance) ratios over which the derivatives were measured was the same in air and R-12, and the test medium density at the simulated condition was about the same, an indication of the effects of Mach number on the flapping derivatives can be obtained by comparing the air and R-12 results. The drag rise associated with operating at high Mach numbers is seen to reduce flapping as Mach number is increased. The calculated results shown were obtained using program ROTDER4.

Flutter Clearance Test of Bell Model 300-A2A

The 1/5-scale full-span rod-mounted aeroelastic model of the Bell Model 300 with the new H-tail was tested in the TDT in March 1972 (fig. 138). The objective of the test was to demonstrate that the design had the required flutter margin of safety and to confirm that the aircraft rigid-body modes were adequately damped over the simulated flight envelope (ref. 242). Aeroelastic and flight mode stability were assessed in both R-12 and air over the simulated flight envelope with windmilling proprotors. The Model 300 was shown to be flutter free up through the 1.2 V_L requirement of the aircraft and to exhibit good flight mode stability beyond the V_L requirement of the aircraft. A cursory investigation of the autorotational characteristics of the model was also conducted (fig. 139).

During this test, the importance of rotor "thrust damping" (forces T in figure 115) on stability of the Dutch Roll mode was dramatically demonstrated when the rotor interconnect shaft broke and the model went into a violent Dutch Roll instability. Tiltrotor aircraft employ an interconnect shaft between the two rotor/engine systems so that in the event of an engine failure either engine may

drive both rotors. The interconnect shaft also maintains synchronization of the rotor speeds during any aircraft motions. This means that yawing motions of the aircraft generate perturbation lift forces that tend to damp the yawing motion, as indicated in figure 115. If this synchronization is lost due to a failed interconnect shaft this damping is lost. The Dutch Roll stability boundary of the model was mapped in air with the interconnect shaft engaged and disengaged to assess the effect of thrust damping. The results are illustrated in figure 140, which shows the variation in the damping of that mode with tunnel airspeed for each of those two cases. The substantial contribution of thrust damping to total damping is quite apparent.

In 1973, NASA and the Army selected Bell to design and build two tiltrotor research aircraft (to be later named the XV-15) based on the Model 300-A2A design. Roll out of the first aircraft occurred in 1976. First flight took place in 1977. The XV-15 (fig. 141) has been an extremely successful research aircraft. Both aircraft are still being used extensively today. The long-term success of the XV-15 tiltrotor, both as a technology demonstrator and as a flight research aircraft, went a long way toward establishing the technical confidence and expertise for proceeding with the development of the V-22. Indeed, it is probably fair to say that if there had not been an XV-15, there would not now be a V-22.

Bell/Boeing JVX (V-22)

A 1/5-scale dynamically and aeroelastically scaled semi-span model (fig. 142) of first a preliminary design and then an updated version of the Bell/Boeing JVX (V-22) was tested in two entries in the TDT during February and June of 1984. The V-22 design features a three-bladed proprotor with highly twisted blades that are attached via coning flexures to a hub assembly that is mounted to the mast with a constant-velocity joint that eliminates two-per-rev torque oscillations of the drive shaft. Hub flapping restraint is employed to increase control power when operating in the helicopter mode. Blade precone is 2.5º and $\delta_3 = -15º$. The blades are stiff inplane so that their lowest inplane natural frequency is above the rotor rpm and remains well separated from the first and second harmonics of the rotor rotational speed. The cantilevered wing beam and chord mode frequencies are well below 1P while the torsion mode frequency is only slightly above 1P. The semi-span model was the right half of the full-span model that was designed and built by Bell for testing in the Boeing V/STOL Wind Tunnel. For this reason, the model was Froude scaled for air. However, like the earlier model of the XV-15, the V-22 model was sized so that it would also be Mach scaled when tested in R-12 (recall discussion in Model Scaling Considerations section). The model proprotor has a diameter of 7.6 feet. Scale factors for the model are listed in table 6.

The main objective of the TDT tests was to confirm predicted stability in the high-speed airplane mode of flight and to provide data for correlation with the aeroelastic stability analyses being used by the contractors in their preliminary design work. Testing was conducted in both R-12 and air. The model was tested in both powered and unpowered conditions. However, most of the testing in the airplane mode of flight was done with a windmilling proprotor. A variety of configurations were tested and analyzed. Parameters that were varied included pylon-to-wing locking (on and off downstop), rotor rpm, blade pitch-flap coupling (δ_3), hub flapping restraint, and wing and blade stiffness distributions. Several configurations of the model with an updated hub design that had offset coning hinges in addition to the gimbal were tested in the second entry. Some illustrative results from the first entry are presented in figures 143 and 144 as the variation with airspeed of the calculated and measured damping and frequency of the three lowest wing modes that are of importance to stability of the rotor-pylon-wing system. The wing beam mode (primarily wing vertical bending) is seen to be critical (lowest flutter speed) for the case shown in figure 143 while the wing chord mode (primarily fore-and-aft wing bending) is critical for the case shown in figure 144. The wing torsion mode was not critical for any of the configurations tested in either of the entries. The "peaks" which are evident in the calculated damping curves for the wing beam and chord modes in both of the cases shown are due to the coupling of those modes with the blade lag (inplane bending) mode as velocity is increased, as can be seen by inspection of the plots showing

the variation of the modal frequencies with airspeed. The calculated results shown were obtained with PASTA1.

Data of the type shown in figures 143 and 144 were obtained for all of the configurations tested in both of the entries. The PASTA code (initially version 1.0 and later 2.0) was used extensively during the tests and comparisons made with measured subcritical damping variation with airspeed up to instability. The demonstrated accuracy of the PASTA code in these comparisons prompted Bell to use the program extensively during the preliminary design phase of the V-22. Since that time, the code has been used in government, industry, and academia for a variety of tiltrotor studies.

The experimental results obtained during the V-22 model tests are documented in internal company reports. A concise summary of the tests may be found in reference 243.

WRATS Tiltrotor Testbed (1995 – 2000)

The 1/5-scale aeroelastic model, which was used by the V-22 contractors to support the preliminary and full-scale design phases of the aircraft, had a long and distinguished test history (ref. 244). Upon completion of that series of tests, the Navy transferred the components for the right-half semi-span configuration of the model to NASA Langley under a loan agreement to be used as the experimental testbed for a new tiltrotor aeroelastic research program that was initiated at AB in 1994. The tiltrotor testbed (fig. 145) was designated the Wing and Rotor Aeroelastic Testing System (WRATS).

The focus, general scope, and initial elements of the new AB tiltrotor research program were laid out in collaboration with Bell Helicopter Textron, Inc. (BHTI), with due regard to NASA's Short Haul Civil Tiltrotor Program that was being planned at the time. It was agreed that the program would focus on those aeroelastic areas that were identified as having the potential for enhancing the commercial viability of tiltrotor aircraft. In particular, considerable emphasis was to be directed to the development and evaluation of modern adaptive control techniques for active vibration control and stability augmentation of tiltrotor aircraft. Attention was also to be given to the use of passive design techniques to enhance aeroelastic stability and aerodynamic performance.

A shakedown test of the WRATS tiltrotor testbed was conducted in the TDT in April 1995. A chronological summary of the tests conducted to-date on the testbed following the shakedown test is given below. BHTI, under a Memorandum of Agreement with NASA, was a partner in all but one of these tests.

August 1995: This was the first research test of the WRATS model in the TDT. The objectives of the test were twofold: (1) to establish the stability characteristics of the baseline configuration; and (2) to evaluate a higher harmonic control (HHC) algorithm for reducing aircraft vibrations by actively controlling the wing flaperon. The test was conducted in air with a windmilling rotor.

The first objective of this test was to establish the stability characteristics of the baseline model, which had a wing spar representing the untailored wing design of the V-22. Stability boundaries measured on the baseline model for two different values of the wing torsion natural frequency are presented in figure 146 as the variation of rotor speed with tunnel airspeed. The wing torsion frequencies were varied by changing a connection spring that represented the stiffness of the pylon/wing downstop locking mechanism. The figure indicates that stability is strongly influenced by wing torsion frequency, with a difference of only 0.2 Hz producing a shift of about 12 knots at constant rpm.

The second objective of this test was to evaluate a higher harmonic control algorithm called MAVSS (Multipoint Adaptive Vibration Suppression System) for its effectiveness in reducing vibrations in the airplane mode of flight by actively controlling the wing flaperon. MAVSS was developed by BHTI for reducing rotor-induced aircraft vibrations occurring at integer multiples of the rotor speed. The MAVSS algorithm, which operates in the frequency domain, assumes that changes in aircraft vibratory responses are linearly related to changes in control inputs through a system transfer matrix that is identified on line. The

deterministic controller on which MAVSS is based is obtained by minimizing a scalar performance index which includes the harmonic vibratory responses to be reduced, the HHC inputs necessary to effect the reduction, and the transfer matrix describing the dynamics of the system. The active flaperon model hardware consisted of a new, stiffer flaperon assembly that replaced the baseline dynamically scaled flaperons and hangers (fig. 147). The active flaperon was driven by a single hydraulic actuator that was mounted on the model splitter-plate inside the fuselage shell. The drive shaft between the actuator and the active flaperon ran along the wing conversion axis where the interconnect drive shaft would be when the model is configured for powered operation. Typical results obtained are illustrated in figure 148, which shows the 3-per-rev vibratory wing torsion loads as a function of tunnel airspeed for the cases in which MAVSS is off and on. The significant reduction in response is evident. The corresponding motions of the flaperon to achieve the load reductions are indicated by the open circles next to the bars. Based on the results of this investigation (ref. 245) it was concluded that active control of an aerodynamic surface (e.g., a flaperon) could produce the forces required for significant vibration reduction in the mode directly influenced by that surface. Multiple responses in different modes are not controlled as well by a single actuator, as might be expected. In all cases, the required motions of the flaperon were found to be quite modest (± 3-deg maximum) and no degradation of aeroelastic stability was noted during activation of MAVSS. The success of the active flaperon test led the way for a 1997 flight test of a MAVSS-controlled active elevator on the XV-15 tiltrotor research aircraft.

December 1995: The objective of this test was to demonstrate that composite wing tailoring could be used to improve proprotor stability. The V-22 has a 23% wing thickness-to-chord (t/c) ratio to provide the wing torsional stiffness required to ensure an adequate level of proprotor-pylon-wing aeroelastic stability within its operating envelope. Studies conducted by Bell as part of a full-scale composite tailored wing study (ref. 246) indicated that by using composite tailoring techniques in the design of tiltrotor wings, a reduction in wing thickness ratio is possible while maintaining acceptable proprotor aeroelastic stability. A reduction in wing thickness would permit higher cruise speeds and/or increased range when operating in the airplane mode of flight. The WRATS testbed was selected for the wind-tunnel evaluation of the composite tailored-wing concept. To this end, Bell designed and fabricated a composite, elastically-tailored graphite-epoxy model wing spar that had the scaled dynamics of a full-scale tailored-wing design having an 18% t/c ratio (ref. 246) and would be interchangeable with the untailored spar of the baseline model (which has a 23% t/c ratio) tested in August 1995. Structural tailoring of the model wing torque box was accomplished by using unbalanced composite laminates in the model wing spar to modify wing bending-torsion coupling. All testing was conducted in air with an unpowered rotor. Some measured and predicted stability boundaries for the baseline and tailored wings over the normal rpm operating range of the model are shown in figure 149. Comparison of the boundaries shows an increase of about 30 KEAS (67 KEAS full scale) in the instability airspeed for the tailored wing. This represents a significant improvement in stability for a full-scale design. Figure 150 shows a typical variation of wing beam mode frequency and damping with tunnel airspeed for the tailored wing in an off-downstop configuration corresponding to the 84% rpm condition of figure 149. The calculated stability boundaries shown in both of these figures were obtained using Bell's ASAP (Aeroelastic Stability Analysis of Proprotors) program. A complete summary of this test may be found in references 247-248.

The tests of the baseline and tailored wings demonstrated that proprotor aeroelastic stability could be increased while reducing the t/c ratio of a wing using composite tailoring techniques. From a broader perspective, this means that composite tailoring can be employed by the designer to increase stability, reduce wing thickness for higher cruise speeds and improved performance, or a combination of these.

January 1996: The August 1995 test was a successful wind-tunnel demonstration of a MAVSS-controlled active flaperon for reducing airframe vibrations. However, it was recognized that a broader evaluation of MAVSS was required

to validate the algorithm for use as an HHC system in tiltrotor applications. The purpose of this January test was to effect this broader evaluation of the MAVSS algorithm. All testing was conducted in air with an unpowered rotor.

The WRATS model was modified to incorporate an HHC system employing both the swashplate and the wing flaperon. The major mechanical modifications made to the baseline model for this test included the replacement of the electric control actuators with high-frequency hydraulic servo-actuators to drive the swashplate, a new servo-controlled wing flaperon (the same one used on the active flaperon test), and the hydraulic lines associated with these actuators. Some of the new components are indicated in figure 151. For convenience, the elastically tailored wing spar from the previous test was retained. The effectiveness of the swashplate and the flaperon acting either singly or in combination in reducing one-per-rev (1P) and three-per-rev (3P) wing vibrations over a wide range of tunnel airspeeds and rotor rotational speeds was demonstrated (ref. 249). The MAVSS algorithm was found robust to variations in tunnel airspeed and rotor speed, requiring only occasional on-line recalculations of the system transfer function. No degradation in aeroelastic stability was noted for any of the conditions tested. The MAVSS control system, when configured to reduce 3P harmonics of the wing loads, was generally able to reduce the wing beam, chord, and torsion load components simultaneously by 85 to 95 percent over the entire range of rotor speeds and tunnel airspeeds considered. Representative results are shown in figure 152. The effectiveness of MAVSS in reducing 1P vibrations was also assessed. For example, figure 153 shows the effect of MAVSS on reducing the 1P vibrations associated with the small inherent imbalance in the rotor. Based on the success of this wind-tunnel demonstration of MAVSS, Bell is currently preparing to test an active vibration suppression system based on MAVSS on the V-22.

April 1998: In 1997, a NASA/Bell team initiated a study (ref. 250) of Generalized Predictive Control to evaluate that method's suitability for implementation as an active stability augmentation system on the WRATS model. GPC is a time-domain predictive control method that uses an ARX representation for the input/output map of the system. The ARX model is used for both system identification and control design. The coefficient matrices of the ARX equation are the quantities determined by the identification algorithm. Closed-loop feedback control is enhanced by performing the system identification in the presence of external disturbances acting on the system. The coefficients of the ARX model are assembled into a multi-step output prediction equation, the desired (target) response is specified, and the resulting expression is used to form a cost function. Minimization of the cost function leads to an expression for the control to be applied to the system.

As part of the GPC study, the team began evaluating a suite of MATLAB m-files for system identification and control that were written by Dr. Jer-Nan Juang of NASA Langley based on the theory of references 251-257. Following extensive numerical simulations that were conducted on simple lumped mass-spring-dashpot math models, and bench tests on the "Cobra stick model" (a 50-lb, 36-inch long multiple-degree-of-freedom lumped-mass dynamic model that approximates the dynamics of a Cobra helicopter), the relevant m-files were assembled into a computer program system for active controls testing of the WRATS model.

The initial evaluation of GPC on the WRATS model was conducted in April 1998 during a one-week test conducted in the AB tiltrotor hover facility in a building adjacent to the TDT. Emphasis of this test was on active control of vibration using only the collective control. To provide a rigorous test of the GPC algorithm, the open-loop response of the model was exaggerated by running the rotor at an rpm that nearly coincided with the natural frequency of the wing beam mode. Additional excitation was provided by the downwash associated with running the rotor at a high thrust level. Some results from reference 250 illustrating the effectiveness of GPC in reducing vibrations are shown in figure 154.

August 1998: The objectives of this TDT test were twofold: (1) to establish new baseline stability boundaries for the WRATS model that included the hydraulic components that had been

added for active controls testing; and (2) begin an investigation into the use of active δ_3 as a means for augmenting mechanical δ_3. Most of the test was conducted in air but some limited testing was carried out in R-134a. All testing was done with the model in an airplane mode and a windmilling proprotor.

Definitive stability boundaries could not be identified for the model. The subcritical damping in the wing beam mode varied with airspeed as expected for speeds up to about 110 knots. However, as tunnel airspeed was increased further the damping did not decrease to zero as usual but rather leveled out at about 1% and held this value up through the maximum safe operating speed of the model (200 knots). This behavior occurred for all configurations of the model tested. Because the observed behavior had the character of a limit cycle, it was thought that there might be some mechanical interference or rubbing that was introducing nonlinearity into the model. However, examination of the model in-situ during the test failed to identify the cause for this unusual behavior. A closer examination of the model after the test identified the cause of the problem: a loose bolt in the bracket that holds the pylon to the downstop spring.

The use of so-called "active δ_3" is being investigated as a means for augmenting mechanical δ_3 in proprotors. Active δ_3 is implemented electronically by introducing cyclic inputs to the swashplate in a manner that introduces blade pitch-flap coupling of the appropriate magnitude and sign. An electronic δ_3 scheme developed by Bell was investigated on the WRATS model during this entry. The measured flapping response associated with the active δ_3 met design requirements. However, the stability augmentation associated with using active δ_3 could not be defined with confidence because of the problem noted above with the model.

October 1999: A brief investigation of the use of GPC to actively control the ground resonance behavior of a soft inplane tiltrotor was conducted in the tiltrotor hover facility in October 1999 (fig. 155) as part of a broader investigation (ref. 258). For this test, the model blades were modified by replacing the stiff inplane flexure at the root of each blade with a spindle incorporating a lag hinge and an adjustable viscous damper and spring. The open-loop behavior (frequency and damping versus rotor rpm) of the modified model was compared with its closed-loop behavior for several values of collective pitch and settings of the lag hinge damping and stiffness. A GPC-based algorithm was used to actively control the cyclic inputs to the swashplate in a manner that produced a whirl of the rotor tip-path-plane in the direction and at the frequency needed to stabilize the critical body mode. For the open-loop configurations of the model in which ground resonance instability was encountered, use of GPC was found to be strongly stabilizing (ref. 258). In particular, damping levels of about 2% critical were noted in the rpm range where the open-loop system was unstable. The results for the configuration with 8-degrees of collective pitch are shown in figure 156. While these results are quite encouraging with respect to the viability of the method, it is recognized that a broader evaluation of the methodology is needed to validate GPC-based algorithms for active stability augmentation of tiltrotor aircraft.

April 2000: The objectives of this TDT test were threefold: (1) to establish the new baseline stability boundaries for the WRATS model that were not identified in the August 1998 test; (2) to continue the investigation begun in the August 1998 test into the use of active δ_3 as a means for augmenting mechanical δ_3; and (3) to initiate wind-tunnel evaluation of GPC for active stability augmentation in the airplane mode of flight. All of the testing was conducted in air with the model in an airplane mode and a windmilling proprotor.

Definitive stability boundaries for the WRATS testbed incorporating the hydraulic components that were added for active controls testing were determined (ref. 259). Considerable progress was made on the active δ_3 study. However, the stability augmentation associated with active δ_3 could not be defined with confidence for all of the operating conditions tested. A review of the data after the test suggested that there might have been in-

strumentation difficulties. A GPC-based active control system was evaluated over a range of operating conditions below the corresponding open-loop stability boundaries of the model in this first wind-tunnel investigation. The method was found to be highly effective in increasing the stability (damping) of the critical wing mode for all of the configurations tested (ref. 260). An indication of the effectiveness of GPC in augmenting stability is given in figure 157, which shows the measured open-loop and closed-loop wing damping versus airspeed for one of the configurations tested.

A concise summary of the GPC experimental investigations conducted during the October 1999 and April 2000 tests is given in reference 261.

October 2000: The Variable Diameter Tilt Rotor (VDTR) is a Sikorsky Aircraft concept for improving tiltrotor aerodynamic performance in hover and cruise by varying rotor diameter in addition to rotor rotational speed between the two modes of flight. Sikorsky has conducted several wind-tunnel tests using low-speed models in a preliminary evaluation of their concept. A high-speed aeroelastic model of the VDTR rotor was tested in the TDT on the WRATS testbed in October 2000. The test had two objectives: (1) experimental validation of the baseline VDTR configuration in the high-speed airplane mode of flight; and (2) establishment of an experimental database to validate the stability analysis codes being used to design the VDTR. Parameters targeted for variation in the latter activity included blade precone, prelag, δ_3, and flapping stiffness, gimbal spring stiffness, rotor underslinging, control system stiffness, hub weight, and pylon weight.

The baseline configuration and several parametric changes to that configuration were successfully tested and compared with pretest predictions when a blade cuff experienced a fatigue failure. The abrupt change in loading associated with the mishap led to the loss of the rotor as well as considerable damage to the transmission and other mechanical systems in the pylon. The WRATS testbed is being repaired and will return to service in late 2001.

Closing Remarks on Tiltrotor Research

The AB/TDT has a long history of propeller and proprotor aeroelastic research. The research has included a broad range of experimental and analytical studies that have made creditable contributions to the technology base that has led to the successful development of the XV-15 and V-22 tiltrotor aircraft. These studies have also contributed substantially to increased understanding of the aeroelastic and dynamic characteristics that are unique to tiltrotor aircraft. The current tiltrotor research program in AB is continuing this tradition and is expected to play an important role in the development of future tiltrotor aircraft such as the Bell/Augusta BA-609 (fig. 158) and the Bell Quad Tilt Rotor (QTR)(fig. 159).

Current and Planned Tiltrotor Aeroelastic Research

Tiltrotor research in AB/TDT continues to consist of a mixture of experimental and analytical activities. On the experimental side, current plans call for several tests in the TDT over the next few years. Those currently on the tunnel schedule include: (1) Continued evaluation of the use of GPC for augmenting stability in the airplane mode of flight; (2) Completion of the active δ_3 study; (3) Aeroelastic stability and active control testing of a Bell soft inplane gimbaled rotor; and (4) A semi-span model of the Bell QTR.

On the analytical side, work is nearly completed on the extension of UMARC/G to include rotor/airframe interactional aerodynamics and a drive system model. Plans are to continue development and evaluation of Generalized Predictive Control for active aeroelastic control. Emphasis will be on improving the suite of computational algorithms that comprise the current GPC software system developed for WRATS. It is expected that enhancements will continue to be made to the UMARC/G and PASTA codes as appropriate to support the in-house studies. Development of the MBDyn code and its application to the WRATS model is also expected to continue in cooperation with the University of Milan.

Concluding Remarks

This paper has presented a historical overview of the contributions of the Langley Aeroelasticity Branch and its associated Transonic Dynamics Tunnel to rotorcraft technology and development since the tunnel's inception in 1960. That research has included a broad range of experimental investigations using a variety of testbeds and scale models, and the development and application of essential analyses. Based on the overview, it is fair to say that the AB/TDT has had a long and creditable history of rotorcraft aeroelastic research that has contributed to the technology base needed by the industry for designing and building advanced rotorcraft systems. In particular, studies conducted in AB/TDT have contributed substantially to supporting rotorcraft research and development programs, to identifying and investigating aeroelastic phenomena unique to rotorcraft systems, and to the resolution of aeroelastic anomalies. Building on this foundation, and with due regard for current and planned research activities in helicopter and tiltrotor aeroelasticity, it is expected that this tradition of service to the nation will continue well into the 21st century.

References

1. Reed, W. H., III: *Aeroelasticity Matters: Some Reflections on Two Decades of Testing in the NASA Langley Transonic Dynamics Tunnel*. NASA TM-83210, September 1981.

2. Doggett, R. V., Jr.; and Cazier, F. W., Jr.: *Aircraft Aeroelasticity and Structural Dynamics Research at the NASA Langley Research Center - Some Illustrative Results*. NASA TM 100627, May 1988.

3. Ricketts, R. H.: *Experimental Aeroelasticity History, Status and Future in Brief*. NASA TM 102651, April 1990.

4. Perry, B., III; and Noll, T. E.: Activities in Aeroelasticity at NASA Langley Research Center. Fourth International Symposium on Fluid-Structure Interactions, Aeroelasticity, Flow-Induced Vibration and Noise, ASME, Dallas, TX, November 16-21, 1997.

5. Kvaternik, R. G.: A Review of Some Tilt-Rotor Aeroelastic Research at NASA-Langley. *Journal of Aircraft*, Vol. 13, No. 5, May 1976, pp. 357-363.

6. Hammond, C. E.; and Weller, W. H.: Wind-Tunnel Testing of Aeroelastically Scaled Helicopter Rotor Blades. *Army Science Conference*, West Point, NY, June 1976.

7. Mantay, W. R.; Yeager, W. T., Jr.; Hamouda, M-N; Cramer, R. G., Jr.; and Langston, C. W.: *Aeroelastic Model Helicopter Rotor Testing in the Langley TDT*. NASA TM 86440 (USA AVSCOM Technical Memorandum 85-B-5), June 1985.

8. Yeager, W. T., Jr.; Mirick, P. H.; Hamouda, M-N; Wilbur, M. L.; Singleton, J. D.; and Wilkie, W. K.: Recent Rotorcraft Aeroelastic Testing in the Langley Transonic Dynamics Tunnel. Presented at the *47th Annual Forum of the American Helicopter Society*, Phoenix, AZ, May 1991.

9. Kvaternik, R. G.: *A Historical Overview of Tiltrotor Aeroelastic Research at Langley Research Center*. NASA TM 107578, April 1992.

10. Notes on the Proceedings of the 1939 Meeting of the Aircraft Industry with the National Advisory Committee for Aeronautics. *Journal of the Aeronautical Sciences*, Vol. 6, Number 7, May 1939, pp. 299-301.

11. Moxey, R. L.: Transonic Dynamics Wind Tunnel. *Compressed Air Magazine*, Vol. 68, Number 10, October 1963, pp. 8-13.

12. Yates, E. C., Jr.; Land, N. S.; and Foughner, J. T., Jr.: *Measured and Calculated Subsonic and Transonic Flutter Characteristics of a 45° Sweptback Wing Planform in Air and in Freon-12 in the Langley Transonic Dynamics Tunnel*. NASA TN-1616, March 1963.

13. Lee, C.; Bruce, C.; and Kidd, D.: *Wind-Tunnel Investigation of a Quarter-Scale Two-Bladed High-Performance Rotor in a Freon Atmosphere*. USAAVLABS Tech. Rep. 70-58, U.S. Army, Feb. 1971.

14. Treon, S. L.; Hofstetter, W. R.; and Abbott, F. T., Jr.: On the Use of Freon-12 for Increasing Reynolds Number in Wind-Tunnel Testing of Three-Dimensional Aircraft Models at Subcritical and Supercritical Mach Numbers. *Facilities and*

Techniques for Aerodynamic Testing at Transonic Speeds and High Reynolds Number, AGARD CP No. 83, Aug. 1971, pp. 27-1 –27-8.

15. Yeager, W. T., Jr.; and Mantay, W. R.: *Correlation of Full Scale Helicopter Rotor Performance in Air with Model-Scale Freon Data*. NASA TN D-8323, November 1976.

16. Corliss, J. M.; and Cole, S. R.: Heavy Gas Conversion of the NASA Langley Transonic Dynamics Tunnel. *20th AIAA Advanced Measurement and Ground Testing Technology Conference*, June 15-18, 1998, Albuquerque, NM (AIAA Paper 98-2710).

17. Cole, S. R.; and Garcia, J. L.: Past, Present and Future Capabilities of the Transonic Dynamics Tunnel From an Aeroelasticity Perspective. Presented at the *AIAA Dynamics Specialists Conference*, Atlanta, GA, April 5-6, 2000 (AIAA Paper 2000-1767).

18. Murphy, G.: *Similitude in Engineering*. The Ronald Press Co., New York, 1950.

19. Baker, W. E.; Westine, P. S.; and Dodge, F. T.: *Similarity Methods in Engineering Dynamics*. Hayden Book Company, Rochelle Park, New Jersey, 1973.

20. USAF/AIA: *Proceedings of Symposium on Aeroelastic & Dynamic Modeling Technology*. Dayton, OH, September 23-25, 1963. (AFFDL Report RTD-TDR-63-4197, Part I, March 1964.)

21. Regier, A. A.: The Use of Scaled Dynamic Models in Several Aerospace Vehicle Studies. Paper presented at *ASME Colloquium on the Use of Models and Scaling in Shock and Vibration*, Philadelphia, PA, November 1963, pp. 34-50.

22. Guyett, P. R.: *The Use of Flexible Models in Aerospace Engineering*. R.A.E. Technical Report No. 66335, November 1966.

23. Kuntz, W. H.; Wasserman, L. S.; and Alexander, H. R.: Dynamically Similar Model Tests of Rotary Wing and Propeller Types of VTOL Aircraft. *Proceedings of the Air Force V/STOL Technology and Planning Conference*, Las Vegas, NV, September 23-25, 1969.

24. Brooks, G. W.: The Application of Models to Helicopter Vibration and Flutter Research. *Proceedings of the Ninth Annual Forum of the American Helicopter Society*, Washington, D.C., May 14-17, 1953.

25. Fradenburgh, E. A.; and Kiely, E. F.: Development of Dynamic Model Rotor Blades for High Speed Helicopter Research. *Journal of the American Helicopter Society*, Vol. 9, Jan. 1964, pp. 3-20.

26. Albrecht, C. O.: Factors in the Design and Fabrication of Powered, Dynamically Similar V/STOL Wind Tunnel Models. *American Helicopter Society Mid-East Region Symposium on the Status of Testing and Modeling Techniques for V/STOL Aircraft*, Essington, PA, Oct. 26-28, 1972.

27. Ormiston, R. A.: Helicopter Modeling. *Aeronautical Journal*, Vol. 77, Nov. 1973, pp. 579-591.

28. Rabbott, J. P., Jr.: Model vs. Full Scale Rotor Testing. *Proceedings of the CAL/AVLABS Symposium on Aerodynamics of Rotary Wing and V/STOL Aircraft* (Vol. II - Wind Tunnel Testing), June 18-20, 1969, Buffalo, NY.

29. Kelly, M. W.: The Role of Wind Tunnel Testing in the Development of Advanced Rotary-Wing Aircraft. Prepared comments made as panel member, Wind tunnel Testing Panel Discussion at the *AHS Mideast Region Symposium on Status of Testing and Modeling Techniques for V/STOL Aircraft*, Essington, PA, Oct. 26-28, 1972.

30. Langhaar, H. L.: *Dimensional Analysis and Theory of Models*. John Wiley and Sons, Inc., 1956.

31. Templeton, H.: *Models for Aero-Elastic Investigations*. Aeronautical Research Council, Technical Report C.P. No. 255, Great Britain, 1956.

32. Molyneux, W. G.: *Aeroelastic Modeling*. RAE Tech Note Structures 353, March 1964.

33. Hunt, G. K.: *Similarity Requirements for Aeroelastic Models of Helicopter Rotors*. RAE Technical Report 72005, January 1972.

34. Lee, C: Weight Considerations in Dynamically Similar Model Rotor Design. Presented at the *27th Annual Conference of the Society of Aeronautical Weight Engineers, Inc.*, New Orleans, LA, May 13-16, 1968 (Paper No. 659).

35. Hanson, P. W.: *An Assessment of the Future Roles of the National Transonic Facility and the Langley Transonic Dynamics Tunnel in Aeroelas-*

tic and Unsteady Aerodynamic Testing. NASA TM 81839, June 1980.

36. Singleton, J. D.; and Yeager, W. T., Jr.: Important Scaling Parameters for Testing Model-Scale Helicopter Rotors. *20th AIAA Advanced Measurement and Ground Testing Technology Conference*, Albuquerque, NM, June 15-18, 1998 (AIAA Paper 98-2881).

37. Ward, John F.; and Huston, Robert J.: A Summary of Hingeless-Rotor Research at NASA-Langley. Presented at the *20th Annual Forum of the American Helicopter Society, Washington*, D.C., May 13-15, 1964.

38. Ward, J. F.: A Summary of Hingeless-Rotor Structural Loads and Dynamics Research. *Journal of Sound and Vibration*, Vol. 4, No.3, 1966, pp. 358 - 377.

39. Hanson, T. F.: *Investigation of Elastic Coupling Phenomena of High-Speed Rigid Rotor Systems*. U. S. Army TRECOM Technical Report 63-75, 1964.

40. Hanson, T. F.: *Wind-Tunnel Tests of an Optimized, Matched-Stiffness Rigid Rotor*. U. S. Army TRECOM Technical Report 64-56, 1964.

41. Lee, Charles D.; and White, James A.: *Investigation of the Effect of Hub Support Parameters on Two-Bladed Rotor Oscillatory Loads*. NASA CR-132435, May 1974.

42. Weller, William H.; and Lee Bill L.: *Wind-Tunnel Tests of Wide-Chord Teetering Rotors With and Without Outboard Flapping Hinges*. NASA Technical Paper 1046, Nov. 1977.

43. Weller, William H.: *Load and Stability Measurements On a Soft-Inplane Rotor System Incorporating Elastomeric Lead-Lag Dampers*. NASA TN D-8437, July 1977.

44. Doggett, R.V., Jr.; and Hammond, C.E.: *Application of Interactive Computer Graphics in Wind-Tunnel Dynamic Model Testing. Applications of Computer Graphics in Engineering*, NASA SP-390, 1975, pp. 325-353.

45. Hammond, Charles E.; and Doggett, Robert V., Jr.: *Determination of Subcritical Damping by Moving-Block/Randomdec. Applications. Flutter Testing Techniques*, NASA SP-415, 1976, pp. 59-76.

46. Lemnios, A. Z.; and Smith, A. F.: *An Analytical Evaluation of the Controllable Twist Rotor Performance and Dynamic Behavior*. USAAMRDL Tech. Rep. 72-16, U.S. Army, May 1972.

47. Lemnios, A. Z.; Nettles, William E.; and Howes, H. E.: Full Scale Wind Tunnel Tests of a Controllable Twist Rotor. *Proceedings of a Symposium on Rotor Technology, American Helicopter Society*, Aug. 1976.

48. Doman, Glidden S.; Tarzanin, Frank J.; and Shaw, John, Jr.: Investigation of Aeroelastically Adaptive Rotor Systems. Proceedings of a *Symposium on Rotor Technology*, American Helicopter Society, Aug. 1976.

49. Blackwell, R. H.: *Investigation of the Compliant Rotor Concept*. Sikorsky Aircraft Division, United Technologies Corporation, USAAMRDL-TR-77-7, Eustis Directorate, USAAMRDL, Fort Eustis, VA. June 1977, AD 1042338.

50. Blackwell, R. H.; and Merkley, D. J.: The Aeroelastically Conformable Rotor Concept. Preprint No. 78-59, *American Helicopter Society*, May 1978.

51. Weller, William H.: *Experimental Investigation of Effects of Blade Tip Geometry on Loads and Performance for an Articulated Rotor System*. NASA Technical Paper 1303, January 1979.

52. Yeager, William T., Jr.; and Mantay, Wayne R.: *Wind-Tunnel Investigation of the Effects of Blade Tip Geometry on the Interaction of Torsional Loads and Performance for an Articulated Helicopter Rotor*. NASA Technical Paper 1926. December 1981.

53. Blackwell, R. H.; Murrill, R. J.; Yeager, William T., Jr.; and Mirick, Paul H.: Wind Tunnel Evaluation of Aeroelastically Conformable Rotors. Preprint 80-23. Presented at the *36th Annual Forum of the American Helicopter Society*, Washington, D. C., May 1980.

54. Blackwell, R. H.; Murrill, R., J.; Yeager, William T., Jr.; and Mirick, P. H.: Wind-Tunnel Evaluation of Aeroelastically Conformable Rotors. *Journal of the American Helicopter Society*, vol. 26, no. 2, Apr. 1981, pp. 31-39.

55. Sutton, Lawrence R.; White, Richard P., Jr.; and Marker, Robert L.: *Wind-Tunnel Evaluation of an Aeroelastically Conformable Rotor*.

USAAVRADCOM-TR-81-D-43, Applied Technology Laboratory, U.S. Army Research and Technology Laboratories, Ft. Eustis, Va., Mar. 1982.

56. Mantay, Wayne R.; and Yeager, William T., Jr.: *Parametric Tip Effects for Conformable Rotor Applications*. NASA Technical Memorandum 85682, August 1983.

57. Mantay, Wayne R.; and Yeager, William T., Jr.*: Aeroelastic Considerations for Torsionally Soft Rotors*. NASA Technical Memorandum 87687, Aug. 1986.

58. Wood, E. R.; and Powers, R. W.: Practical Design Considerations for a Flightworthy Higher Harmonic Control System. Presented at the *36th Annual Forum of the American Helicopter Society*, Washington, D.C., May 1980.

59. Hammond, C. E.; and Cline, J. H.: On the Use of Active Higher Harmonic Blade Pitch for Helicopter Vibration Reduction. Presented at the *12th Army Science Conference*, West Point, New York, June 17-20, 1980.

60. Hammond, C.E.: Wind-Tunnel Results Showing Rotor Vibratory Loads Reduction Using Higher Harmonic Blade Pitch. *Journal of the American Helicopter Society*, Jan. 1983, pp. 10-15.

61. Molusis, J. A.; Hammond, C. E.; and Cline, John H.: A Unified Approach to the Optimal Design of Adaptive and Gain Scheduled Controllers to Achieve Minimum Rotor Vibration. *Journal of the American Helicopter Society*, Apr. 1983.

62. Wood, E. R.; Powers, R. W.; Cline, J. H.; and Hammond, C. E.: On Developing and Flight Testing a Higher Harmonic Control System. Presented at the *39th Annual Forum of the American Helicopter Society*, St. Louis, Missouri, May 1983.

63. Straub, F. K.; and Byrns, E. V., Jr.: *Application of Higher Harmonic Blade Feathering on the OH-6A Helicopter for Vibration Reduction.* NASA CR-4031, December 1986.

64. Yeager, William T., Jr.; Hamouda, M-Nabil; and Mantay, Wayne R.: Aeromechanical Stability of a Hingeless Rotor in Hover and Forward Flight: Analysis and Wind Tunnel Tests. Presented at the *Ninth European Rotorcraft Forum*, Stresa, Italy, Sept. 1983.

65. Yeager, William T., Jr.; Hamouda, M-Nabil; and Mantay, Wayne R.: *An Experimental Investigation of the Aeromechanical Stability of a Hingeless Rotor in Hover and Forward Flight*. NASA TM-89107, USAAVSCOM TM 87-B-5, June 1987.

66. Johnson, W.: *A Comprehensive Analytical Model of Rotorcraft Aerodynamics and Dynamics, Part I – Analysis Development*. NASA TM-81182, 1980.

67. Johnson, W.: *A Comprehensive Analytical Model of Rotorcraft Aerodynamics and Dynamics, Part II – User's Manual*. NASA TM-81183, 1980.

68. Bingham, Gene J.: The Aerodynamic Influences of Rotor Blade Airfoils, Twist, Taper and Solidity on Hover and Forward Flight Performance. Proceedings of the *37th Annual Forum, American Helicopter Society*, May 1981, pp. 37-50.

69. Yeager, William T., Jr.; Mantay, Wayne R.; Wilbur, Matthew L.; Cramer, Robert G., Jr.; and Singleton, Jeffrey D.: *Wind-Tunnel Evaluation of an Advanced Main-Rotor Blade Design for a Utility-Class Helicopter*. NASA Technical Memorandum 89129, Sept. 1987.

70. Singleton, Jeffrey D.; Yeager, William T., Jr.; and Wilbur, Matthew L.: *Performance Data From a Wind-Tunnel Test of Two Main-Rotor Blade Designs for a Utility-Class Helicopter.* NASA Technical Memorandum 4183, June 1990.

71. Yeager, William T., Jr.; Hamouda, M-Nabil; Idol, Robert F.; Mirick, Paul H.; Singleton, Jeffrey D.; and Wilbur, Matthew L.: *Vibratory Loads Data From a Wind-Tunnel Test of Structurally Tailored Model Helicopter Rotors*. NASA Technical Memorandum 4265, Aug. 1991.

72. Yen, J. G.: Coupled Aeroelastic Hub Loads Reduction. Proceedings of the *Theoretical Basis of Helicopter Technology Seminar, Part 3*. Nanjing Aeronautical Inst. (Peoples's Republic of China) and American Helicopter Society, Inc., 1985, pp.D4-1-D4-9.

73. Yen, Jing G.;Yuce, Mithat; Chao, Chen-Fu; and Schillings, John: Validation of Rotor Vibratory Airloads and Application to Helicopter Response.

Journal of the American Helicopter Society, vol. 35, no. 4, Oct. 1990, pp. 63-71.

74. Taylor, Robert B.: Helicopter Vibration Reduction by Modal Shaping. Presented at the *38th Annual Forum of the American Helicopter Society*. Anaheim, Calif., May 1982.

75. Wilbur, Matthew L.: Experimental Investigation of Helicopter Vibration Reduction Using Rotor Blade Aeroelastic Tailoring. Presented at the *47th Annual Forum of the American Helicopter Society*, Phoenix, Ariz., May 1991.

76. Wilbur, Matthew L.; Yeager, William T., Jr.; Singleton, Jeffrey D.; Mirick, Paul H.; and Wilkie, W. Keats: *Wind-Tunnel Evaluation of the Effect of Blade Nonstructural Mass Distribution on Helicopter Fixed-System Loads*. NASA TM-1998-206281, Jan. 1998.

77. Hardin, J. C.; and Lamkin, S. L.: Concepts for Reduction of Blade/Vortex Interaction Noise. *Journal of Aircraft*, Vol.24, No.2, Feb. 1987, pp. 120-125.

78. Splettstoesser, W.R.; Schultz, K. L.; and Martin Ruth M.: Rotor Blade/Vortex Interaction Noise Source Identification and Correlation with Rotor Wake Predictions. *AIAA 11th Aeroacoustics Conference*, AIAA-87-2744, Oct. 1987.

79. Brooks, Thomas K.; and Booth, Earl R., Jr.: Rotor Blade-Vortex Interaction Noise Reduction and Vibration Using Higher Harmonic Control. *16th European Rotorcraft Forum*, Glasgow, U. K., Paper No.9.3, Sept. 1990.

80. Lowson, Martin Vincent; St. David, Barton; Hawkings, David Leonard; Byham, Geoffrey Malcolm; Perry, Frederick John; and Denham, Corton: Helicopter Rotor Blades. U. S. Pat. 4,077,741. Mar. 7, 1978.

81. White, R. W.: Developments in UK Rotor Blade Technology. *AIAA Aircraft Design, Systems and Technology Meeting*, Oct. 1983. (Available as AIAA-83-2525).

82. Wanstall, Brian: BERP Blades - Key to the 200 kn Helicopter. *INTERAVIA*, vol. 3, 1986, pp. 322 - 324.

83. Perry, F. J.: Aerodynamics of the Helicopter World Speed Record. Proceedings of the *43rd Annual Forum of the American Helicopter Society*, May 1987, pp. 3-15.

84. Yeager, William T., Jr.; Noonan, Kevin W.; Singleton, Jeffrey D.; Wilbur, Matthew L.; and Mirick, Paul H.: *Performance and Vibratory Loads Data From a Wind-Tunnel Test of a Model Helicopter Main-Rotor Blade With a Paddle-Type Tip*. NASA Technical Memorandum 4754, ARL Technical Report 1283, ATCOM Technical Report 97-A-006. May 1997.

85. Noonan, Kevin W.; Yeager, William T., Jr.; Singleton, Jeffrey D.; Wilbur, Matthew L.; and Mirick, Paul H.: Evaluation of Model Helicopter Main Rotor with Slotted Airfoils at the Tip. Presented at the *American Helicopter Society 55th Annual Forum*. Montreal, Quebec, Canada, May 25 - 27, 1999.

86. Derham, R.; and Hagood, N.: Rotor Design Using Smart Materials to Actively Twist Blades. *American Helicopter Society 52nd Annual Forum Proceedings*, Vol. 2, Washington, D.C., June 4 - 6, 1996, pp. 1242 - 1252.

87. Wilkie, W. Keats; Belvin, W. Keith; and Park, K. C.: Aeroelastic Analysis of Helicopter Rotor Blades Incorporating Anisotropic Piezoelectric Twist Actuation. *ASME 1996 World Congress and Exposition, Adaptive Structures Symposium*, Proceedings, Aerospace Division. Nov. 1996.

88. Wilkie, W. Keats: *Anisotropic Piezoelectric Twist Actuation of Helicopter Rotor Blades: Aeroelastic Analysis and Design Optimization*. Ph. D. thesis, University of Colorado, Boulder, Colorado, 1997.

89. Wilkie, W. Keats; Park, K. C.; and Belvin, W. Keith: Helicopter Dynamic Stall Suppression Using Active Fiber Composite Rotor Blades. AIAA Paper No. 98-2002, presented at *the AIAA/ASME/AHS Structures, Structural Dynamics, and Materials Conference*, Long Beach, Calif., April 20 -23, 1998.

90. Rodgers, John P.; and Hagood, Nesbitt W.: Preliminary Mach-Scale Hover Testing of an Integral Twist-Actuated Rotor Blade. Presented at the *SPIE 5th Annual International Symposium on Smart Structures and Materials*, San Diego, Calif., March, 1998.

91. Cesnik, Carlos E. S.; Shin, SangJoon; Wilkie, W. Keats; Wilbur, Matthew L.; and Mirick, Paul H.:

Modeling, Design, and Testing of the NASA/Army/MIT Active Twist Rotor Prototype Blade. Presented at the *American Helicopter Society 55th Annual Forum*, Montreal, Canada, May 25-27, 1999.

92. Wilkie, W. Keats; Wilbur, Matthew L.; Mirick, Paul H.; Cesnik, Carlos E. S.; and Shin, Sang-Joon: Aeroelastic Analysis of the NASA/Army/MIT Active Twist Rotor. Presented at the *American Helicopter Society 55th Annual Forum*, Montreal, Canada, May 25-27, 1999.

93. Johnson, Wayne: *CAMRAD-II, Comprehensive Analytical Model of Rotorcraft Aerodynamics and Dynamics*, Johnson Aeronautics, Palo Alto, Calif. 1994.

94. Taylor, Robert B.: *Helicopter Blade Design for Minimum Vibration*. NASA CR-3825, Oct. 1984.

95. He, C.: *A Parametric Study of Harmonic Rotor Hub Loads*. NASA CR-4558, Nov. 1993.

96. Bousman, William G.; and Mantay, Wayne R.: A Review of Research in Rotor Loads. Presented at *NASA/Army Rotorcraft Technology Conference*, Mar. 14 – 16, 1987, NASA - AMES Research Center.

97. Ormiston, Robert A.: Comparison of Several Methods for Predicting Loads on a Hypothetical Helicopter Rotor. *Journal of the American Helicopter Society*, Vol. 19, No. 4, Oct. 1974, pp. 2 – 13.

98. Blackwell, R. H., Jr.: Blade Design for Reduced Helicopter Vibration. *Journal of the American Helicopter Society*, Vol. 28, No. 3, July 1983, pp. 33 –41.

99. Hansford, R. E.; and Vorwald, J.: Dynamics Workshop on Rotor Vibratory Loads Prediction. *Journal of the American Helicopter Society*, Vol. 43, No. 1, Jan. 1998, pp. 76 –86.

100. Bingham, Gene J.; and Noonan, Kevin W.: *Two-Dimensional Aerodynamic Characteristics of Three Rotorcraft Airfoils at Mach Numbers From 0.35 to 0.90*. NASA TP-2000, AVRADCOM TR-82-B-2, 1982.

101. Noonan, Kevin W.: *Aerodynamic Characteristics of Two Rotorcraft Airfoils Designed for Application in the In-board Region of a Main Rotor Blade*. NASA TP-3009, AVSCOM TR-90-B-005, 1990.

102. Wilbur, M. L.; Mirick, P. H.; Yeager, W. T., Jr.; Langston, C. W.; Cesnik, C. E. S.; and Shin, S: Vibratory Loads Reduction Testing of the NASA/Army/MIT Active Twist Rotor. Presented at the American Helicopter Society 57th Annual Forum, Washington, DC, May 9-11, 2001.

103. Peters, D. A.; and Hohenemser, K. H.: Application of the Floquet Transition Matrix to Problems of Lifting Rotor Stability. *Journal of the American Helicopter Society*, Vol. 16, No. 2, April 1971, pp. 25-33.

104. Hammond, C. E.: An Application of Floquet Theory to Prediction of Mechanical Instability. *AHS/NASA Ames Specialists' Meeting on Rotorcraft Dynamics*, Moffett Field, CA, Feb. 13-15, 1974 (Also, *J. Amer. Hel. Soc*., Vol. 19, No. 4, Oct. 1974, pp. 14-23).

105. Hammond, C. E.: Helicopter Ground Resonance in Light of Army Requirements. Presented at the *Ninth Army Science Conference*, West Point, NY, June 18-21, 1974.

106. Coleman, R. P.; and Feingold, A. M.: *Theory of Self-Excited Mechanical Oscillations of Helicopter Rotors With Hinged Blades.* NACA Report 1351, 1958.

107. Bennett, R.L.: *Digital Computer Program DF1758 Fully Coupled Natural Frequencies and Mode Shapes of a Helicopter Rotor Blade.* NASA CR-132662, 1975.

108. McLarty, Tyce T.: *Rotorcraft Flight Simulation With Coupled Rotor Aeroelastic Stability Analysis. Volume 1 – Engineers Manual.* USAAMRDL-TR-76-41A, U.S. Army, May 1977. (Available from DDC as AD A042462.)

109. Weller, W. H.; and Minick, R. E.: *An Improved Computational Procedure for Determining Helicopter Rotor Blade Natural Modes.* NASA TM 78670, August 1978.

110. Kaza, K. R. V.; and Hammond, C. E.: An Investigation of Flap-Lag Stability of Wind-Turbine Rotors in the Presence of Velocity Gradients and Helicopter Rotors in Forward Flight. Presented at the 17th Structures, Structural Dynamics and Materials Conference, Valley Forge, PA, May 5-7, 1976.

111. Kaza, K. R. V.; and Kvaternik, R. G.: A Critical Examination of the Flap-Lag Dynamics of Helicopter Rotor Blades in Hover and Forward flight. Presented at the *32nd Annual Forum of the American Helicopter Society*, Washington, DC, May 1976.

112. Kaza, K. R. V.; and Kvaternik, R. G.: Examination of the Flap-Lag Stability of Rigid Articulated Rotor Blades. *Journal of Aircraft*, Vol. 16, No. 12, December 1979, pp. 876-884.

113. Hohenemser, K. H.; and Yin, S-K: Some Applications of the Method of Multiblade Coordinates. *Journal of the American Helicopter Society*, Vol. 17, No. 3, July 1972, pp. 3-12.

114. Biggers, J. C.: Some Approximations to the Flapping Stability of Helicopter Rotors. *AHS/NASA Ames Specialists' Meeting on Rotorcraft Dynamics*, Moffett Field, CA, Feb. 13-15, 1974 (Proceedings available as *Rotorcraft Dynamics*, NASA SP-352, 1974). Also, *Journal of the American Helicopter Society*, Vol. 19, No. 4, October 1974, pp. 24-33.

115. Friedmann, P.; Hammond, C. E.; and Woo, T-H: Efficient Numerical Treatment of Periodic Systems with Application to Stability Problems. *International Journal for Numerical Methods in Engineering*, Vol. 11, 1977, pp. 1117-1136.

116. Kaza, K. R. V.; and Kvaternik, R. G.: Nonlinear Flap-Lag-Axial Equations of a Rotating Beam. *AIAA Journal*, Vol. 15, No. 6, June 1977, pp. 871-874.

117. Kvaternik, R. G.; and Kaza, K. R. V.: *Nonlinear Curvature Expressions for Combined Flapwise Bending Chordwise Bending, Torsion and Extension of Twisted Rotor Blades.* NASA TM X-73997, December 1976.

118. Kaza, K. R. V.; and Kvaternik, R. G.: *Nonlinear Aeroelastic Equations for Combined Flapwise Bending, Chordwise Bending, Torsion, and Extension of Twisted Nonuniform Rotor Blades in Forward Flight.* NASA TM 74059, August 1977.

119. Novozhilov, V. V.: *Foundations of the Nonlinear Theory of Elasticity*. Graylock Press, Rochester, NY, 1953.

120. Vigneron, F. R.: Comment on Mathematical Modeling of Spinning Elastic Bodies for Modal Analysis. *AIAA Journal*, Vol. 13, January 1975, pp. 126-128.

121. Kaza, K. R. V.; and Kvaternik, R. G.: *Aeroelastic Equations of Motion of a Darrieus Vertical-Axis Wind-Turbine Blade.* DOE/NASA/1028-79/25 (NASA TM-79295), December 1979.

122. Kaza, K. R. V.: *Nonlinear Aeroelastic Equations of Motion of Twisted, Nonuniform, Flexible Horizontal-Axis Wind Turbine Blades*. DOE/NASA/3139-1 (NASA CR-159502), July 1980.

123. Kaza, K. R. V.; and Kvaternik, R. G.: Application of Unsteady Airfoil Theory to Rotary Wings. *Journal of Aircraft*, Vol. 18, No. 7, July 1981, pp. 604-605.

124. Kvaternik, R. G.; White, W. F., Jr.; and Kaza, K. R. V.: Nonlinear Flap-Lag-Axial Equations of a Rotating Beam with Arbitrary Precone Angle. Presented at the *AIAA/ASME 19th Structures, Structural Dynamics and Materials Conference*, Bethesda, MD, April 3-5, 1978 (AIAA Paper 78-491).

125. White, W. F., Jr.; Kvaternik, R. G.; and Kaza, K. R. V.: Buckling of Rotating Beams. *Int. J. Mech. Sci*., Vol. 21, 1979, pp. 739-745.

126. Lakin, W. D.: *Integrating Matrices for Arbitrarily Spaced Grid Points*. NASA CR-159172, November 1979.

127. Lakin, W. D.: *Differentiating Matrices for Arbitrarily Spaced Grid Points*. NASA CR 172556, January 1985 (also, *Int. J. Numer. Meth. Engrg*., Vol. 23, 1986, pp. 209-218).

128. Lakin, W. D.: *Integrating Matrix Formulations for Vibrations of Rotating Beams Including the Effects of Concentrated Masses*. NASA CR-165954, June 1982.

129. Lakin, W. D.; and Kvaternik, R. G.: An Integrating Matrix Formulation for Buckling of Rotating Beams Including the Effects of Concentrated Masses. *Int. J. Mech. Sci.*, Vol. 31, No. 8, 1989, pp. 569-577.

130. Lakin, W. D.: *Two-Dimensional Integrating Matrices on Rectangular Grids*. NASA CR 165668, February 1981.

131. Lakin, W. D.: A Combined Integrating- and Differentiating-Matrix Formulation for Boundary-Value Problems on Rectangular Domains. *Journal of Engineering Mathematics*, Vol. 20, 1986, pp. 203-215.

132. Vakhitov, M. B.: Integrating Matrices as a Means of Numerical Solution of Differential Equations in Structural Mechanics. *Izvestiya VUZ. Aviatsionnaya Teknika*, Vol. 3, 1966, pp. 50-61.

133. Hunter, W. F.: *Integrating-Matrix Method for Determining the Natural Vibration Characteristics of Propeller Blades.* NASA TN D-6064, December 1970.

134. White, W. F., Jr.; and Malatino, R. E.: *A Numerical Method for Determining the Natural Vibration Characteristics of Rotating Nonuniform Cantilever Blades*. NASA TM X-72751, October 1975.

135. Hinnant, H. E.: *Derivation of a Tapered p-Version Beam Finite Element*. NASA TP 2931, 1989.

136. Hodges, R. V.; Nixon, M. W.; and Rehfield, L. W.: *Comparison of Composite Rotor Blade Models: A Coupled-Beam Analysis and an MSC/NASTRAN Finite-Element Model*. NASA TM 89024, 1987.

137. Nixon, M. W.: Extension-Twist Coupling of Composite Circular Tubes with Application to Tilt Rotor Blade Design. *Presented at the 28th Structures, Structural Dynamics and Materials Conference*, Monterey, CA, April 1987.

138. Nixon, M. W.: *Improvements to Tilt Rotor Performance Through Passive Blade Twist Control*. NASA TM 100583 (AVSCOM TM-88-B-010), April 1988.

139. Nixon, M. W.: Analytical and Experimental Investigations of Extension-Twist-Coupled Structures. Master of Science Thesis, George Washington University, May 1989.

140. Nixon, M. W.; and Hinnant, H. E.: Dynamic Analysis of Pretwisted Elastically-Coupled Rotor Blades. Presented at the *1992 ASME Winter Annual Meeting*, Anaheim, CA, November 8-13, 1992.

141. Lake, R. C.; and Nixon, M. W.: *A Preliminary Investigation of Finite-Element Modeling for Composite Rotor Blades*. NASA TM 100559 (USAAVSCOM TM 88-B-001), January 1988.

142. Lake, R. C.; Izadpanah, A. P.; and Baucom, R. M.: *Experimental and Analytical Investigation of Dynamic Characteristics of Extension-Twist-Coupled Composite Tubular Spars.* NASA TP 3225 (ARL TR 30), February 1993.

143. Lake, R. C.; Nixon, M. W.; Wilbur, M. L.; Singleton, J. D.; and Mirick, P. H.: *A Demonstration of Passive Blade Twist Control Using Extension-Twist Coupling*. NASA TM 107642 (USAAVSCOM TR 92-B-010), June 1992.

144. Lake, R. C.; Nixon, M. W.; Wilbur, M. L.; Singleton, J. D.; and Mirick, P. H.: Demonstration of an Elastically Coupled Twist Control Concept for Tilt Rotor Blade Application. *AIAA Journal*, Vol. 32, No. 7, July 1994, pp. 1549-1551.

145. Nixon, M. W.: Aeroelastic Response and Stability of Tiltrotors with Elastically-Coupled Composite Rotor Blades. Ph.D. Dissertation, 1993, University of Maryland, College Park, Maryland. (A synopsis of this work may be found in: Parametric Studies for Tiltrotor Aeroelastic Stability in High Speed Flight. *J. Amer. Hel. Soc.*, Vol. 38, Oct. 1993, pp. 71-79.)

146. Rehfield, L. W.: Design Analysis Methodology for Composite Rotor Blades. *Proceedings of the Seventh DoD/NASA Conference on Fibrous Composites in Structural Design*, AFWAL-TR-85-3094, June 1985.

147. Vanderplaats, G. N.: *CONMIN - A FORTRAN Program for Constrained Function Minimization, User's Manual*. NASA TM X-62282, August 1973.

148. Murthy, V. R.; and Hammond, C. *E.:* Vibration Analysis of Rotor Blades with Pendulum Absorbers. Presented at the *AIAA/ASME/ASCE/AHS 20th Structures, Structural Dynamics and Materials Conference*, St. Louis, Mo. April 4-6, 1979, AIAA Paper 79-0730.

149. Murthy, V. R.; and Hammond, C.E.: Vibration Analysis of Rotor Blades with Pendulum Absorbers. *Journal of Aircraft*, Vol. 18, No. 1, Jan. 1981, pp. 23-29.

150. Pierce, G. A.; and Hamouda M-N. H.: *Helicopter Vibration Suppression Using Simple Pendulum*

Absorbers on the Rotor Blade. NASA CR-3619, Sept. 1982.

151. Reichert, G.: Helicopter Vibration Control - A Survey. *Sixth European Rotorcraft and Powered Lift Aircraft Forum*, Bristol, UK, September 1980.

152. Amer, K. B.; and Neff, J.R.: Vertical-Plane Pendulum Absorbers for Minimizing Helicopter Vibratory Loads. *Journal of American Helicopter Society*, Vol. 19, Oct. 1974, pp. 44-48.

153. Paul, W. F.: Development and Evaluation of the Main Rotor Bifilar Absorber. *25th Annual National Forum of the American Helicopter Society*, May 1969.

154. Gabel, R.; and Gunther, R.: Pendulum Absorbers Reduce Transition Vibration. *31st Annual National Forum of the American Helicopter Society*, May 1975.

155. Taylor, R. B.; and Teare, P. A.: Helicopter Vibration Reduction with Pendulum Absorbers. *Journal of the American Helicopter Society*, Vol. 20, July 1975, pp. 9-17.

156. Houbolt, J. C.; and Brooks, G. W.: *Differential Equations of Motion for Combined Flapwise Bending, Chordwise Bending and Torsion of Twisted Nonuniform Rotor Blades*. NACA Report 1346, 1958.

157. Pestal, E. C.; and Leckie, F. A.: *Matrix Methods in Elastomechanics*. McGraw-Hill Book Co., 1963.

158. Kvaternik, R. G.; and Walton, W. C., Jr.: *A Formulation of Rotor-Airframe Coupling for Design Analysis of Vibrations of Helicopter Airframes.* NASA RP 1089, June 1982.

159. Advanced Rotorcraft Technology Task Force Report. Office of Aeronautics and Space Technology, NASA, October 15, 1978.

160. Gabel, R.; Ricks, R.; and Magiso, H: *Planning, Creating, and Documenting a NASTRAN Finite Element Vibrations Model of a Modern Helicopter, Planning Report*. NASA CR-165722, April 1981.

161. Gabel, R.; Kesack, W. J.; and Reed, D. A.: *Planning, Creating, and Documenting a NASTRAN Finite Element Vibrations Model of a Modern Helicopter, Modeling Documentation Report.* NASA CR-166077, March 1983.

162. Gabel, R.; and Reed, D. A.: *Planning, Creating, and Documenting a NASTRAN Finite Element Vibrations Model of a Modern Helicopter, Test Requirements Report*. NASA CR-165855, April 1982.

163. Gabel, R.; Reed, D. A.; and Ricks, R.: *Planning, Creating, and Documenting a NASTRAN Finite Element Vibrations Model of a Modern Helicopter, Ground Shake Test - Results and Correlation Report*. NASA CR-166107, May 1983.

164. Gabel, R.; Kesack, W. J.; Reed, D. A.; and Ricks, R.: *Planning, Creating, and Documenting a NASTRAN Finite Element Vibrations Model of a Modern Helicopter, Summary Report*. NASA CR-172229, October 1983.

165. Gabel, R.; Reed, D.; Ricks, R.; and Kesack, W.: Planning, Creating, and Documenting a NASTRAN Finite Element Model of a Modern Helicopter. *AHS/NASA Ames 2nd Decennial Specialists' Meeting on Rotorcraft Dynamics*, Moffett Field, CA, Nov. 7-9, 1984 (Proceedings available as *Rotorcraft Dynamics 1984*, NASA CP 2400, November 1985).

166. Dompka, R. V.; Sciascia, M. C.; Lindsay, D. R.; and Chung, Y. T.: *Plan, Formulate, and Discuss a NASTRAN Finite Element Vibrations Model of the Bell ACAP Helicopter Airframe*. NASA CR-181774, May 1989.

167. Dompka, R. V.; Hashish, E.; and Smith, M. R.: *Ground Vibration Test Comparisons of a NASTRAN Finite Element Model of the Bell ACAP Helicopter Airframe*. NASA CR-181775, May 1989.

168. Gabel, R.; Lang, P. F.; Smith, L. A.; and Reed, D. A.: *Plan, Formulate, Discuss and Correlate a NASTRAN Finite Element Vibrations Model of the Boeing Model 360 Helicopter Airframe*. NASA CR-181787, April 1989.

169. Reed, D. A.; and Gabel, R.: *Ground Shake Test of the Boeing Model 360 Helicopter Airframe*. NASA CR-181766, March 1989.

170. Christ, R.; Ferg, D.; Kilroy, K.; Toossi, M.; and Weisenburger, R.: *Plan, Formulate and Discuss a NASTRAN Finite Element Model of the AH-64A*

Helicopter Airframe. NASA CR-187446, October 1990.

171. Ferg, D.; Foote, L.; Korkosz, G.; Straub, F.; Toossi, M.; and Weisenburger, R.: *Plan, Execute, and Discuss Vibration Measurements and Correlations to Evaluate a NASTRAN Finite Element Model of the AH-64A Helicopter Airframe*. NASA CR-181973, January 1990.

172. Dinyovszky, P.; and Twomey, W. J.: *Plan, Formulate, and Discuss a NASTRAN Finite Element Model of the UH-60A Helicopter Airframe*. NASA CR-181975, February 1990.

173. Howland, G. R.; Durno, J. A.; and Twomey, W. J.: *Ground Shake Test of the UH-60A Helicopter Airframe and Comparison with NASTRAN Finite Element Model Predictions*. NASA CR-181993, March 1990.

174. Stebbins, R. F.; and Twomey, W, J.: *Plan, Formulate, and Discuss a NASTRAN Finite Element Model of the Sikorsky ACAP Helicopter Airframe*. NASA CR-182059, June 1990.

175. Ferg, D.; and Toossi, M.: *Finite Element Modeling of the Higher Harmonic Controlled OH-6A Helicopter Airframe*. NASA CR-187449, October 1990.

176. Hashemi-Kia, M.; Kilroy, K.; and Parker, G.: *Development and Applications of a Multi-Level Strain Energy Method for Detecting Finite Element Modeling Errors*. NASA CR-187447, October 1990.

177. Bielawa, R. L.; Hefner, R. E.; and Castagna, A.: *Static Strain and Vibration Characteristics of a Metal Semimonocoque Helicopter Tail Cone of Moderate Size*. NASA CR-187576, June 1991.

178. Hashemi-Kia, M.; and Toossi, M.: *Development and Application of a Technique for Reducing Airframe Finite Element Models for Dynamics Analysis*. NASA CR-187448, October 1990.

179. Dompka, R. V.: *Investigation of Difficult Component Effects on Finite Element Model Vibration Prediction for the Bell AH-1G Helicopter. Volume I - Ground Vibration Test Results. Volume II - Correlation Results.* NASA CR-181916, October 1989 (A summary of this work may be found in *Journal of the American Helicopter Society*, Vol. 35, No. 1, Jan. 1990, pp. 64-74).

180. Dompka, R. V.; and Calapodas, N. J.: Finite Element Correlation of the U. S. Army/BHTI ACAP Composite Airframe Helicopter. *Presented at the 47th Annual Forum of the American Helicopter Society*, Phoenix, AZ, May 6-8, 1991, pp. 1009-1028.

181. Dompka, R. V.: *Investigation of Difficult Component Effects on Finite Element Model Vibration Prediction for the Bell ACAP Helicopter*. NASA CR-187493, February 1991.

182. Cronkhite, J. D.; Berry, V. L.; and Brunken, J. E.: *A NASTRAN Vibration Model of the AH-1G Helicopter Airframe*. U. S. Army Armament Command Report No. R-TR-74-045, June 1974.

183. Cronkhite, J. D.; Berry, V. L.; and Dompka, R. V.: *Summary of the Modeling and Test Correlations of a NASTRAN Finite Element Vibrations Model for the AH-1G Helicopter*. NASA CR-178201, January 1987.

184. Dompka, R. V.; and Cronkhite, J. D.: *Summary of AH-1G Flight Vibration Data for Validation of Coupled Rotor-Fuselage Analyses*. NASA CR-178160, November 1986.

185. Cronkhite, J. D.; Dompka, R. V.; Rogers, J. P.; Corrigan, J. C.; Perry, K. S.; and Sadler, S. G.: *Coupled Rotor/Fuselage Dynamic Analysis of the AH-1G Helicopter and Correlation with Flight Vibrations Data*. NASA CR-181723, January 1989.

186. DiTaranto, R. A.; and Sankewitsch, V.: *Calculation of Flight Vibration Levels of the AH-1G Helicopter and Correlation with Existing Flight Vibration Measurements.* NASA CR-181923, November 1989.

187. Sangha, K.; and Shamie, J.: *Correlation of AH-1G Airframe Flight Vibration Data with a Coupled Rotor-Fuselage Analysis.* NASA CR-181974, August 1990.

188. Sopher, R.; and Twomey, W. J.: *Calculation of Flight Vibration Levels of the AH-1G Helicopter and Correlation with Existing Flight Vibration Measurements.* NASA CR-182031, April 1990.

189. Bauchau, O. A.; and Kang, N. K.: *Nonlinear Dynamic Analysis of Flexible Multibody Systems*. NASA CR-187597, July 1991.

190. Hanagud, S. V.; Zhou, W.; Craig, J. I.; and Weston, N. J.: Use of System Identification Techniques for Improving Airframe Finite Element Models Using Test Data, *AIAA/ASME/ASCE/AHS/ASC 32nd Structures, Structural Dynamics, and Materials Conference*, Baltimore, MD, April 8-10, 1991 (Paper AIAA-91-1260-CP).

191. Kvaternik, R. G.: The NASA/Industry Design Analysis Methods for Vibrations (DAMVIBS) Program - Accomplishments and Contributions. Presented at the *AHS National Technical Specialists' Meeting on Rotorcraft Structures*, Williamsburg, VA, October 29-31, 1991. (Also available as NASA TM 104192, December 1991).

192. Kvaternik, R. G.: *The NASA/Industry Design Analysis Methods for Vibrations (DAMVIBS) Program - A Government Overview*. NASA TM 107579, April 1992.

193. Kvaternik, R. G.: DAMVIBS Looks at Rotorcraft Vibrations. *Aerospace America*, September 1992, pp. 22-24.

194. Many authors: A Government/Industry Summary of the Design Analysis Methods for Vibrations (DAMVIBS) Program. Special session on "Finite Element Analysis of Rotorcraft Vibrations" at the *33rd Structures, Structural Dynamics and Materials Conference*, April 13-15, 1992, Dallas, TX (Session papers also available as NASA CP 10114, January 1993).

195. Murthy, T. S.: Design Sensitivity Analysis of Rotorcraft Airframe Structures for Vibration Reduction. *NASA/VPISU Symposium on Sensitivity Analysis in Engineering*, Langley Research Center, Sept. 25-26, 1986 (Proceedings available as: *Sensitivity Analysis in Engineering*. NASA CP 2457, Sept. 1987).

196. Murthy, T. S.: Optimization of Helicopter Airframe Structures for Vibration Reduction - Considerations, Formulations and Applications. *AIAA Aircraft Design, Systems and Operations Meeting*, September 7-9, Atlanta, GA, 1988 (also, *J. of Aircraft*, Vol. 28, No. 1, January 1991, pp. 66-73).

197. Sareen, A. K.; Shrage, D. P.; and Murthy, T. S.: Rotorcraft Airframe Structural Optimization for Combined Vibration and Fatigue Constraints. Presented at the *47th Annual Forum of the American Helicopter Society*, Phoenix, AZ, May 6-8, 1991.

198. Murthy, T. S.; and Kvaternik, R. G.: Experiences at Langley Research Center in the Application of Optimization Techniques to Helicopter Airframes for Vibration Reduction. Presented at the *AHS National Technical Specialists' Meeting on Rotorcraft Structures*, Williamsburg, VA, October 29-31, 1991. (Also available as NASA TM 104193, December 1991).

199. Murthy, T. S.: Investigation on the Use of Optimization Techniques for Helicopter Airframe Vibrations Design Studies. In Leondis, C. T. (editor): *Control and Dynamic System, Volume 54: System Performance Improvement and Optimization Techniques and Their Applications in Aerospace Systems*, Academic Press, San Diego, CA, 1992.

200. Kvaternik, R. G.; and Murthy, T. S.: *Airframe Structural Dynamic Considerations in Rotor Design Optimization*. NASA TM 101646, August 1989.

201. MSC/NASTRAN (Version 65) User's Manual, Volumes I and II. The MacNeal-Schwendler Corporation, 1985.

202. Hanson, H. W.: Investigation of Vibration Reduction Through Structural Optimization. USAAVRADCOM-TR-80-D-13, July 1980.

203. Young, M. I.: On Passive Spot Damping Anomalies. *Proceedings of Damping '89*, WRDC-TR-89-3116, Vol. I, pp. DCB 1-14 (Conference sponsored by the Air Force Flight Dynamics Laboratory and held in West Palm Beach, Fl, Feb. 8-10, 1989).

204. Young, M. I.: Spot Damping Anomalies. *Journal of Sound and Vibration*, 1989, Vol. 131, No. 1, pp. 160-163.

205. Young, M. I.: On Lightly Damped Linear Systems. *Journal of Sound and Vibration*, 1990, Vol. 139, No. 3, pp. 515-518.

206. Young, M. I.: On Dynamic Stability Boundaries for Binary Systems. *Journal of Sound and Vibration*, 1990, Vol. 136, No. 3, pp. 520-524.

207. Young, M. I.: *Structural Dynamics and Vibrations of Damped, Aircraft-Type Structures*. NASA CR 4424, February 1992.

208. Berman, A.; Chen, S-Y.; Gustavson, B.; and Hurst, P.: *Dynamic System Coupler Program (DYSCO 4.1). Volume I - Theoretical Manual*. USAAVSCOM TR-88-D-14A, January 1989.

209. Wilbur, M. L.: Development of a Rotor/Body Coupled Analysis for an Active-Mount, Aeroelastic Rotor Testbed. Master of Science Thesis, George Washington University, 1996.

210. CAMRAD-II Theory. Version 1.2. Volumes 1-3, Johnson Aeronautics, Palo Alto, CA, 1994.

211. Dynamic Analysis and Design System Reference Manual. Revision 7.5. Volumes 1 and 2, CADSI, Coralville, Iowa. 1993.

212. Haug, E. J.: *Computer Aided Kinematics and Dynamics of Mechanical Systems. Volume 1: Basic Methods*. Allyn and Bacon, Boston, 1989.

213. du Plessis, A.; and Hagood, N.: Performance Investigation of Twist Actuated Single Cell Composite Beams for Helicopter Blade Control. *Sixth International Conference on Adaptive Structures Technology*, Key West, Florida, Nov. 13-15, 1995.

214. Peters, D. A.: Toward a Unified Lift Model For Use in Rotor Blade Stability Analyses. *Journal of the American Helicopter Society*, Vol. 30, No.3, July 1985, pp. 32-42.

215. Petot, D.: Differential Equation Modeling of Dynamic Stall. *Recherche Aerospatiale*, Vol. 5, No. 5, 1989.

216. Peters, D. A.; Chouchane, M.; and Fulton, M.: Helicopter Trim with Flap-Lag-Torsion and Stall by an Optimized Controller. *Journal of Guidance, Control and Dynamics*, Vol. 13, No. 5, Sept.-Oct., 1990, pp. 824-834.

217. *MATLAB Reference Guide*, The MathWorks, Inc., 1992.

218. Abbott, F. T., Jr.; Kelly, H. N.; and Hampton, K. D.: *Investigation of 1/8-Size Dynamic-Aeroelastic Model of the Lockheed Electra Airplane in the Langley Transonic Dynamics tunnel.* NASA TM SX-456, November 1960. (Also published as: *Investigation of Propeller-Power-Plant Autoprecession Boundaries for a Dynamic-Aeroelastic Model of a Four-Engine Turboprop Transport Airplane*. NASA TN D-1806, August 1963).

219. Bennett, R. M.; Kelly, H. N.; and Gurley, J. R., Jr.: *Investigation in the Langley Transonic Dynamics Tunnel of a 1/8-Size Aeroelastic-Dynamic Model of the Lockheed Electra Airplane with Modifications in the Wing-Nacelle Region*. NASA TM SX-818, March 1963.

220. Reed, W. H., III; and Bland, S. R.: *An Analytical Treatment of Aircraft Propeller Precession Instability*. NASA TN D-659, November 1960.

221. Houbolt, J. C.; and Reed, W. H., III: Propeller-Nacelle Whirl Flutter. *J. Aeronautical Sci.*, March 1962, pp. 333-345.

222. Bland, S. R.; and Bennett, R. M.: *Wind-Tunnel Measurements of Propeller Whirl-Flutter Speeds and Static-Stability Derivatives and Comparison with Theory*. NASA TN D-1807, August 1963.

223. Bennett, R. M.; and Bland, S. R.: *Experimental and Analytical Investigation of Propeller Whirl Flutter of a Power Plant on a Flexible Wing*. NASA TN D-2399, August 1964.

224. Reed, W. H., III; and Bennett, R. M.: Propeller Whirl Considerations for V/STOL Aircraft. *CAL/TRECOM Symposium Proceedings: Vol. II - Dynamic Load Problems Associated with Helicopters and V/STOL Aircraft*, June 1963.

225. Richardson, J. R.; and Naylor, H. F. W.: *Whirl flutter of Propellers with Hinged Blades*. Report No. 24, Engineering Research Associates, Toronto, Canada, March 1962.

226. Reed, W. H., III: *Review of Propeller-Rotor Whirl Flutter*. NASA TR R-264, July 1967.

227. Rainey, A. G.: Aeroelastic Considerations for Transports of the Future - Subsonic, Supersonic, and Hypersonic. Presented at the *AIAA Aircraft Design for 1980 Operations Meeting*, Washington, D.C., Feb. 12-14, 1968.

228. Kvaternik, R. G.: Studies in Tilt-Rotor VTOL Aircraft Aeroelasticity. Ph.D. Dissertation, June 1973, Case-Western Reserve University, Cleveland, Ohio.

229. Singleton, J. D.: Coupled Rotor-Fuselage Aeroelastic Analysis for Tiltrotor Configurations. *Eighth ARO Workshop on Aeroelasticity of Rotorcraft Systems*, October 18-20, 1999, State College, PA.

230. Wang, J. M.; Torok, M. S.; and Nixon, M. W.: Experimental and Theoretical Study of Variable Diameter Tilt Rotor Dynamics. Presented at the *AHS Vertical Lift Aircraft Design Conference*, San Francisco, CA, January 18-20, 1995.

231. Wang, J. W.; Jones, C. T.; and Nixon, M. W.: A Variable Diameter Short Haul Civil Tiltrotor. Presented at the *55th Annual Forum of the American Helicopter Society*, Montreal, Canada, May 25-27, 1999.

232. Ghiringhelli, G. L.; Masarati, P.; Mantegazza, P.; and Nixon, M. W.: Multi-Body Analysis of the 1/5-Scale Wind Tunnel Model of the V-22 Tiltrotor. Presented at *the 55th Annual Forum of the American Helicopter Society*, Montreal, Canada, May 25-27,1999.

233. Ghiringhelli, G. L.; Masarati, P.; Mantegazza, P.; and Nixon, M. W.: Multi-Body Analysis of an Active Control for a Tiltrotor. *CEAS/AIAA/ICASE/NASA Langley Forum on Aeroelasticity and Structural Dynamics 1999. NASA CP-1999-209136/PT 1, June 1999.*

234. Ghiringhelli, G. L.; Masarati, P.; Mantegazza, P.; and Nixon, M. W.: Multi-Body Analysis of a Tiltrotor Configuration. *Nonlinear Dynamics*, Vol. 19, 1999, pp. 333-357.

235. Gaffey, T. M.: The Effect of Positive Pitch-Flap Coupling (Negative δ_3) on Rotor Blade Motion Stability and Flapping. *Journal of the American Helicopter Society*, Vol. 14, No. 2, April 1969, pp.49-67.

236. Gaffey, T. M.; Yen, J. G.; and Kvaternik, R. G.: Analysis and Model Tests of the Proprotor Dynamics of a Tilt-Proprotor VTOL Aircraft. Presented at the *Air Force V/STOL Technology and Planning Conference*, Las Vegas, NV, September 23-25, 1969.

237. Kvaternik, R. G.: Experimental and Analytical Studies in Tiltrotor Aeroelasticity. *AHS/NASA Ames Specialists' Meeting on Rotorcraft Dynamics*, Moffett Field, CA, Feb. 13-15, 1974 (Proceedings available as *Rotorcraft Dynamics*, NASA SP-352, 1974).

238. Yen, J. G.; Weber, G. E.; and Gaffey, T. M.: *A Study of Folding Proprotor VTOL Aircraft Dynamics*. AFFDL-TR-71-7 (Vol. I), September 1971.

239. Marr, R. L.; and Neal, G. T.: Assessment of Model Testing of a Tilt-Proprotor VTOL Aircraft. Presented at the *AHS Mid-East Region Symposium on the Status of Testing and Modeling Techniques for V/STOL Aircraft*, Essington, PA, Oct. 26-28, 1972.

240. Baird, E. F.; Bauer, E. M.; and Kohn, J. S.: Model Tests and Analysis of Prop-Rotor Dynamics for Tilt-Rotor Aircraft. Presented at the *AHS Mid-East Region Symposium on the Status of Testing and Modeling Techniques for V/STOL Aircraft*, Essington, PA, Oct. 26-28, 1972.

241. Kvaternik, R. G.; and Kohn, J. S: *An Experimental and Analytical Investigation of Proprotor Whirl Flutter*. NASA TP 1047, December 1977.

242. Edenborough, H. K.; Gaffey, T. M.; and Weiberg, J. A.: Analyses and Tests Confirm Design of Proprotor Aircraft. *AIAA 4th Aircraft Design, Flight Test, and Operations Meeting*, Los Angeles, CA, August 7-9, 1972.

243. Popelka, D.; Sheffler, M.; and Bilger, J.: Correlation of Test and Analysis for the 1/5 Scale V-22 Aeroelastic Model. Presented at the *41st Annual Forum of the American Helicopter Society*, Fort Worth, TX, May 15-17, 1985. (Also, *J. Amer. Hel. Soc.*, Vol. 32, No. 2, April 1987, pp. 21-33).

244. Settle, T. B.; and Kidd, D. L.: Evolution and Test History of the V-22 0.2-Scale Aeroelastic Model. *Journal of the American Helicopter Society*, Vol. 37, No. 1, January 1992, pp. 31-45.

245. Settle, T. B.; and Nixon, M. W.: MAVSS Control of an Active Flaperon for Tiltrotor Vibration Reduction. *53rd Annual Forum of the American Helicopter Society*, Virginia Beach, VA, April 29-May 1, 1997.

246. Popelka, D.; Lindsay, D.; Parham, T.; Berry, V.; and Baker, D.: Results of an Aeroelastic Tailoring Study for a Composite Tiltrotor Wing. *51st Annual Forum* of the *American Helicopter Society*, Fort Worth, TX, May 9-11, 1995.

247. Corso, L. M.; Popelka, D. A.; and Nixon, M. W.: Design, Analysis, and Test of a Composite Tailored Tiltrotor Wing. *53rd Annual Forum of the American Helicopter Society*, Virginia Beach, VA, April 29-May 1, 1997.

248. Nixon, M. W.; Piatak, D. J.; Corso, L. M.; and Popelka, D. A.: Aeroelastic Tailoring for Stability Augmentation and Performance Enhancements of Tiltrotor Aircraft. *55th Annual National Forum of the American Helicopter Society*, Montreal, Canada, May 25-27, 1999.

249. Nixon, M. W.; Kvaternik, R. G.; and Settle, T. B.: Tiltrotor Vibration Reduction through Higher Harmonic Control. *53rd Annual Forum of the American Helicopter Society*, Virginia Beach, VA, April 29-May 1, 1997. (Also: *Journal of the American Helicopter Society*, July 1998, pp. 235-245).

250. Kvaternik, R. G.; Juang, J-N.; and Bennett, R. L: Exploratory Studies in Generalized Predictive Control for Active Aeroelastic Control of Tiltrotor Aircraft. *AHS Northeast Region Active Controls Technology Conference*, Bridgeport, CT, October 4-5, 2000.

251. Juang, J.-N., *Applied System Identification*, Prentice Hall, Inc., Englewood Cliffs, New Jersey, 1994.

252. Phan, M. Q.; and Juang, J-N: Predictive Feedback Controllers for Stabilization of Linear Multivariable Systems. *AIAA Guidance, Navigation and Control Conference*, San Diego, CA, July 29-31, 1996.

253. Juang, J.-N.: *State-Space System Realization With Input- and Output-Data Correlation*. NASA TP 3622, April 1997.

254. Juang, J-N; and Phan, M. Q.: Deadbeat Predictive Controllers. NASA TM 112862, May 1997.

255. Eure, K. W.: *Adaptive Predictive Feedback Techniques for Vibration Control*. Ph.D. Dissertation, Virginia Polytechnic Institute and State University, May 1998.

256. Phan, M. Q.; and Juang, J.-N.: Predictive Controllers for Feedback Stabilization. *Journal of Guidance, Control, and Dynamics*, Vol. 21, No. 5, Sept.-Oct. 1998, pp. 747-753.

257. Juang, J-N; and Eure, K. W.: *Predictive Feedback and Feedforward Control for Systems with Unknown Disturbances*. NASA TM-1998-208744, December 1998.

258. Nixon, M. W.; Langston, C. W.; Singleton, J. D.; Piatak, D. J.; Kvaternik, R. G.; Corso, L. M.; and Brown, R. K.: Aeroelastic Stability of a Soft-Inplane Gimballed Tiltrotor Model in Hover. *42nd AIAA/ASME/ASCE/AHS/ASC Structures, Structural Dynamics, and Materials Conference*, Seattle, WA, April 16-19, 2001.

259. Piatak, D. J.; Kvaternik, R. G.; Nixon, M. W.; Langston, C. W.; Singleton, J. D.; Bennett, R. L.; and Brown, R. K.: A Wind-Tunnel Parametric Investigation of Tiltrotor Whirl-Flutter Stability Boundaries. *57th Annual Forum of the American Helicopter Society*, Washington, DC, May 9-11, 2001.

260. Kvaternik, R. G.; Piatak, D. J.; Nixon, M. W.; Langston, C. W.; Singleton, J. D.; Bennett, R. L.; and Brown, R. K.: An Experimental Evaluation of Generalized Predictive Control for Tiltrotor Aeroelastic Stability Augmentation in Airplane Mode of Flight. *57th Annual Forum of the American Helicopter Society*, Washington, DC, May 9-11, 2001.

261. Nixon, M. W.; Langston, C. W.; Singleton, J. D.; Piatak, D. J.; Kvaternik, R. G.; Corso, L. M.; and Brown, R. K.: Experimental Investigations of Generalized Predictive Control for Tiltrotor Stability Augmentation. *2001 CEAS/AIAA/AIAE International Forum of Aeroelasticity and Structural Dynamics*, Madrid, Spain, June 5-7, 2001.

Table 1. - General Aeroelastic Scale Factors Applicable to Rotorcraft Models in TDT for Equal Lock Numbers (Mass Ratios) and Advance Ratios (Reduced Frequencies)

	Mach Numbers Equal				**Froude Numbers Equal**			
Parameter	General	Air	R-12	R-134a	General	Air	R-12	R-134a
Length	L	L	L	L	L	L	L	L
Mass	$L^3\rho$	$L^3\rho$	$L^3\rho$	$L^3\rho$	$L^3\rho$	$L^3\rho$	$L^3\rho$	$L^3\rho$
Time	$L(\gamma RT)^{-1/2}$	$L\,T^{-1/2}$	$2.23\,L\,T^{-1/2}$	$2.07\,L\,T^{-1/2}$	$L^{1/2}g^{-1/2}$	$L^{1/2}$	$L^{1/2}$	$L^{1/2}$
Mach number	1	1	1	1	$(Lg/\gamma RT)^{1/2}$	$(L/T)^{1/2}$	$2.23(L/T)^{1/2}$	$2.07(L/T)^{1/2}$
Froude number	$(Lg)^{-1}(\gamma RT)$	$L^{-1}T$	$.202\,L^{-1}T$	$.234\,L^{-1}T$	1	1	1	1
Reynolds number	$L\rho\mu^{-1}(\gamma RT)^{1/2}$	$L\rho T^{-.26}$	$.449\,L\rho\mu^{-1}T^{1/2}$	$.484\,\rho\mu^{-1}T^{1/2}$	$L^{3/2}\rho\mu^{-1}g^{1/2}$	$L^{3/2}\rho T^{-.76}$	$L^{3/2}\rho\mu^{-1}$	$L^{3/2}\rho\mu^{-1}$
Force	$L^2\rho(\gamma RT)$	$L^2\rho T$	$.202\,L^2\rho T$	$.234\,L^2\rho T$	$L^3\rho g$	$L^3\rho$	$L^3\rho$	$L^3\rho$
Speed	$(\gamma RT)^{1/2}$	$T^{1/2}$	$.449\,T^{1/2}$	$.484\,T^{1/2}$	$L^{1/2}g^{1/2}$	$L^{1/2}$	$L^{1/2}$	$L^{1/2}$
Acceleration	$L^{-1}(\gamma RT)$	$L^{-1}T$	$.202\,L^{-1}T$	$.234\,L^{-1}T$	g	1	1	1
Frequency	$L^{-1}(\gamma RT)^{1/2}$	$L^{-1}T^{1/2}$	$.449\,L^{-1}T^{1/2}$	$.484\,L^{-1}T^{1/2}$	$L^{-1/2}g^{1/2}$	$L^{-1/2}$	$L^{-1/2}$	$L^{-1/2}$
Angular Accel.	$L^{-2}(\gamma RT)$	$L^{-2}T$	$.202\,L^{-2}T$	$.234\,L^{-2}T$	$L^{-1}g$	L^{-1}	L^{-1}	L^{-1}
Moment, Work	$L^3\rho(\gamma RT)$	$L^3\rho T$	$.202\,L^3\rho T$	$.234\,L^3\rho T$	$L^4\rho g$	$L^4\rho$	$L^4\rho$	$L^4\rho$
Power	$L^2\rho(\gamma RT)^{3/2}$	$L^2\rho T^{3/2}$	$.091\,L^2\rho T^{3/2}$	$.113\,L^2\rho T^{3/2}$	$L^{7/2}\rho g^{3/2}$	$L^{7/2}\rho$	$L^{7/2}\rho$	$L^{7/2}\rho$
Moment of Inertia	$L^5\rho$	$L^5\rho$	$L^5\rho$	$L^5\rho$	$L^5\rho$	$L^5\rho$	$L^5\rho$	$L^5\rho$
Pressure, Stress	$\rho(\gamma RT)$	ρT	$.202\,\rho T$	$.234\,\rho T$	$L\rho g$	$L\rho$	$L\rho$	$L\rho$
Stiffness (EI,GJ)	$L^4\rho(\gamma RT)$	$L^4\rho T$	$.202\,L^4\rho T$	$.234\,L^4\rho T$	$L^5\rho g$	$L^5\rho$	$L^5\rho$	$L^5\rho$

Scale factors equal ratio of model to full-scale values of the quantities indicated; e.g., $L = L_M/L_F$, $\gamma RT = (\gamma RT)_M/(\gamma RT)_F$, etc., where T = temperature, ρ = test medium density, R = gas constant, μ = viscosity, γ = specific heat ratio for gas, and g is the acceleration due to gravity.

Air constants based on $\gamma = 1.4$, R = 1716 $ft^2/sec^2\,°R$
R-12 constants based on $\gamma = 1.137$, R = 427.3 $ft^2/sec^2\,°R$ (95% R-12/air mixture)
R-134a constants based on $\gamma = 1.114$, R = 505.3 $ft^2/sec^2\,°R$ (95% R-134a/air mixture)

Table 2. - Chronology of Tiltrotor Aeroelastic Analysis Development at AB/TDT

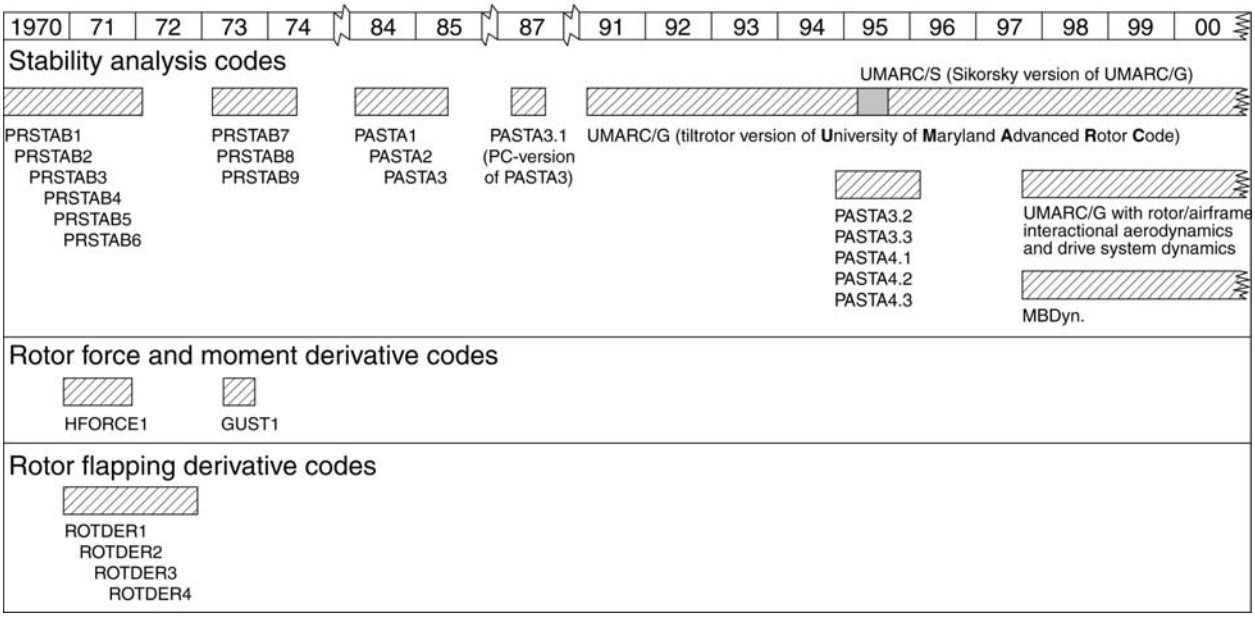

Table 3. - Scale factors for 1/7.5-scale aeroelastic model of Bell Model 266

Parameter	Scale Factor (Model/Airplane)
Froude number	1.00
Lock number	1.00
Mach number	0.365
Advance ratio	1.00
Reynolds number	0.0487
Length	0.1333
Density	1.0
Velocity	0.365
Time	0.365
Mass	0.00237
Frequency	2.738
Force	0.002369
Bending moment	0.0003157
Stiffness	0.000042095
Bending spring rate	0.01777
Torsion spring rate	0.0003157

Table 4. - Scale factors for 1/5-scale aeroelastic model of Bell Model 300 tiltrotor

Parameter	Scale Factor (Model/Full-Scale) Air	R-12
Froude number	1.0	1.0
Lock number	1.0	1.0
Mach number	0.447	1.016
Advance ratio	1.0	1.0
Reynolds number	0.0894	0.1265
Length	0.2	0.2
Density	1.0	1.0
Velocity	0.447	0.447
Time	0.447	0.447
Mass	0.008	0.008
Frequency	2.24	2.24
Force	0.008	0.008
Bending moment	0.0016	0.0016
Stiffness	0.00032	0.00032
Bending spring rate	0.04	0.04
Torsion spring rate	0.0016	0.0016

Table 5. - Scale factors for 1/4.5-scale aeroelastic model of Grumman Helicat

Parameter	Scale Factor (Model/Airplane)
Froude number	1.00
Lock number	1.00
Mach number	1.00
Advance ratio	1.00
Reynolds number	0.1047
Length	0.222
Density	1.0
Velocity	0.471
Time	0.471
Mass	0.01099
Frequency	2.12
Force	0.01099
Bending stiffness	0.0005420
Torsion stiffness	0.0005420
Bending spring rate	0.05
Torsion spring rate	0.002439

Table 6. - Scale factors for 1/5-scale aeroelastic model of Bell/Boeing V-22 tiltrotor

Parameter	Scale Factor (Model/Full-Scale) Air	R-12
Froude number	1.0	1.0
Lock number	1.0	1.0
Mach number	0.447	1.016
Advance ratio	1.0	1.0
Reynolds number	0.0894	0.1265
Length	0.2	0.2
Density	1.0	1.0
Velocity	0.447	0.447
Time	0.447	0.447
Mass	0.008	0.008
Frequency	2.24	2.24
Force	0.008	0.008
Bending moment	0.0016	0.0016
Stiffness	0.00032	0.00032
Bending spring rate	0.04	0.04
Torsion spring rate	0.0016	0.0016

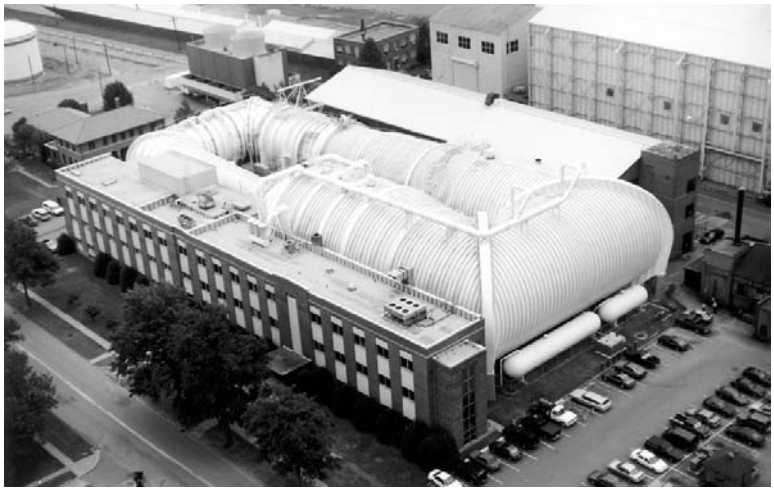

Figure 1. - The Langley Transonic Dynamics Tunnel (TDT).

(a) Lockheed Aircraft Company helicopter testbed

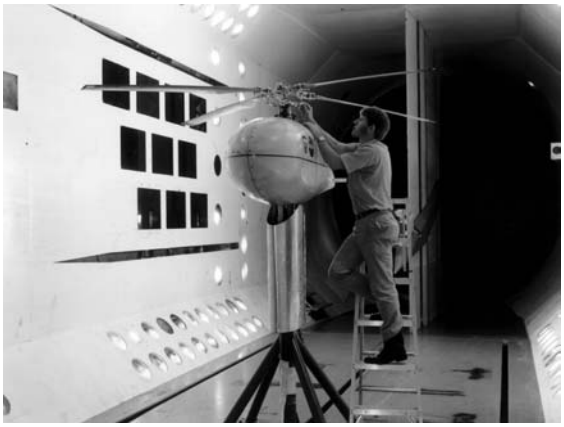

(c) Generalized Rotor Aeroelastic Model (GRAM) testbed

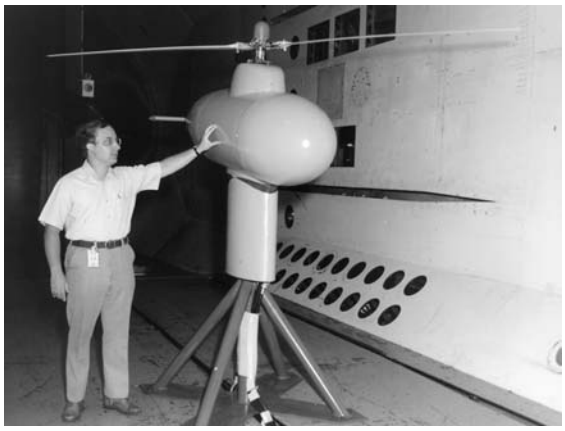

(b) Bell Helicopter Company helicopter testbed

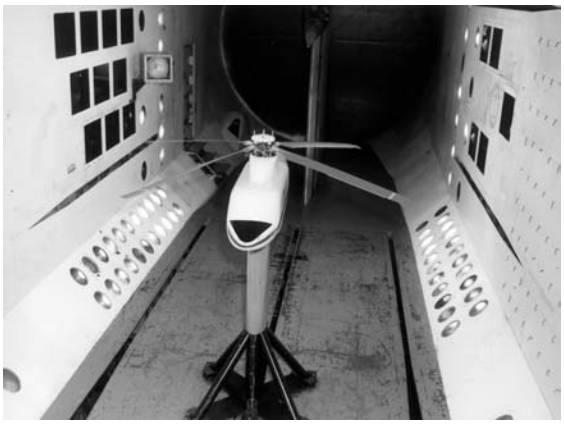

(d) Aeroelastic Rotor Experimental System (ARES) testbed

Figure 2. - Helicopter testbeds used in TDT.

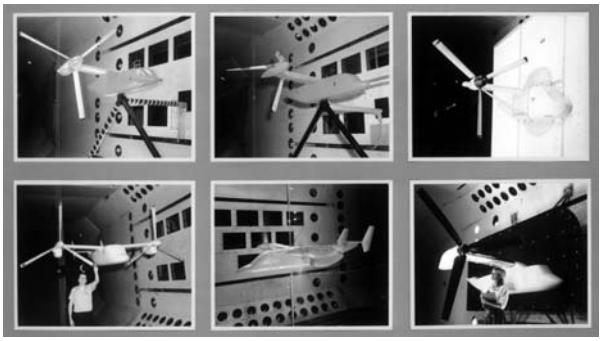

Figure 3. - Some tiltrotor models tested in the TDT.

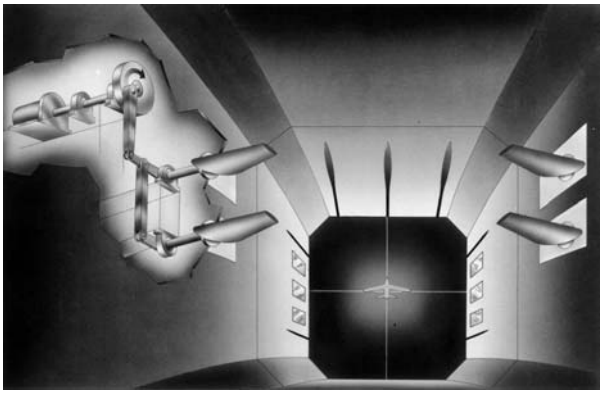

Figure 5. - Sketch of TDT airstream oscillator showing cutaway of driving mechanism.

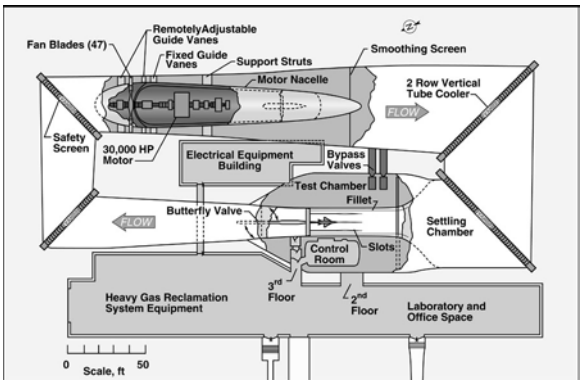

(a) Plan view

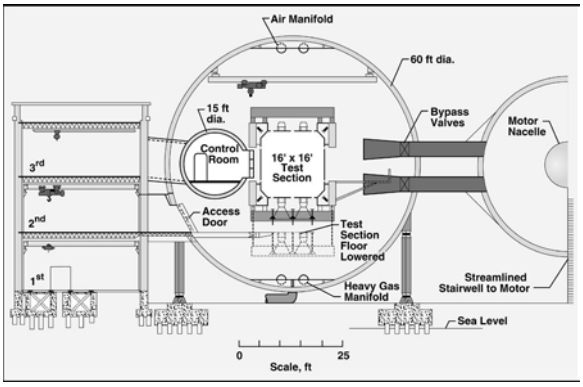

(b) Cross-section through test section

Figure 4. - General arrangement of TDT.

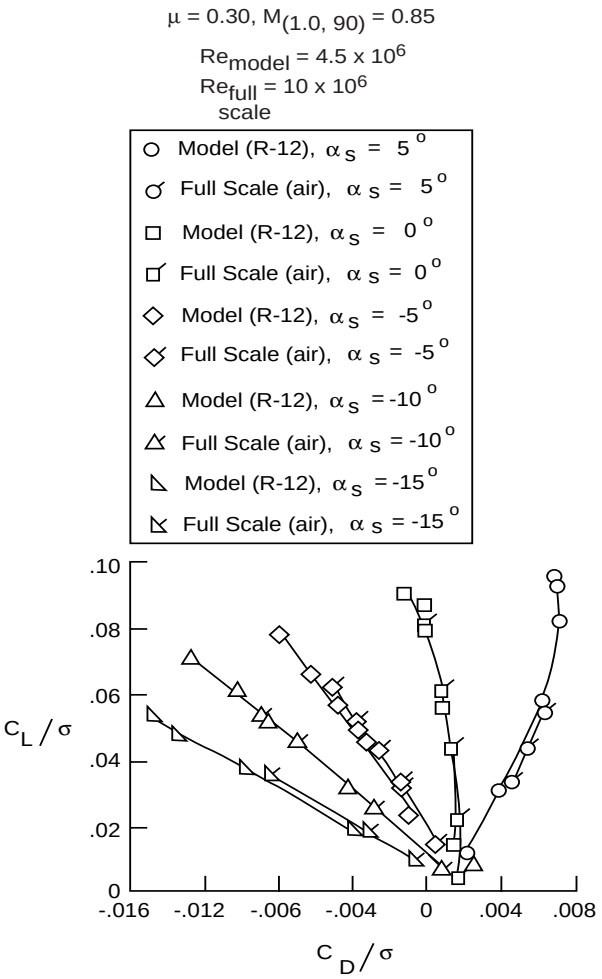

Figure 6. - Full-scale and model rotor performance.

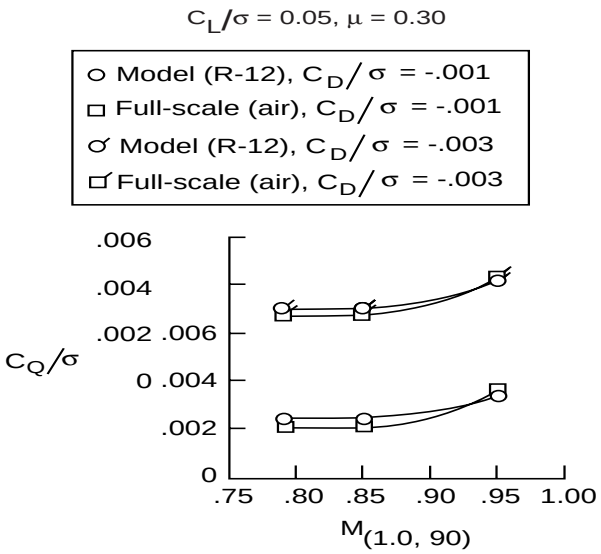

Figure 7. - Full-scale and model rotor performance.

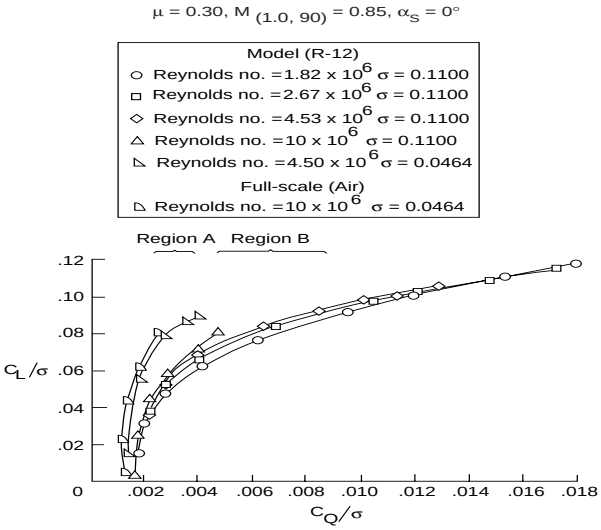

Figure 8. - Effect of scaling parameters on Freon model and full-scale rotor performance.

Figure 9.- GRAM testbed with AH-1G rotor.

Figure 10. - GRAM testbed with hinged wide-chord rotor.

Figure 11. - GRAM testbed with wide-chord rotor (no mid-span flap hinge).

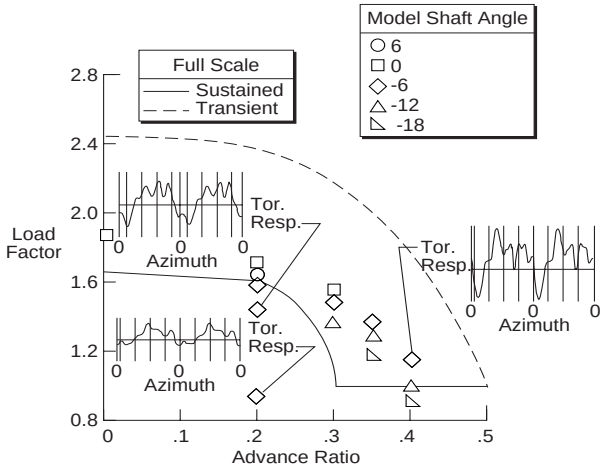

Figure 12. - Model Cobra test conditions compared to full-scale flight envelope with selected blade torsional waveforms.

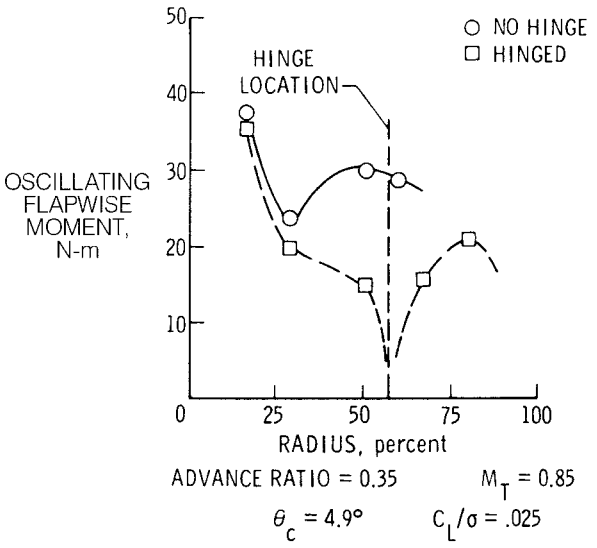

Figure 13. - Comparison of oscillatory blade loadings as a function of span for the wide-chord teetering rotors.

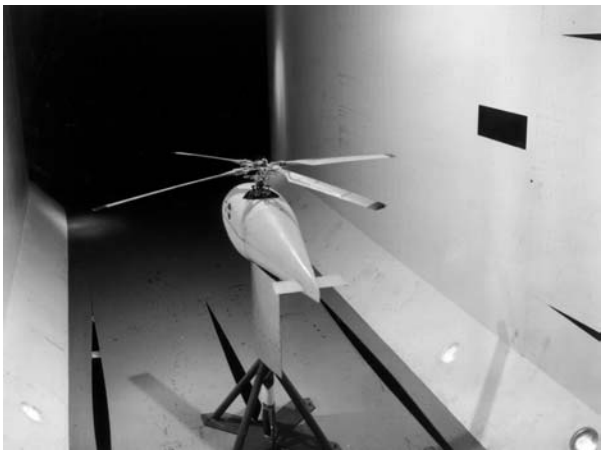

Figure 14.- Flex-hinge rotor mounted on the GRAM testbed.

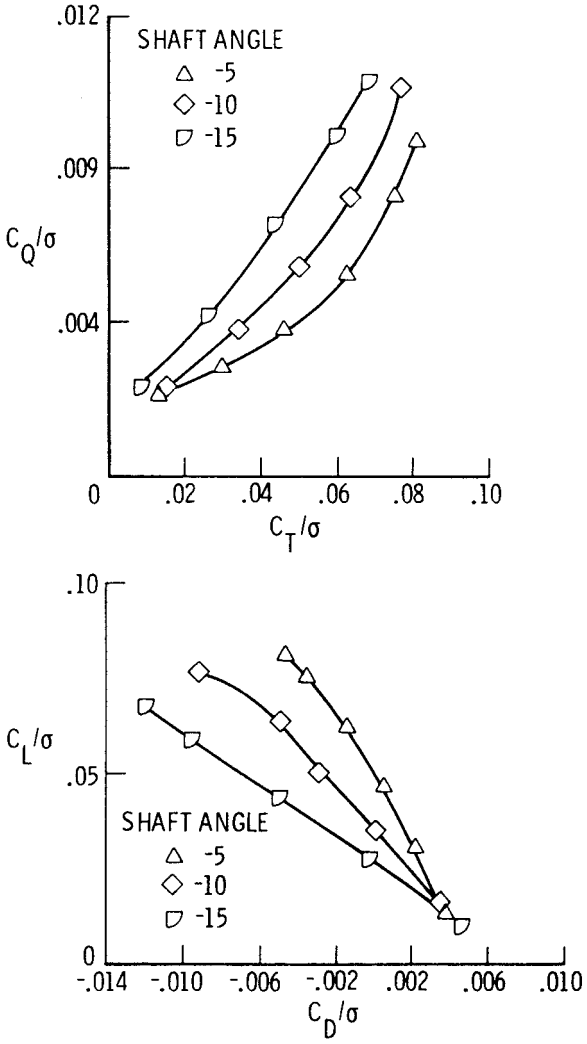

Figure 15. - Rotor performance data for the flex-hinge rotor at an advance ratio of 0.35.

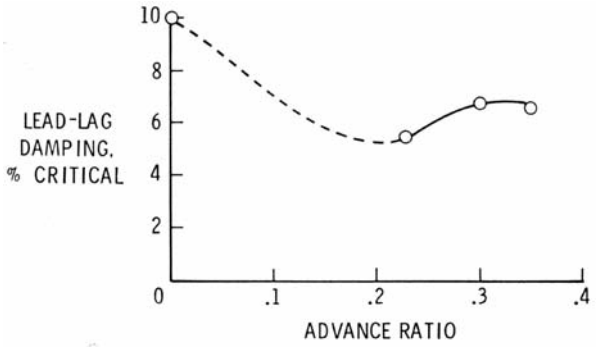

Figure 16. - Blade lead-lag mode damping as a function of advance ratio for the flex-hinge rotor.

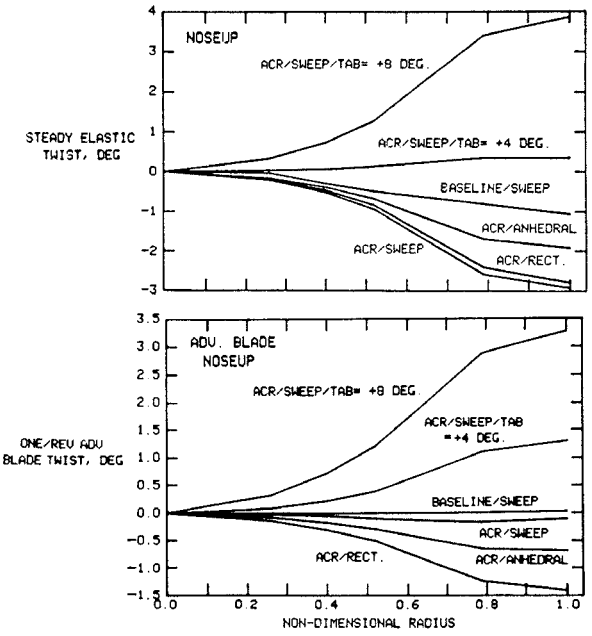

Figure 17. - One/rev lateral twist of ACR configurations and baseline rotor at $\mu = 0.30$, $\alpha_S = -5$ deg, and $C_L / \sigma = 0.08$.

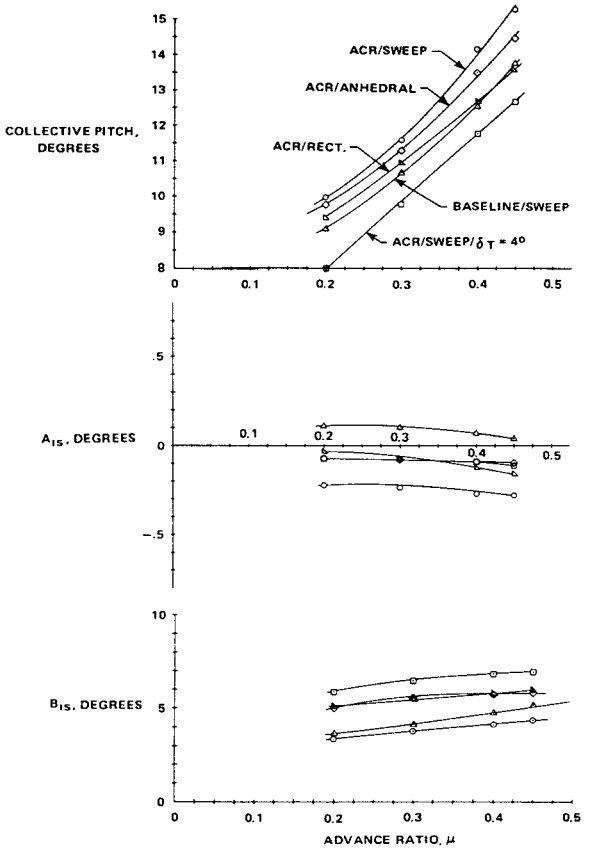

Figure 18. - Trim requirements of ACR and baseline model rotors at $C_L / \sigma = 0.07$ and $f = 30$ ft^2.

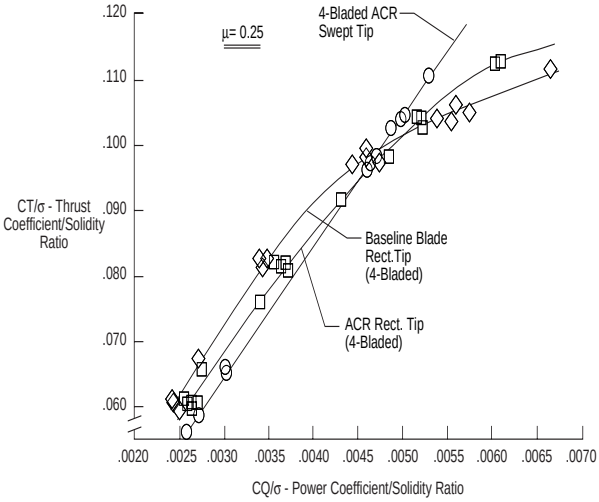

Figure 19. - Coefficient of thrust / solidity ratio vs. coefficient of power / solidity ratio at $\mu = 0.25$.

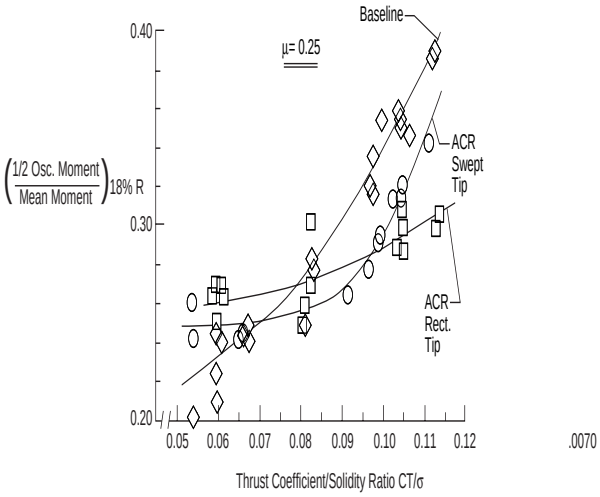

Figure 20. - Nondimensional oscillatory flapwise bending moment at 18% radius vs. thrust coefficient / solidity ratio at $\mu = 0.25$.

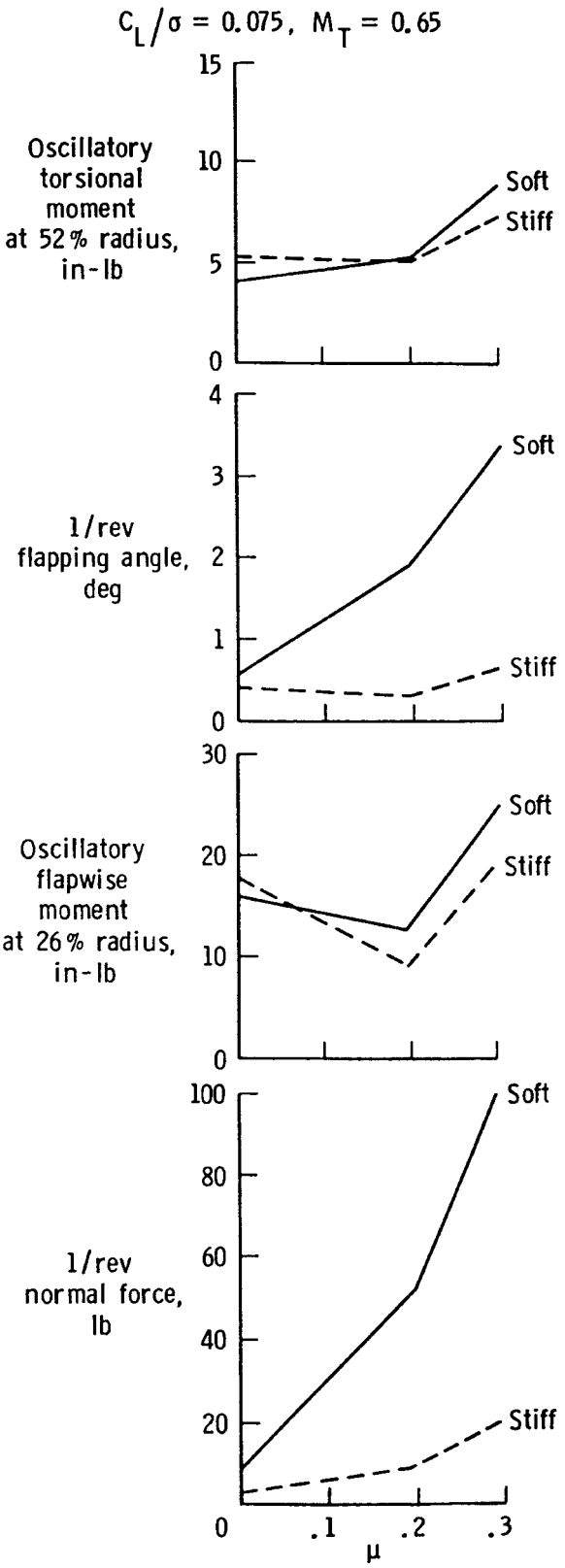

Figure 21. - Effect of 4 deg tab deflection on torsionally soft and stiff blade response.

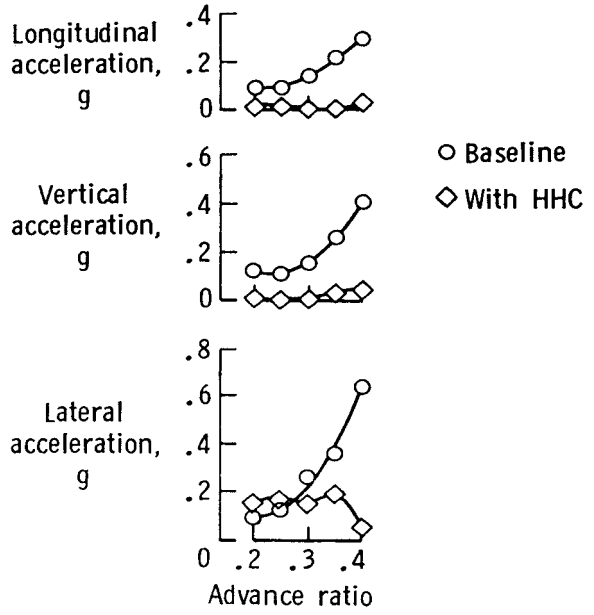

Figure 22. - Effect of higher harmonic control on fixed-system 4-per-rev vibration levels.

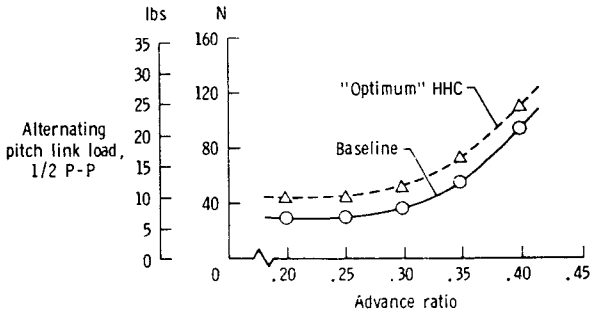

Figure 23. - Variation of alternating pitch link load (1/2 peak-to-peak values) with advance ratio.

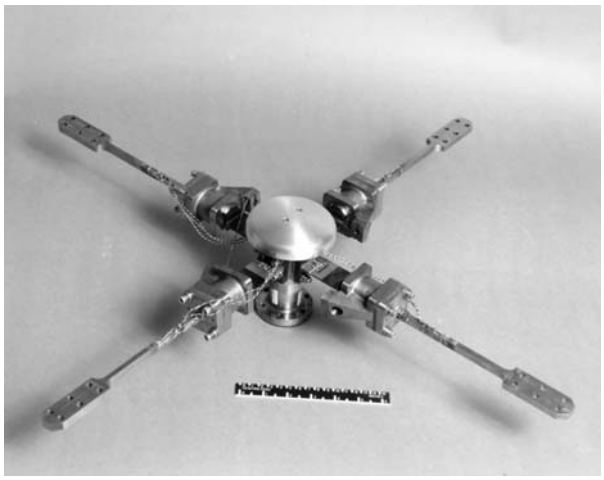

Figure 24. - Model hingeless rotor hub.

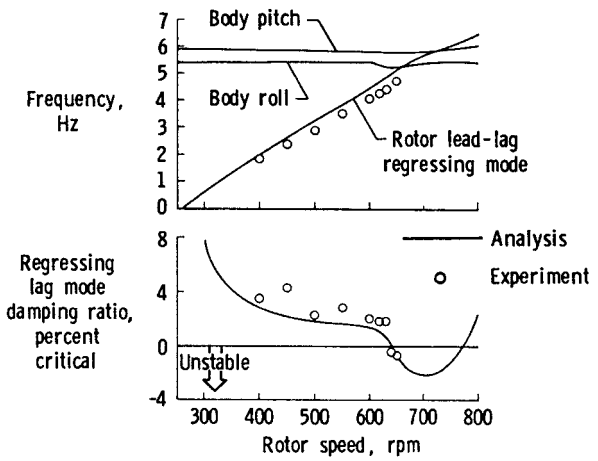

Figure 25. - Comparison of predicted and measured stability as a function of rotor speed in hover.

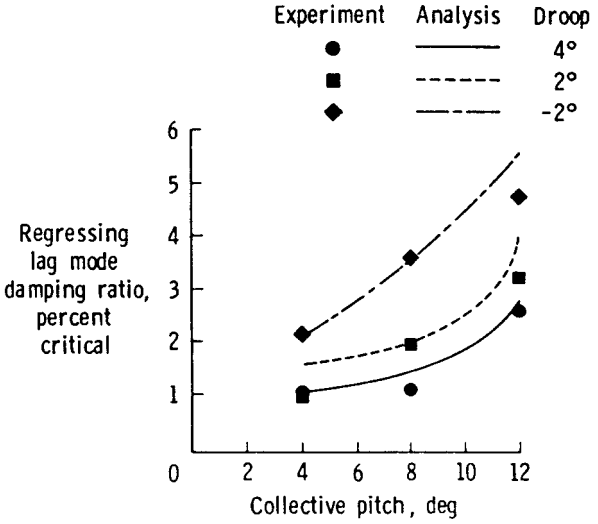

Figure 26. - Effect of blade droop angle on lead-lag damping at advance ratio = 0.30.

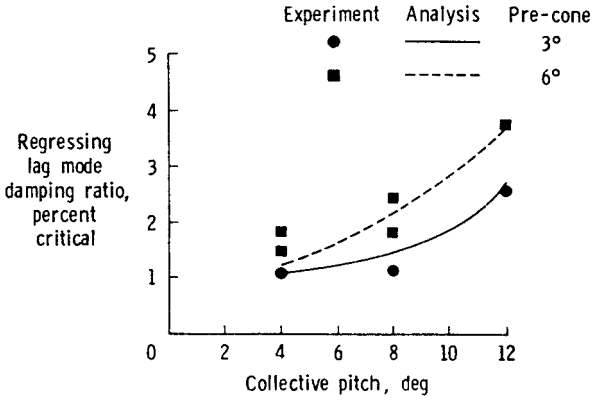

Figure 27. Effect of blade pre-cone angle on lead-lag damping at advance ratio = 0.30.

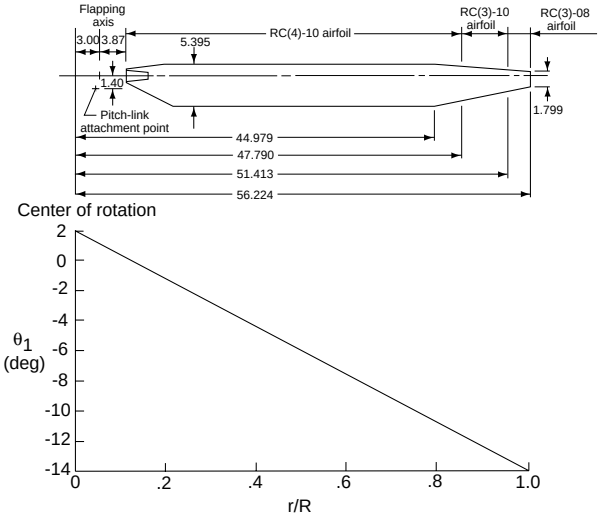

Figure 28. - Advanced rotor blade geometry and built-in twist distribution. Linear dimensions are in inches.

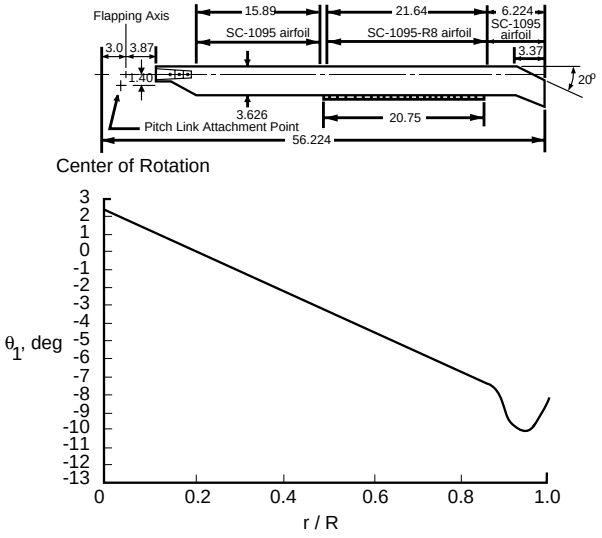

Figure 29. - Baseline rotor blade geometry and built-in twist distribution. Linear dimensions are in inches.

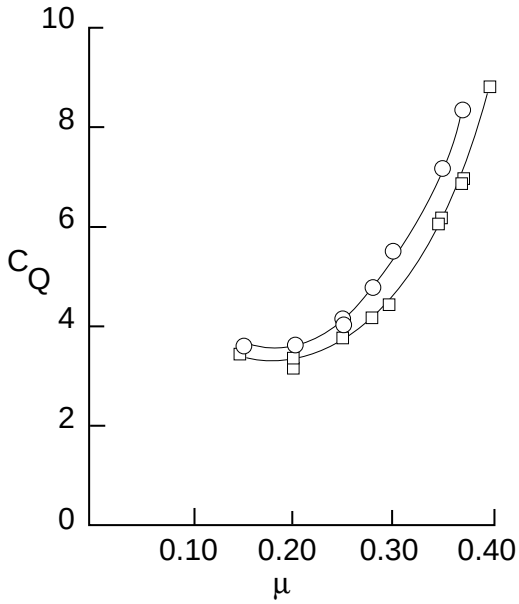

(a) Gross Weight = 18,500 lb: C_L = 0.00810.

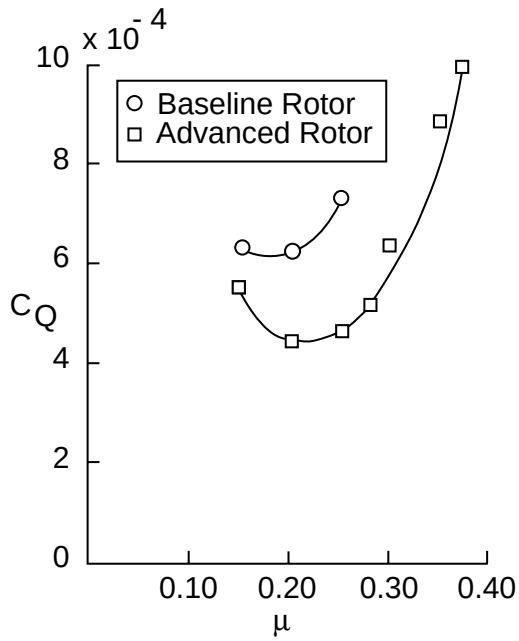

(b) Gross Weight = 24,000 lb: C_L = 0.0107.

Figure 30. - Comparison of baseline and advanced rotor C_Q for 4000 ft geometric altitude, 95 deg F ambient temperature and vehicle equivalent parasite area of 29.94 ft^2.

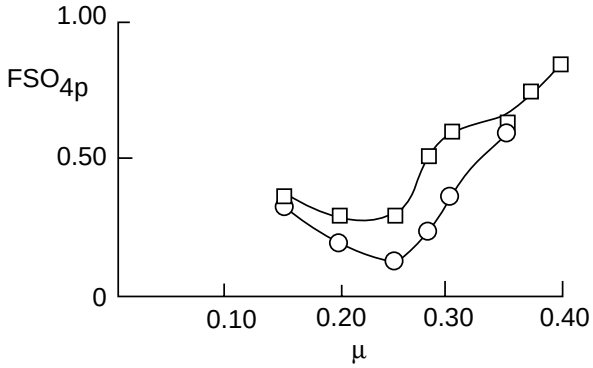

(a) Gross Weight = 18,500 lb: C_L = 0.00810.

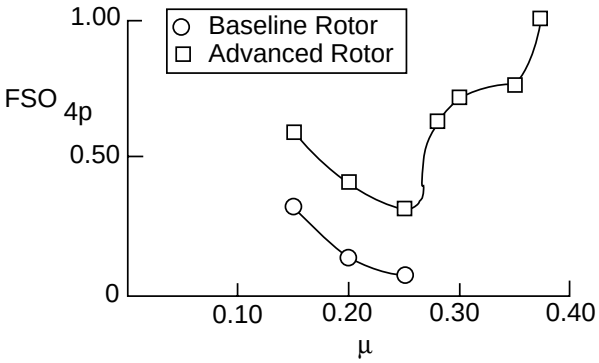

(b) Gross Weight = 24,500 lb: C_L = 0.0107.

Figure 31. - Comparison of 4-per-rev vertical fixed-system loads for baseline and advanced rotor configurations at 4000 ft geometric altitude, 95 deg F ambient temperature and vehicle equivalent parasite area of 29.94 ft^2.

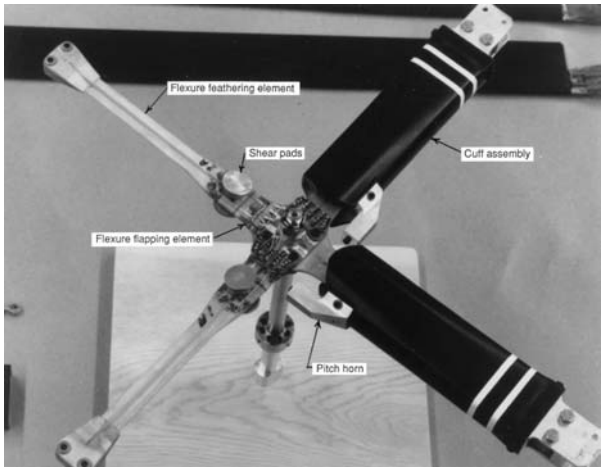

Figure 32. - Model bearingless rotor hub.

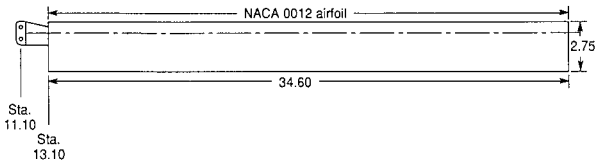

Figure 33. - Geometry of Froude-scaled model rotor blades. All dimensions are in inches.

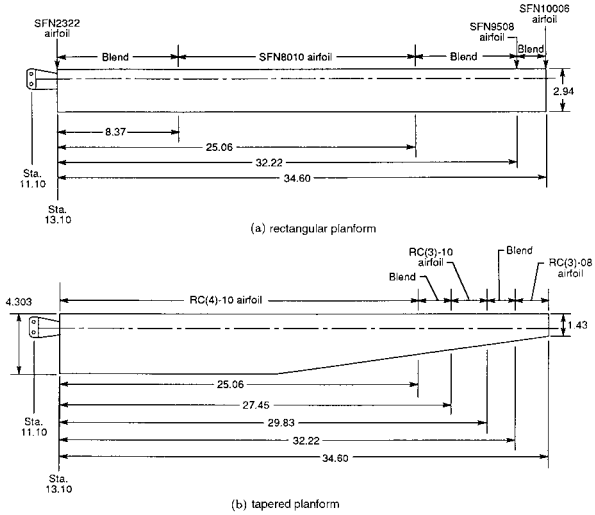

Figure 34. - Geometry of Mach-scaled model rotor blades. All dimensions are in inches.

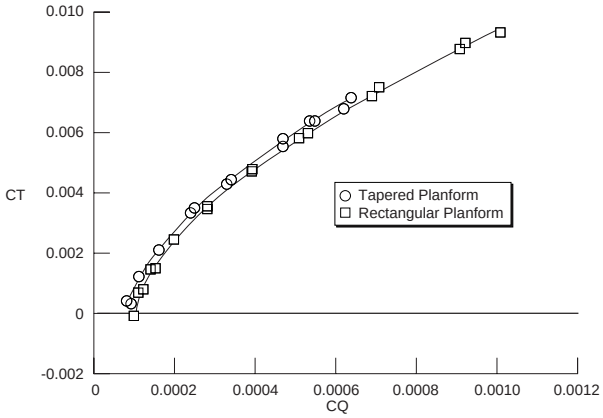

Figure 35. - Comparison of hover performance (IGE, M_T = 0.626) of the rectangular and tapered planform blades.

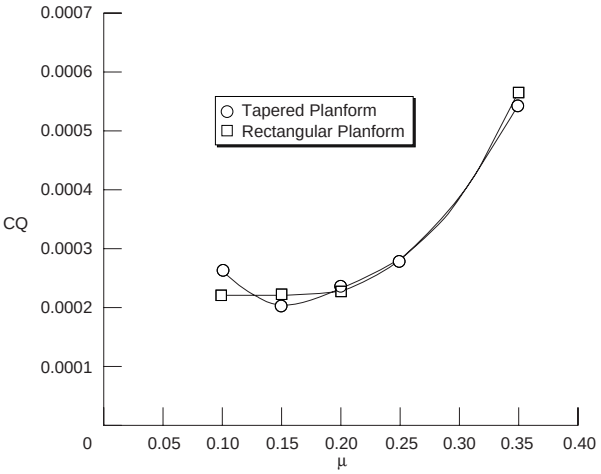

Figure 36. - Comparison of the forward flight performance of the rectangular and tapered planform blades (vehicle equivalent parasite area = 20.65 ft^2).

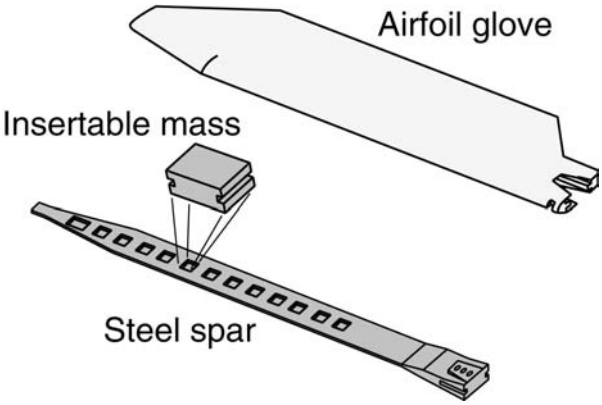

Figure 37. - Components of advanced model rotor blade used for vibration reduction research.

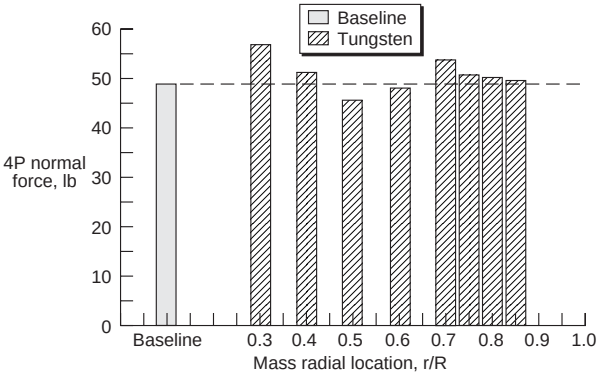

Figure 38. - Effect of non-structural mass on 4-per-rev fixed-system loads for T= 285 lbs and μ = 0.35.

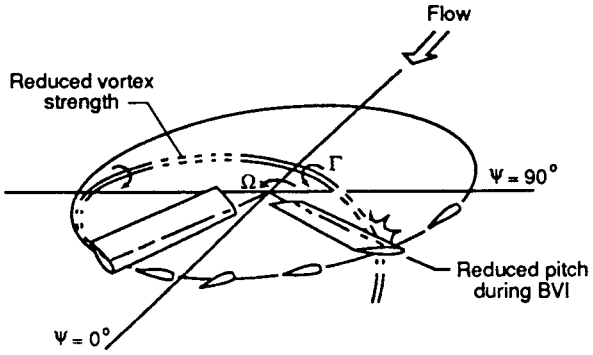

Figure 39. - Illustration of noise reduction concept.

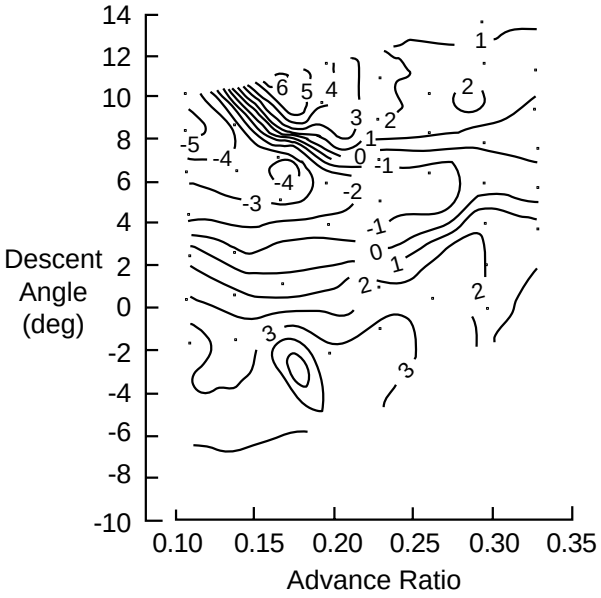

Figure 40. - Effect of higher harmonic pitch (HHP) on rotor noise levels (db).

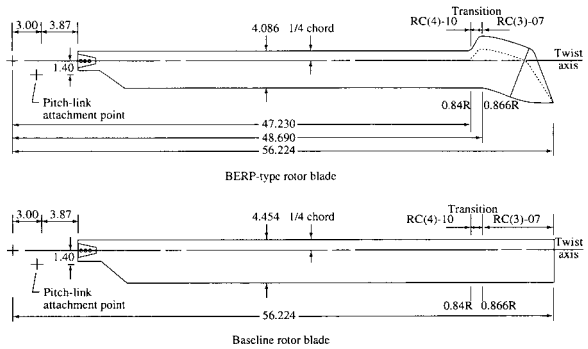

Figure 41. - BERP-type and baseline rotor blade geometries. Linear dimensions are in inches.

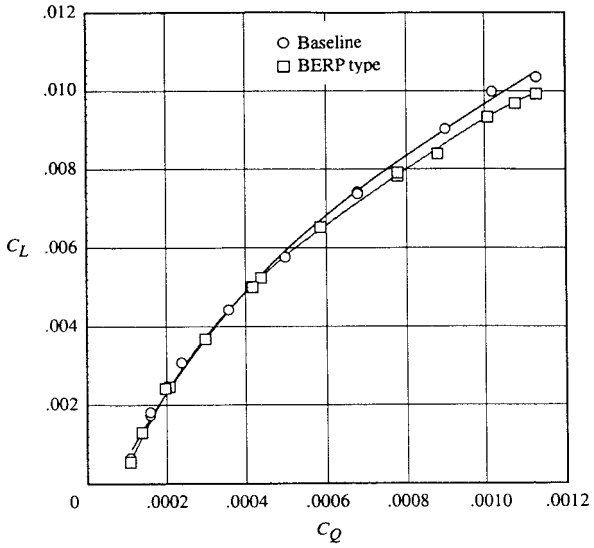

Figure 42. - Rotor hover performance at $M_T = 0.628$ and z / d = 0.83.

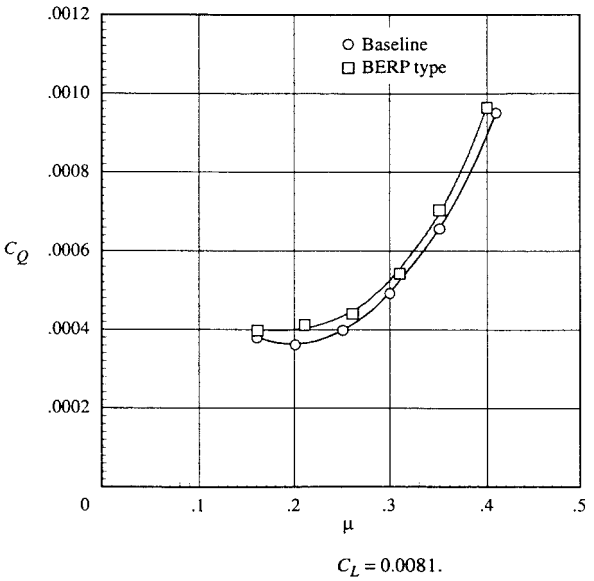

Figure 43. - Variation of rotor torque coefficient with advance ratio for $M_T = 0.628$ and vehicle equivalent parasite area = 29.94 ft^2.

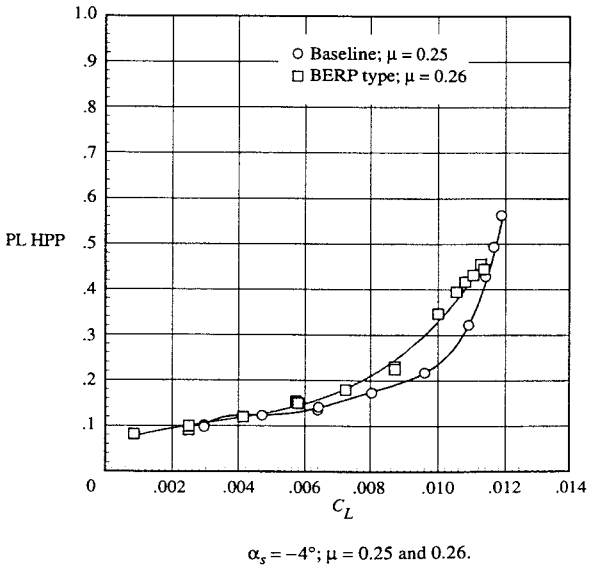

Figure 44. - Pitch-link oscillatory loads for baseline and BERP-type rotors at α_S = -4 deg; μ = 0.25 and 0.26.

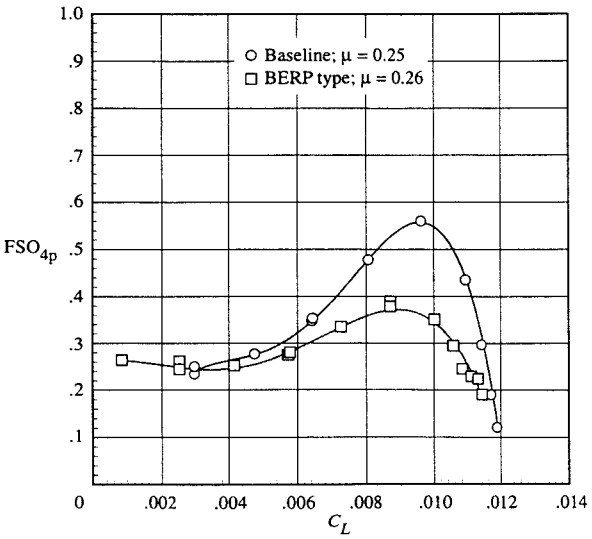

Figure 45. - The 4-per-rev vertical fixed-system loads for baseline and BERP-type rotors at α_S = -4 deg; μ= 0.25 and 0.26.

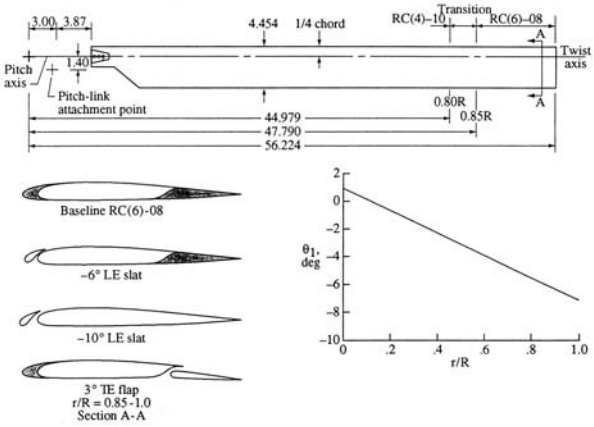

Figure 46. - HIMARCS-I rotor blade geometry and twist distribution. Linear dimensions in inches.

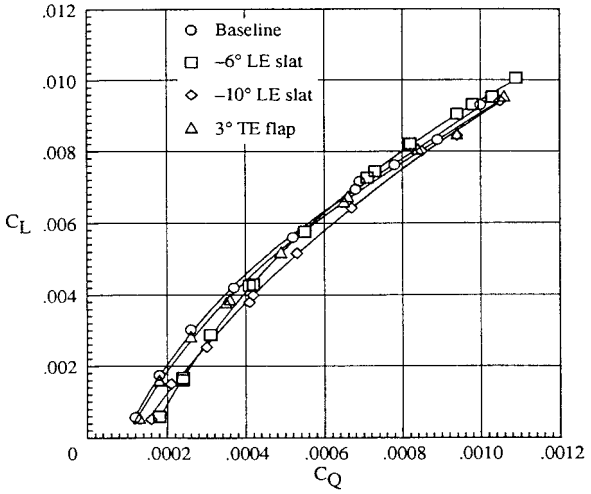

Figure 47. - Rotor hover performance at M_T=0.627 and z/d =0.83.

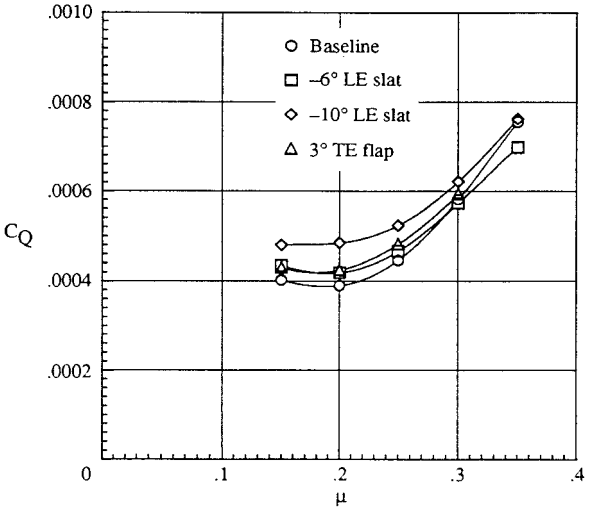

Figure 48. - Variation of rotor torque coefficient with advance ratio for C_L = 0.0081, M_T = 0.627 and vehicle equivalent parasite area = 29.94 ft^2.

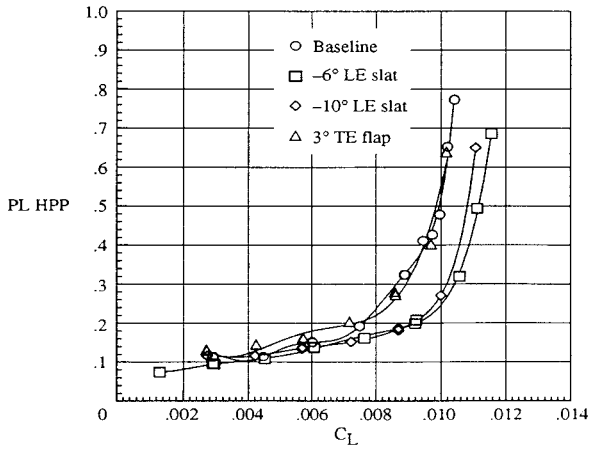

Figure 49. - Variation of pitch-link oscillatory loads with rotor lift coefficient for $M_T = 0.627$, $\mu = 0.25$, and $\alpha_S = -4$ deg.

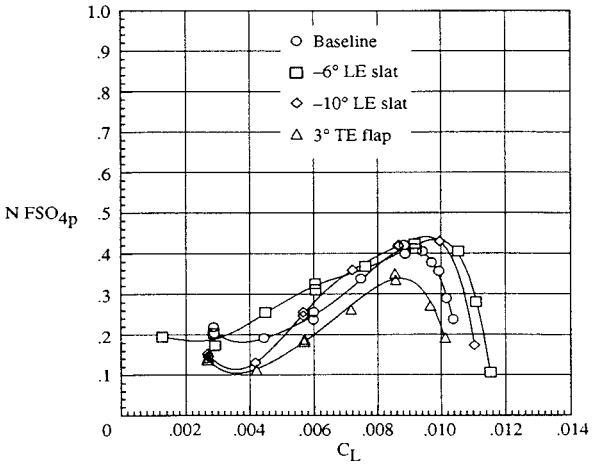

Figure 50. - Variation of 4-per-rev vertical fixed-system loads with rotor lift coefficient for $M_T = 0.627$, and $\alpha_S = -4$ deg.

Figure 51. - Baseline (Advanced S-61) model rotor blade.

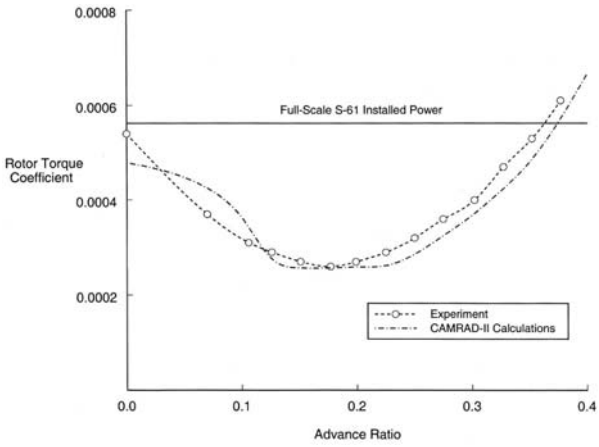

Figure 52. - Comparison of analytical and experimental forward flight rotor performance of advanced S-61 rotor at GW = 20,000 lbs, vehicle equivalent parasite area = 34.55 ft^2 and SLS.

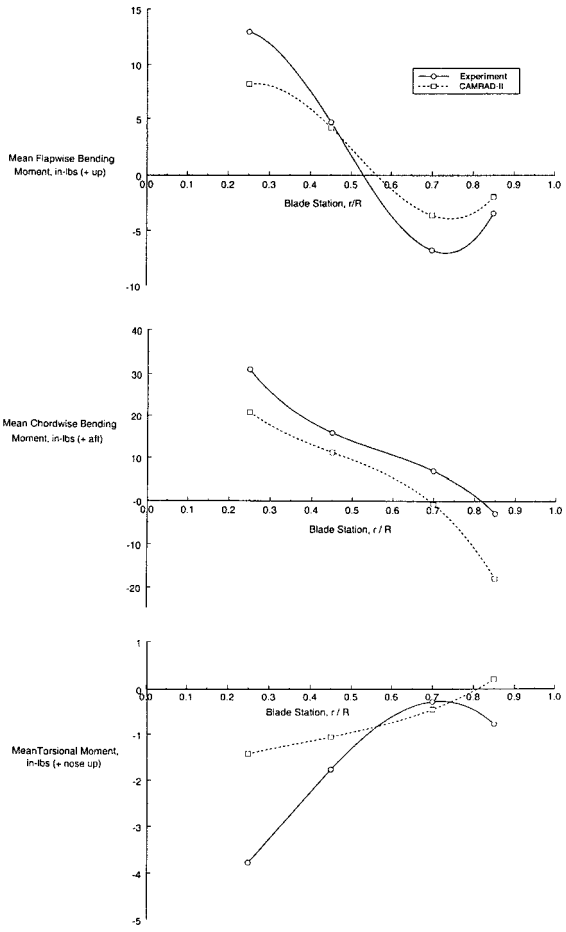

Figure 53. - Comparison of analytical and experimental mean blade bending and torsion moments for advanced S-61 rotor at GW = 20,000 lbs, advance ratio = 0.25, vehicle equivalent parasite area = 34.55 ft^2, and SLS.

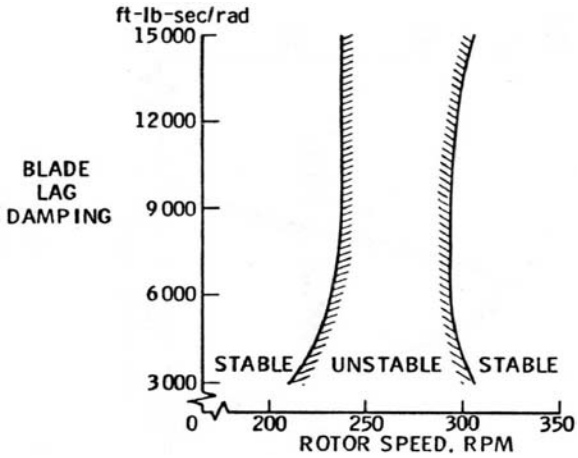

Figure 54. - Ground resonance instability region as a function of blade lag damping for non-isotropic hub with one blade damper inoperative.

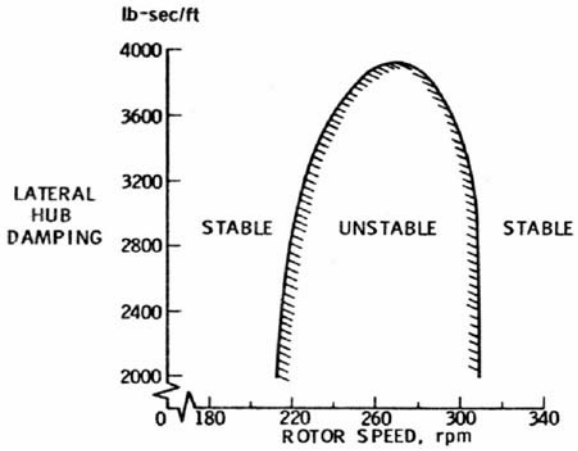

Figure 55. - Effect of lateral hub damping on region of instability with one blade damper inoperative.

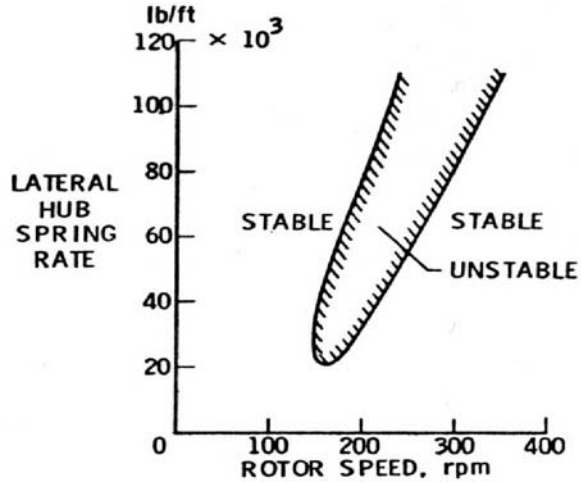

Figure 56. - Effect of lateral hub spring rate on region of instability with one blade damper inoperative.

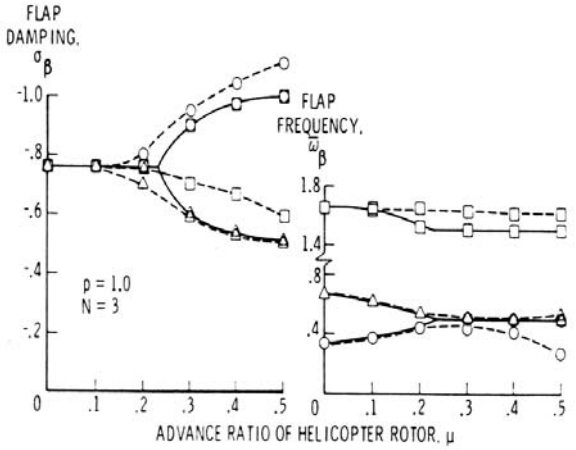

(a) $\delta_3 = 0$

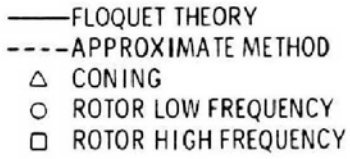

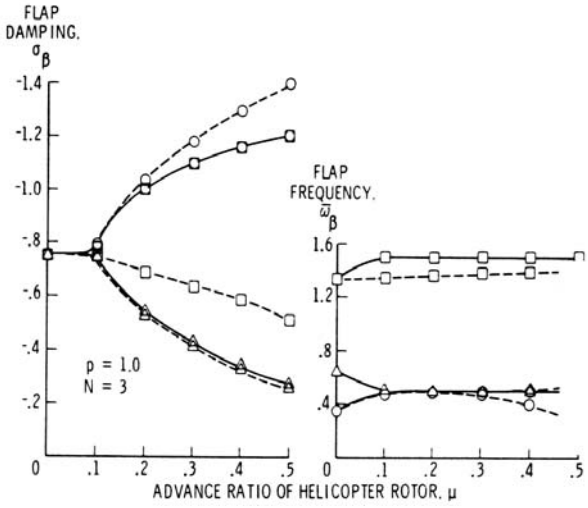

(b) $\delta_3 = -11.46°$

Figure 57. - Comparison of pure flapping stability boundaries as obtained from Floquet theory and approximate method.

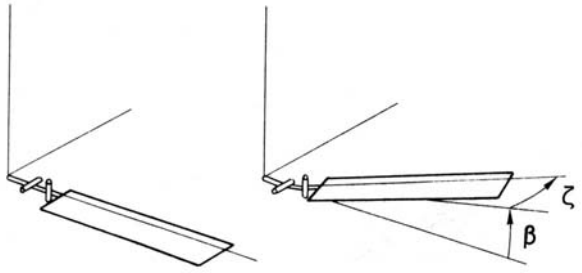

(a) Lag hinge outboard of flap hinge ("Flap-lag hinge sequence")

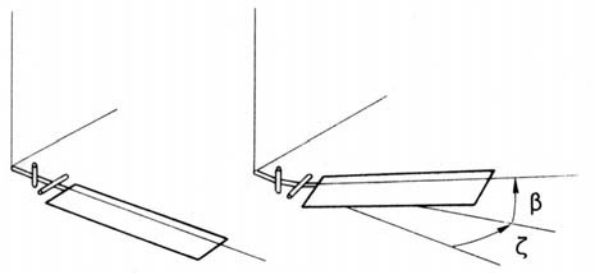

(b) Lag hinge inboard of flap hinge ("Lag-flap hinge sequence")

Figure 58. - Hinge geometry for articulated blade.

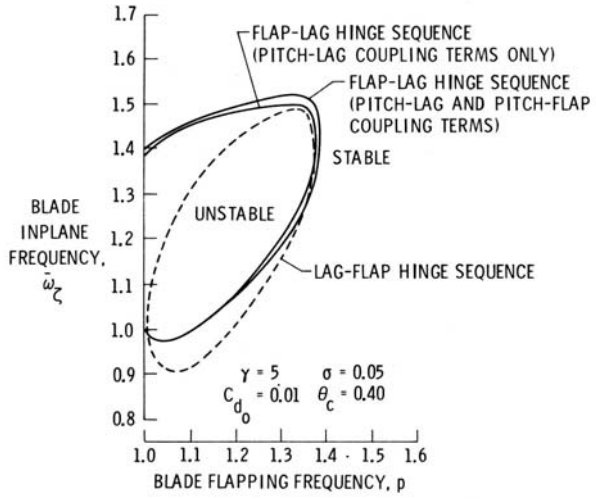

Figure 59. - Effect of pitch-lag and pitch-flap coupling due to steady state flapping and lagging on flap-lag stability in hover.

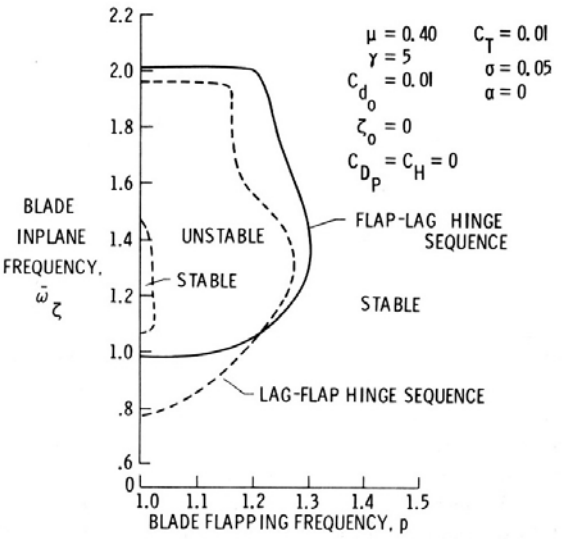

Figure 60. - Effect of hinge sequence on flap-lag stability in forward flight (approximate method).

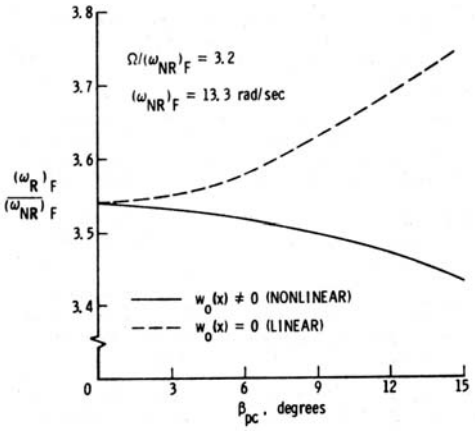

(a) First flapwise bending mode

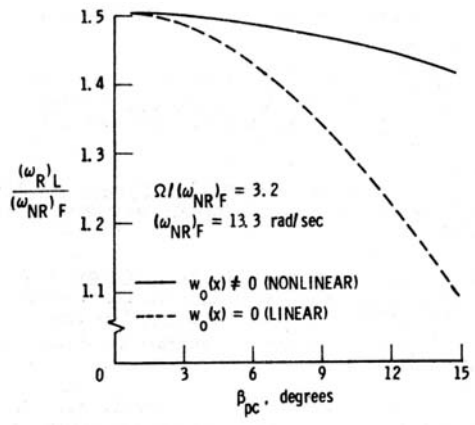

(b) First lagwise bending mode

Figure 61. - Effect of steady-state deformation $w_o(x)$ induced by rotation for non-zero values of precone on bending mode frequencies of a symmetric beam.

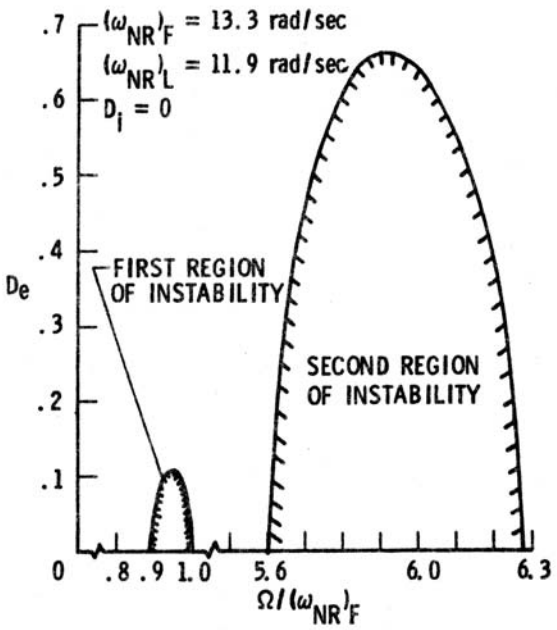

Figure 62. - Effect of external viscous damping on stability of an asymmetric rotating shaft.

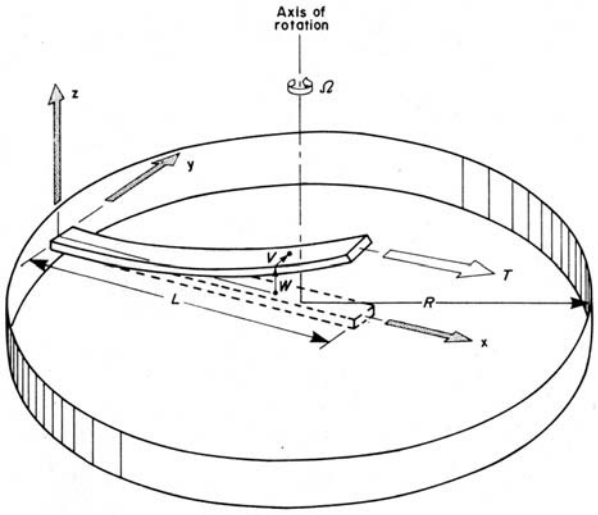

Figure 63. - Rotating beam clamped off the axis of rotation.

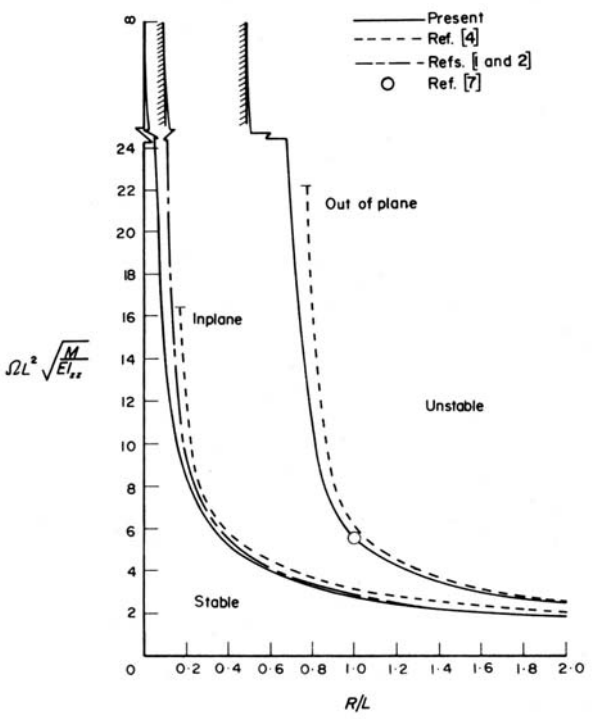

Figure 64. - Critical speed for inplane and out-of-plane buckling of a symmetric rotating beam clamped off the axis of rotation (continuous mass representation of uniform beam).

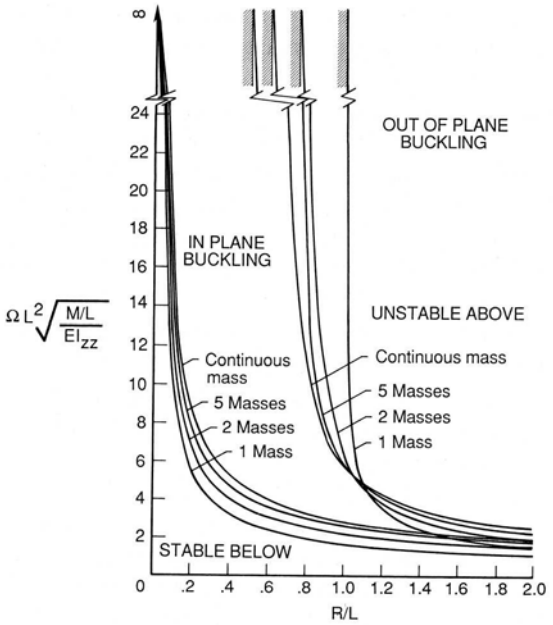

Figure 65. - Critical speed for buckling of a symmetric rotating beam clamped off the axis of rotation (discrete mass representation of uniform beam).

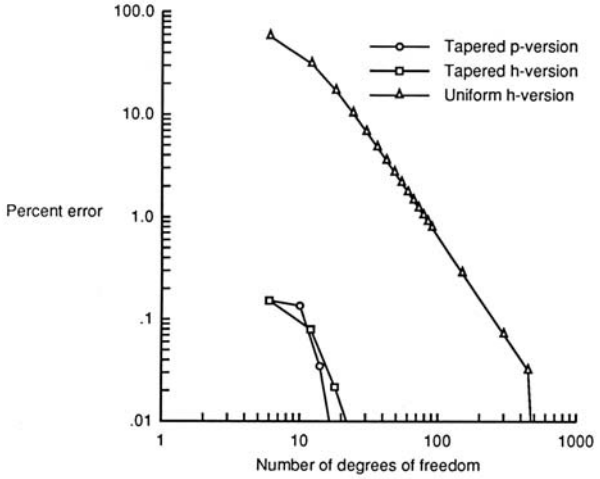

(a) First bending mode frequency

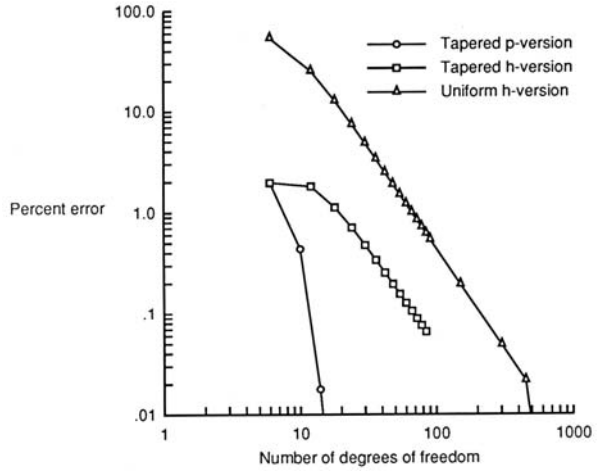

(b) First torsional mode frequency

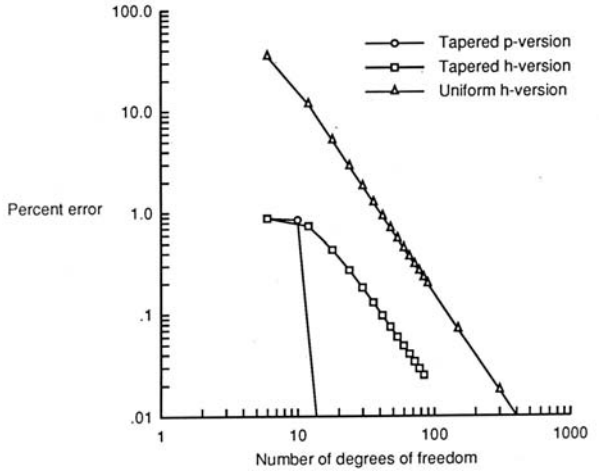

(c) First axial mode frequency

Figure 66. - Percent error in calculated frequencies of a tapered beam versus the number of finite-element degrees of freedom used to model the beam.

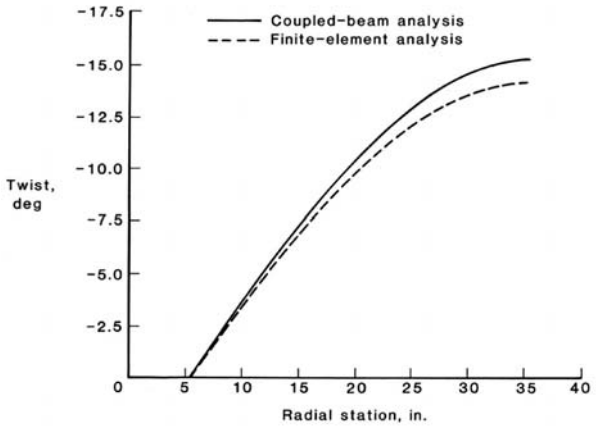

Figure 67. - Calculated twist of model rotor blade due to a statically-applied centrifugal force loading.

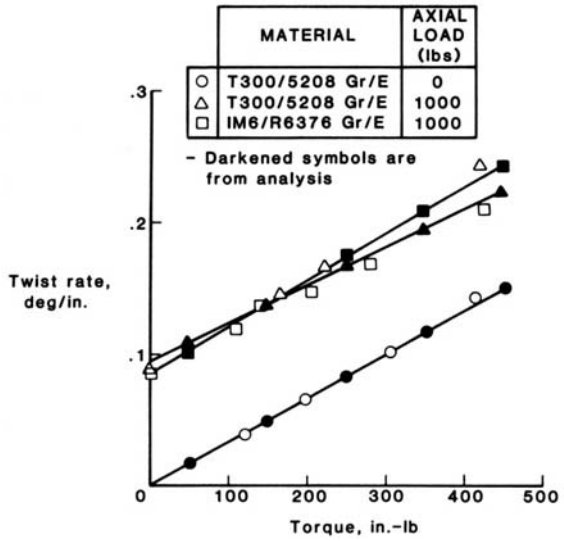

Figure 68. - Measured twist rate as a function of torque for composite tube with $[(+20/-70)_2]_S$ lay-up.

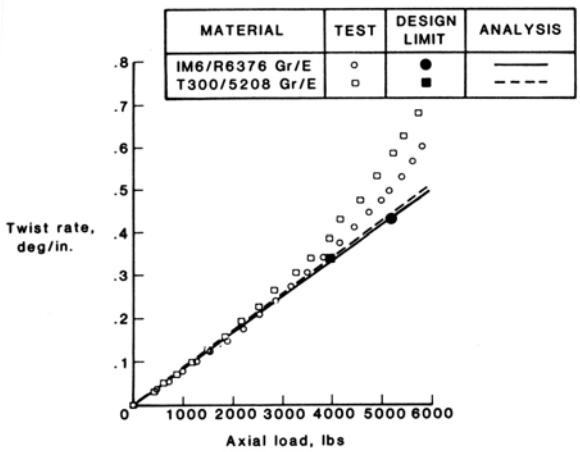

Figure 69. - Variation of measured and calculated twist rates with axial load for tube with $[(+20/-70)_2]_S$ lay-up.

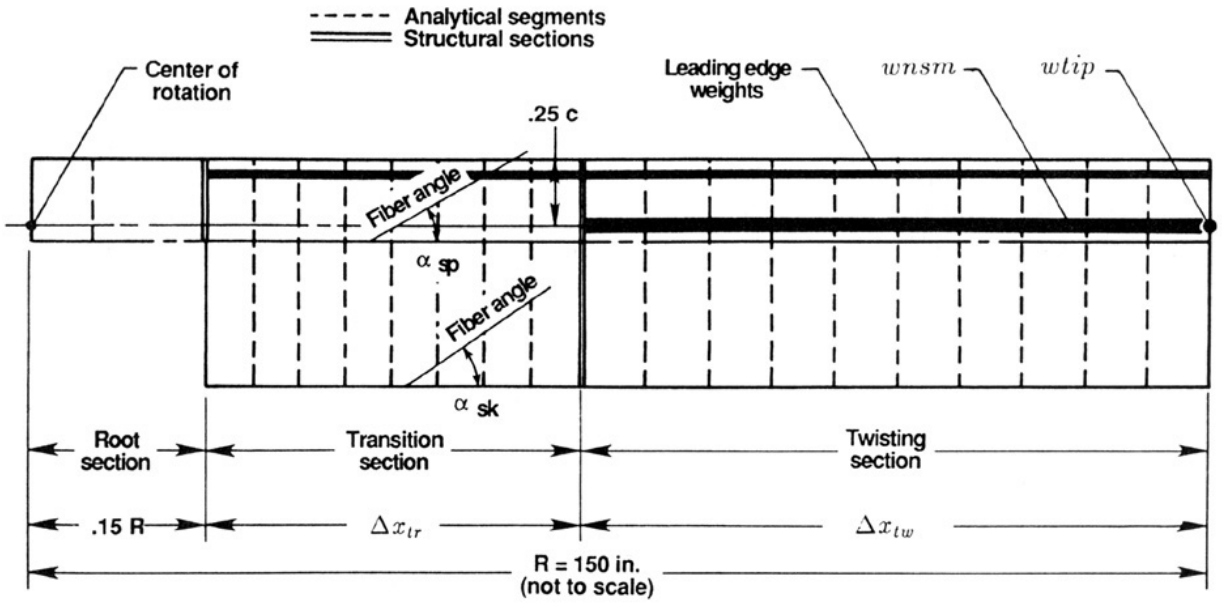

(a) Blade planform

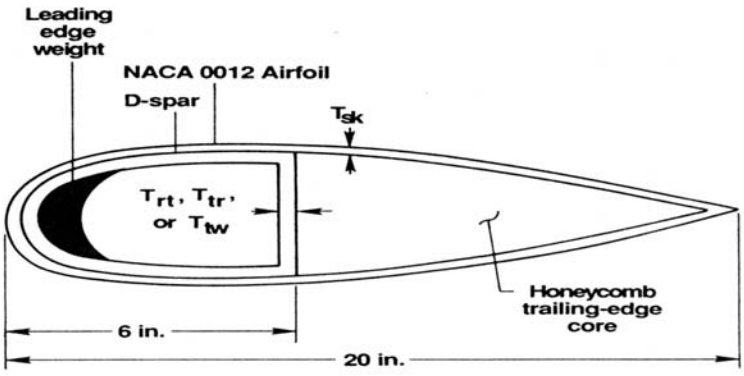

(b) Blade cross section

Figure 70. - Structural configuration of a hypothetical model rotor blade used to analytically study passive blade twist control via extension-twist elastic coupling.

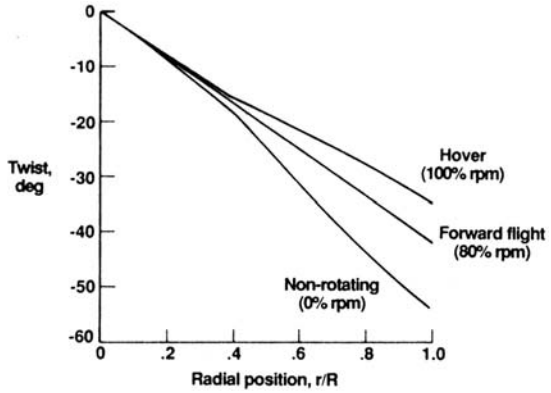

Figure 71. - Variations in blade twist distribution calculated for an extension-twist-coupled design obtained using the structural model shown in figure 70.

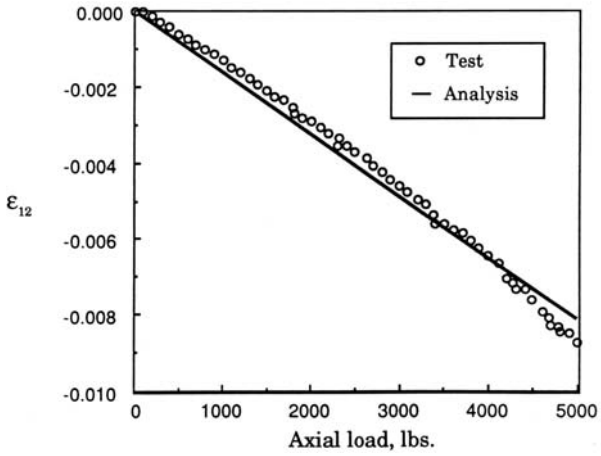

Figure 74. - Principal shear strain as a function of axial load for the hollow D-shaped composite tube.

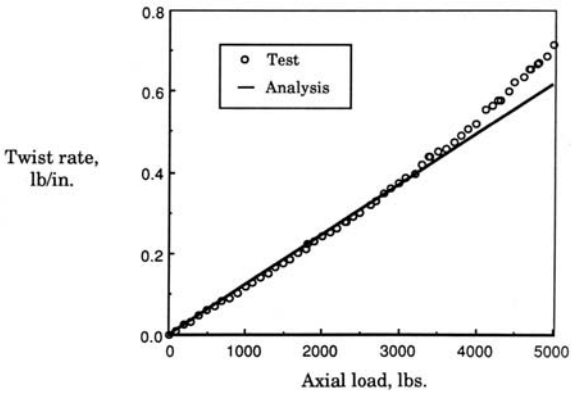

Figure 72. - Twist rate as a function of axial load for hollow D-shaped composite tube.

Figure 75. - Composite tubular spars with D-shaped, elliptical, and square cross sections, respectively.

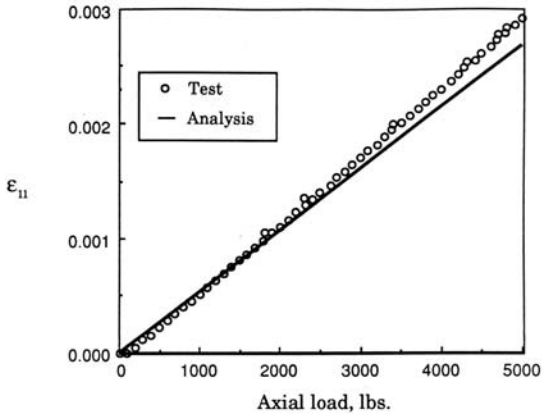

Figure 73. - Principal fiber strain as a function of axial load for the hollow D-shaped composite tube.

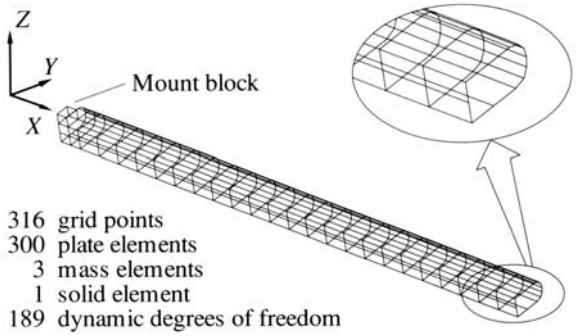

Figure 76. - Finite-element model of D-shaped composite spar.

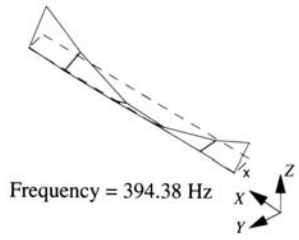

(a) First vertical bending.

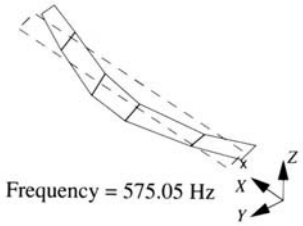

(b) First lateral bending.

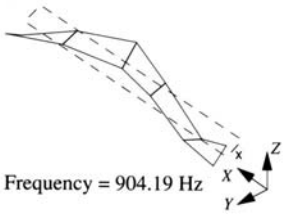

(c) Second vertical bending.

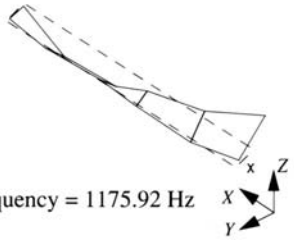

(d) First torsion.

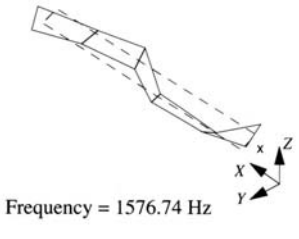

(e) Second lateral bending.

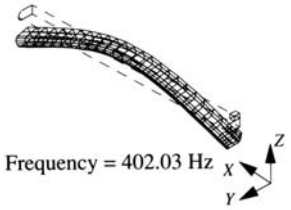

(a) First vertical bending.

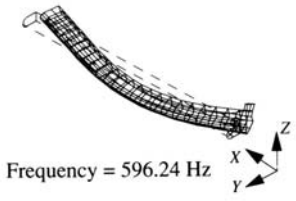

(b) First lateral bending.

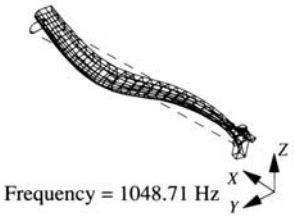

(c) Second vertical bending.

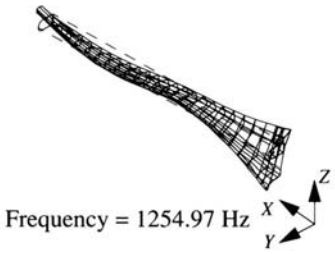

(d) First torsion.

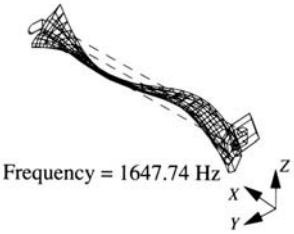

(e) Second lateral bending.

Figure 77. - Measured (left) and calculated (right) mode shapes for D-shaped composite spar.

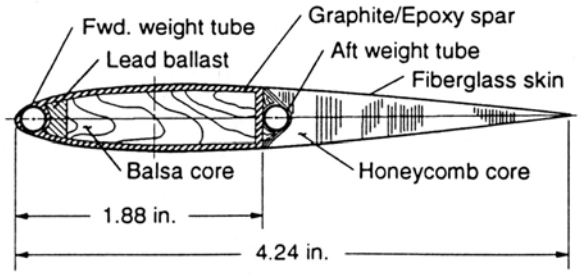

Figure 78. - Cross section of extension-twist-coupled model rotor blade used in hover test.

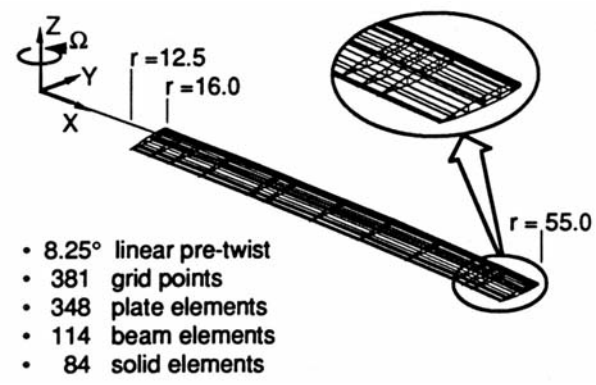

Figure 79. - Finite-element model of extension-twist-coupled model rotor blade shown in figure 78.

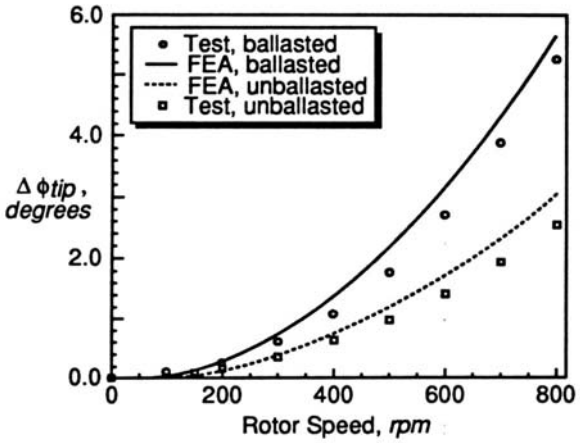

Figure 80. - Change in blade elastic twist at tip as a function of rotor speed.

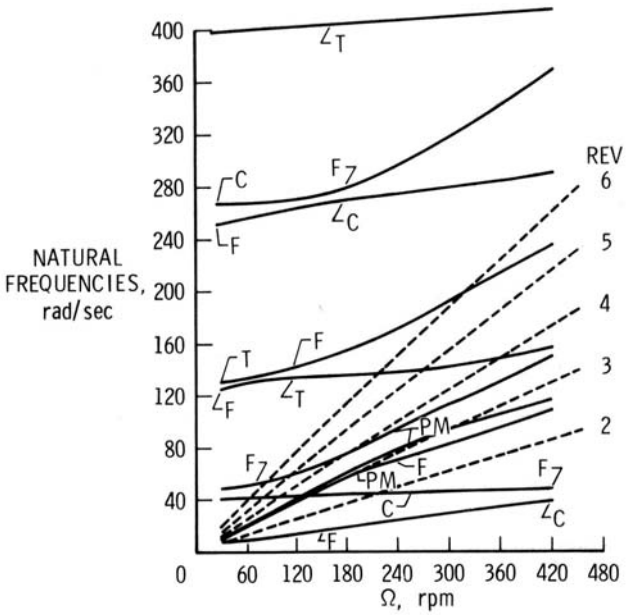

Figure 81. - Variation of blade natural frequencies with rotational speed for a hingeless blade with a spherical pendulum and 12 degrees of collective pitch (F=flap, C=chord, T=torsion, PM=pendulum mode).

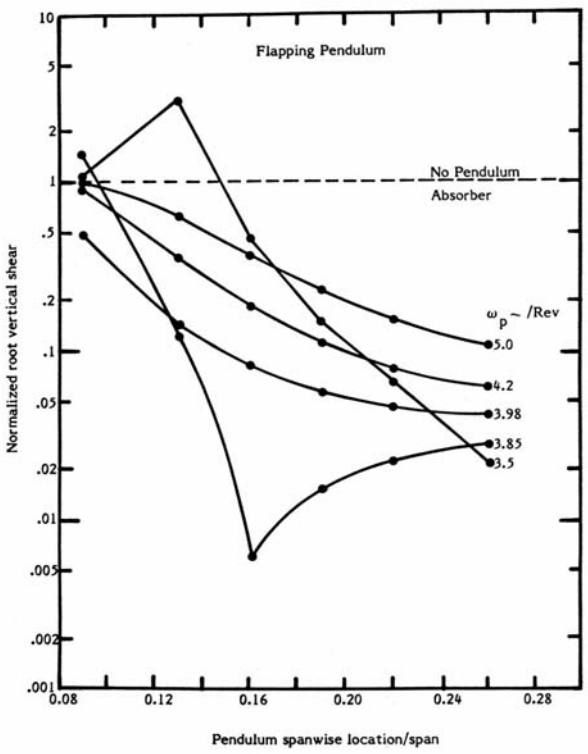

Figure 82. - Root vertical shear for 4/rev concentrated excitation of a nonuniform blade with a flapping pendulum.

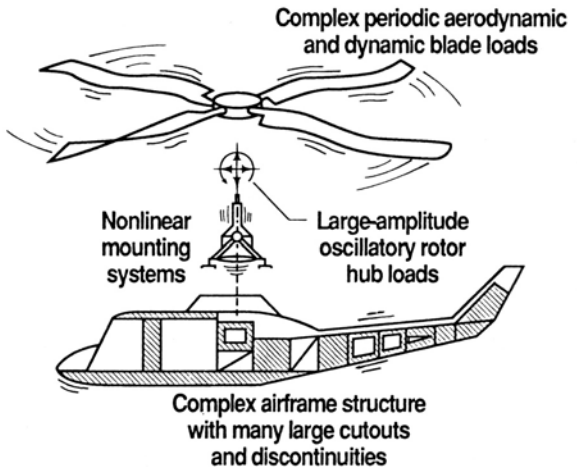

Figure 83. - Challenges confronting analysts in predicting helicopter vibrations.

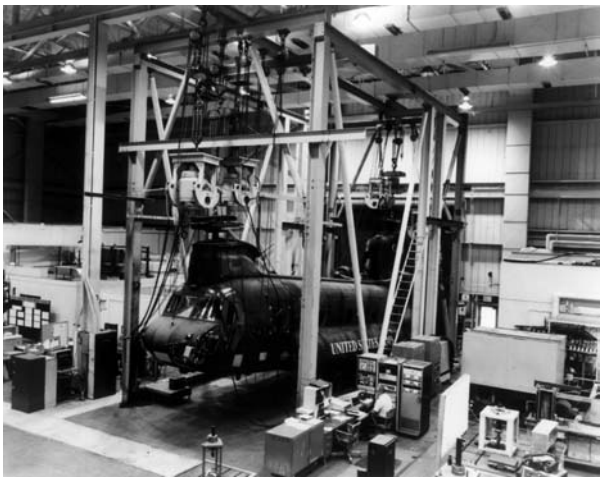

Figure 86. - Ground vibration test of CH-47D.

Figure 84. - CH-47D helicopter.

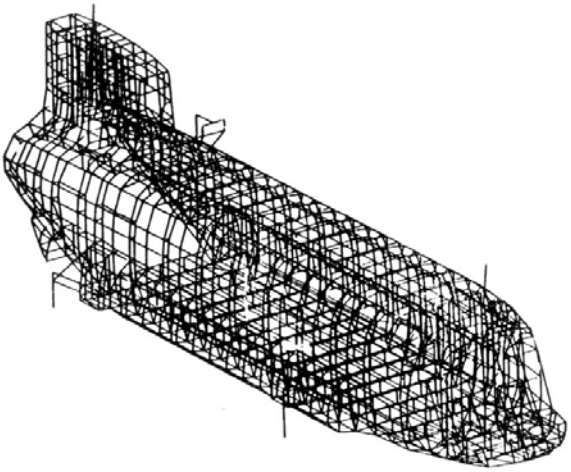

Figure 85. - CH-47D NASTRAN finite-element model.

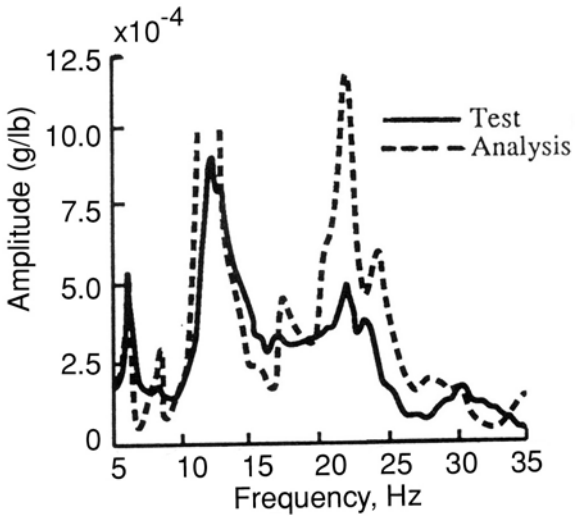

Figure 87. - Comparison of measured and calculated lateral responses of CH-47D cockpit for lateral excitation at the forward hub.

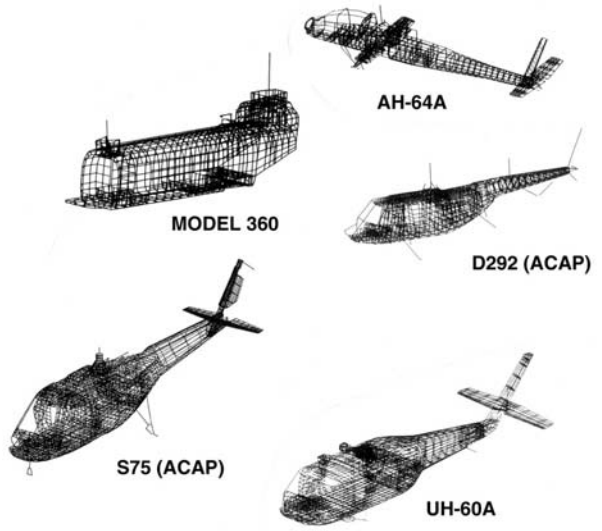

Figure 88. - Finite-element models formed under DAMVIBS program.

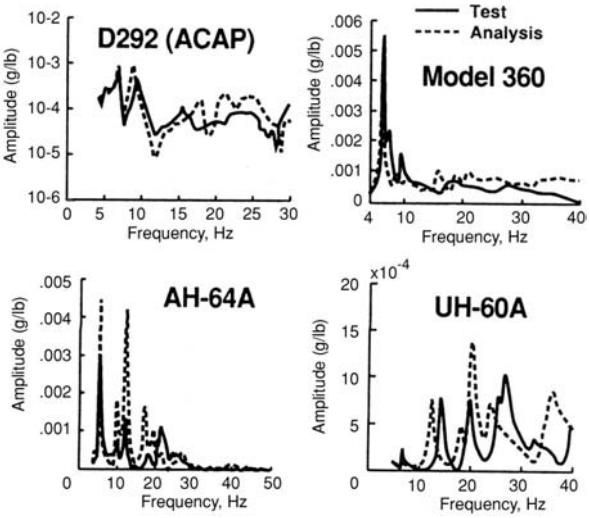

Figure 90. - Typical test/analysis comparisons of airframe frequency response amplitudes.

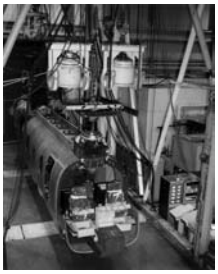

Model 360

UH-60A

D292 (ACAP)

AH-64A

Figure 89. - Ground vibration tests conducted under DAMVIBS program.

(a) Complete airframe

(b) Stripped-down airframe

Figure 91. - Difficult components study of AH-1G helicopter airframe.

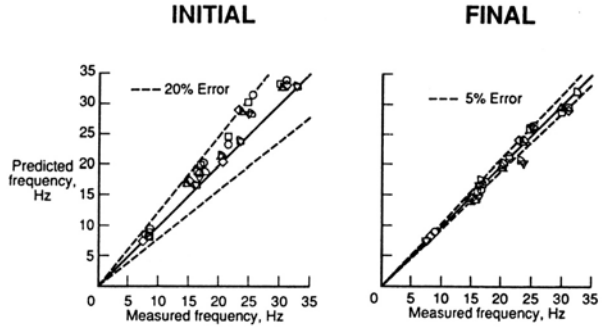

Figure 92. - AH-1G natural frequency comparisons using initial and improved finite-element models.

Figure 93. - AH-1G helicopter.

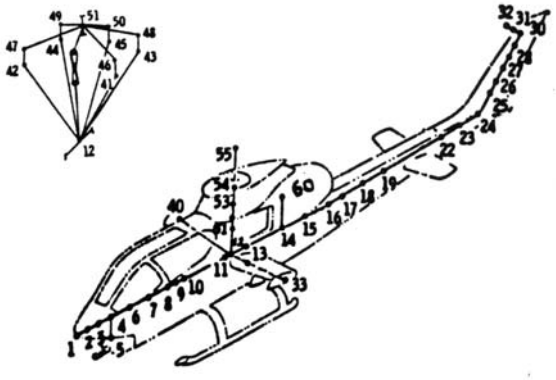

Figure 94. - Elastic line or "stick" finite-element model of AH-1G helicopter airframe.

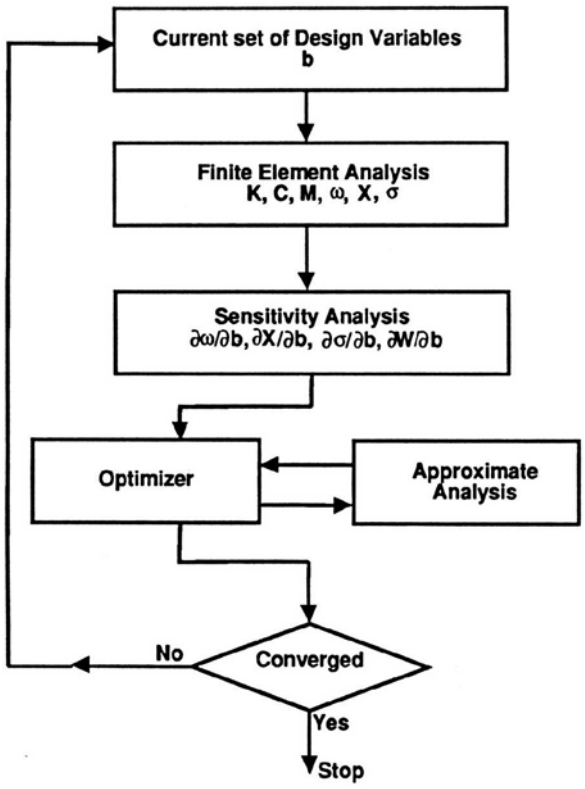

Figure 95. - Major computational steps in DYNOPT optimization program.

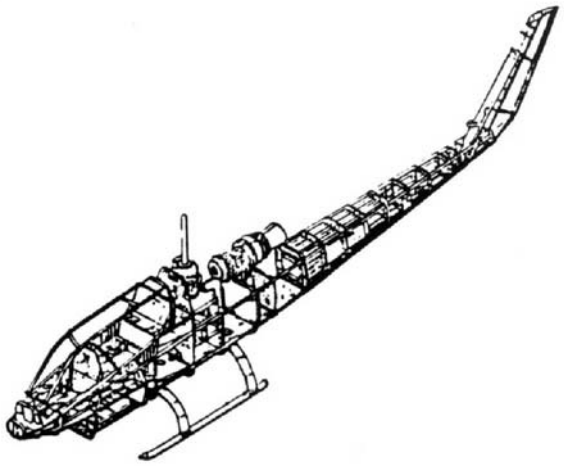

Figure 96. - AH-1G helicopter airframe with skins removed.

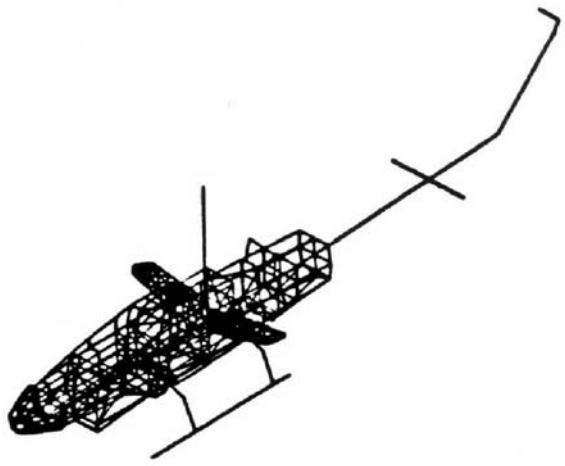

Figure 97. - AH-1G finite-element model used in optimization studies.

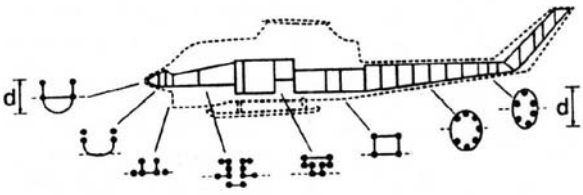

Figure 98. - Preliminary design model for optimization.

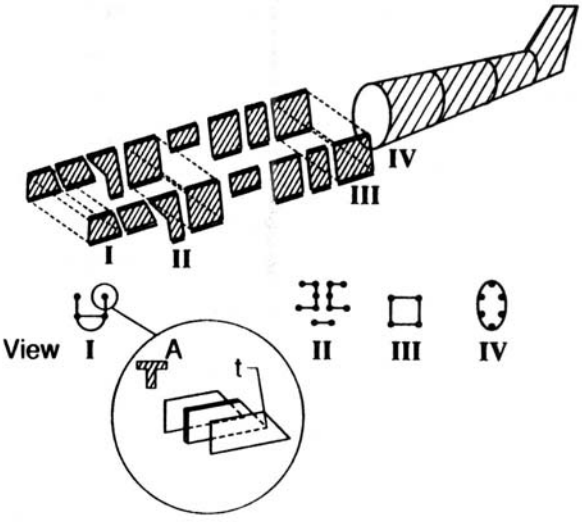

Figure 99. - Detailed design model for optimization.

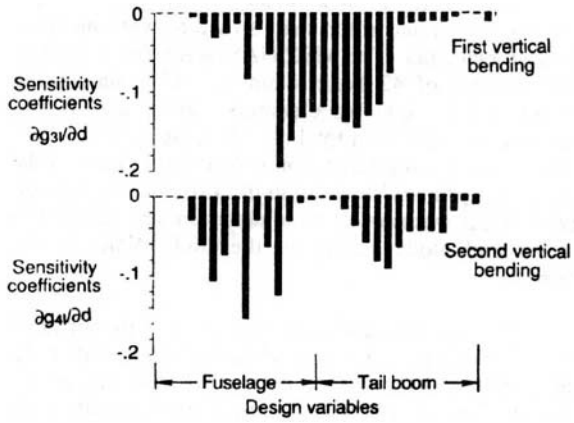

Figure 100. - Sensitivity of airframe vertical bending natural frequencies to changes in design variables.

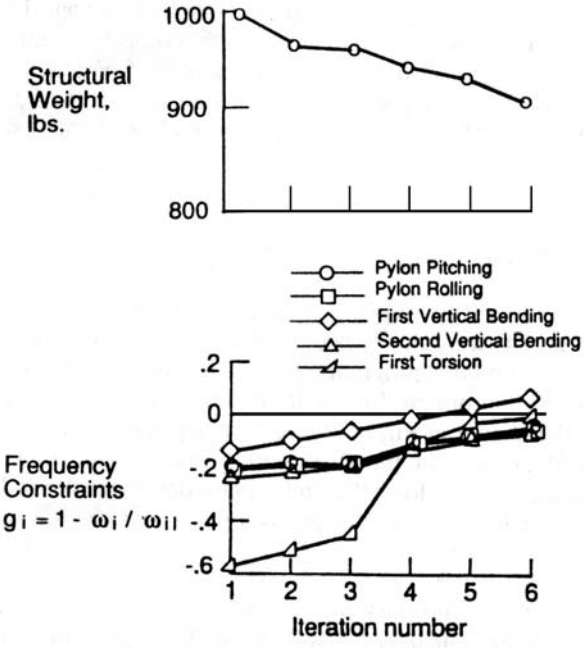

Figure 101. - Iteration history of objective function and frequency constraints.

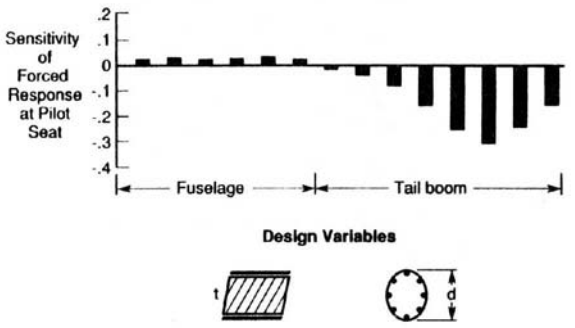

Figure 102. - Sensitivity of forced response displacement constraint at pilot seat location to changes in design variables.

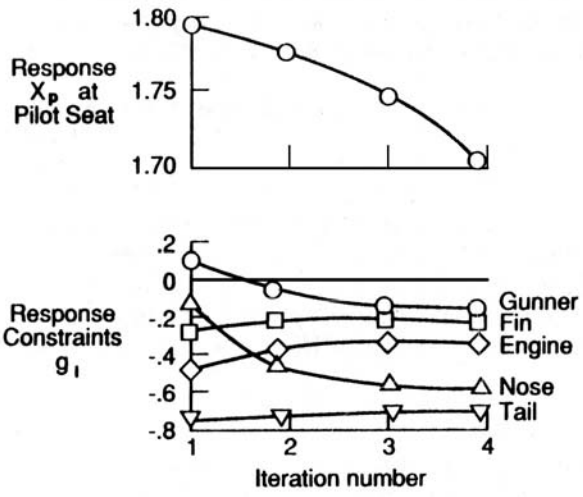

Figure 103. - Iteration history of the objective and constraint functions for detailed design model.

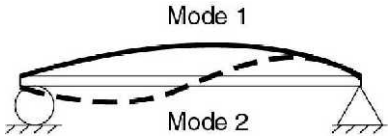

(a) Simply supported beam

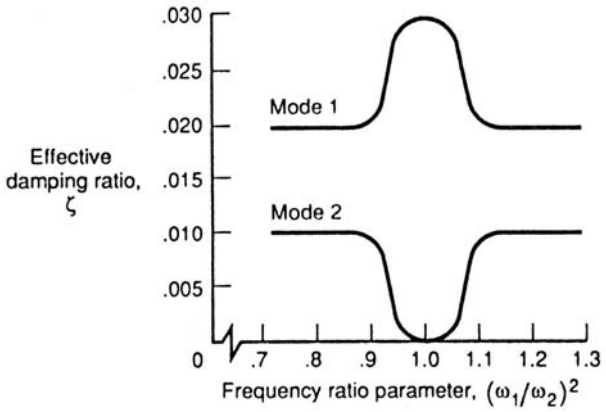

(b) Variation of effective modal damping with frequency ratio for simply supported beam.

Figure 104. - Illustrative example of a resonating structure not benefiting from damping treatment to reduce its vibratory response.

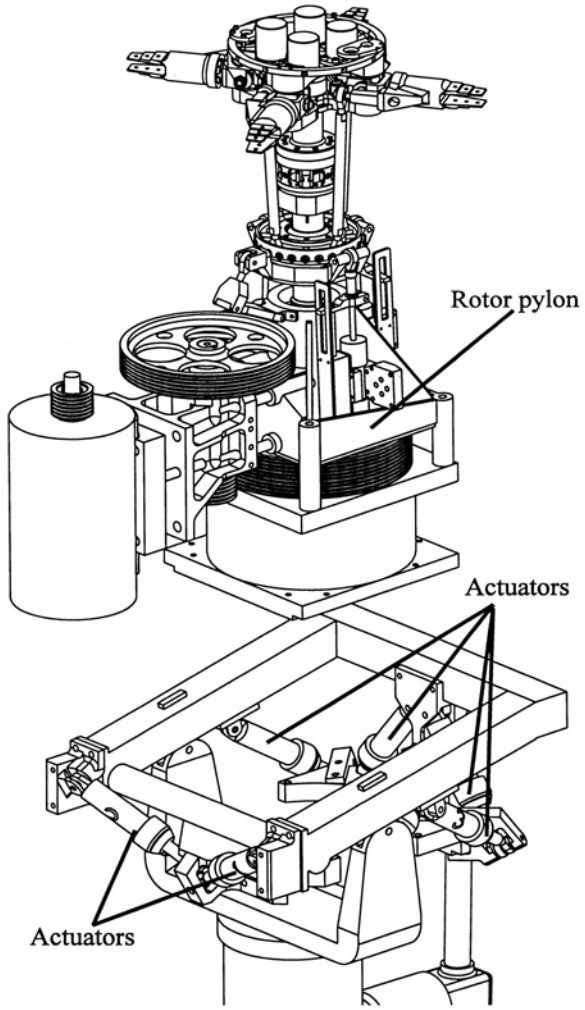

Figure 105. - Exploded view of the ARES-II rotor pylon and the Stewart platform.

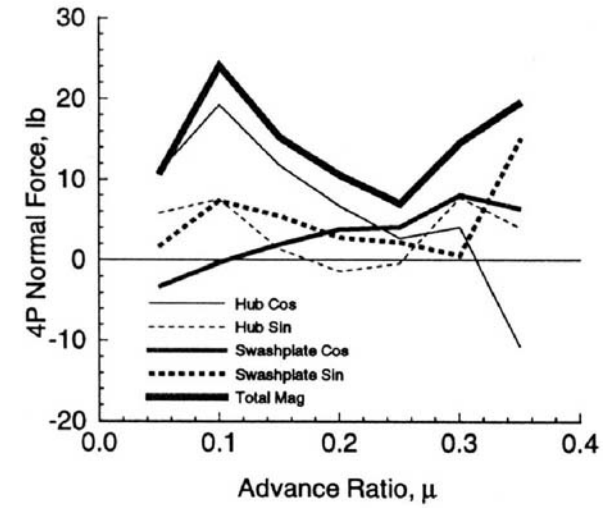

(a) Normal force

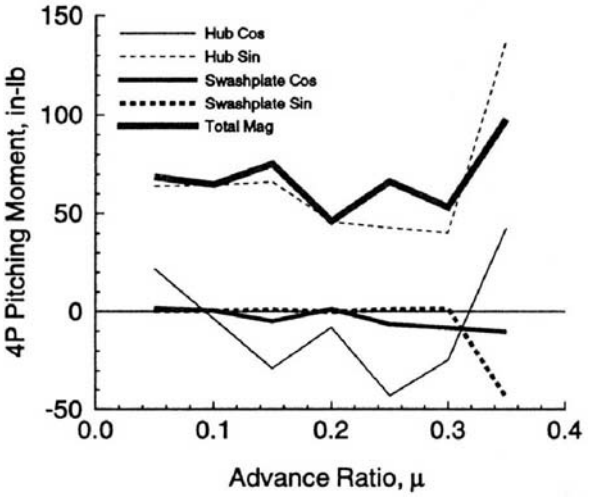

(b) Pitching moment

Figure 106. - Fixed-system loads for uncoupled Baseline Research Rotor model.

Figure 107. - Bell/Boeing V-22 tiltrotor aircraft.

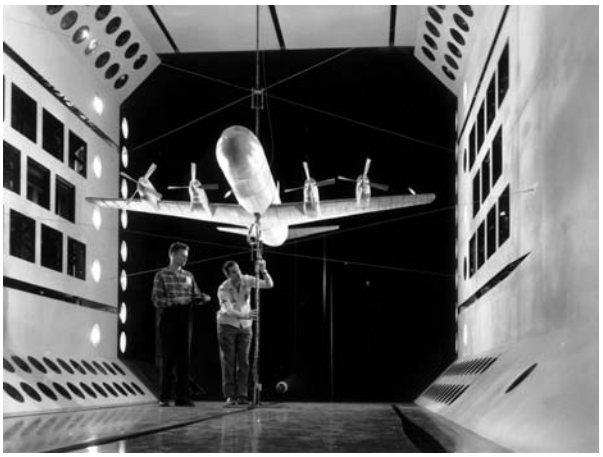

Figure 108. - 1/8-size Lockheed Electra model in TDT for propeller whirl flutter investigation.

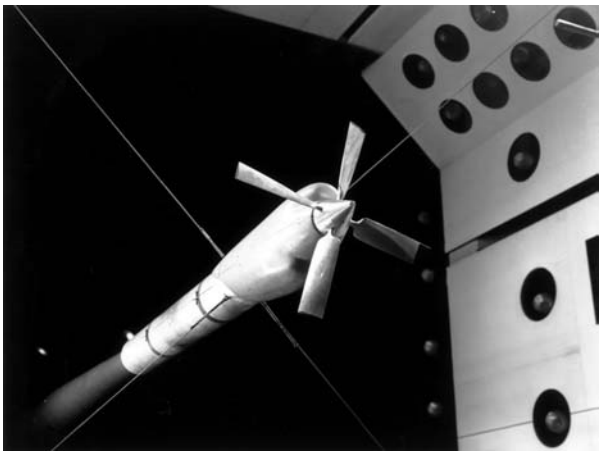

Figure 109. - Sting-mounted propeller/nacelle whirl flutter model.

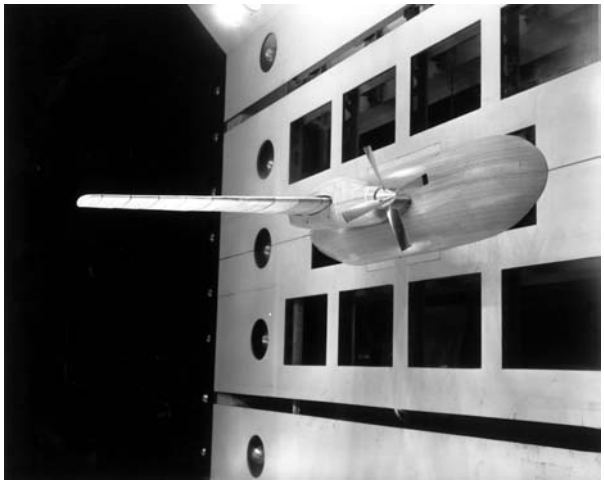

Figure 110. - Wing-mounted propeller/nacelle whirl flutter model.

(a) Blades fixed like propeller

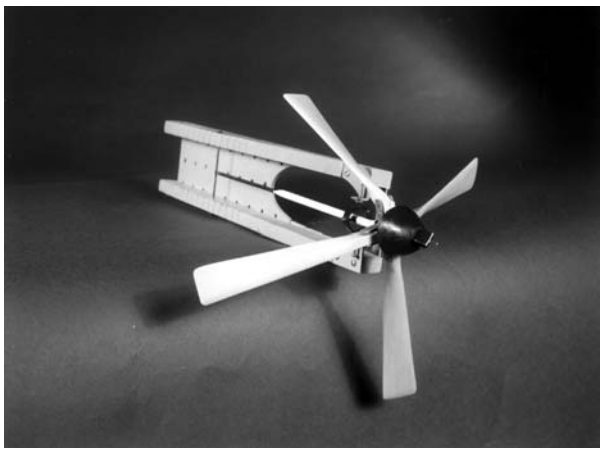

(b) Blades free to flap

Figure 111. - Flapping-blade propeller whirl flutter model.

Figure 112. - Ducted fan whirl flutter model.

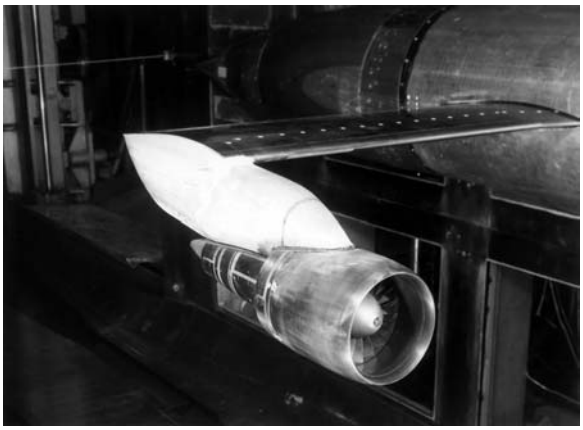

Figure 113. - Model of high bypass ratio fan-jet engine in Langley 8-foot Transonic Pressure Tunnel.

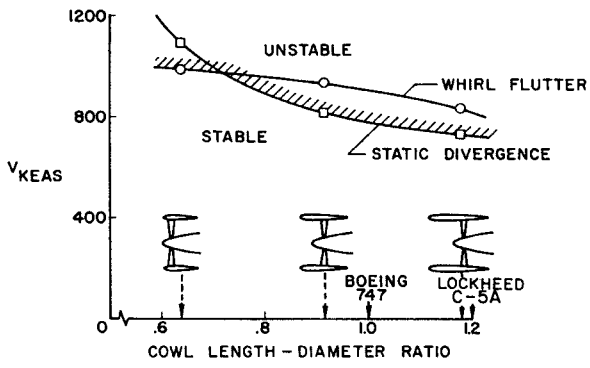

Figure 114. - Estimated stability boundaries for high bypass ratio fan-jet nacelle-pylon.

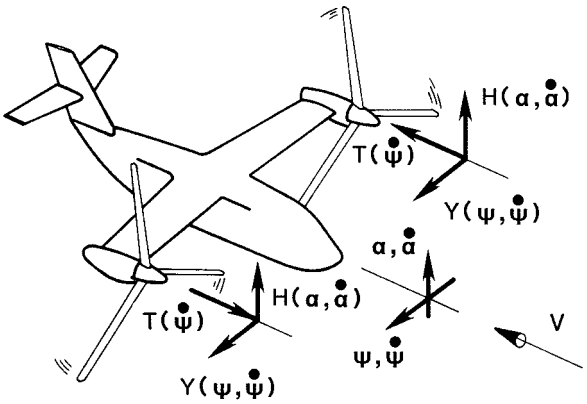

Figure 115. - Perturbation rotor-induced aerodynamic forces acting on a tiltrotor aircraft during pitching and yawing oscillations (rotors interconnected).

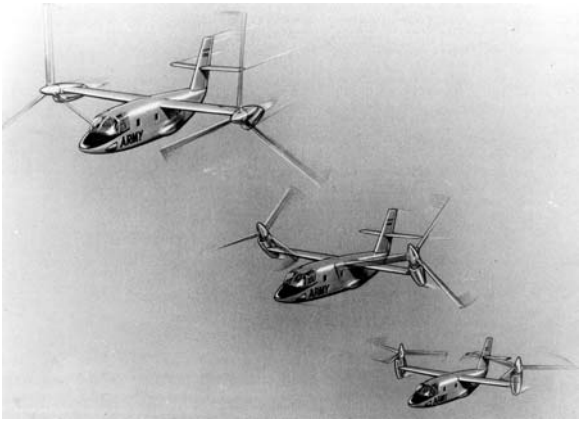

Figure 116. - Artist's conception of Bell Model 266 tilt-rotor design evolved during the Army Composite Aircraft Program.

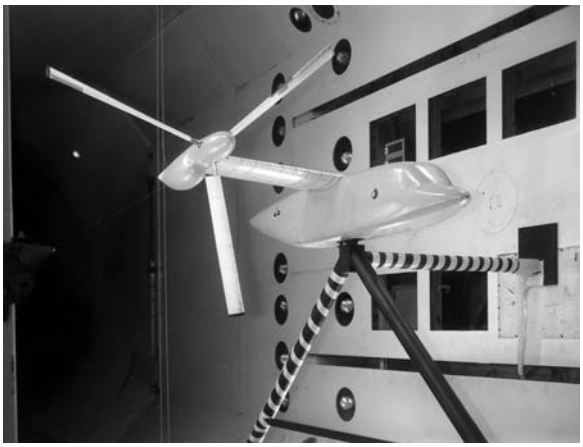

Figure 117. - 1/7.5-scale semispan aeroelastic model of Bell Model 266 in TDT.

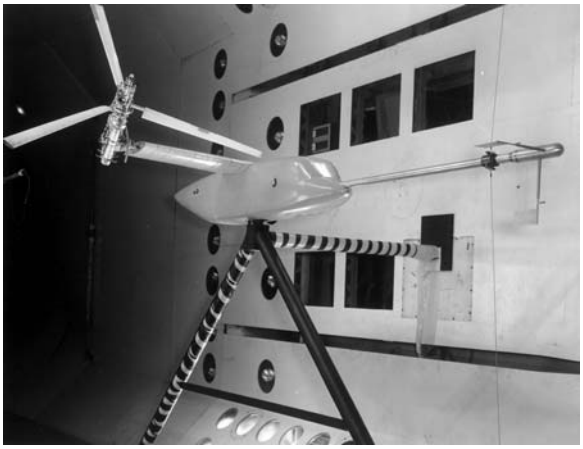

Figure 118. - 1/7.5-scale semispan model in simulated conversion mode with boom-mounted flow direction transmitter used in gust studies.

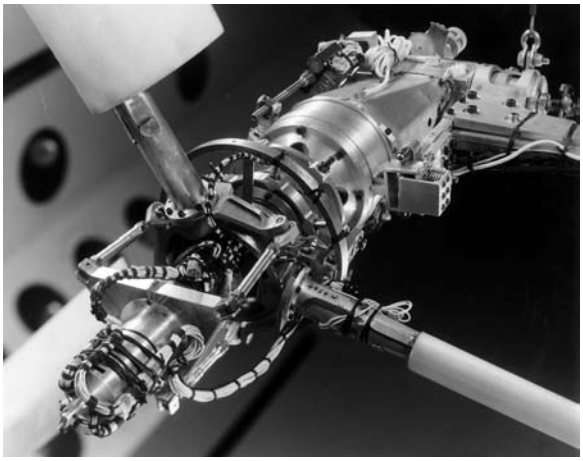

Figure 119. - Close-up view of model pylon with covers removed showing control system used for unpowered testing in airplane mode of flight.

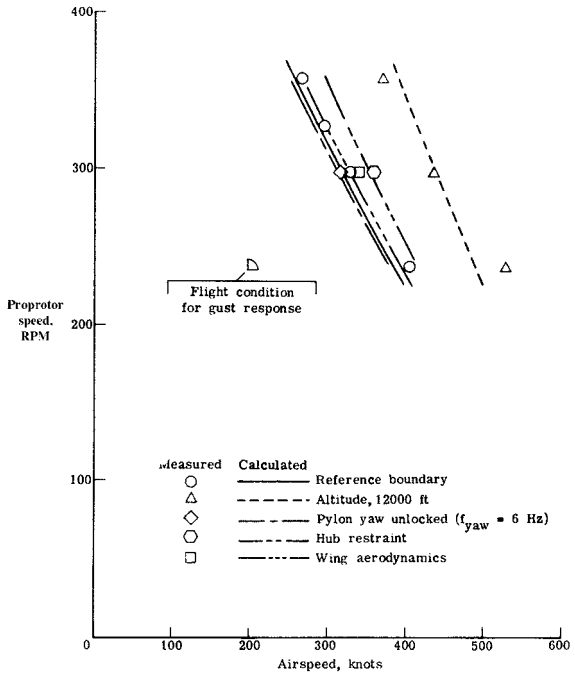

Figure 120. - Effect of some system parameters on proprotor/pylon/wing stability.

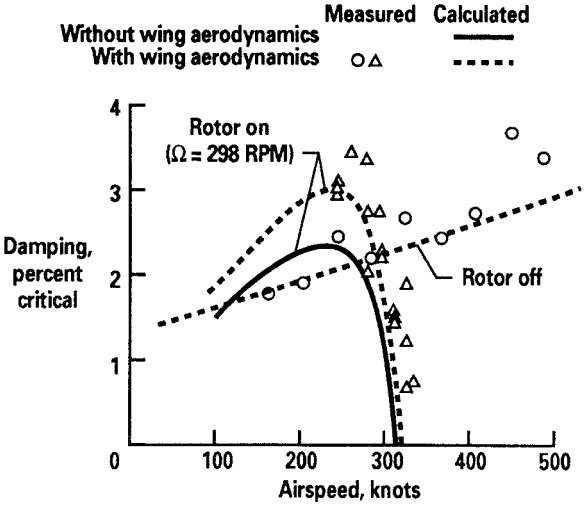

Figure 121. - Effect of proprotor aerodynamics on damping of wing beam mode.

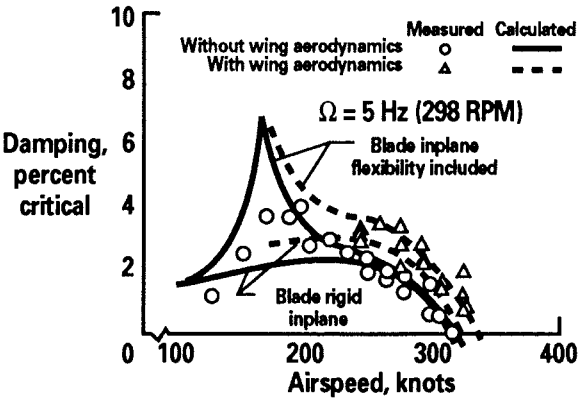

Figure 122. - Effect of wing aerodynamics and blade inplane flexibility on damping of wing beam mode.

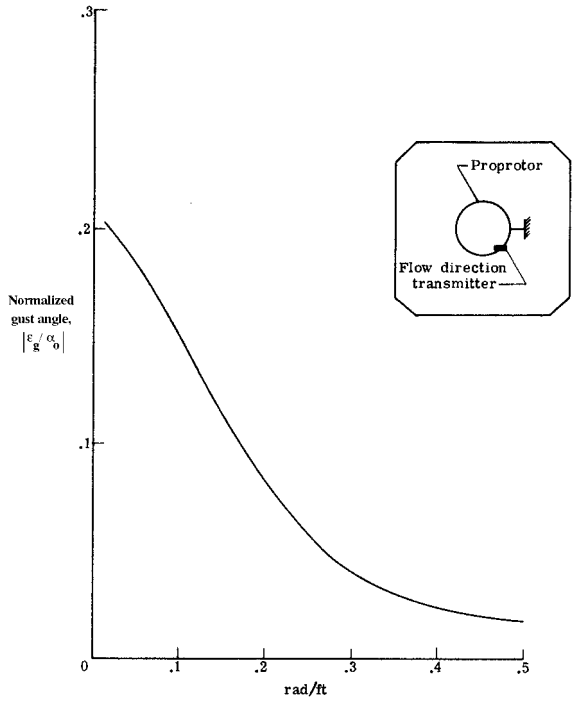

Figure 123. - Measured variation of gust-induced angle of attack with frequency of airstream oscillator.

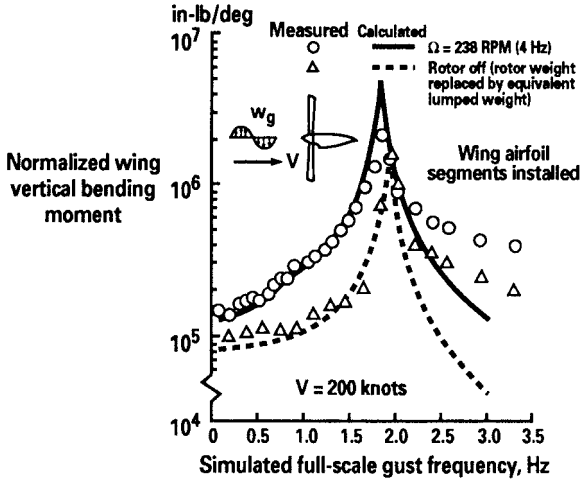

Figure 124. - Effect of proprotor aerodynamics on frequency response of wing vertical bending moment during vertical gust excitation.

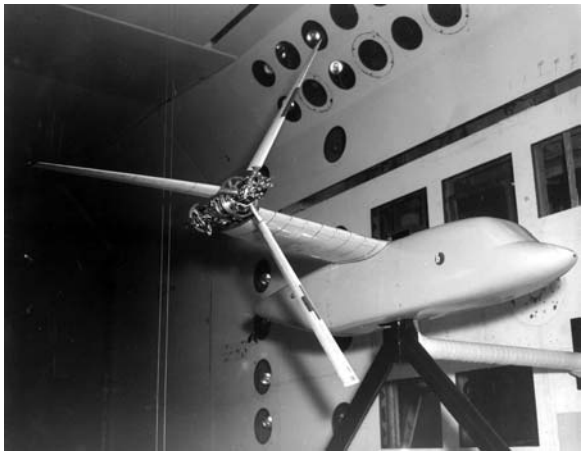

Figure 125. - Model 266 configured for rotating and stop-start portion of folding proprotor investigation.

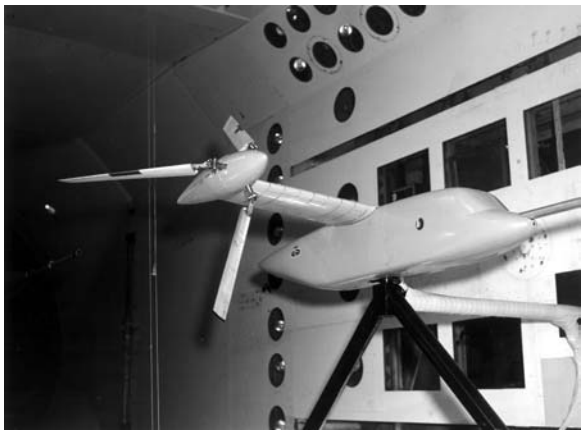

Figure 126. - Model 266 in simulated blade folding configuration.

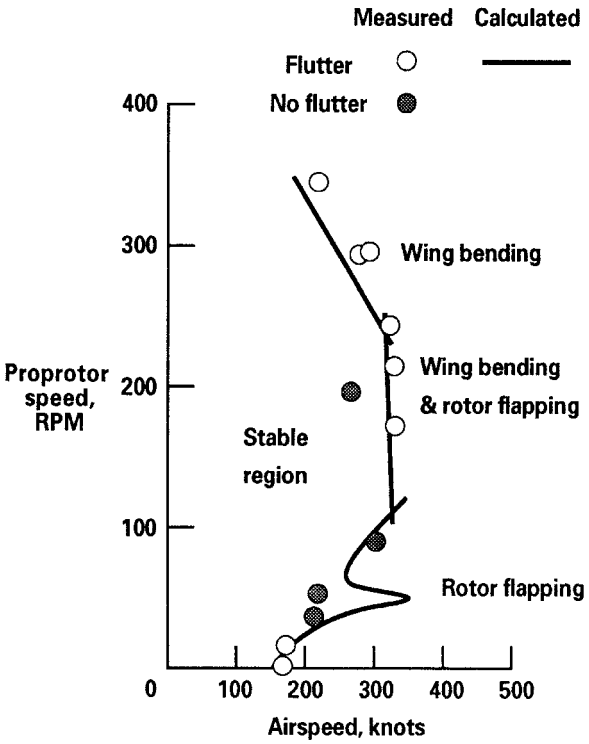

Figure 127. - Model 266 flutter boundaries showing variation in character of flutter modes as rpm is reduced to zero ($\delta_3 = -32°$).

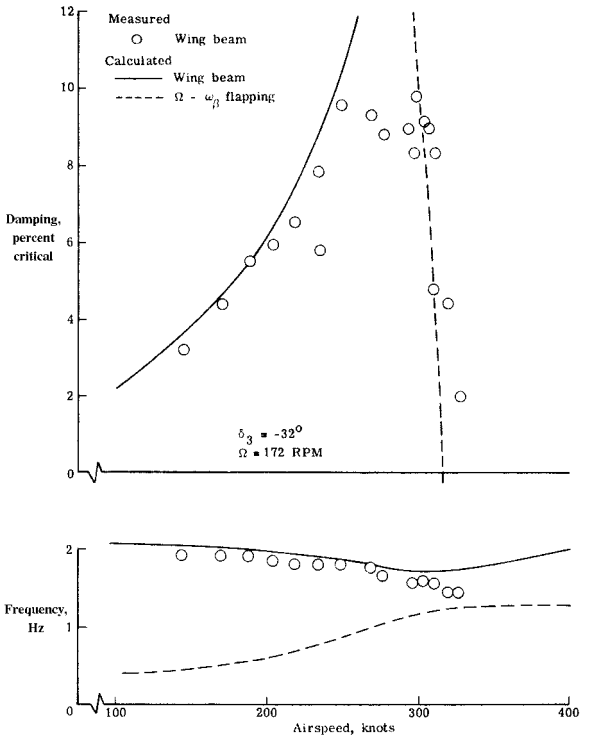

Figure 128. - System subcritical response for Ω = 172 rpm case in figure 127.

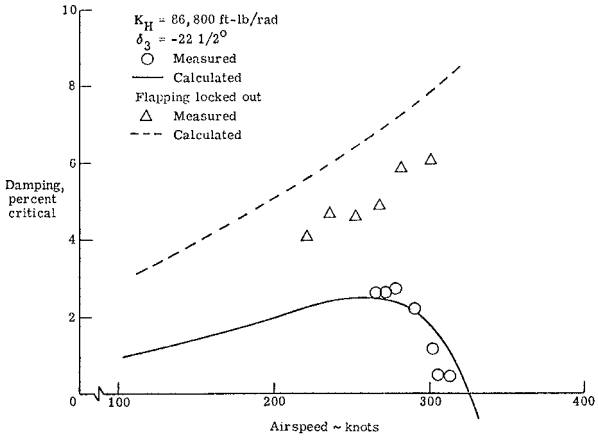

Figure 129. - Effect of blade flapping degree of freedom on wing beam mode damping (Ω = 300 rpm).

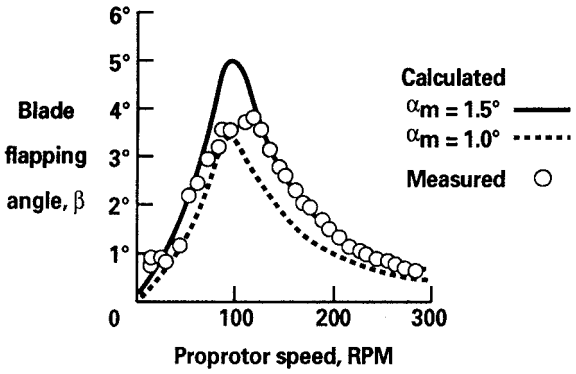

Figure 130. - Variation of blade steady-state flapping with rotor rpm.

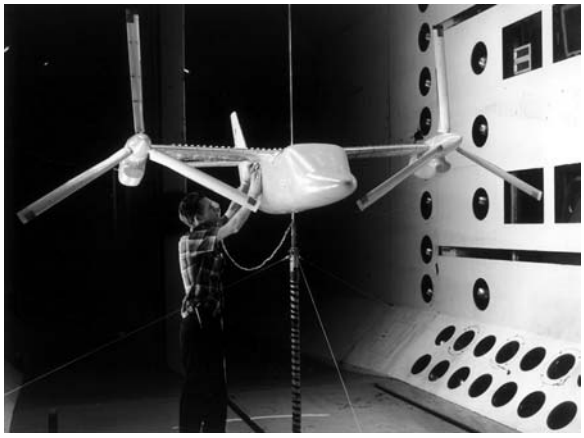

Figure 131. - 1/5-scale aeroelastic model of Bell Model 300-A1A in TDT.

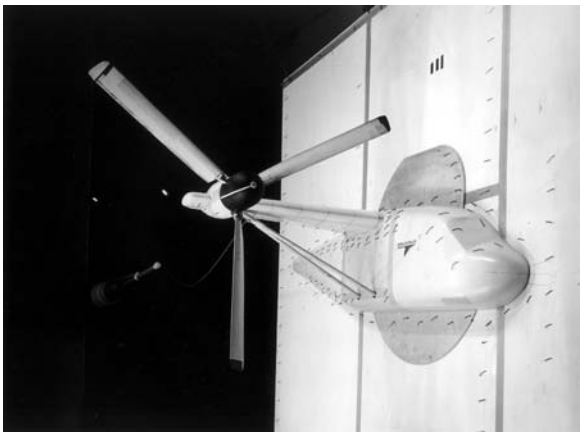

Figure 132. - 1/4.5-scale aeroelastic model of Grumman "Helicat" tiltrotor design in TDT.

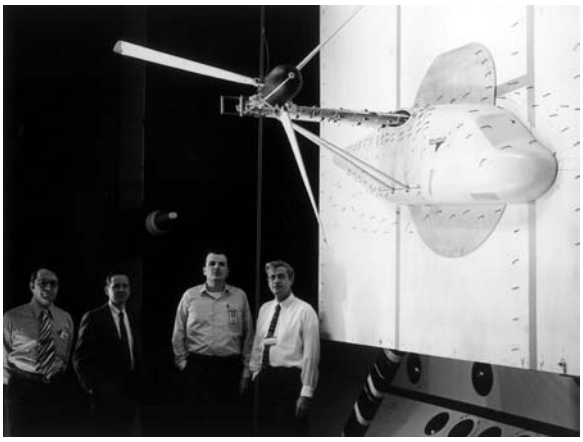

Figure 133. - Grumman tiltrotor model in whirl flutter research configuration.

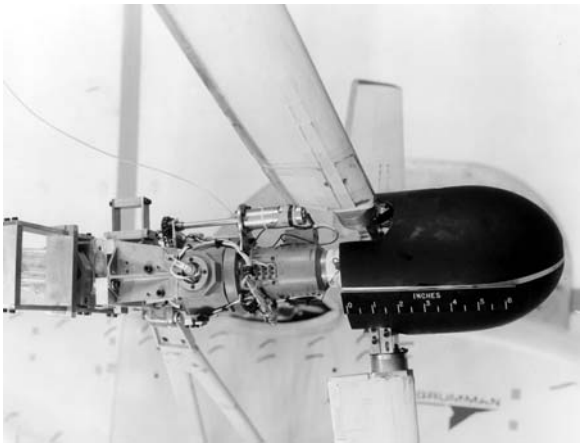

Figure 134. - Close-up view of model pylon in research configuration.

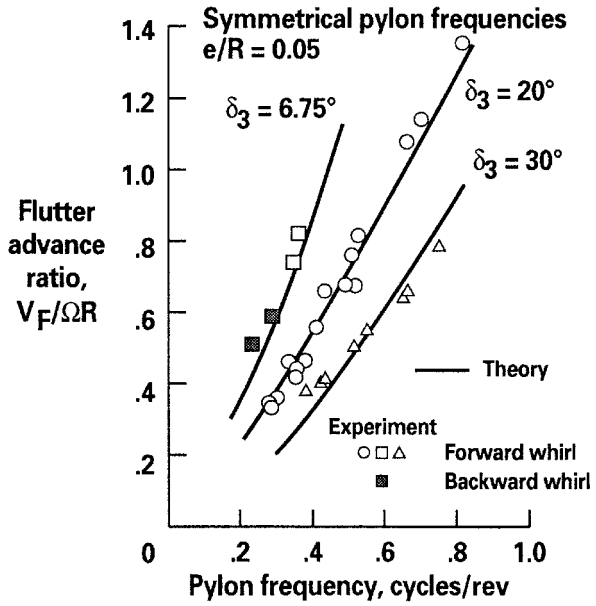

Figure 135. - Effect of blade pitch-flap coupling (δ_3) on whirl flutter.

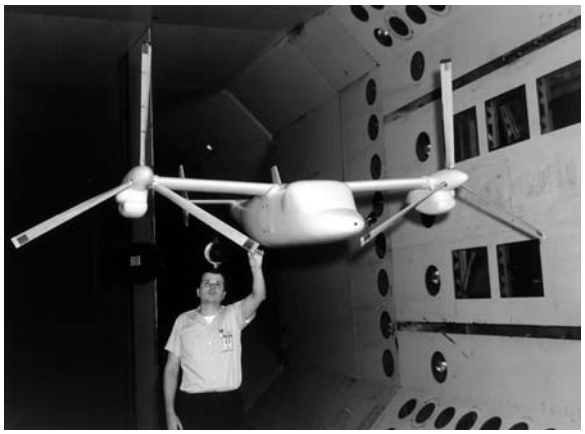

Figure 136. - 1/5-scale rigid aerodynamic force model of Bell Model 300-A2A (XV-15) with rotors from aeroelastic model in TDT.

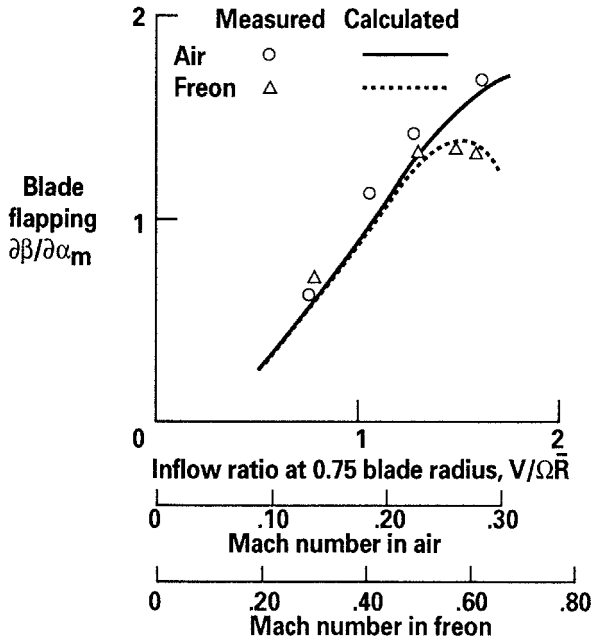

Figure 137. -Effect of Mach number on blade flapping.

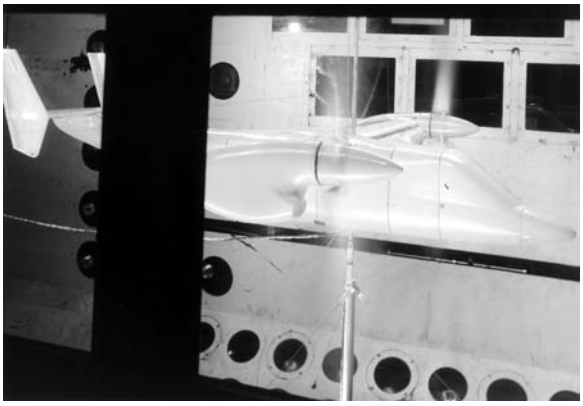

Figure 138. - 1/5-scale aeroelastic model of Bell Model 300-A2A (XV-15) in TDT.

Figure 139. - 1/5-scale model in simulated helicopter autorotational configuration.

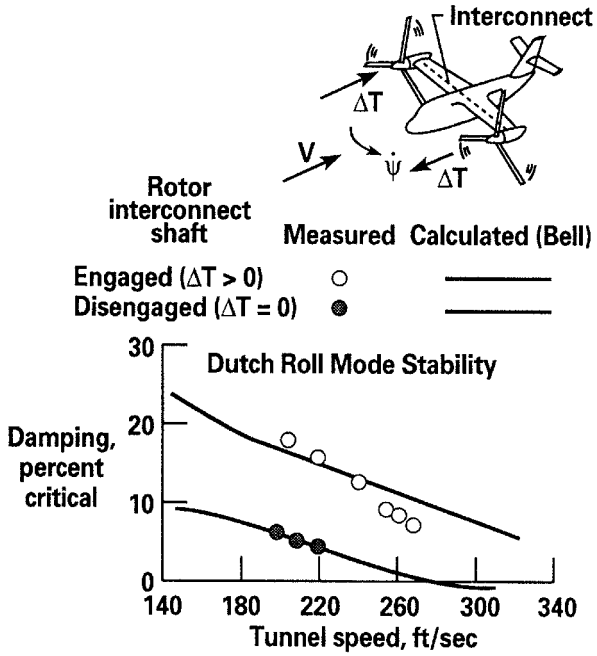

Figure 140. - Proprotor thrust damping effect on model Dutch roll mode stability.

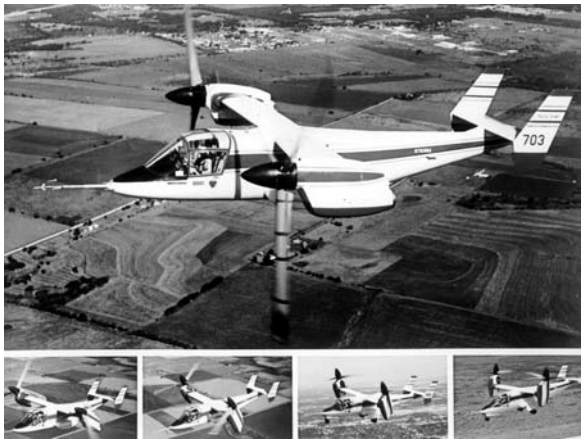

Figure 141. - The XV-15 tiltrotor research aircraft.

Figure 142: 1/5-scale semispan aeroelastic model of Bell/Boeing V-22 in TDT.

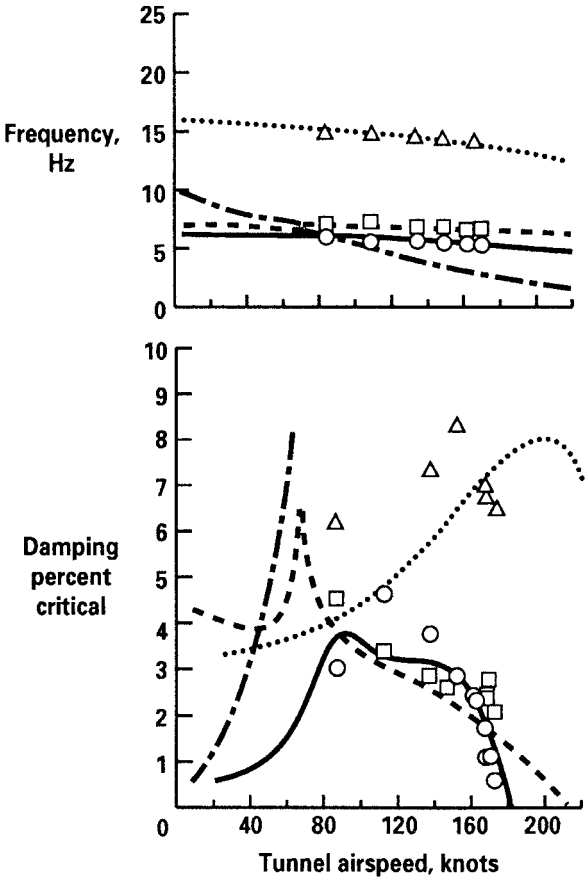

Figure 143. - Stability of wing modes for V-22 model with design stiffness wing spar.

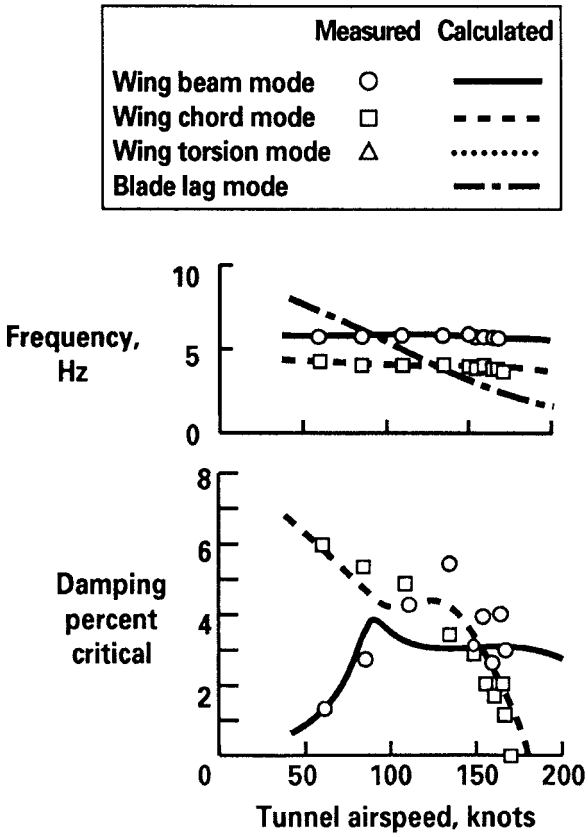

Figure 144. - Stability of wing modes for V-22 model with off-design stiffness wing spar.

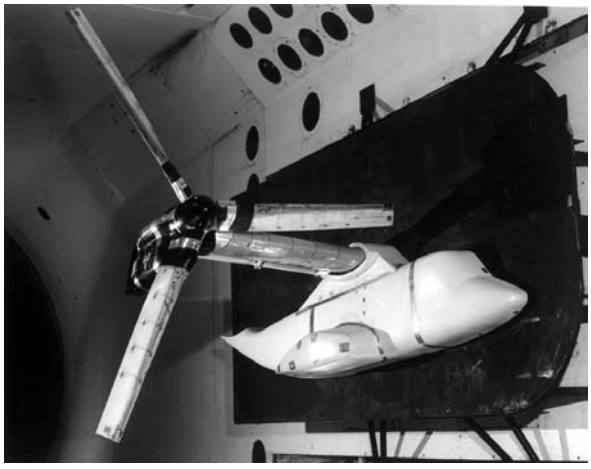

Figure 145. - WRATS testbed installed in TDT.

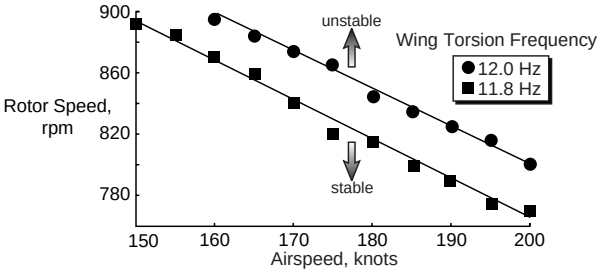

Figure 146. - Effect of wing torsional frequency on stability of WRATS testbed.

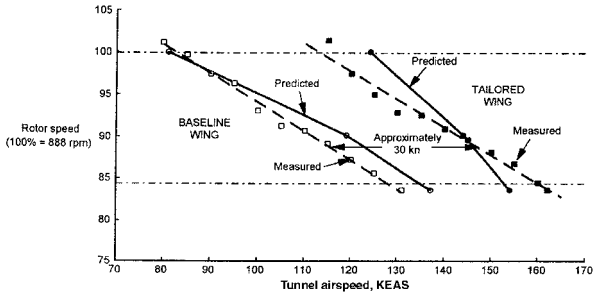

Figure 149. - Stability boundaries for 1/5-scale baseline and tailored wings.

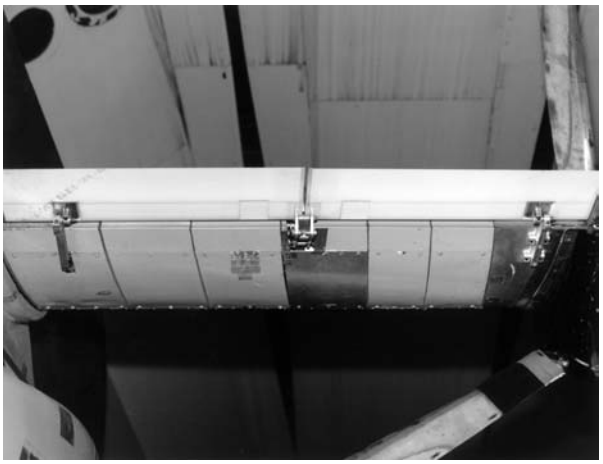

Figure 147. - Active flaperon installed on WRATS testbed.

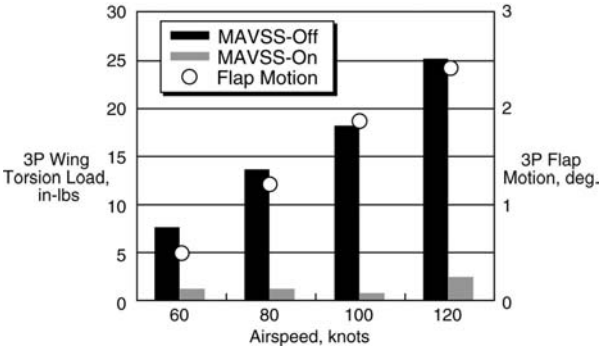

Figure 148. - MAVSS control of 3P torsional vibration using active flaperon.

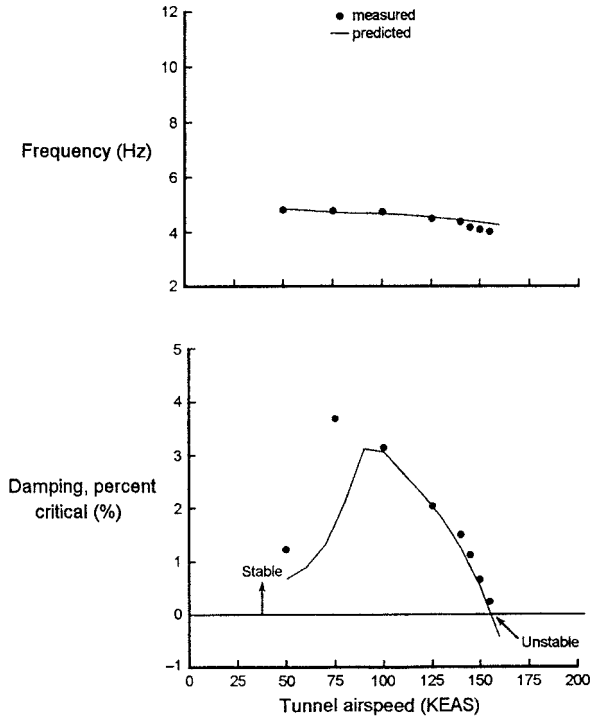

Figure 150. - Stability of wing beam mode for model with tailored wing spar.

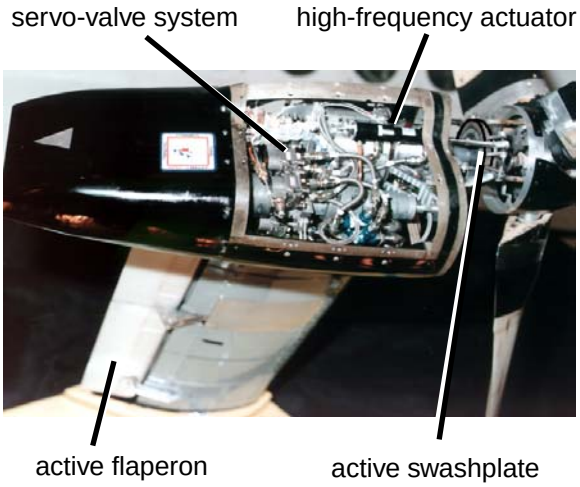

Figure 151. - Hardware components of WRATS active swashplate/flaperon higher harmonic control system.

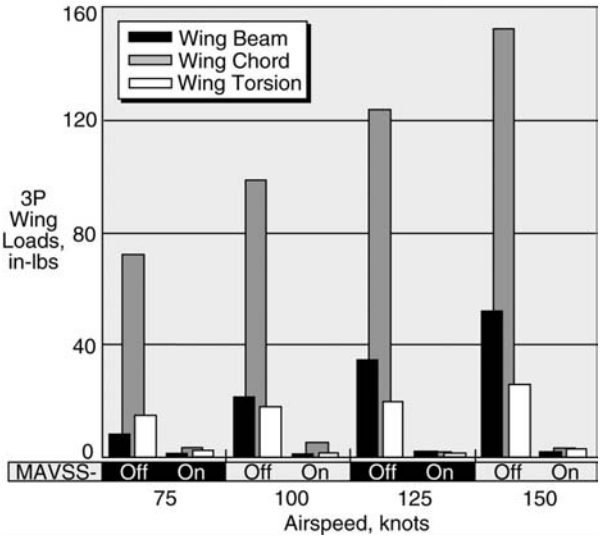

Figure 152. - MAVSS control of 3P wing bending and torsion loads as a function of airspeed.

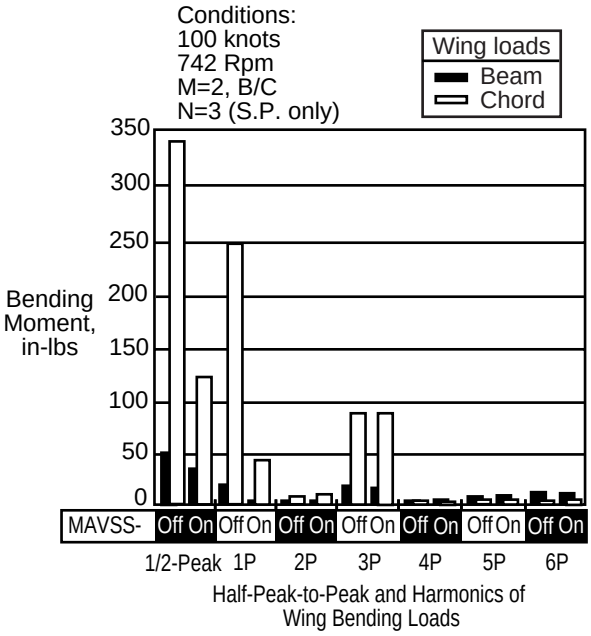

Figure 153. - MAVSS control of 1P wing bending loads.

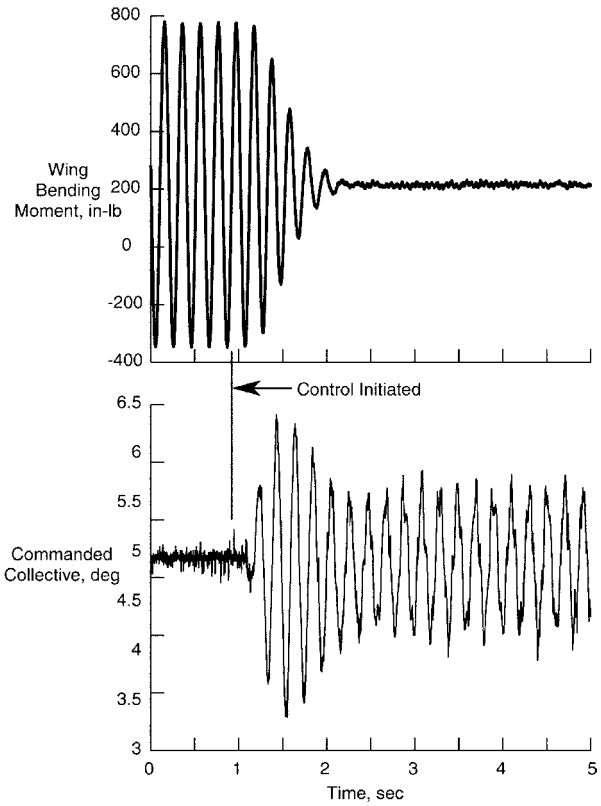

Figure 154. - GPC control of wing vibration on WRATS testbed in hover configuration.

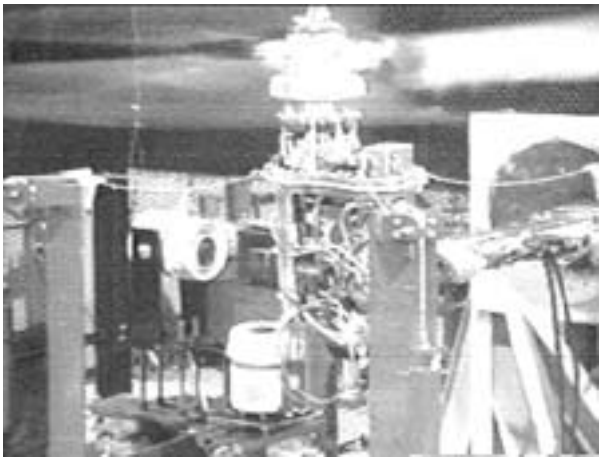

Figure 155. - WRATS tiltrotor testbed with soft-inplane rotor in hover test facility.

Figure 158. - Full-scale mock-up of Bell/Agusta BA609 tiltrotor now in development.

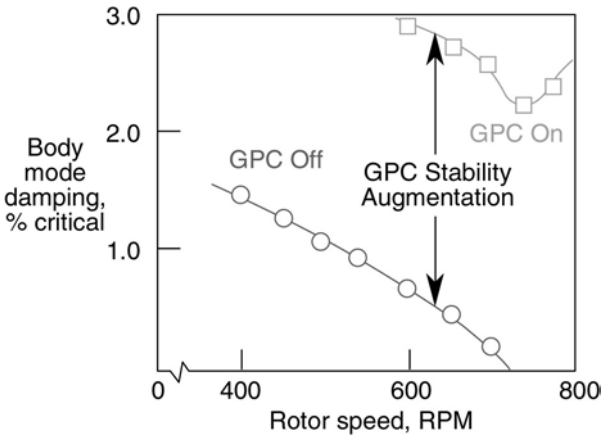

Figure 156. - Use of GPC to actively control ground resonance behavior of soft-inplane model rotor.

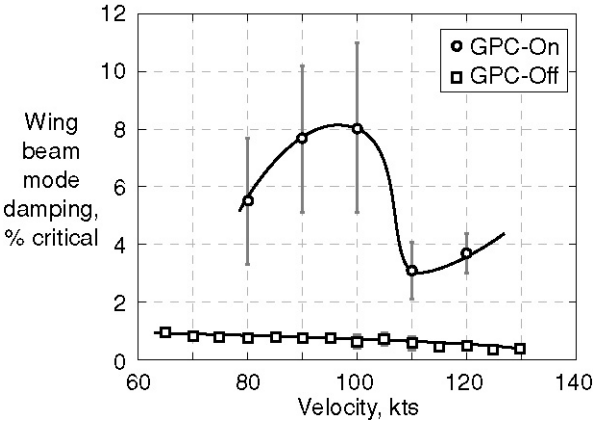

Figure 157. - Comparison of wing beam mode damping versus airspeed with GPC on and off for $\delta_3 = -15°$.

Figure 159. - Artist's conception of a "Quad Tilt Rotor" under study by Bell.

REPORT DOCUMENTATION PAGE

Form Approved
OMB No. 0704-0188

1. AGENCY USE ONLY (*Leave blank*)	2. REPORT DATE	3. REPORT TYPE AND DATES COVERED
	August 2001	Technical Memorandum

4. TITLE AND SUBTITLE
A Historical Overview of Aeroelasticity Branch and Transonic Dynamics Tunnel Contributions to Rotorcraft Technology and Development

5. FUNDING NUMBERS
WU 712-20-21-01

6. AUTHOR(S)
William T. Yeager, Jr., and Raymond G. Kvaternik

7. PERFORMING ORGANIZATION NAME(S) AND ADDRESS(ES)
NASA Langley Research Center
Hampton, VA 23681-2199

U.S. Army Research Laboratory
Vehicle Technology Directorate
NASA Langley Research Center
Hampton, VA 23681-2199

8. PERFORMING ORGANIZATION REPORT NUMBER
L-17983

9. SPONSORING/MONITORING AGENCY NAME(S) AND ADDRESS(ES)
National Aeronautics and Space Administration
Washington, DC 20546-0001
and
U.S. Army Research Laboratory
Adelphi, MD 20783-1145

10. SPONSORING/MONITORING AGENCY REPORT NUMBER
NASA/TM-2001-211054
ARL-TR-2564

11. SUPPLEMENTARY NOTES
A significantly expanded version of the paper "Contributions of the Langley Transonic Dynamics Tunnel to Rotorcraft Technology and Development" that was presented at the AIAA Dynamics Specialists Conference, Atlanta, GA, April 5-6, 2000 (AIAA Paper 2000-1771).

12a. DISTRIBUTION/AVAILABILITY STATEMENT
Unclassified -Unlimited
Subject Category 99 Distribution: Standard
Availability: NASA CASI (301) 621-0390

12b. DISTRIBUTION CODE

13. ABSTRACT *(Maximum 200 words)*
A historical account of the contributions of the Aeroelasticity Branch (AB) and the Langley Transonic Dynamics Tunnel (TDT) to rotorcraft technology and development since the tunnel's inception in 1960 is presented. The paper begins with a summary of the major characteristics of the TDT and a description of the unique capability offered by the TDT for testing aeroelastic models by virtue of its heavy gas test medium. This is followed by some remarks on the role played by scale models in the design and development of rotorcraft vehicles and a review of the basic scaling relationships important for designing and building dynamic aeroelastic models of rotorcraft vehicles for testing in the TDT. Chronological accounts of helicopter and tiltrotor research conducted in AB/TDT are then described in separate sections. Both experimental and analytical studies are reported and include a description of the various physical and mathematical models employed, the specific objectives of the investigations, and illustrative experimental and analytical results.

14. SUBJECT TERMS
Langley Transonic Dynamics Tunnel (TDT); Rotorcraft aeroelastic models; Helicopter models; Tiltrotor models; Rotor blade stability and dynamics; Finite element modeling; Active controls; Optimization; Rotorcraft comprehensive analyses; Rotorcraft vibrations

15. NUMBER OF PAGES
115

16. PRICE CODE
A06

17. SECURITY CLASSIFICATION OF REPORT	18. SECURITY CLASSIFICATION OF THIS PAGE	19. SECURITY CLASSIFICATION OF ABSTRACT	20. LIMITATION OF ABSTRACT
Unclassified	Unclassified	Unclassified	UL